PIUS - Hydrofaction(TM) Platform with Integrated Upgrading Step

Jensen, Claus Uhrenholt

Publication date:
2018

Document Version
Publisher's PDF, also known as Version of record

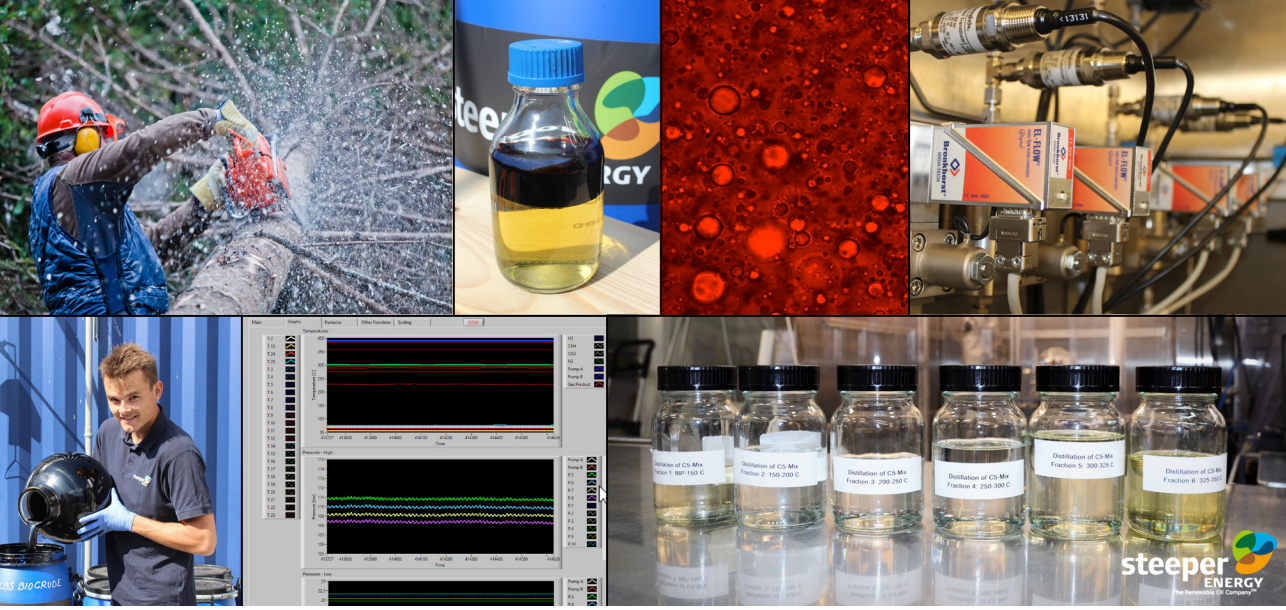

PIUS – HYDROFACTION™ PLATFORM WITH INTEGRATED UPGRADING STEP

BY
CLAUS UHRENHOLT JENSEN

DISSERTATION SUBMITTED 2018

AALBORG UNIVERSITY
DENMARK

PIUS - Hydrofaction^{TM} Platform with Integrated Upgrading Step

Ph.D. Dissertation
Claus Uhrenholt Jensen

Dissertation submitted January, 2018

Dissertation submitted:	January, 2018
PhD supervisors:	Prof. Lasse A. Rosendahl Aalborg University, Denmark
	PhD Steen B. Iversen Steeper Energy ApS, Denmark
Assistant PhD supervisor:	PhD Göran Olofsson Steeper Energy ApS, Denmark
External PhD Supervisor:	Prof. William C. McCaffrey University of Alberta, Canada
PhD committee:	Associate Professor Marco Maschietti (chairman) Aalborg University, Denmark
	Professor Arno de Klerk University of Alberta, Edmonton, AL, Canada
	Senior Research Scientist Brajendra K. Sharma University of Illinois, Urbana-Champaign, USA
PhD Series:	Faculty of Engineering and Science, Aalborg University
Department:	Department of Energy Technology

ISSN (online): 2446-1636
ISBN (online): 978-87-7210-134-7

Published by:
Aalborg University Press
Langagervej 2
DK – 9220 Aalborg Ø
Phone: +45 99407140
aauf@forlag.aau.dk
forlag.aau.dk

Printed in Denmark by Rosendahls, 2018

Preface

This dissertation is submitted for the degree of Doctor of Philosophy at the Faculty of Engineering and Science, Aalborg University. The industrial PhD project span from January 2015 to January 2018, and is funded by Innovation Fund Denmark (grant no. 4135-00126) and Steeper Energy ApS.

With a process engineering background I soon realized that I jumped right into a maze of chemistry, and the list of people who helped me on the way out is long. I am grateful to my supervisors Prof. L.A. Rosendahl, CTO S.B. Iversen and PhD G. Olofsson for your excellent guidance and support and friendly attitude during a highly educational and enjoyable part of my life.

I also want to express gratitude to all my additional colleagues of Team Steeper; in particular CEO Perry Toms for inspiration and motivation, Julie K. Rodriquez for fruithful collaboration on the upgrading research; Bob Moll, Sergios Karatzos, Andrew Ironside and Ling Lee for your help, friendship and great experiences during my visits to Calgary; and last but not least Anne V.K. Rasmussen, Henrik Egholm, Hans-Henrik Pedersen, Johnny L. Callisen and Jan Petersen for support, friendship and laughter. It has been a pleasure to do an industrial PhD for a company with such dedication to research and detail, and where novel data is so abundant.

I highly appreciate the educational and friendly collaboration with academic employees at AAU; Daniele Castello, Thomas H. Pedersen, Henrik Sørensen, Jessica Hoffmann and past and present fellow PhD students. I want to thank Prof. W.C. McCaffrey and his group at University of Alberta for hospitality and guidance during my research visits as both PhD and graduate student. I am thankful to Prof. Nader Mahinpey and Prof. Pedro P. Almao for welcoming me in your laboratories at the University of Calgary. Also, a sincere thank you to the PhD committee for allowing your time.

Finally, I want to direct a special thanks to my family and friends, and particularly Rikke, who encouraged, supported and traveled with me.

Claus Uhrenholt Jensen
Aalborg University, January 15, 2018

Contents

Nomenclature

Names and definitions

Catliq®	Catalytic liquefaction process owned by Altaca Enerji
Cat-HTR™	Catalytic Hydrothermal Reactor, HTL process developed by Licella
CBS1	Continuous Bench Scale HTL pilot unit installed at AAU
H2T	Hydrotreating pilot unit designed and commisioned at AAU as part of the PhD
HTP	Hydrothermal processing, HTL process developed by PNNL and Genifuel
HTU®	Hydrothermal Upgrading, HTL process developed by Shell and Biofuel B.V
Lights	Volatile organic distillate (IBP-140 °C) of HTL oil
NL	Normal liter at standard conditions (0.0 °C and 1.01325 bar)
SECA	Sulphur emission control areas
TCP	Thermal conversion process, developed by CWT (Changing World Technologies)

Acronyms

AA	Acetic acid
AAU	Aalborg University, Denmark
AET	Atmospheric equivalent temperature
BPR	Back pressure regulator
CA	Citric acid
CCAI	Calculated Carbon Aromaticity Index
CCI	Calculated cetane index
CFPP	Cold filter plugging point
C-NMR	Carbon-13 nuclear magnetic resonance
CoMo	Cobalt molybdenum
CS_2	Carbon disulphide
CTO	Crude tall oil
DMDS	Dimethyl disulphide
DTO	Distilled tall oil
FT	Fischer-Tropsh synthesis
GHG	Greenhouse gas
GTL	Gas to liquid
H_2S	Hydrogen sulphide
H/C	Molar hydrogen to carbon ratio
HCL	Hydrocloric acid
HDM	Hydrodemetallation
HDN	Hydrodenitrogenation
HDO	Hydrodeoxygenation
HDS	Hydrodesulphurisation
HHV	Higher heating value
H-NMR	Proton nuclear magnetic resonance
HoS	Hours on stream
HTL	Hydrothermal Liquefaction
HVO	Hydrotreated vegetable oil
HYD	Hydrogenation
IBP	Initital boiling point
ICP	Inductively Coupled Plasma
IP	Intellectual property
MB	Mass balance
MCR	Micro carbon residue
MEK	Methyl Ethyl Ketone
MFC	Mass flow controller
NiMo	Nickel molybdenum
NiW	Nickel Wolfram
PAH	Polyaromatic hydrocarbon
PCL	Pseudo critical line
PFD	Process flow diagram
PW	Process water from HTL
RO	Reverse osmosis water
Rx	Reactor no. x, e.g. R1
SiC	Silicon carbide
TAN	Total acid number
TBP	True boiling point
TOC	Total organic content
WHSV	Weight hourly space velocity
WP	Water phase from washing

Thesis Details

Thesis Title:	PIUS - Hydrofaction^{TM} Technology Platform with Integrated Upgrading Step
Ph.D. Student:	Claus Uhrenholt Jensen
Supervisors:	PhD Steen B. Iversen, Steeper Energy ApS Prof. Lasse A. Rosendahl, Aalborg University PhD Göran Olofsson, Steeper Energy ApS

The main body of this thesis consist of the following papers.

[A] Claus Uhrenholt Jensen, Julie Katerine Rodriguez Guerrero, Sergios Karatzos, Göran Olofsson, Steen Brummerstedt Iversen, "Hydrofaction^{TM} of Forestry Residues to Drop-in Renewable Transportation Fuels", *Direct Thermochemical Liquefaction for Energy Applications*, Elsevier, 2018, ISBN: 9780081010259.

[B] Claus Uhrenholt Jensen, Julie Katerine Rodriguez Guerrero, Sergios Karatzos, Göran Olofsson, Steen Brummerstedt Iversen, "Fundamentals of Hydrofaction^{TM} : Renewable crude oil from woody biomass", *Biomass Conversion and Biorefinery*, vol. 7, no. 4, pp. 495–509, 2017.

[C] Thomas H. Pedersen, Claus Uhrenholt Jensen, Linda Sandström, Lasse A. Rosendahl, "Full characterization of compounds obtained from fractional distillation and upgrading of a HTL biocrude", *Applied Energy*, vol. 202, pp. 408–419, 2017.

[D] Claus Uhrenholt Jensen, Lasse A. Rosendahl, Göran Olofsson, "Impact of nitrogenous alkaline agent on continuous HTL of lignocellulosic biomass and biocrude upgrading", *Fuel Processing Technology*, vol. 159, pp. 376–385, 2017.

[E] Jessica Hoffmann, Claus Uhrenholt Jensen, Lasse A. Rosendahl "Co-processing potential of HTL bio-crude at petroleum refineries - Part 1: Fractional distillation and characterization", *Fuel*, vol.165, pp. 526–535, 2016.

[F] Claus Uhrenholt Jensen, Jessica Hoffmann, Lasse A. Rosendahl "Co-processing potential of HTL bio-crude at petroleum refineries - Part 2: A parametric hydrotreating study", *Fuel*, vol. 165, pp. 536–543, 2016.

Patent applications

[G] Steen Brummerstedt Iversen, Claus Uhrenholt Jensen, Julie Katerine Rodriguez Guerrero, Göran Olofsson, "Process for producing low sulphur renewable oil", *International PCT Application no. PCT/EP2017/067264*.

[H] Steen Brummerstedt Iversen, Claus Uhrenholt Jensen, Julie Katerine Rodriguez Guerrero, Göran Olofsson, "Separation system for high pressure process system", *Danish patent application no. PA201770234*.

[I] Steen Brummerstedt Iversen, Claus Uhrenholt Jensen, Andrew Ironside, Göran Olofsson, "Heating system for high pressure process system", *Danish patent application no. PA201700160*.

[L] Steen Brummerstedt Iversen, Claus Uhrenholt Jensen, Julie Katerine Rodriguez Guerrero, Göran Olofsson, "Process for upgrading oxygen containing renewable oil", *Danish patent application*.

In addition to the main papers, the following publications have also been made.

[J] T.H. Pedersen, I.F. Grigoras, J. Hoffmann, S.S. Toor, I.M. Daraban, C.U. Jensen, S.B. Iversen, R.B. Madsen, M. Glasius, K.R. Arturi, R.P. Nielsen, E.G. Søgaard, L.A. Rosendahl, "Continuous hydrothermal co-liquefaction of aspen wood and glycerol with water phase recirculation", *Applied Energy*, vol. 162, pp. 1034–1041, 2016.

[K] I.M. Daraban, I.F. Grigoras, C.U. Jensen, S.S. Toor, T.H. Pedersen, L.A. Rosendahl, "Two-stage alkaline hydrothermal liquefaction of wood to biocrude in a continuous bench-scale system", *Biomass Conversion and Biorefinery*, vol. 7, no. 4, pp. 425–435, 2017.

Conference contributions

- Claus Uhrenholt Jensen, T.H. Pedersen, Lasse A. Rosendahl, P. Biller, "Hydrotreatment and Compound Identification of Distillate Bio-crude Fractions from Continuous Hydrothermal Liquefaction of Wood", *Oral presentation at TC Biomass 2015, Chicago*, 2nd–5th of November 2015.
- Claus Uhrenholt Jensen, Julie Katerine Rodriguez Guerrero, Ling Li, "Recent Advancements in Upgrading of Hydrofaction^{TM} Oil", *Poster presentation at EUBCE 2016, Amsterdam*, 6th–9th of June 2016.

- Claus Uhrenholt Jensen, Julie Katerine Rodriguez Guerrero, Sergios Karatzos, Göran Olofsson, Steen Brummerstedt Iversen, "Continuous Hydrotreatment of Hydrofaction^{TM} Oil to Drop-In Diesel", *Oral presentation at Symposium on Thermal and Catalytic Sciences for Biofuels and Biobased Products, Chapel Hill*, 1st–3rd of November 2016.
- Claus Uhrenholt Jensen, Julie Katerine Rodriguez Guerrero, Sergios Karatzos, Göran Olofsson, Steen Brummerstedt Iversen, "Hydrofaction^{TM} – The Path to Renewable Drop-in Biofuels", *Oral presentation at International Conference on Gas, Oil and Petroleum Engineering, Las Vegas*, 14th–16th of November 2016.

This thesis has been submitted for assessment in partial fulfillment of the PhD degree. The thesis is based on the submitted or published scientific papers which are listed above. Parts of the papers are used directly or indirectly in the extended summary of the thesis. As part of the assessment, co-author statements have been made available to the assessment committee and are also available at the Faculty.

Abstract

Steeper Energy's proprietary Hydrofaction^{TM} pathway for production of advanced drop-in transportation fuels comprise thermochemical conversion of lignocellulosic biomass residues through hydrothermal liquefaction (HTL) and subsequent upgrading. HTL enables a feedstock flexible liquefaction of wet or dry, low-value, non-food biomass residues to liquid biocrude. Similar to petroleum crude oil, the oxygenated biocrude is an intermediate that needs further upgrading to meet liquid fuel specifications. On that basis, this thesis focuses on development of an integrated separation, demineralization and upgrading technology platform for Hydrofaction^{TM} , enabling production of advanced biofuel blendstocks for the heavy transport sector.

The HTL oil product is a water in oil emulsion containing 10-15 wt.% water and 3-4 wt.% inorganics, and demineralization is a requirement for catalyst lifetime and stability during subsequent hydrotreating. Filtering, centrifugation and electrocoalescence have been found ineffective, as the emulsion alkalinity needs to be reduced for effective demineralization. A washing procedure using a diluent and 0.1 M citric acid was developed for pilot scale, resulting in repeatable demineralization of Hydrofaction^{TM} oil to <50 ppm metals. Another novel approach using the CO_2 rich gaseous HTL product in the form of carbonated water as acidifying agent during product separation and demineralization was successfully tested. The findings have been implemented in an integrated product separation and demineralization system that is being commissioned at the HTL pilot plant in 2018.

A continuous dual-reactor hydrotreating pilot unit has been designed, built and commissioned and the present work advances the state of the art on hydrotreating of HTL oil by completing several continuous campaigns with up to 660 hours on stream. Upon several iterations a 3-Zone hydrotreating process was developed, proving the upgrading of Hydrofaction^{TM} oil to drop-in transportation fuel at yields around 100 vol.%. Due to the oxygenated nature of liquefaction oil, a critical step was configuration of the first reactor to keep reaction rates and exothermic heat release at manageable levels.

Upgraded oils have been distilled and evaluated against fuel specifications. HTL oil volatility and fuel compatibility are significantly improved by hydrotreating. The diesel equivalent fraction represents an advanced fuel blendstock comprising 50-60 wt.% of the upgraded oil, and complete analysis may even prove that it meets the current D975 diesel specifications. Blending in substantial proportions is also applicable for the gasoline, jet fuel and marine bunker fractions, the latter being an attractive low sulphur residue with desirable blend properties in relation to the recent sulphur restrictions on marine fuels. Thereby, the PhD project has contributed to the development of Hydrofaction^{TM} , as a technology that provides the entire path from tree to tank.

Resumé

Steeper Energy's proprietære Hydrofaction^{TM} teknologi til produktion af vedvarende transport brændstoffer indebærer en termokemisk konvertering af lignocellulosisk biomasse affald gennem hydrothermal liquefaction (HTL) med efterfølgende opgradering. HTL muliggør konvertering af en bred vifte af våd eller tør, lav-værdi biomasse affald til en flydende bio-råolie. I lighed med fossil råolie, den iltede bio-råolie er af en kvalitet der kræver yderligere opgradering for at opfylde gældende brændstof specifikationer. På det grundlag fokuserer denne afhandling på udvikling af en integreret separations, demineraliserings og opgraderings teknologi til Hydrofaction^{TM} , der muliggør produktion af vedvarende biobrændstoffer til den tunge transport sektor.

HTL bio-råolien er en vand i olie emulsion indeholdende 10-15 % vand og 3-4 % uorganiske salte. Demineralisering er et krav for at opretholde katalysatorens levetid og stabilitet i den efterfølgende opgradering. Filtrering, centrifugering og elektrocoalescense blev konkluderet ineffektive, da pH af emulsionsen skal reduceres for at opnå en komplet separation. En vaskeprocedure med anvendelse af en solvent og 0.1 M citronsyre blev udviklet til pilotskala, hvilket siden har resulteret i demineralisering af Hydrofaction^{TM} olie til <50 ppm metaller. En alternativ fremgangsmåde er også udviklet, hvor den CO_2 rige gas fra HTL processen anvendes i synergi som forsurende middel under separation og olievask. Metoderne bliver implementeret på HTL pilotanlægget i 2018 i form af et integreret separations- og demineraliseringssystem.

Et kontinuert multi-reaktor hydrogeneringsanlæg er blevet designet, bygget og idriftsat og arbejdet med opgradering af HTL olie avancerer state-of-the-art kva kontinuerte kampagner med op til 660 timers varighed. Gennem flere iterationer er der udviklet en 3-zoners proces, som kan opgradere Hydrofaction^{TM} olie til vedvarende transport brændstof med udbytter omkring 100 vol.%. På grund af iltindholdet i bio-råolien, var det et kritisk trin at konfigurere den første reaktions zone så reaktionshastigheder og eksoterm varmeafgivelse holdes på et håndterbart niveau.

Opgraderede olier er blevet destilleret og evalueret i forhold til gældende brændstof specifikationer, og opgraderingen forbedrer oliens volatilitet og brændstofkompatibilitet betydeligt. Dieselfraktionen udgør 50-60 % af den opgraderede olie og er af en kvalitet der kan iblandes diesel, muligvis opfylder den endog de gældende D975 diesel specifikationer. Ligeledes er benzin, flybrændstof og marine fraktionerne af en kvalitet der tillader væsentlig iblanding. Den tunge marine fraktion udgør et attraktivt lav-svovls produkt i relation til de seneste svovlrestriktioner for marine brændstoffer. Dermed har PhD projektet bidraget til udviklingen af Hydrofaction^{TM} , så teknologien omfatter hele processen fra træ til tank.

Part I

Extended Summary

Chapter 1

Introduction

1 Shortage of Transportation Fuel Alternatives

Decarbonisation of the long haul transportation sector has become the difficult piece of the puzzle regarding our climate, energy access and air quality goals. While passenger vehicles are expected to become electric, no renewable fuel alternatives exist in tangible volumes for road freight, aviation and marine. As a consequence, the global oil consumption will continue to rise. Solely due to increasing demands from the petrochemicals and long haul transportation sectors [18], which will remain at least partially dependent on liquid fuels.

The European Commission aims at implementing a framework that accelerates the share of advanced biofuels within the heavy transportation sector. A blending mandate or an obligation to reduce greenhouse gas (GHG) emissions from the fuel has been proposed [11]. Advanced biofuels are defined as sustainable fuels, providing significant GHG emissions reduction compared to fossil equivalents, and produced from non-food feedstocks mitigating ILUC effects. Conventional biofuels account for 4% of world road transport fuel production, while advanced biofuels represents 1% of the 4% [17]. In support of this and recognising that legislative framework is likely to improve the economic incentives, the short and long term market potential for advanced transportation biofuels is enormous.

Direct thermochemical biomass liquefaction processes such as pyrolysis and hydrothermal liquefaction (HTL) are emerging as potential resource effective, cost competitive pathways for production of advanced biofuels, fungible with fossil equivalents [7, 27]. Furthermore, projections of a commercial scale HTL plant [Paper A] indicate higher energy efficiency and lower well-

to-wheel GHG emissions as compared to pathways for bioethanol, biodiesel, hydrotreated vegetable oil (HVO), gas to liquid (GTL) fuel and conventional diesel [10].

HTL enables a feedstock flexible liquefaction of wet or dry, low-value, non-food biomass residues, thereby mitigating feedstock supply risks. Generally, the feedstock is diluted in an aqueous pumpable slurry at 10-30 wt.% dry matter and reacted at near-critical water conditions. More specific operating details depend on the particular HTL process. The main product is an oxygenated liquid biocrude intermediate that needs further refining to meet any liquid fuel specifications. On that basis, the research focus of the current PhD project is development of the process steps necessary to perform demineralisation and upgrading of HTL biocrude to advanced biofuel.

2 History of Hydrothermal Liquefaction

The history of HTL goes back about a century. To the best of knowledge, the first publications in this context were a number of patents by Doctor Carl Krauch from the 1920's on liquefaction of carbonaceous substances such as coals, distillation residues, heavy oils and wood in the presence of hydrogen [21]. Since then, interrelated fluctuations in political stability, oil prices and security of supply have dictated the amount of R&D conducted in the field of HTL. The oil crises of the 1970's sparked grand efforts by a number of groups, Shell (Netherlands), Bureau of Mines, Lawrence Berkeley Laboratory and Pacific Northwest Laboratory (USA), who are often referred to as the pioneers of HTL. Around 1980 the US based laboratories conducted early development work at a continuous 1-3 ton wood chips per day facility at Albany, Oregon. They tested among other things the effect of biomass pretreatment, oil recycling and co-processing with carbon monoxide and hydrogen [6, 9]. The first catalytic hydrotreatment studies with focus on gasoline production were also carried out with oil from the Albany facility [2, 8, 14]. In the same period, Shell developed the HTU® process and treated woody biomass in subcritical water for production of liquid fuels. Despite promising results, Shell discontinued development of the HTU® process in 1988, due to low crude oil prices around $10/barrel [31].

As a response to the increased focus on sustainability and demand for advanced biofuels, the number of publications, patents and commercial activities within HTL has increased notably the last two decades. For example R&D of Shell's HTU® process was reinitiated in 1996 by Biofuel B.V., who is currently in the phase of developing commercial projects [31]. A selection of additional major initiatives need mentioning in relation to the more recent

history of HTL.

The Catliq® process was developed from 1996 to 2010 in Denmark under the auspices of first F.L.S Miljø A/S (1996-2003) and later SCF Technologies A/S (2003-2010) with several employees from Steeper Energy in key roles. Several engineering studies of commercial plants were conducted both internally and with external partners [24], and five continuous pilot plants were built with feed slurry capacities ranging from a few $^{kg}/_{h}$ up to 250 $^{kg}/_{h}$ [19]. 40 different feedstocks were processed in about 500 unpublished test runs [19]. SCF Technologies A/S failed an emission on Copenhagen stock exchange in 2010, and suffered a controlled shut down in 2011, where the Catliq® pilot plant and intellectual property rights were sold to the Turkish company Altaca Enerji. Altaca Enerji focus on agricultural and municipal wastes as HTL feedstock, and the most recent news indicate that Altaca Enerji is currently building a 15 $^{ton}/_{h}$ demonstration plant in Gönen, Turkey [22, 30].

Changing World Technologies (CWT), founded in 1997, developed the thermal conversion process (TCP) and commissioned a large plant in Carthage, Missouri in 2003 on offal from a neighboring turkey processing plant [5]. Surprising and unlikely oil yield and quality figures are provided on CWT's website, claiming production volumes that, if converted to mass yields, are well above unity [5]. According to one of their patents [1], the turkey offal is heavily diluted (1:3) in used engine oil. Without being conclusive, this may possibly explain the high yields of very high quality oil. The 'commercial-scale' plant went bankrupt in 2009 due to odor complaints. The plant reopened in 2011 using a different feedstock and was acquired by Calgary based Ridgeline Energy Services in 2013 [15]. Information on the activity level since then has not been found.

Australian based Licella developed the subcritical Cat-HTR™ process from 2005-2007 and commissioned its first pilot plant in 2008 in Sommersby, Australia [23]. Licella is currently in the funding phase of a commercial-scale waste plastic to chemicals plant. The project is a joint venture with Armstrong Chemicals, Canada. Additionally, a €9 million Canadian cleantech grant was awarded to Canfor Pulp in Q1 2017 to pursue a commercial scale project with Licella's technology [23].

Genifuel Corporation, founded in 2006, arose from the extensive research within HTL carried out by Pacific Northwest Laboratory (PNNL). Genifuel has exclusive license to patents developed by PNNL, and are currently developing different demonstration scale projects on their hydrothermal processing (HTP) process [12, 25]. This includes planning of a €5-6 million pilot project on HTP of waste water solids from the Metro Vancouver, Canada. The

400 kg/h plant is to be commissioned late 2018 [3, 25].

Additional milestones in the history of HTL include commissioning of the 10-30 kg/h continuous bench scale (CBS1) unit at Aalborg University (AAU), Denmark in 2013; a similar pilot plant at Aarhus University, Denmark in 2015; and finally two pilot units (HPPS and MHTLS) designed by PNNL and Genifuel in 2015/2016 [4, 13].

3 Steeper Energy and Hydrofaction™

Steeper Energy ApS (now Steeper) was founded in 2011 with offices in Copenhagen and Aalborg, Denmark and in Calgary, Canada. Steeper's core business is development and commercialization of its proprietary Hydrofaction™ technology platform, rooted in the generic field of HTL. Steeper is both a technology provider and licensor as well as a project developer with a view to build, own and operate biomass-to-liquids facilities. Steeper is well on its way to advance the commercial adoption of Hydrofaction™ having had various significant potential users and licensees undertake deep due diligence as to the technology's performance and quality of bio-fuel production. To this end, the company announced a €50.6 million demonstration project with joint venture Silva Green Fuel on the 15th of December 2017 [28]. The demonstration project is a mid-step in the eventual development of a full-scale commercial facility processing some 225.000 dry tonnes of forestry residues per annum for production of diesel fuel at Tofte, Norway. The announcement is not only a milestone for Steeper but for commercial development and adoption of HTL in general.

Figure 1.1 provides a process flow diagram (PFD) of the Hydrofaction™ platform divided into a 1st HTL stage and a 2nd upgrading stage. HTL in a Hydrofaction™ context implies supercritical water conditions, use and recovery of homogenous alkali metal catalysts and recirculation of biocrude and water soluble organics. The 2nd stage represents hydrotreating and fractionation into advanced drop-in biofuels. Gaseous by-products from both stages are utilized to provide heat for the process. The above combination of features make Hydrofaction™ unique from other commercial HTL activities.

Hydrofaction™ is flexible in terms of feedstock, but currently Steeper's primary focus is on forestry residues, as it is the only source of residual biomass that is both relatively homogenous in composition and available in 'petrochemical volumes'. Besides, production of biofuels from forestry residues bridges a synergy between 1. a heavy transportation sector that needs to be decarbonised; 2. a forestry sector that needs to valorise their

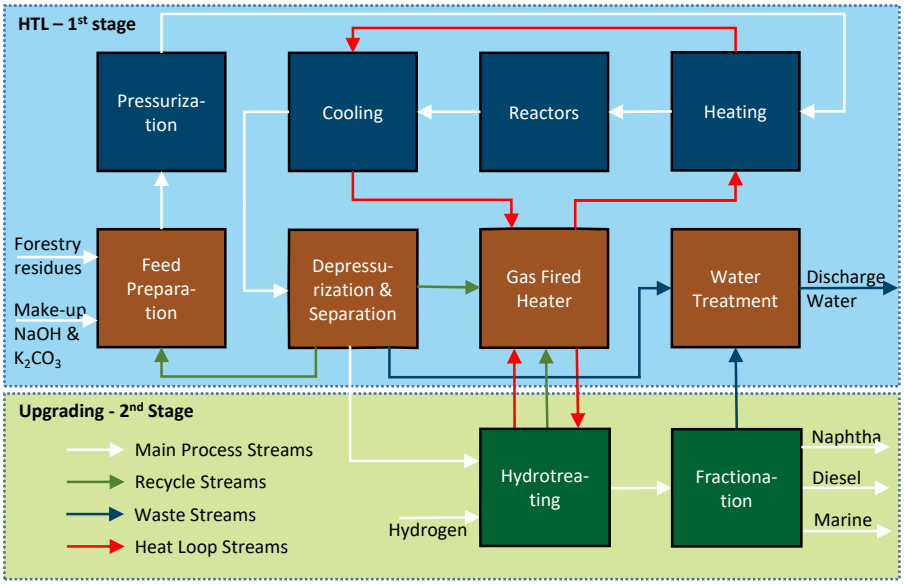

Fig. 1.1: Schematic of the Hydrofaction™ platform consisting of supercritical HTL stage and subsequent hydrotreating stage [Paper A].

waste streams, due to increased competition and reduced demand from the paper industry; 3. a resource that, when used efficiently, provides a GHG mitigation strategy according to the Kyoto protocol [26]. Forestry residues in a biofuel context are further described in the introduction of [Paper A].

3.1 IP of Steeper Energy

Steeper Energy pursues an active and offensive patent strategy addressing the whole value chain from raw material e.g. a tree in the forest to finished products and their use, when considering patent rights and opportunities. The current patent portfolio comprises more than 100 national patents and patents pending divided into 21 patent families of which the PhD candidate has co-invented 4 (Patent Applications G,H,I,L). The patented areas are complementary and range from the core process described below, over individual steps of the process, biocrude upgrading and controls. [29]

3.2 Steeper Energy & Aalborg University

The industrial/academic collaboration between Steeper and AAU started with approval of funding and building of the CBS1 unit. The unit that has been designed and operated by Steeper, has facilitated >1750 oil production hours since commissioning in Q2 2013. The CBS1 represents a centerpiece

in development of the Hydrofaction^{TM} technology, in experimental academic research by AAU and in the development of HTL in general.

HTL activities at AAU, managed by Professor Lasse Rosendahl, has accelerated notably during the last decade, and the facilities have improved from batch reactors and limited analysis capabilities to continuous HTL and hydrotreating units and a wide range of analytical instruments. This is at least partly the outcome of a fruitful and ongoing collaboration between Steeper and AAU, where knowledge sharing combine industrial and academic perspectives on HTL. A most recent product of the collaboration is the current industrial PhD project.

4 Thesis Objectives and Outline

The industrial PhD project is funded partly by Innovation Fund Denmark grant no. 4135-00126B and Steeper Energy ApS. The PhD candidate is enrolled at the Doctoral School of Engineering and Science at AAU.

4.1 Aims and Focus of Research

At initiation of the PhD project on 1st of January 2015, the Hydrofaction^{TM} upgrading approach was undefined and the amount of experimental upgrading work carried out on Hydrofaction^{TM} oil was limited to that of former PhD fellow Jessica Hoffmann [16] and in-house graduate student projects by the PhD candidate [20]. Thus formulation of an upgrading technology pose a major research objective. Further, the preferred HTL operating conditions were not yet fully defined for Hydrofaction^{TM} at initiation of the project, nor an effective product separation approach. Thus, the research focus also includes variations in feedstock composition, operating conditions, product separation and their effect on biocrude quality and upgradability. On that basis, the overall research objective has been to design an integrated separation and upgrading platform for the Hydrofaction^{TM} technology in order to bring the Hydrofaction^{TM} products to a quality that enables transport biofuel market penetration.

The major focus areas of the project are indicated with magnifying glasses in the modified PFD of Hydrofaction^{TM} in Figure 1.2. The capital letters are given to indicate focus of the publications, e.g. Paper A focuses on both HTL conversion and hydrotreating results.

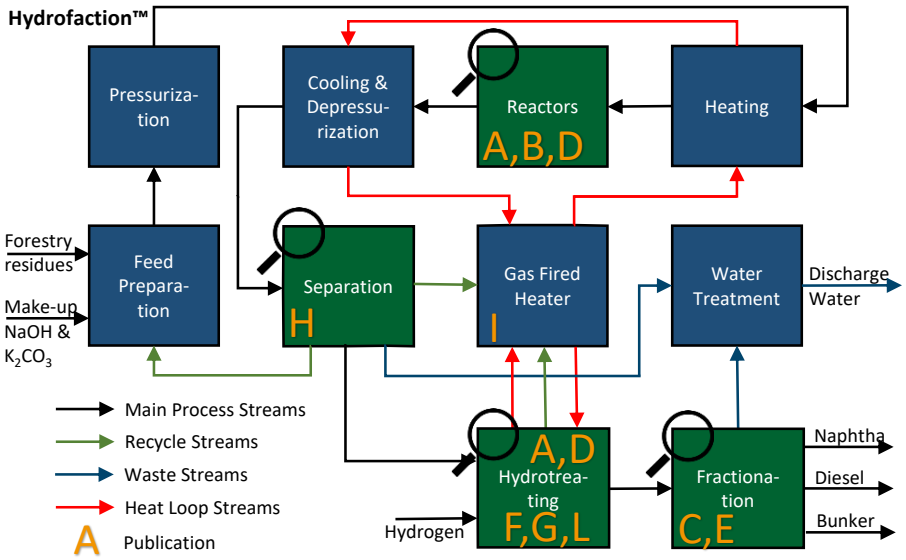

Fig. 1.2: A modified PFD of the Hydrofaction^{TM} platform to indicate and divide research focus and publications between the different stages of Hydrofaction^{TM} .

4.2 Reading guidelines

The thesis is divided into three parts. *Part 1, Extended Summary* sets the scene with background knowledge on the competitive landscape of HTL and fundamentals of HTL and Hydrofaction^{TM} in particular. Those of the experimental findings that have been published are briefly summarized, while a selection of unpublished findings will be described in more detail. Part 1 is structured in 5 chapters as described below. References are listed at the end of each chapter. *Part 2, Appendices* provide documentation of a continuous hydrotreater that has been designed, build and commissioned as part of the project. *Part 3, Publications* contains the project outcome in terms of publications. Patent applications are only appended by title for proprietary reasons.

Chapter 1 introduces the context and research objectives of the project.

Chapter 2 describes Hydrofaction^{TM} in a HTL context and presents selected experimental results on continuous HTL, fractionation of HTL oils and analytical characterization of Hydrofaction^{TM} biocrude. It defines the interphase between the HTL process and the separation and upgrading platform that is to be designed.

Chapter 3 focus on development of a product separation and demineral-

isation technique for the Hydrofaction^{TM} platform. The content include a description of potential demineralization techniques, experimental tests and a final process design for implementation at the CBS1 pilot.

Chapter 4 summarise the work conducted on hydrotreating, including parametric screening studies, design and commisioning of a multi-reactor continuous hydrotreater and unpublished results from the latter.

Chapter 5 presents fractionation results of upgraded Hydrofaction^{TM} oils and evaluate the physiochemical properties of the various fractions against relevant fuel specifications.

Finally, the PhD project is condensed to conclusive remarks in the *Conclusions*.

4.3 Main contributions

The main contributions of this research are:

- Contributions to the pilot oil production facility, CBS1 include standardization of operating and data logging protocols. The effect of various start-up oils on operating stability and final oil quality has been evaluated and a preferred start-up oil selected. Finally, the effect of operating pressure is sought explained in Paper B and the operating pressure of the pilot has been adapted to the findings of that study. All contributing to improved operation and providing basis for Papers A,B,D.
- The effect of a nitrogenuous alkaline agent (NH_3) versus NaOH on continuous HTL of wood and biocrude upgrading is published in Paper D with focus on product distribution, quality and biocrude upgradability. The paper also touches on the scalability between microbatch and continuous reaction systems, the effect oxygen has on biocrude volatility and novel Py-GCxGC-MS of products before and after upgrading.
- Development and test of a demineralization by washing technique that can reduce the inorganics content of the Hydrofaction^{TM} oil before fixed bed hydrotreating. The technique is currently standard procedure during Hydrofaction^{TM} at the pilot facility. The technique is claimed in Patent Application H.
- Development and test of an integrated product separation & demineralization process, where the CO_2 rich HTL product gas is applied in synergy to improve phase separation efficiency and as acidifying agent during subsequent demineralization. The process is claimed in Patent Application H.

- An integrated, continuous separation and demineralization platform based on the above contributions has been designed for the CBS1 pilot, parts have been acquired/manufactured, and the system will be commissioned ultimo Q3 2018.
- Results from hydrotreating of Hydrofaction^{TM} oil evolve from parametric and catalyst screening in microbatch reactors (80+ experiments in doubles) to focus on operability and catalyst stability in continuous hydrotreating systems. Selected upgrading results are published in Papers A, C, D, F, G and L.
- Design, acquirement, assembling and commissioning of a multi-reaction zone hydrotreating unit at AAU constituted most of the workload during Q1 2017 to Q3 2017. 5 experimental campaigns with up to 470 hours on stream (HoS) contributed to development of a 3-Zone upgrading process, proving hydrotreating of Hydrofaction^{TM} oil to advanced drop-in fuel at volumetric yields around 100%.
- Fractional distillation of Hydrofaction^{TM} oils, academic oils and upgraded oils provide basis for characterization of the different fractions, comparison with fuel specifications and blending studies targeting diesel fuel and marine bunker. Selected fractionation results are applied in Papers C, D and E. Recent yet unpublished results show that hydrotreated Hydrofaction^{TM} oil has been produced with sufficient quality to enable drop-in as diesel, jet, gasoline and/or marine fuel blendstock. The diesel fraction produced in present work may even prove to meet the D975 diesel specification.

References

[1] T. N. Adams, B. S. Appel, C. T. Einfeldt, and J. H. Freiss, "Depolymerization process of conversion of organic and non-organic waste materials into useful products," Aug. 10 2010, US Patent 7771699.

[2] E. G. Baker and D. C. Elliott, "Catalytic hydrotreating of biomass-derived oils," https://web.anl.gov/PCS/acsfuel/preprint%20archive/Files/32_2_DENVER_04-87_0257.pdf, Pacific Northwest Lab., Richland, WA (USA), Tech. Rep., 1988.

[3] S. Bauer, J. Oyler, D. Bradley, and C. Capuco, "Fuel from sewage is the future – and it's closer than you think," https://www.pnnl.gov/news/release.aspx?id=4317, 2016, accessed: 18-12-17.

[4] J. Billing, D. Anderson, R. Hallen, T. Hart, G. Maupin, A. Schmidt, and D. Elliott, "Design, Fabrication, and Testing of the Modular Hydrothermal Liquefaction System (MHTLS)," https://projects.ncsu.edu/mckimmon/cpe/opd/tcs2016/pdf/oral/Session3.3_5-Billing.pdf, 2016, accessed: 29-09-17.

[5] Changing World Technologies, "Feedstock types," http://www.changingworldtech.com/index.html, 2017, accessed: 05-12-17.

[6] H. Davis, C. Figueroa, and L. Schaleger, "Hydrogen or carbon monoxide in the liquefaction of biomass," Lawrence Berkeley Lab., CA (USA), Tech. Rep., 1982.

[7] S. De Jong, R. Hoefnagels, A. Faaij, R. Slade, R. Mawhood, and M. Junginger, "The feasibility of short-term production strategies for renewable jet fuels - a comprehensive techno-economic comparison," *Biofuels, Bioproducts and Biorefining*, vol. 9, no. 6, pp. 778–800, 2015.

[8] D. Elliott and E. Baker, "Catalytic hydrotreating of biomass liquefaction products to produce hydrocarbon fuels: Interim report," https://www.osti.gov/scitech/servlets/purl/6912635, Pacific Northwest Lab., Richland, WA (USA), Tech. Rep., 1986.

[9] D. C. Elliott, "Process development for biomass liquefaction," *Am. Chem. Soc., Div. Fuel Chem., Prepr.;(United States)*, vol. 25, no. CONF-800814-P3, 1980.

[10] European Commission, "State of the art on alternative fuels transport systems in the european union, final report," Tech. Rep., 2015.

[11] European Commission, "Communication from the commission to the european parliament, the council, the european economic and social committee and the committee of the regions - a european strategy for low-emission mobility, swd/2016/0244 final," Tech. Rep., 2016.

[12] Genifuel, "News," http://www.genifuel.com/news.html, 2017, accessed: 05-12-17.

[13] Genifuel Corporation, "Genifuel corporation closeout report for NAABB program, DE-FOA-0000123," https://energy.gov/sites/prod/files/2016/01/f28/naabb_genifuel_pilot_system_final_report.pdf, 2015, accessed: 29-09-17.

[14] B. Gevert, P. Andersson, S. Jaeras, and S. Sandqvist, "Hydroprocessing of desalted directly liquefied biomass," *Prepr. Pap., Am. Chem. Soc., Div. Fuel Chem. (United States)*, vol. 33, no. CONF-8809228, 1988.

[15] J. Hacker, "Canadian firm acquires Carthage RES plant," http://www.carthagepress.com/article/20130416/NEWS/130419181, 2013, accessed: 14-01-18.

[16] J. Hoffmann, "Bio-oil production - process optimization and product quality, PhD Thesis," http://vbn.aau.dk/files/202396082/jessica_hoffmann.pdf, Department of Energy Technology, Aalborg University, Tech. Rep., 2014.

[17] International Energy Agency, "Technology roadmap - delivering sustainable bioenergy," OECD/IEA, Tech. Rep., 2017.

[18] International Energy Agency, "World energy outlook 2017, executive summary," OECD/IEA, Tech. Rep., 2017.

[19] S. B. Iversen, "Personal communication," 2018, accessed: 13-01-18.

[20] C. U. Jensen and K. M. Rasmussen, "Co-processing Bio-crude at Petroleum Refineries: Fractional distillation and deoxygenation of HTL bio-crude to evaluate the potential as co-processing feed, Master Thesis,"

http://projekter.aau.dk/projekter/files/198489791/Co_processing_Bio_crude_at_Petroleum_Refineries.pdf, Department of Energy Technology, Aalborg University, Tech. Rep., 2014.

[21] C. Krauch and M. Pier, "Conversion of solid fuels and products derived therefrom or other carbonaceous materials into valuable products," Feb. 6 1926, US Patent 1890434.

[22] J. Lane, "4 minutes with... Taner Onoglu, Vice President, Altaca Energy," http://www.biofuelsdigest.com/bdigest/2015/06/04/4-minutes-with-taner-onoglu-vice-president-altaca-energy/, 2015, accessed: 14-01-18.

[23] Licella Pty Ltd, "Licella.com.au - Latest News," http://www.licella.com.au/latest-news/, 2017, accessed: 05-12-17.

[24] M. Nielsen, "Final eudp project report: Demonstration of sustainable biooil production using catliq technology - phase 1." https://energiforskning.dk/sites/energiteknologi.dk/files/slutrapporter/final_report_-_journal_no_64010-0067.pdf, SCF Technologies A/S, Tech. Rep., 2010.

[25] J. Oyler, "Hydrothermal processing in wastewater treatment, overview and update," http://www.genifuel.com/text/20170712%20Genifuel%20Presentation%20for%20IR2%20Forum.pptx, 2017, accessed: 14-01-18.

[26] P. Ramachandran Nair, B. Mohan Kumar, and V. D. Nair, "Agroforestry as a strategy for carbon sequestration," *Journal of plant nutrition and soil science*, vol. 172, no. 1, pp. 10–23, 2009.

[27] L. Rosendahl, *Direct Thermochemical Liquefaction for Energy Applications*. Woodhead Publishing, 2018, ISBN: 978-0-08-101029-7.

[28] Steeper Energy, "Steeper energy announces eur 50.6 m (dkk 377 m) advanced biofuel project with norwegian-swedish joint venture silva green fuel in licensing deal," http://steeperenergy.com/media/, 2017, accessed: 15-12-17.

[29] Steeper Energy, "Steeper energy intellectual property rights," 2018, internal document.

[30] M. Unsal, H. Livatyali, P. Aksoy, S. Gul, and A. Onoglu, "Catliq catalytic hydrothermal liquefaction process from pilot scale to demo scale, conference proceedings," https://www.omicsonline.org/2090-4541/2090-4541.S1.002_023.pdf, 2015, accessed: 14-01-18.

[31] W. P. van Swaaij, S. R. Kersten, and W. Palz, *Biomass power for the world*, Vienna ed. Pan Stanford Publishing, 2015, ISBN: 978-981-4669-24-5.

Chapter 2

Hydrofaction^{TM} HTL

HTL is the core process during Hydrofaction^{TM} from tree to tank. The quality of the HTL oil intermediate defines how much further it has to be upgraded to meet drop-in fuel specifications. Thus, tuning of the HTL process to balance oil yield, quality and upgradability may improve the starting point of the downstream processes. Additionally, knowledge on how HTL modifications will impact demineralization and upgrading, significantly improves the chances of designing a robust separation and upgrading platform. With this reasoning, Figure 2.1 summarises the steps covered as part of the PhD project towards understanding and tuning of the HTL stage. The learning curve has included a lot of hands-on tasks including pilot operation and product analysis to evaluate the effect of operating conditions and feedstock variations. This chapter will briefly summarise the fundamentals of the liquefaction part of Hydrofaction^{TM} ; introduce intellectual property (IP) on competing HTL technologies; and finally summarize selected findings of experimental work on HTL.

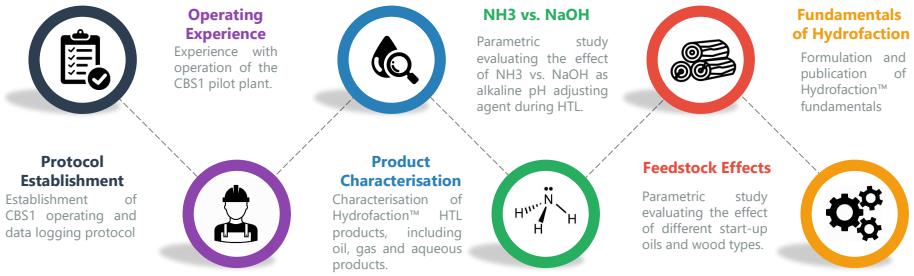

Fig. 2.1: A summary of the HTL related tasks covered as part of the PhD project.

1 Fundamentals of Hydrofaction^{TM} HTL

A phase diagram of water is given in Figure 2.2 to show the 'conventional' subcritical HTL regime and the fact that Hydrofaction^{TM} operates in the supercritial regime above pseudo-critial pressures (300–350 bar & 390-420 °C). The pseudo critical line (PCL) is somewhat a continuation of the saturation pressure curve into the supercritical regime, because the properties of supercritical water change rapidly from liquid-like to steam-like, when crossing the PCL from left to right in Figure 2.2. On the other hand, the PCL has nothing to do with phase change, and pseudo-critical pressure should not be confused with saturation pressure, as only one phase exists in the supercritical regime. None of the competing HTL technologies mentioned later in Section 2 operate at pressures above 300 bar [1, 2, 4, 7, 11, 13, 15, 16]. In fact most operate at subcritical temperatures and pressures below 260 bar. Similarly, most open literatue from academia operates subcritically, except from Professor Rosendahls group at Aalborg University.

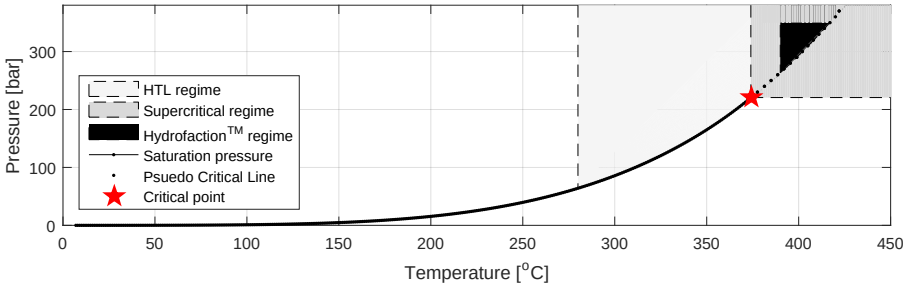

Fig. 2.2: Phase diagram of water to visualize the different operating regimes. [Paper B]

Paper B describes the reasoning behind the supercritical operating conditions of Hydrofaction^{TM} and argues for a number of benefits including improved reaction kinetics of certain desirable reaction mechanisms. Details will not be repeated here, but a different perspective on what is believed to be a major misconception can be emphasized again. The following differentiation for the ionic product of water: ionic reactions>10^{-14}>radical reactions is often used to determine what type of reactions are favored in a near-critical water reaction medium. Supercritical water is often being associated with radical reactions used in gasification type reactions, while subcritical water is believed to be required for ionic type reactions, which are desirable during HTL. However, as given in Figure 2.3, the ionic product of water is a direct function of density and only indirectly of pressure and temperature. Consequently, water can have the same ionic product at sub- and supercritical temperatures if the density is kept constant. Similarly, the dielectric constant, another important property of water in relation to HTL, is a direct function

of density. Figure 2.3 emphasizes that by operating above the saturation or pseudo-critical pressure the ionic product for water will always be above 10^{-14}. This explains why the relatively high temperature of Hydrofaction^{TM} is combined with a pressure above the pseudo critical pressure.

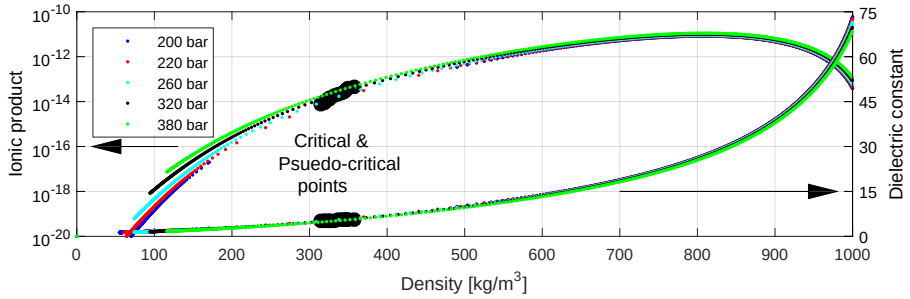

Fig. 2.3: Ionic product and dielectric constant of water as function of density for different isobars. [Paper B]

Besides the supercritical operating conditions, the technology applies the following list of additional features, and the motivations behind are described from a theoretical perspective in Paper B.

- Operation above the critical point of water at relatively high pressures (300-350 bar) and temperatures (390-420 °C);
- Recirculation of produced organic compounds in the form of water-soluble organics and oil for improved feed characteristics, improved energy balance, desired chemical kinetics and improved oil yields;
- Use of homogeneous catalyst in the form of potassium carbonate (K_2CO_3) for desired catalytic effects;
- Control of pH to alkaline conditions for desired catalytic effects and minimization of corrosion;
- Recovery and recycling of homogeneous catalysts for improved process economics;
- Self-sustained with process heat when in steady state.

Paper A provides a more practical description of the HTL part of Hydrofaction^{TM} and on the configuration of the different operations given as PFD blocks in Figure 1.1.

2 IP of Competing HTL Technologies

Development of the HTL technology for production of renewable liquid transportation fuels has been underway for almost a century, yet no commercial scale production facilities have been built. Though, a substantial amount of IP in the field of HTL has been developed by different organisations, and a selection is introduced in the following.

Biofuel B.V. continued the development of Shell's HTU® process and have updated IP accordingly. The broadest form of their patent [15] does not have an upper reaction temperature limit, though it has a pressure range of 100-250 bar, which in turn adds a temperature limit below 400 °C due to the undesirable properties of supercritical water when crossing the PCL (Figure 2.2).

The HTU® process does not apply alkali metal catalysts to shift the equilibrium of the water gas shift and reforming reactions. This is clear from high CO concentrations in the gas compositions reported in [15, 16]. Finally, it is characteristic to the HTU® process to run slightly acidic with aqueous phase pH of 4-5 [16]. The aqueous product is separated off and a substantial amount is recycled to the feed at elevated temperature, which heats the feed mixture to pulping temperature. The pulping, carried out at 100-250 bar and 180-280 °C, depolymerises the macrostructures of the biomass, making it a more homogenous and pumpable slurry.

Combustion of byproducts in a furnace supplies heat to a hot oil heat transfer medium, which is distributed in various heat exchangers. This is similar to the preferred Hydrofaction™ technique [Paper I]. Note, they observed a heat transfer coefficient for the biomass paste, which was half relative to water [16].

Licella Pty Ltd are located in Australia. Unique for Licella's Cat-HTR™ technology is the use of an aqueous solvent, often methanol or ethanol in a concentration between 1-30 wt.%. The organic matter feedstock is mixed with the aqueous solvent and processed subcritically at 260-350 °C and 80-260 bar according to the US patent [7]. The European patent span up to supercritical conditions, 250-400 °C and 100-300 bar [11]. Their US patent indicate that the hemicellulose fraction is extracted using a solvent before liquefaction [7]. Their European patent claim that at least one base catalyst is added in an aqueous solution after heating the feed slurry to operating temperature and pressure. This base catalyst is claimed to be a transition- or alkali metal salt catalyst [11].

A recent patent application from Licella mentions a selectable capillary system as the preferred pressure reduction methodology [6]. This is similar to the technique used in the CBS1. The same patent application claims that problems related to increasing pressure drops across the reaction zone of a liquefaction reactor is removed by co-processing the organic matter feedstock with a solid substrate that can be either carbonaceous such as coal, lignite, char etc. or non-carbonaceous such as ash, metal oxide, insoluble metals salts etc. A similar approach was mentioned to avoid carbon deposition in the early patent by Dr. Krauch in 1926 [9].

ExxonMobil has a granted patent [13] claiming both sub- and supercritical liquefaction of a broad range of feedstocks including lignocellulosic residues, algae etc. They claim the right to recycle a portion of the aqueous product including water soluble organics, and to add an organic solvent to the feed, which can, but does not have to be an alcohol, a phenol or a carboxylic acid. This is all similar to Hydrofaction^{TM} conditions, but the ExxonMobil patent is unique by contacting the feed with carbon monoxide at a partial pressure of 50 to 100 bar during reaction, similar to the early studies by [5].

The Catliq® process was developed in Denmark by SCF Technologies A/S and currently owned by Turkish Altaca Enerji. The process operates at about 250 bar and temperatures just below the critical temperature of water. Further, Catliq® uses a combination of homogeneous and heterogeneous catalysts as well as a recirculation loop with trim heating to ensure almost instantaneous heat up in the last part of the process [8].

Changing World Technologies developed the thermal conversion process (TCP) and has a few granted patents on different feedstocks including shredder residues, offal, animal manures, sewadge sludge etc. Unique for the TCP patents is that they all include a separation of solids (bones, metals etc.) during pretreatment. Operating conditions vary between 220-400 °C and pressure above the saturation pressure of water.

Muradel Pty Ltd. is an Australian based company in the field of HTL. Regarding IP no granted patents were found, but a patent application [4] comprising HTL of algae with the possibility of co-processing an algae feedstock with a carbonaceous material such as biosolids, manure, coal etc. The HTL conditions are subcritical (250-350 °C and 40-200 bar) and with a solids loading of maximum 20 % w/v [4]. Muradel is operating a liquefaction facility with a process capacity of 3 ton per day [10]. Feedstock at this facility is both algae, sewadge sludge and biosolids. A relatively long double pipe con-

figuration represents a combined heat exchanger and plug flow reactor [10].

Genifuel Corporation & PNNL The PNNL group was among the pioneers on HTL of woody biomass and have published extensively in the field, recently focusing on algae and waste water streams as HTL feedstock. The PNNL and Genifuel HTP technology is characterised by subcritical operating conditions, a variety of feedstocks and it relies on catalytic hydrothermal gasification as the water treatment technology.

3 Pilot Results and Product Analysis

The CBS1 pilot facility was commissioned Q1 2013 and has been a centerpiece in the development of the Hydrofaction^{TM} platform with more than 1750 oil production hours. It is a semi-continuous plant, where 100 kg slurry batches are prepared and processed continuously at a flow rate around 20 kg/h. Figure 2.4 illustrates a PFD of the CBS1, and Paper B provides a detailed experimental procedure on how Hydrofaction^{TM} oils are produced at the CBS1. Note how liquid products are manually separated at ambient conditions by gravimetric separation. The wood content of the slurries are 17-20 wt.% on a dry ash free basis, but a slurry loading of 25 wt.% was achieved by alkaline pulping as pretreatment prior to slurry preparation [Paper K].

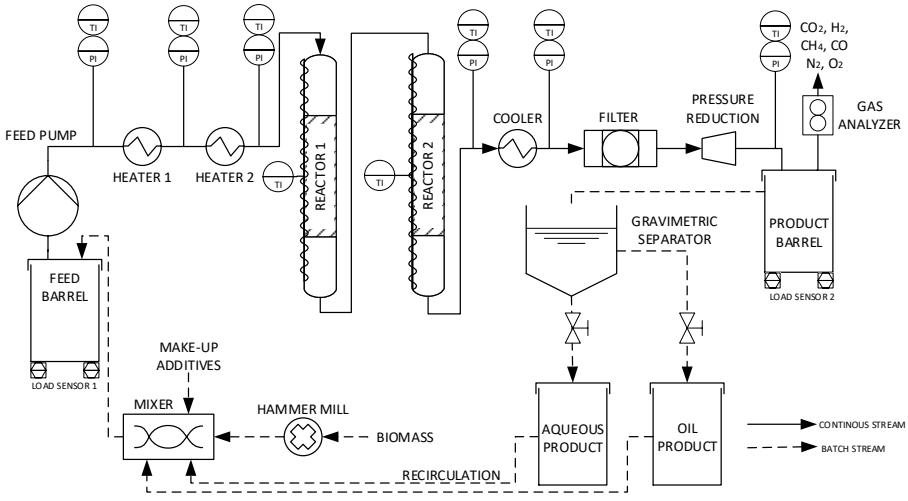

Fig. 2.4: Process flow diagram of the Pilot. [Paper B]

3.1 Recirculation of Oil and Aqueous Products

Recirculation of aqueous and oil products is characteristic to Hydrofaction^{TM} . This is demonstrated in the CBS1 by using tall oil as start-up oil and recycling the products 4-6 cycles until the start-up oil is diluted sufficiently to reflect steady state operation. Figure 2.5 illustrate experimental data from Paper B on variation of oil and aqueous product characteristics as function of recirculation cycle. The water content of the oil approaches a stable level around 10-15 wt.% after 4 recirculation cycles, while the ash content is relatively stable around 3-4 wt.%. Note in particular the ash content that is several orders of magnitude higher than what can be allowed in relation to catalytic hydrotreating, thus requiring a demineralisation step before further upgrading.

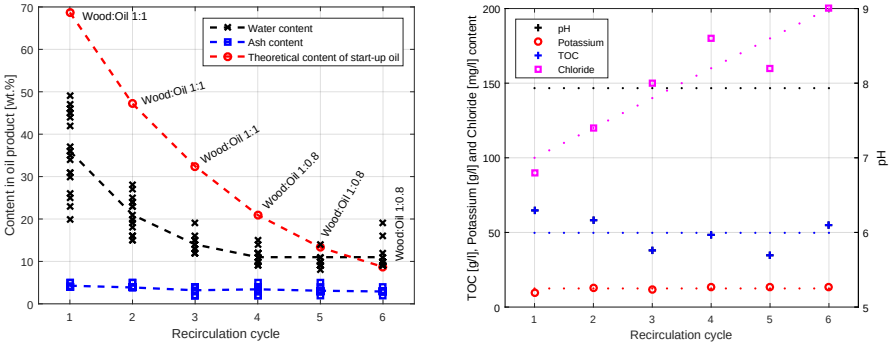

Fig. 2.5: Right) Water content, ash content and theoretical start-up oil content in oil product as function of recirculation cycle. The content of start-up oil is calculated based on the wood to oil ratio in the slurry, the wood to oil yield and a conservative assumption that the start-up oil does not convert. Left) Average values for pH and concentration of potassium, TOC and chloride in aqueous product as function of recirculation cycle. [Paper B]

The analysis given of the aqueous phase in Figure 2.5 indicate stable potassium and pH levels, but an increasing chloride level. While the former are being controlled by addition of make-up K_2CO_3 and NaOH during feed preparation, the latter is increasing when aqueous products are recycled and additional chloride is added through the biomass. In an up-scaled design with continuous water recirculation, there will be purge of a chloride rich concentrate to avoid build-up of wood impurities such as chloride. Finally, the relatively stable total organic carbon (TOC) content of Figure 2.5 indicate no net production of water soluble organics. This results in more carbon being directed to the oil phase, which in turn increases the oil yield and carbon efficiency.

A study on the effect of wood type and start-up oil on final oil quality was conducted and published in Paper A. Crude tall oil (CTO) and distilled tall oil (DTO) was each used as start-up oil in 3 different campaigns with 4-6 recirculation cycles. Table 2.1 lists the resulting oil quality and it is evident that both the type of wood and start-up oil have negligible impact on the final oil quality. The simulated distillation profiles of the 6 oils are also very similar, despite the very different volatility of the two start-up oils [Paper A]. As a result, Table 2.1 provides a good baseline for the oil quality that can be expected from Hydrofaction^{TM} .

Oil	Cycle	Start-up oil	Wood	Visc. [a][cP]	HHV[b] [MJ/kg]	MCR[b,c] [wt.%]	C[b] [wt.%]	H[b] [wt.%]	N[b] [ppm]	S[b] [ppm]	O[d] [wt.%]	H/C [-]
A	6	CTO	P/S	17360	38.6	21.0	81.4	8.6	1124	100	9.8	1.26
B	4	CTO	P/S	714	38.0	16.4	80.4	9.0	822	195	10.4	1.34
C	5	CTO	Bi	813	38.0	15.6	80.8	9.1	2635	215	9.8	1.34
D	5	DTO	Bi	2084	37.7	18.6	80.2	9.2	2201	159	10.4	1.37
E	5	DTO	P/S	3313	37.2	19.7	80.0	9.0	1447	104	10.9	1.34
F	5	DTO	Ba/P/S	1954	37.9	18.1	81.4	9.7	973	100	8.8	1.42

[a] Viscosity at 40 °C [b] on dry basis [c] Micro Carbon Residue (ASTM D4530) [d] Oxygen by difference

Table 2.1: Physio-chemical properties of renewable crude oils produced by Hydrofaction^{TM} of various wood types (P/S=Pine/Spruce, Bi=Birch, Ba/P/S=10 wt.% bark in P/S) using different start-up oils. The initial boiling point (IBP) to 140 °C fraction (now lights) was lost during production of Oil A, which affected viscosity, MCR and H/C ratio. [Paper A]

3.2 Effect of Nitrogenous Alkaline Agent

A CBS1 campaign with 4 recirculation cycles was conducted to test the use of ammonia instead of sodium hydroxide as homogenous pH adjusting agent. The motivation was that ammonia is cheaper, it may have a hydrogen donating effect during reaction, and it is a non-metal which reduces the ash content of the oil, making it easier to demineralize before upgrading.

The study that is published as Paper D evaluated the effect of NH_3 versus NaOH both during HTL and subsequent upgrading. In line with the hypothesis, ammonia was observed to improve the molar hydrogen to carbon (H/C) ratio of the resulting product and reduce the ash content of the oil to 1-2 wt.%. On the other hand, operating difficulties such as increasing pressure drops and lack of mass balance closure, were encountered during the experiments using ammonia as catalyst. Microbatch experiments were conducted to investigate this observation further, and a very high yield of carbonacous solids were formed in the presence of NH_3. The coke formation was 11.1 wt.% and 1.8 wt.%, when using NH_3 and NaOH respectively. This explains the operating difficulties that were characteristic to the continuous ammonia runs. Moreover, the introduction of a nitrogenous catalyst polluted the biocrude with 2.7 wt.% nitrogen. Various substituted pyrrole and

pyrazine structures were identified by GC-MS in the volatile fraction of the NH_3 oil. Subsequent hydrotreating was less successful for the NH_3 oil compared to that produced using NaOH, and nitrogen is likely to be the inhibitor.

As a result, potential use of ammonia was discarded based on both nitrogen pollution of the oil and the coke formation during HTL. These findings are relevant to consider in relation to HTL of other nitrogenous feedstocks such as algae, manure and sewadge sludge, where the nitrogen content of the oil is also known to be relatively high.

3.3 Fractional Distillation of HTL Oils

Fractional distillation enables detailed analysis of the different distillate cuts and evaluation of their potential as drop-in fuels. Numerous distillations of liquefaction oils have been carried out during the PhD project, but only published data will be discussed here. The distillation presented in Paper E was of one of the first oils produced at the CBS1, and it was only subjected to 2 oil recirculation cycles. As mentioned previously, it was later found that at least 4 recirculation cycles are needed to reflect steady state quality, and thus this oil is left out of the following summary.

Figure 2.6 depicts an example of the 'green liquids' obtained from fractionation of wood derived HTL oil. The picture on the right shows how the distillates that are rather clear upon distillation, quickly change to red and dark colors when exposed to air. This is a consequence of minor concentrations of nitrogen, phenolics and/or active hydrocarbon color precursors such as olefins.

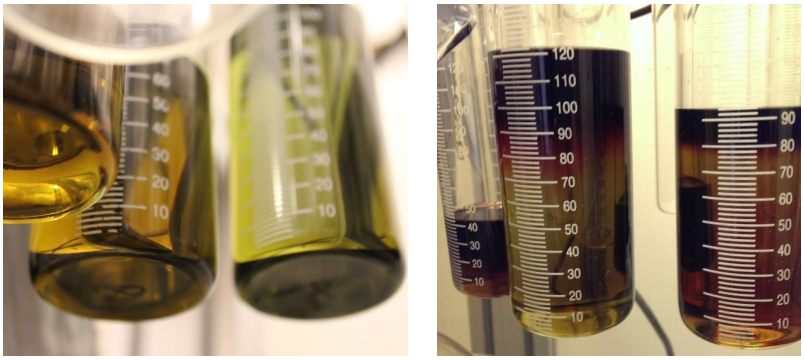

Fig. 2.6: Distillates from fractionation of liquefaction oil change color from clear/green to red/dark when exposed to air.

Table 2.2 lists selected physio-chemical properties of three different lique-

faction oils and their respective fractions obtained from 15-theoretical plate fractional distillation following ASTM D2892. The so-called HDO0 oil reflect standard Hydrofaction^{TM} oil quality. In comparison the oils produced in the presence of ammonia [Paper D] or glycerol [Paper C and J] contain more oxygen and nitrogen, respectively. Both oils have also been observed to be more resistant towards upgrading. The amount of +350 °C residue is generally high for the wood derived HTL oils and relative to petroleum crudes, they are indeed very heavy and of low quality in a fuel context. Meanwhile, it is important to acknowledge oxygen's effect on biocrude volatility, in order not to underestimate the fuel potential of HTL biocrude. Deoxygenation by mild hydrotreating has been shown to reduce the distillation profile roughly 100 °C in average [Paper D]. Thereby, distillation quality of the oil shifts from a heavy and troublesome crude, to one having a larger diesel fraction than the benchmark Brent crude oil. This emphasizes the need and potential value-add of further upgrading.

	Cut [°C]	Yield [wt.%]	Acc. Yield [wt.%]	Density [kg/m3]	HHV, DB [MJ/kg]	TAN [mg KOH/g]	Elemental comp. [wt.%] C	H	N	O	H/C [-]
HDO0[a]	-	-	-	1051	37.6	55.7	81.4	8.5	0.1	10.1	1.25
F1	IBP-180	3.9%	3.9%	842	41.3	6.02	80.5	11.9	-	7.6	1.76
F2	180-260	11.6%	15.5%	943	39.0	3.75	80.3	10.3	-	9.4	1.53
F3	260-344	21.1%	36.6%	1024	37.8	8.15	82.3	9.5	-	8.2	1.38
Residue	344+	62.5%	99.0%	1154	37.5	-	84.8	8.0	-	7.2	1.12
HDN0[a]	-	-	-	1036	38.6	33.6	79.8	9.3	2.7	8.2	1.39
F1	IBP-180	6.9%	6.9%	857	37.6	0.4	66.2	9.3	2.6	21.9	1.67
F2	180-260	6.0%	12.9%	945	39.0	6.7	78.3	10.6	1.2	9.9	1.61
F3	260-375	25.5%	38.4%	1009	39.1	21.8	81.7	10.1	0.1	8.0	1.48
Residue	375+	56.8%	95.2%	1093	37.8	-	82.2	8.4	2.1	7.4	1.22
C3BO oil[b]	-	-	-	1091	34.3	50.0	76.4	8.4	-	15.2	1.31
F1	IBP-200	12.0%	12.0%	925	35.5	19.2	74.1	11.9	-	14.0	1.92
F2	200-250	6.0%	18.0%	978	37.1	14.0	78.8	10.5	-	10.7	1.59
F3	250-350	25.6%	43.6%	1074	34.6	48.3	75.3	9.1	-	15.6	1.44
Residue	350+	51.8%	95.4%	1135	35.2	-	81.0	6.3	-	12.8	0.92

[a] Paper D [b] Paper C

Table 2.2: Selected physio-chemical properties of different liquefaction oils produced at the CBS1 and their corresponding boiling point fractions.

Figure 2.7 depicts selected properties from Table 2.2 as function of true boiling point (TBP), and three general conclusions can be drawn. Firstly, Figure 2.7 shows that the H/C ratio decreases as function of boiling point, and that the H/C ratio and density indicate a significant amount of aromatic and napthenic hydrocarbons in the middle distillates and heavies. Secondly, oxygenated compounds are distributed rather evenly (by mass) throughout the different boiling fractions, resulting in elevated densities, reduced heating values and low compatibility with commodity fuels in general. As a consequence, the biooil cannot be purified by distillation to obtain any straight run fractions with no or little oxygen, which is different from petroleum crudes, for which it is characteristic that the concentration of heteroatoms (N,S,O) increase with boiling point. Lastly, Figure 2.7 shows an increasing total acid

number (TAN) with TBP, indicating that acids groups are mostly positioned on high molecular weight compounds.

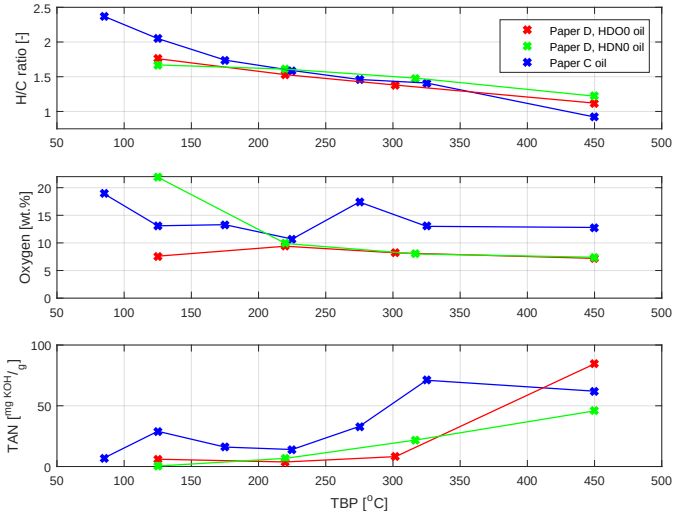

Fig. 2.7: H/C ratio, oxygen content and TAN as function of TBP for the liquefaction oils presented in Table 2.2.

Liquid Fuel Potential of Liquefaction Oil

The incompatibility of liquefaction oil distillates as drop-in fuels is a major conclusion as well as prerequisite for the need of upgrading. Acidity, density, aromaticity and heteroatom distribution make the middle distillates far from suitable as diesel fuel. Further, the polarity of such oxygenated product reduce its solubility with commodity fuels, and it makes the fuel susceptible to water uptake. Blending with fossil streams could potentially introduce the liquefaction distillates in low concentrations. Though, the HTL distillates does not excel with any desirable blend properties and would have to be sold at a low price, unless there is a 'green premium'.

The possibility of using the liquefaction oil residue fraction as a low-sulphur bunker fuel blendstock have been tested during the PhD project. The idea came during participation of a bunker blending course in Singapore. Low sulphur bunker fuels are often associated with density and viscosity 'give away', because severe desulphurisation of fossil residues is unfeasible. However, this potential use had to be disregarded due to lack of miscibility with conventional bunker blendstocks without further upgrading.

The heavy fraction containing inorganics could possibly be recycled to the liquefaction process and co-processed with the biomass for additional cracking in supercritical water. A project on the effect of residue recycling during liquefaction was proposed to an AAU master student and it was carried out as a graduation project [3]. A +475 °C distillation residue from Hydrofaction^{TM} oil was used and the residue to wood ratio was varied during liquefaction in microbatch reactors. Liquefaction of the residue did result in a more volatile product having about 20 % less heavies (estimated by thermogravimetric analysis). The oxygen content was lower than the corresponding wood derived oil, but the volatility and molar H/C ratio was also reduced when wood was co-processed with the highly aromatic residue [3]. As a result, co-processing of the heavy fraction was proven possible, but additional complications associated with char and coke formation are likely.

As a conclusion, the potential added value that can be gained by upgrading justifies Steeper's incentive with further research in this direction.

4 Process Interface between HTL and the Upgrading Platform

Operating conditions and slurry composition were not definitive at initiation of the PhD project. However, a preferred set of Hydrofaction^{TM} conditions has now been established for forestry residues, based in part on the findings of this PhD project. With Hydrofaction^{TM} HTL defined, a baseline for the expected product quality can also be defined, which in turn provides details on the interface between the HTL process and the demineralization and upgrading platform.

4.1 HTL Product Composition

The products of the HTL process comprise the feedstock for the separation platform. Knowledge on the composition of the aqueous, gaseous and oil products provide important input to the design of a continuous product separation process. The products obtained from current continuous HTL pilot operation provide a best estimate on the product composition and will be used as baseline throughout this dissertation. With that said, product compositions are expected to change slightly, when product separation becomes an integrated part of the continuous process rather than being by manual gravimetric separation. In particular, distribution of inorganics, water and low molecular weight organics depend on the product separation design.

The gaseous product is rich in carbon dioxide (around 90 wt.%), with the remaining composition being mainly light hydrocarbons and hydrogen (Paper B for details). The aqueous phase is alkaline with a pH around 8.0 and it contains about 50 g/L TOC. Additionally, the aqueous phase has an ash content of 8-15 wt.%, as most of the alkali metal catalysts are dissolved herein. The Hydrofaction^{TM} oil is a water in oil emulsion containing 3-4 wt.% ash and 10-15 wt.% water as produced. Table 2.3 lists the elements detected by ICP of a representable Hydrofaction^{TM} oil produced at the HTL pilot.

Analysis	Al	Cr	Fe	K	Mg	Mn	Sn	Zn	P	Ca	Na	Total
ICP [ppm]	392	56	987	5096	53	50	13	<10	<10	171	4506	<11344
Ash [wt.%]												3.45

Table 2.3: Major elements (>5 ppm) detected by ICP of a wood derived Hydrofaction^{TM} oil as received after gravimetric separation. The ash content is given for comparison.

On a dry ash free basis, the oil contains 10 wt.% oxygen, 1000–2000 ppm nitrogen and 100–200 ppm sulphur. It is rich in phenolics, fatty and napthenic acids and polyaromatic hydrocarbon (PAH) type compounds. Finally, it is relatively heavy boiling with more than 50 wt.% +350 °C residue, and it posses a higher heating value (HHV) around 38 MJ/kg and a H/C ratio around 1.3 to 1.4. Significant deoxygenation takes place during liquefaction of the biomass, but remaining oxygen content of the Hydrofaction^{TM} oil affects its miscibility and compatibility with commodity fuels. Thereby, liquefaction oil is an intermediate that, similar to petroleum crude oils, need further upgrading/refining to gain transportation fuel value.

4.2 Potential Configurations of Integrated Upgrading Platform

An integrated separation and upgrading platform can be designed in different configurations with different degrees of complexity. Three different pathways to finished fuel are illustrated in Figure 2.8, and the pros and cons of each will be discussed in the following.

Stand-alone Refining

A process configuration, where the entire oil is upgraded to maximize the yield of liquid fuel products. The potential yield when upgrading the entire biocrude is around 100 vol.% based on input oil, or potentially up to 450 liter of fuel products per dry ton of wood. On the downside, stand-alone upgrading requires the most severe hydrotreating conditions and the most hydrogen, which is associated with significant operational costs. This is required

to deoxygenate and hydrogenate the relatively aromatic Hydrofaction™ oil sufficiently to meet fuel specifications of e.g. diesel and bunker fuel.

Following this pathway, the hydrotreating process including catalyst selection etc. can be designed around the Hydrofaction™ oil and the hydrotreater can be an integrated part of a Hydrofaction™ plant. Finally, the higher value of a finished fuel compared to a partially upgraded crude provides a larger so called 'crack spread', which is a petroleum term for the margin between feedstock cost and wholesale product value.

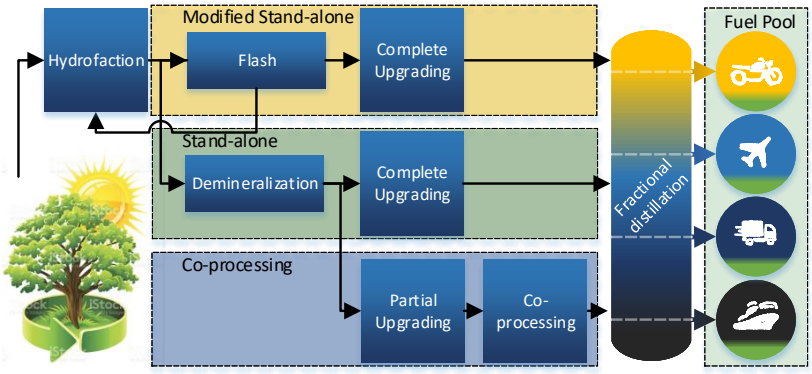

Fig. 2.8: Three potential upgrading pathways have been considered for Hydrofaction™ from tree to tank.

Modified Stand-alone Refining

A process design is where the Hydrofaction™ oil is flashed into a light and heavy organic fraction and only the light fraction is hydrotreated to finished fuel. According to open literature, this is the preferred configuration of the HTU® process [15] and Licellas Cat-HTR™ technology [12]. It does not require complete demineralization, because inorganics have been observed to remain in the heavy fraction allowing the light fraction to be hydrotreated. Another advantage is that hydrotreating severity can be reduced compared to the stand-alone configuration, because deep hydrogenation of the heavy fraction is avoided. As a consequence, the hydrogen consumption is also reduced. In general, this pathway reflect a less complex upgrading configuration, but at the expense of a lower yield of liquid fuel products.

The heavy fraction is found inadequate as bunker blendstock, and not particularly advantageous as liquefaction feed. The only meaningful use of the heavy fraction in this configuration is for combined heat and power production, but it reduces the accumulated product value. As a result, the modified

stand-alone configuration is not of further interest, due to the relatively low yields of finished fuel products.

Co-processing

Co-processing implies partial upgrading before shipping the oil to a refinery for co-processing with a petroleum crude. This configuration is also discussed in Paper E. Partial upgrading is required for different reasons. Firstly, the Hydrofaction^{TM} oil may not be compatible with petroleum products. Secondly, heteroatoms are distributed evenly in Hydrofaction^{TM} oil, whereas heteroatom removal operations are focused on the heavy boiling fractions in a conventional refinery. Finally, the refinery processes would have to be adapted to accommodate the lower thermal stability and exothermic reactivity that is characteristic to an oxygenated oil.

Quality requirements to the partially upgraded oil are eased compared to the stand-alone configuration. This reduces hydrotreating complexity and hydrogen consumption. In general, the option represents a simpler process with high yields, but also a significantly lower product value. A partially upgraded Hydrofaction^{TM} oil will most likely be referred to as an opportunity crude, which is the term for alternative refinery feedstocks that are characterized by high TAN (>1$^{mg\ KOH}/_{g}$) and/or densities above 900 $^{kg}/_{m^3}$ [14]. Co-processing of an opportunity crude induces the risk of corrosion and fouling issues, cetane reduction and product instability. As a consequence, refiners are relatively conservative towards opportunity crudes, which is why they are sold at a discount compared to benchmark products. Though, again an eventual 'green premium' may sweeten the deal and improve the incentives for co-processing.

Stand-alone upgrading and the co-processing option may both be beneficial in a particular Hydrofaction^{TM} plant setting. But from a commercial perspective, it is of Steeper's interest to be able to provide the entire technology platform from tree to tank. As a result, it is the stand-alone configuration in Figure 2.8 that will be in focus from now on, and Chapter 3, 4 and 5 address demineralization, upgrading and distillation, respectively.

References

[1] T. N. Adams, B. S. Appel, C. T. Einfeldt, and J. H. Freiss, "Depolymerization process of conversion of organic and non-organic waste materials into useful products," Aug. 10 2010, US Patent 7771699.

[2] J. Billing, D. Anderson, R. Hallen, T. Hart, G. Maupin, A. Schmidt, and D. Elliott, "Design, Fabrication, and Testing of the Modular Hydrothermal Liq-

uefaction System (MHTLS)," https://projects.ncsu.edu/mckimmon/cpe/opd/tcs2016/pdf/oral/Session3.3_5-Billing.pdf, 2016, accessed: 29-09-17.

[3] L. Casamassima, "Coliquefaction of wood and fractionation residue to ease production of drop in biofuels, Master thesis," Department of Energy Technology, Aalborg University, Tech. Rep., 2016.

[4] S. Chinnasamy, S. Bhaskar, J. Nallasivam, S. K. Ratha, D. M. Lewis, A. Meenakshisundaram, M. Lavanya, V. Selvavathi *et al.*, "Method of processing algae, carbonaceous feedstocks, and their mixtures to biocrude and its conversion into biofuel products," Jun. 24 2015, US Patent App. 15315723.

[5] H. Davis, C. Figueroa, and L. Schaleger, "Hydrogen or carbon monoxide in the liquefaction of biomass," Lawrence Berkeley Lab., CA (USA), Tech. Rep., 1982.

[6] L. J. Humphreys, "Assembly for reducing slurry pressure in a slurry processing system," Sep. 10 2010, US Patent App. 13496484.

[7] L. J. Humphreys, "Bio-oil production method," Apr. 14 2015, US Patent 9005312 B2.

[8] S. B. Iversen, K. S. Felsvang, T. Larsen, and V. Lüthje, "Method and apparatus for converting organic material," Mar. 16 2010, US Patent 7678163.

[9] C. Krauch and M. Pier, "Conversion of solid fuels and products derived therefrom or other carbonaceous materials into valuable products," Feb. 6 1926, US Patent 1890434.

[10] D. Lewis, "Personal communication, former CEO of Muradel Pty Ltd," 2016, accessed: 10-06-16.

[11] T. Maschmeyer and L. J. Humphreys, "Methods for biofuel production," Apr. 14 2015, WO 2011123897.

[12] Y. Mathieu, L. Sauvanaud, L. Humphreys, W. Rowlands, T. Maschmeyer, and A. Corma, "Opportunities in upgrading biomass crudes," *Faraday Discussions*, vol. 197, pp. 389–401, 2017.

[13] M. Siskin, G. E. Phillips, and S. R. Kelemen, "Biomass conversion using carbon monoxide and water," Aug. 6 2013, US Patent 8502003 B2.

[14] J. G. Speight, *The refinery of the future*. William Andrew, 2010, ISBN: 978-0-81-552041-2.

[15] L. Van de Beld, F. R. Boerefijn, G. M. Bos, F. Goudriaan, J. E. Naber, and J. A. Zeevalkink, "Process for the production of liquid fuels from biomass," Aug. 28 2007, US Patent 7262331 B2.

[16] W. P. van Swaaij, S. R. Kersten, and W. Palz, *Biomass power for the world*, Vienna ed. Pan Stanford Publishing, 2015, ISBN: 978-981-4669-24-5.

Chapter 3

Product Separation and Demineralization

This chapter focus on development and design of an integrated separation and demineralisation platform for the Hydrofaction^{TM} technology. As produced from the HTL pilot, the oil product subject to demineralisation and upgrading is a water in oil emulsion containing 3-4 wt.% ash and 10-15 wt.% water. Within conventional hydrotreating such concentrations of pollutants are unacceptable and pose a distinct risk of fouling and deactivation of catalyst beds [7–9].

This chapter presents a literature review on relevant separation and demineralization techniques. Secondly, experimental results obtained as part of developing a demineralization process is presented. Finally, a continuous separation system for the CBS1 pilot is designed. Figure 3.1 pictures the progress from development and test of various methods, to a final system design that is being acquired for the pilot at the time of writing.

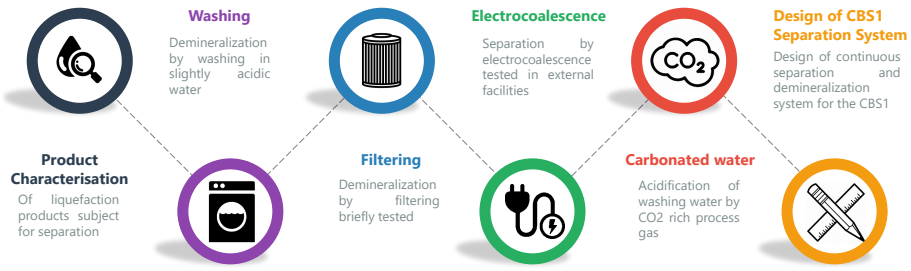

Fig. 3.1: Project phases from development of a separation and demineralisation technique to a detailed system design for the CBS1 pilot.

1 The HTL Oil Emulsion

Considering the entire HTL reactor effluent including gaseous, oil and aqeuous phases, water is quite likely to be the continuous phase of the product 'emulsion'. However, a so-called phase inversion occurs upon the gravimetric separation, during which the oil becomes the continuous phase. The resulting water in oil emulsion as received by gravimetric separation is depicted in Figure 3.2, and it is clear that oil is the continuous phase.

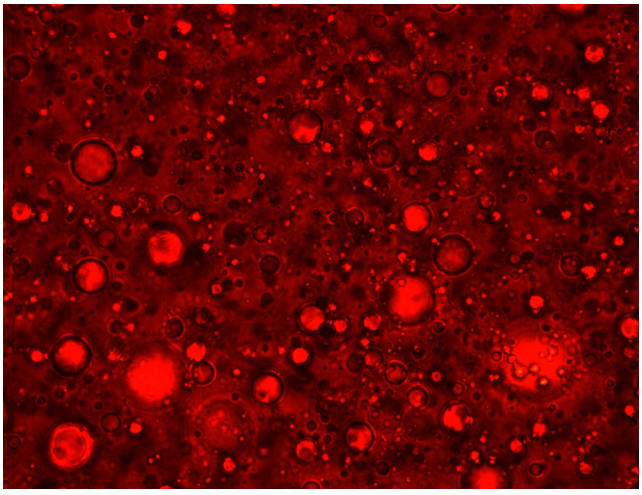

Fig. 3.2: Transferring light optical microscopy (100x) of as produced Hydrofaction^{TM} oil.

The HTL oil product given in Figure 3.2 contains 3-4 wt.% ash (mainly potassium and sodium) and 8-15 wt.% water. As given later, the TAN is about an order of magnitude higher than for a 'high TAN' petroleum crude. This is very relevant in relation to separation of the emulsion. High TAN makes desalting more difficult, because the inorganics and carboxylic acids form carboxylates. E.g. soaps from fatty acids or naphthenates from naphthenic acids. Such carboxylates are surfactants that stabilise the emulsion due to their amphiphilic nature. Furthermore, Figure 2.7, presented previously, shows that the TAN of HTL biocrude increases as function of boiling point, making high molecular weight acids the major acids present. High molecular weight carboxylates are particularly resistant to phase separation, due to reduced water solubility [9, 25]. Along this line, sodium and potassium naphthenates are particularly water soluble and water-dispersible, resulting in tight emulsions [19]. This is relevant as sodium and potassium represent 85% of the total oil inorganics listed in Table 2.3.

Polarity of the oxygenated oil causes a stronger affinity for water compared to petroleum derived hydrocarbons. The water in oil HTL product emulsion is further stabilised by minor concentrations of organic solids, such as resins from the woody feedstock with melting points above 120 °C. Thus, the water in oil emulsion is stabilised by solids and amphihilic surfactants, alkaline pH, interfacial films and van der Walls forces and electrostatic repulsive forces [3, 5, 6].

Important parameters that affect the separation of a water in oil emulsion can be derived from Stokes equation on sedimentation speed, v of a dispersed droplet.

$$v = \frac{2r^2 \Delta\rho g}{9\mu} \tag{3.1}$$

It is evident that the sedimentation speed is proportional to the square of the droplet radius, r. Further, sedimentation increases with a larger density difference, $\Delta\rho$ between the continuous and dispersed phase. And finally, it depends on the gravitational force and viscosity of the continuous phase.

As produced, the Hydrofaction^{TM} oil is viscous and the density is very close to that of the dispersed water phase. This stabilises the water in oil emulsion as evident from Stokes equation. However, both viscosity and density differences can be improved in terms of sedimentation by use of a diluent. A diluent is also beneficial in terms of dissolving the before mentioned organic resin like solids. Likewise, separation at elevated temperature will reduce viscosity and increase the density differences. A higher temperature will also increase coalescence by higher kinetics and rate of drop collisions [3].

2 Potential Demineralization Techniques

This section serves as a literature study on demineralisation procedures applied by both competing HTL technologies and by the petrochemical industry.

2.1 Flashing or Extraction

Solvent extraction or distillation is used to concentrate metals of a 'dirty' petroleum crude with e.g. 1000 ppm metals, before further hydrotreating of the extractives/distillates [9]. Similarly, **Biofuel B.V.** claims flashing or solvent extraction as techniques for demineralization of the HTU biocrude prior to hydroprocessing [22]. The flashing technique implies fractionation into a light and heavy oil fraction. The light distillate fraction is suitable for hydrotreating to transportation fuel, while the coal like residue fraction can be

combusted for electricity and heat generation. Alternatively, either the entire organic product or the heavy fraction from flashing can undergo extraction with a polar solvent. The extractives can then be further hydroprocessed into fuel grade products [22].

Flashing is also the method used by **Licella** according to a recent publication, where it is stated that the heaviest 20-30% of the wood derived biocrude is separated off by flashing [14]. The method is very effective, but the relatively high loss of heavies is a disadvantage of this technique.

2.2 Filtering

PNNL's approach towards demineralization is separation and/or filtration of the reactor effluent at reaction conditions (350 °C and 207 bar) [4]. The inorganics have low solubility in near-critical water, and the reactor effluent is passed through a precipitation vessel, where inorganic and mineral solids flocculate and settle for collection. The effluent may also be passed through a <10 micron filter to avoid passage of any precipitates [4]. A similar system is currently being commissioned at the pilot plant in Foulum, **Aarhus University**, Denmark.

No information, such as separation efficiency is given in [4] on the final ash/minerals content of the biocrude. Though, recent publications by PNNL, report 2900 ppm ash in biocrude from municipal wastewater sludge [18], 600-4600 ppm ash in sewadge sludge derived oils [17], and an iron content around 1000 ppm for two algae derived biocrudes [11]. Assuming that these oils are treated according to the preferred technology, but without being conclusive on numbers provided by others, it seems that an additional demineralization step is unavoidable.

2.3 Centrifugation

Centrifugation is another mechanical separation technique that can be used to break water in oil emulsions. In Stokes equation (3.1), centrifugation enhances the gravitational force. However, centrifugation is an expensive solution to maintain due to several moving parts. And based on several ineffective centrifugation tests, this technique will not be discussed further.

2.4 Electrocoalescence

Electrocoalescence is a popular technique in e.g. crude oil desalting units to improve separation of water in oil emulsions. Application of an electric field across such emulsion polarise the water droplets and induces flocculation

and coalescence, due to the different conductivity of water and oil. When droplets coalesce and become larger, the settling speed improves according to Stokes law [5, 6].

Coalescence of the small water droplets apparent from Figure 3.2 is very appealing in relation to separation of Hydrofaction^{TM} products. Though, the difference in conductivity between the aqueous and oil phases are likely lower, due to the polar nature of HTL oil. This may reduce the potential of electrocoalescence, as both the water and oil droplets will be polarised when exposed to the electric field. Another parameter to consider is the relative high water content of the oil phase, which is around 10-15 wt.%. High water contents induce the risk of short circuiting in relation to electro coalescers.

2.5 Desalting or Washing

Desalting is a well known technique widely used by petroleum refiners to demineralise crudes and especially reduce the content of NaCl and suspended solids (sand, clay etc.) before any further processing. In brief the crude is mixed with 3-10 vol.% water at temperatures from 90-150 °C. Electrocoalescence, pH adjustment using acids, de-emulsifying agents and the water to oil ratio are parameters that can be varied to improve the separation efficiency. For heavy crude oils, a diluent such as gas oil may be added as viscosity- and density reducing agent to improve separation. For high mineral content crudes, two- or even three-stage desalting is used to demineralise the feed, in particular if the residue fractions are subject for catalytic processing.

Demineralisation by washing was also published in the early HTL literature. [10] washed a wood derived HTL oil prior to hydrotreating by dissolving it in 10 % isooctane, mixing with 2:1 water to oil and separating the mixture gravimetrically. This procedure was repeated and thereby the oil sodium content was reduced from 0.92 to 0.12 wt.%.

UOP recently patented a method for decontamination of oils in general, but claimed for algae derived HTL oils specifically [13]. The method comprises contacting the oil with a base to form a stable emulsion, contacting the emulsion with an acid to break the emulsion, and separate the demineralized organic phase from the aqueous phase. There is no information on the particular acids used, but the base is suggested to be sodium hydroxide for metal removal [13]. In relation to demineralization of Hydrofaction^{TM} biocrude, the first base contacting step of UOP's procedure is unnecessary, as the aqueous product contain NaOH and is alkaline with a pH around 8.0.

Washing with deionized or acidified water is also used within biodiesel production to purify the biodiesel from water and traces of methanol, glycerol and alkaline catalysts. [20] and [23] presents reviews of purification of biodiesel, and the use of citric acid for e.g. calcium removal is concluded to be particularly efficient considering both yields and use of reagents. Acetic acid is also used to acidify the water during washing of biodiesel.

2.6 Washing with Carbonated Water

ExxonMobil has an interesting patent, [1] on 'CO_2 treatment to remove organically bound metal ions from crude'. The patent focuses on demineralization of petroleum crude by contacting the crude with carbonated water. The patent is relevant in a Hydrofaction^{TM} context, because the HTL reactor effluent consists of a CO_2 rich gas product, an aqueous phase and the oil. 14 examples are provided in [1] that show how a total concentration of 1920 ppm of calcium, magnesium, potassium and sodium can be reduced to around 100 ppm. More specifically, the examples show an effect of the initial mineral concentration, CO_2 to oil ratio, contacting time, temperature/pressure during separation and that the demineralization efficiency is significantly reduced in the absence of water, where only CO_2 and oil is present. Along this line, **Chevron** claimed in 1988 the use of carbonic acid for calcium removal of carbonaceous feedstock, such as petroleum vacuum residue [16].

The pH of pure water is reduced to about 3-4 at CO_2 pressures higher than 10 bar and ambient temperatures [2, 15]. A slightly higher CO_2 pressure is required to reduce pH of an alkaline solution, but the pH becomes rather independent of pressure above 30 bar. A higher temperature reduces the solubility of CO_2 in water, resulting in a slightly higher pH value. Moreover, it can be derived from [2, 15] that the effect CO_2 pressure has on pH increases, the more alkaline the intial aqueous solution is. This is important in relation to the aqueous Hydrofaction^{TM} product, which is alkaline due to the NaOH and K_2CO_3.

3 Experimental Demineralization Results

Of the techniques mentioned in the previous literature review, it is only PNNL's hot separation technique that has not been tested. Filtering, electrocoalescence, centrifugation, distillation and in particular desalting/washing with deionized, acidic and carbonated water have all been tested. Selected results from these experiments will be presented in the following section.

3.1 Filtering

The major advantage of mechanical separation techniques such as filtering and electrocoalescence is the avoided need of washing water, which generates waste. Filtering was tested by diluting a Hydrofaction^{TM} oil in methyl ethyl ketone (MEK) (1:4) to reduce viscosity, and circulating the mixture in a 100 micron CC Jensen filter for 70 hours. The filter (Figure 3.3) consists of a 27 liter pre-filter and main cellulose filter that should enable water separation. Figure 3.3 (right) depicts water and ash contents of the filtered product as function of recirculation time. With stable ash content and only slightly decreasing water content, it is evident that demineralisation and dehydration using this filter is ineffective.

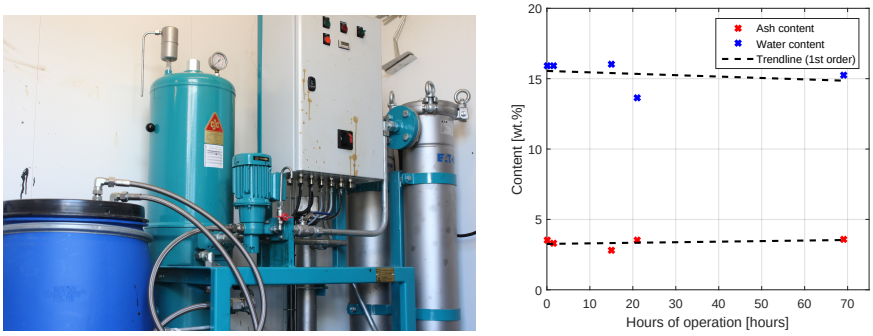

Fig. 3.3: Left) CCJensen filter setup. Right) Water and ash contents of filtered products as function of recirculation time.

As presented later, a demineralization technique has been developed, which reduces the ash content of Hydrofaction^{TM} oil to around 300 ppm. Preliminary filtering tests using 0.5 micron syringe filters showed that additional demineralisation below 300 ppm can potentially be obtained by a fine filter. In principle, the filtering presented in Figure 3.3 may have removed certain types of inorganics in the ppm range, but when compared to percentage levels it is very difficult to measure.

3.2 Electrocoalescence

Electrocoalescence tests on Hydrofaction^{TM} oil was tested by external technology providers, varying the voltage (<10 kV), temperature (<90 °C) and use of deemulsifiers. As a matter of safety, the equipment did not allow temperatures above 90 °C nor addition of a diluent in combination with the high voltage. Electrocoalescence does improve the speed of separation/dehydration compared to gravimetric separation, which is likely due to improved coales-

cence to larger droplets that improve the sedimentation speed (Stokes Equation (3.1)). However, electrocoalescence does not dehydrate the oil below 10 wt.% (Figure 3.4). This may be related to the higher conductivity of an oxygenated oil compared to petroleum products, which disturbs the selectivity of the electric field. Further, it is likely because electrocoalescence does not affect emulsion stabilisers such as napthenate complexes or heavy organic compunds that melt or re-dissolve at temperatures above 130 °C.

As given in Figure 3.4, the relation between degree of dehydration and demineralization by electrocoalescence, indicate that part of the inorganics is bound to the oil as organometallics, and thus the minerals cannot be removed simply by dehydration.

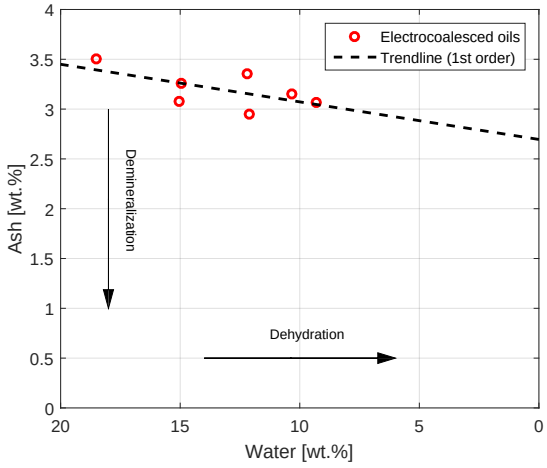

Fig. 3.4: Relation between dehydration and demineralization by electrocoalescence of a Hydrofaction^{TM} oil.

Despite the initial testing being unsuccessful in terms of demineralization, electrocoalescence may be a suitable technique to improve the speed of separation once combined with a technique that breaks the emulsion.

3.3 Demineralization by Washing - Labscale

More than 50 washing experiments have been conducted in 100mL glass flasks. Oil and washing agents were mixed at ambient temperature and pressure using a magnetic stirrer for more than 12 hours and left for gravimetric separation for more than 10 hours. Figure 3.5 depicts a mixture after settling, which is ready for separation by pipetting. The major findings of the study will be presented in this section.

Fig. 3.5: Washing experiment with citric acid and MEK after 10 hours of settling.

Parametric Screening

pH of the aqueous phase increase during washing, as the major part of inorganics in the biocrude is alkali metal catalysts from the liquefaction. In fact the relative pH increase is a useful indicator of the demineralization. Acetic acid (AA), citric acid (CA), hydrocloric acid (HCl) and reverse osmosis (RO) water were tested. No alkaline agents were evaluated as it was quickly found that pH of the aqueous phase after washing has to be below 7 for good phase separation to occur. This observation is illustrated in Figure 3.6 a), where the reduction in oil ash content by washing, expressed as demineralization, is highest when pH of the aqueous phase is below 7. The observation matches the guidelines for petroleum desalters, where pH should be below 8 and preferable around 6 to obtain good dehydration and avoid napthenate-stabilised emulsions [9, 21].

Due to alkaline pH after separation, deionized water resulted in poor demineralization. Regarding the acids, CA was superior to AA, which was again superior to HCl, despite HCl being the strongest acid. CA has three acid functional groups, which makes it a good chelating agent, as compared to the others with only one acid functional group each. This is included in Figure 3.6 b) that compares the experiment on basis of moles of acid functional groups per gram of oil. It can be derived that CA provides the highest demineralisation per mole of acid groups, which is most likely related to CA being a better chelating agent.

Significant variation of the data in Figure 3.6 b) is because the washing agent to oil ratio and acid concentration were also varied in some tests. Figure 3.6 c) shows how demineralisation decreases if the washing agent to oil ratio is reduced, despite compensation by a higher acid concentration. Likewise, it shows how excess acid does not improve demineralization.

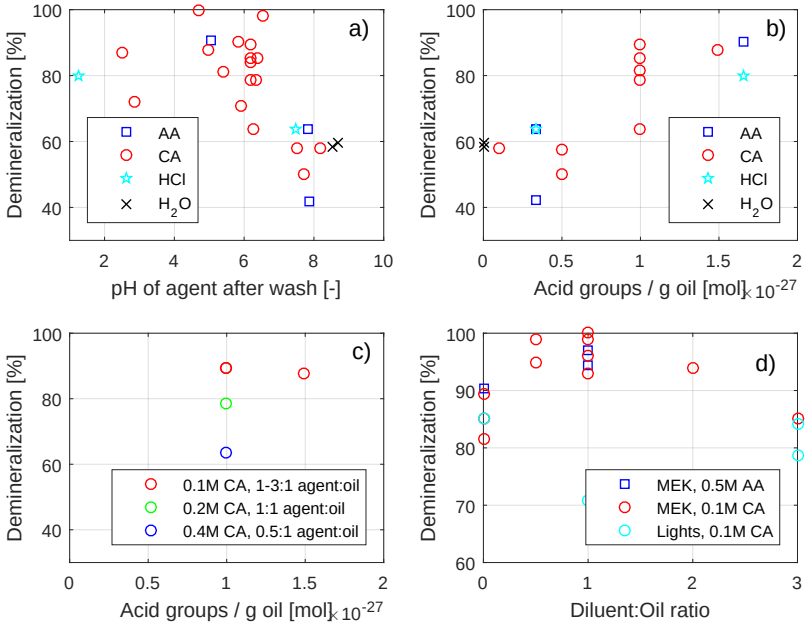

Fig. 3.6: AA = acetic acid, CA = citric acid, HCl = Hydrochloric acid.

Use of a density- and viscosity-reducing agent is important to obtain complete demineralization by washing. The biocrude density is above 1.0 kg/m^3 at ambient temperatures and it becomes the bottom layer upon washing with the aqueous washing agents if no diluent is used. This affects demineralization, but so does the choice of diluent. Toluene results in stable emulsions that are difficult to separate, while the IBP-140 °C distillates (lights) of Hydrofaction^{TM} oil seems to affect inorganics removal negatively. But as given in Figure 3.6 d), demineralization increases for both CA and AA when MEK is used as diluent. This figure also indicates that use of excess diluent affects demineralization negatively. Separation at elevated temperatures has a similar effect on viscosity and density, which could potentially result in similar demineralization efficiencies without the use of a diluent. A test at 70 °C did not improve inorganics removal compared to the test at ambient temperatures, indicating that higher temperatures are needed.

Optimal Washing Conditions

The highest biocrude demineralization is obtained using 0.1 M CA in 2:1 agent to oil ratio and MEK in a 1:1 diluent to oil ratio. The applicability and robustness of this demineralization procedure is evaluated by testing

it on four different wood derived industrial and academic HTL biocrudes. As given in Table 3.1, more or less complete demineralization was achieved for the biocrudes. For the Paper D, NH_3 oil, the aqueous phase contained 5.6 g/L nitrogen after demineralization. This corresponds to approximately 1.5 wt.% nitrogen that is removed from the oil during washing, which is an additional benefit in relation to the downstream upgrading. The +475 °C Hydrofaction^{TM} residue, which is rock-solid at ambient temperature, was more difficult to wash. It required more diluent to dissolve and contained 0.17 wt.% ash after the first wash, but 0.02 wt.% ash after a second wash.

Conditions				Oil, Ash [wt.%]		WP, Ash
Oil	Oil:diluent	Agent	$\frac{Agent}{Oil}$	Before	After	[wt.%]
Paper B oil	1:1 MEK	0.1M CA	2.0	3.32	0.00[a]	1.24
Paper D, NH_3 oil	1:1 MEK	0.1M CA	2.0	1.65	0.01	0.45
Paper J oil	1:1 MEK	0.1M CA	2.0	0.62	0.02	0.17
Residue from Paper B oil[b]	1:3 MEK	0.1M CA	2.0	1.10	0.02	[b]

[a] = below detection level [b] = required 2 washes

Table 3.1: Applicability of washing method on different HTL oils.

3.4 Demineralization by Washing - Pilot Scale

The washing experiments described above where completed in Q3 2015, just before 100 kg of Hydrofaction^{TM} oil produced at the pilot had to be delivered to a partner. Through a few iterations, suitable equipment for upscaled demineralisation by washing was acquired, and the following procedure, depicted in Figure 3.7, has been used for demineralization of Hydrofaction^{TM} biocrude at the pilot since then.

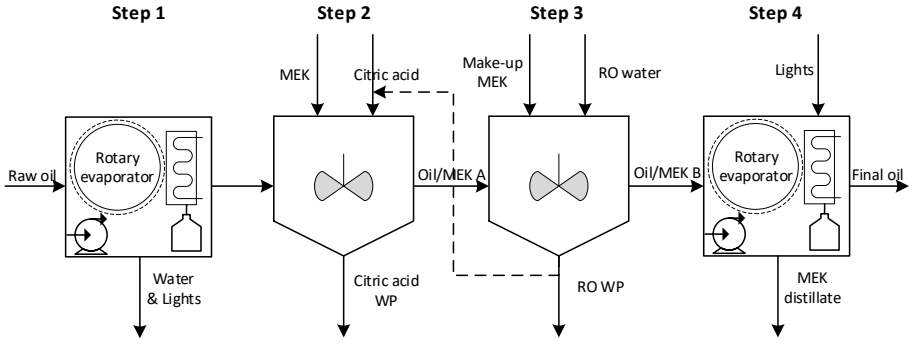

Fig. 3.7: Schematic of pilot scale washing set-up.

Step 1: Evaporation of Water and Lights
Collection of the organic lights by evaporation to an atmospheric equivalent

temperature (AET) equal to 140 °C in a rotary evaporator. The lights need to be collected prior to dilution with MEK in order not to loose them under subsequent MEK removal. The water and organic lights can be separated either by gravimetric separation (Figure 3.8) or by freezing to -10 °C and decanting.

Step 2: Dilution and Acidic Washing

The dewatered oil from Step 1 is diluted in a 1:1 ratio with MEK and washed using 0.1M citric acid in a 2:1 washing agent to oil ratio for 8 hours. After >10 hours of separation, the aqueous phase is collected.

Step 3: Washing with Deionized Water

An additional wash with RO water in a 2:1 agent to oil ratio is included, based on a hypothesis that left over water, containing both citric acid and trace alkali metals, in the oil phase can be diluted to reduce TAN and ash content of the final oil product. The aqueous phase of the RO wash are collected after settling. This product may be mixed with citric acid and used for the next oil to be washed, in order to reduce waste water and loss of water soluble organics from the oil.

Step 4: Diluent Recovery and Reintroduction of Lights

Recovery of MEK and trace water from the washing in Step 3 by rotary evaporation. The AET should match that of Step 1. After recovery of the diluent, the lights recovered in Step 1 is mixed back into the washed and dewatered oil. This is preferably done while the oil is hot in order to achieve thorough mixing.

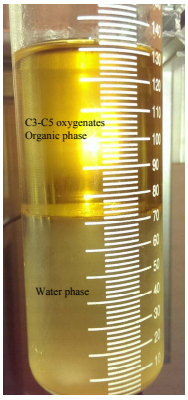

Fig. 3.8: Distillate products from dehydration of Hydrofaction^{TM} oil. The aqueous and organic phase separate instantaneously.

Validation of Procedure in Upscaled Washing

The following discusses major findings from an example of upscaled demineralization of oil at the pilot. The oil was produced at the pilot according to the procedure described in Paper B, and the washing example is given in patent application H. Figure 3.7 visualises the procedure, where mixing is done by a high speed disperser build in stainless steel that facilitates both high speed dispersion and low speed mixing. The high speed mixer creates a dispersion of oil, MEK and water phase, which is very difficult to separate, and thus the low speed mixer is used to avoid such emulsion. Please note that Step 1, evaporation of water and lights, was omitted in this example (Oil A, Table 2.1), but due to the findings of this example, it has been standard procedure since.

Oil and Aqueous Streams

Table 3.2 lists ash content, water content and TAN for the raw, intermediate and final oil. The main washing step with 0.1 M citric acid reduces the ash content from 3.7 wt.% to around 850 ppm in oil A. The water content is also reduced during the acid wash from 14.3 to 8.3 %. Assuming that the 850 ppm ash is situated in the trace water only, the ash content of the trace water should be 1.03 wt.%. This matches quite well with the ash content of 1.17 wt.% in the citric acid water phase (WP) that was separated from this particular wash (see Table 3.3). This is one argument for an additional wash with RO water to dilute the water phase that is bounded in the oil. Likewise, an additional RO wash could potentially dilute any remaining citric acid and reduce the TAN of the final oil. However, allowing some uncertainty in the measurements, the TAN values given in Table 3.2 indicate that the RO wash has no or little effect on the TAN. TAN of the raw oil is relatively low at 8 compared to 45 $^{\text{mg KOH}}/_{\text{g}}$ in the final oil and the increase in TAN during washing is discussed later.

Analysis	Raw oil	Oil/MEK A	Oil A[a]	Oil/MEK B	Oil B[a]	MEK dist.	Final Oil
Ash [ppm]	37000	470	850	180	330	0	370
Metals [ppm]	11351						41
Water [wt.%]	14.3	4.6	8.3	4.3	7.8	8.8	0.6
TAN [$^{\text{mg KOH}}/_{\text{g}}$]	8	24	44	22	40	0	45

[a] dry & MEK free basis

Table 3.2: Parameter change during each step of the improved washing.

Table 3.3 lists additional parameters for the in- and output aqueous streams of each washing step. Ash content, pH and potassium content of the citric acid increase, emphasizing that the majority of alkali metal catalysts are removed from the oil during the first wash. Another important note need to

be made in relation to Table 3.3. A substantial amount of MEK is lost to the water phase, due to the relatively high solubility of MEK in water. This is a drawback of using MEK as diluent, because it need to be recovered from the water phase to reduce consumables and subsequent water treatment.

Analysis	0.1M Citric acid	Citric acid WP	RO water	RO WP
Ash [wt.%]	0.00%	1.17%	0.00%	0.05%
pH	1.8	6.3	6.0	5.9
TAN [mg KOH/g]	17.0	1.0	0.0	0.1
TOC [g/L]	4	57	0	66
MEK calc. [wt.%]	0%	7%	0%	10%
Alcohol [g/L]	0.3	5.7	0.0	2.9
Phenol [mg/L]	0.0	246	0.0	204
Potassium [g/L]	0.0	2.9	0.0	0.1

Table 3.3: Parameter change during each step of the upscaled washing.

Mass Balance

Table 3.4 lists the mass balances of the overall washing to be 99.8 %. The oil yield on a dry ash free basis is determined to be 92.6 %. Losses are believed to be mostly lights lost due to the omitted step 1, and water soluble compounds lost to the water phases. Based on the alcohol and phenol content of the water phases after washing (Table 3.3) 2-3 wt.% of the oil is lost to the aqeuous phase. This is related to the lack of evaporation of lights in this example. It has been found that reintroduction of lights have a significant effect on biocrude quality in terms of viscosity and thermal stability and step 1 is now standard procedure during washing. Hydrofaction^{TM} oil viscosity is given as function of amount of lights that is reintroduced in Figure 3.9. A GC-MS analysis of the lights is given later in Table 5.3.

Sample	Total in	Total out	Ash	Water	Oil DAF	MEK	Citric acid
Total in [kg]	246.9		1.4	161.5	31.0	51.5	1.47
Total out [kg]		246.3	1.17	161.61	28.73	53.36	1.47
Loss [kg]		0.6	0.22	-0.11	2.29	-1.83	0.00
Recovery		99.8%	83.9%	100.1%	92.6%	103.6%	

Table 3.4: Mass balance of the improved washing

Remaining Contaminants

The final bio-oil contains 0.6 wt.% water, around 370 ppm ash and 41 ppm metals (detected by ICP). The difference between inorganics measured by ash and ICP is partly because ICP only quantifies the mass of the metal, whereas the mass of the entire e.g. iron oxide is included in the ash content. Figure

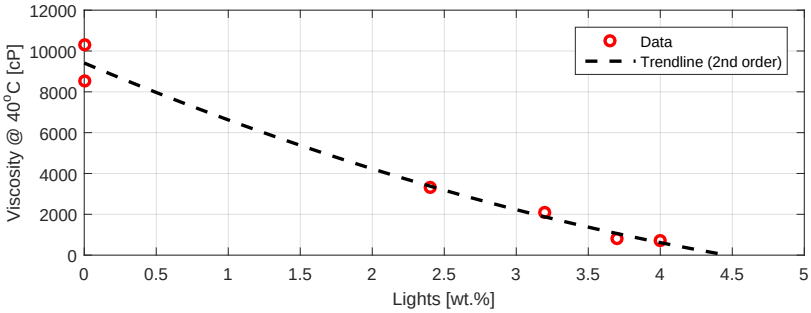

Fig. 3.9: Viscosity of the oil depend on the amount of lights that are reintroduced in Step 4 of the washing procedure. Based on oils from Table 2.1.

3.10 reflects the metals content measured by ICP of the ash before and after washing. Sodium and potasium are reduced to <5 ppm, despite their significant presence in the raw oil. The accumulated metals content of the final oil is 41 ppm, with iron being the only metal which has a concentration above 5 ppm. It is not surprising that iron is the major contaminant, as the ash after analysis is red as rust. But the origin of the iron gave rise to speculation. After several hypotheses on corrosion of reactors, product barrels or washing hardware were turned down, the reason was found to be the hammer mill. The hammers degrade during milling of the woody biomass, and both the ash content and iron measured by ICP was found to increase during milling of the birch and energy wood.

Based on the ICP measurement, demineralization by washing seems to reduce the inorganics content to a level that is manageable in relation to downstream catalytic upgrading.

Pilot Results over Time

The 4-step washing procedure has been used frequently during the last two years for demineralisation of Hydrofaction^{TM} oils produced at the CBS1. Figure 3.11 plots the resulting ash contents after oil washing for the last two years, and a few conclusions can be drawn. Firstly, use of acetic acid as washing agent is ineffective compared to citric acid. This matches the conclusion of the micro scale washing experiments presented previously. Secondly, issues regarding low quality and extremely high viscosity of the oil product from the pilot was observed around Q1 2017. These issues seem to affect the demineralization. Finally, if the Q1 2017 outliers are disregarded, the average ash content from citric acid wash is 307 ppm.

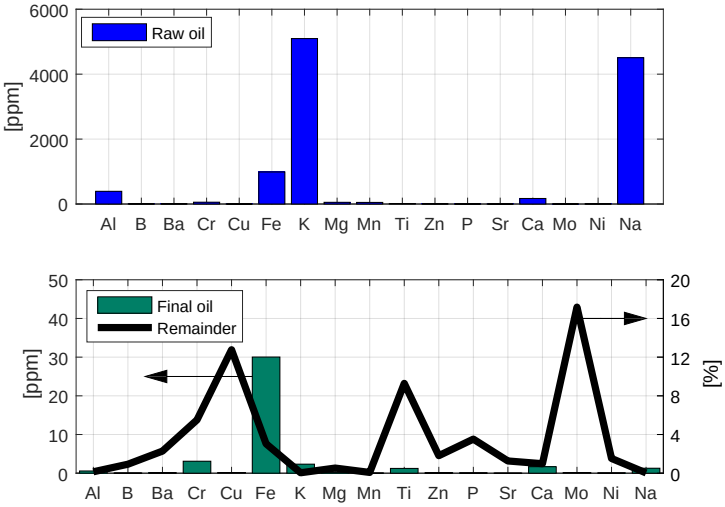

Fig. 3.10: Metal content by ICP before and after upscaled washing.

Increase in TAN during Washing

TAN of the oil increases significantly during washing. It has been speculated whether this increase in TAN is caused by acid that remains in the oil phase after washing. While CA has a boiling point of 310 °C, AA boils at 117 °C and will be recovered together with diluent and water in Step 4 of the washing procedure (Section 3.4).

Table 3.5 lists the TAN of similar Hydrofaction^{TM} oils washed with different acidifying agents (see Section 3.5 for demineralization using carbonated water). The TAN of the oil washed with AA is highest, emphasizing that

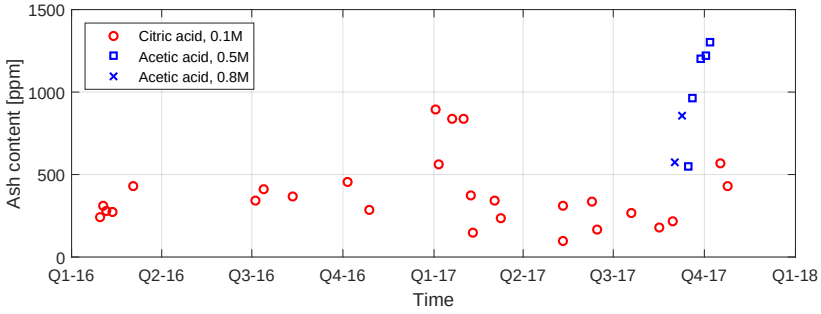

Fig. 3.11: Ash content of Hydrofaction^{TM} oils produced and washed at the CBS1 since establishment of the 4-step washing procedure.

the increase in TAN during washing is not due to the presence of remaining acid. Instead, it is believed to be the direct effect of demineralization. By demineralizing e.g. sodium naphthenate, the corresponding naphthenic acid will contribute to a higher TAN after washing.

Washing Agent	Citric acid	Acetic acid	Carbonated water	
Exp. #	CBS1-342	CBS1-339	SFS1	SFS4
TAN [$^{mg\ KOH}/_{g}$]	67	80	64	62

Table 3.5: Total acid number of oils washed using different acidifying agents.

3.5 Demineralization using Process CO_2

CO_2 is the major constituent of the liquefaction process gas. Pressurized CO_2 in water (carbonated water) has been observed to improve phase separation through its ability to lower the pH similar to the citric acid solution used in Section 3.3. Experimental results around CO_2 treatment have not been published, but are included in Patent Application H, and the major findings will be presented in the following.

Initially, the visual effect of separation in a CO_2 atmosphere was tested at the University of Alberta, Canada using a reflecting light microscope and a pressure and temperature resistant reactor with see-through bottom. The dynamics are difficult to document on print, but there was a clear visible effect on water coalescence during and after changing the atmosphere to CO_2. Figure 3.12 pictures an as produced Hydrofaction^{TM} oil in 30 bar N_2 and CO_2 respectively. The CO_2 seems to reduce surface tension and induce coalescence resulting in larger droplets after settling, compared to small, spherical droplets and no or little coalescence in N_2.

Parametric Screening in Microbatch Vessels

A series of separation experiments have been carried out using 15ml microbatch reactors to determine the effect of carbonated water as washing agent. The reagents were mixed, mildly shaken and left for separation for 20 hours in vertical position. Initially, the vessels were depressurized prior to separation, but similar to opening a soda, the 'fizz' was found to disturb phase separation and thus demineralization. Instead, products were recovered at pressure through a needle valve in the bottom.

A set of experiments were conducted to study separation in different atmospheres. Table 3.6 compares separation in 10 bar and 30 bar CO_2 with gravimetric separation at atmospheric pressure and separation in 30 bar N_2.

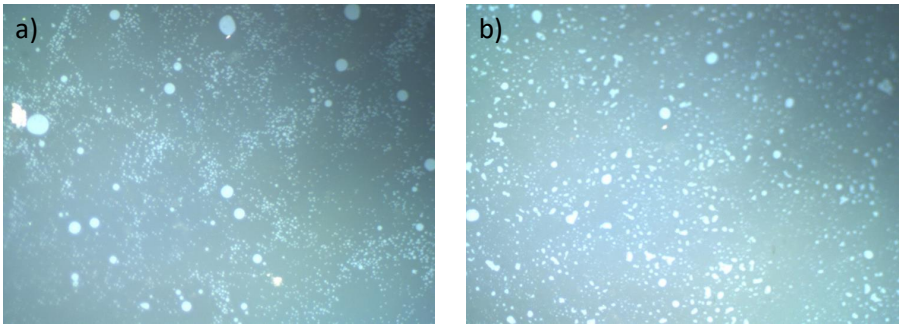

Fig. 3.12: 100x reflecting light microscopy of as produced Hydrofaction^{TM} oil at 20 °C, a) 40 min after pressuring the sample with 30 bar N_2, b) 40 min after flushing and pressuring the same sample with 30 bar CO_2. The width of the pictures correspond to 1mm of the sample.

Due to the elevated pH of the mixtures, no phase separation occurred in neither N_2 nor in air. In comparison, 30 bar CO_2 reduced the ash content of the oil from 4.2 wt.% to 1505 ppm in one step, hence a clear effect of carbonated water

Exp.#	Agent	Diluent	Gas	P [bar]	T [°C]	pH WP [-]	Ash Oil[a] [ppm]
SA19	RO (4:1)	MEK (1:1)	Air	atm.	20	8.1	NA[b]
SA20	RO (4:1)	MEK (1:1)	N_2	30	20	8.3	NA[b]
SA18	RO (4:1)	MEK (1:1)	CO_2	10	20	7.0	3133
SA1&2	RO (4:1)	MEK (1:1)	CO_2	30	20	6.9	1505

[a] MEK free basis [b] No phase separation observed

Table 3.6: Effect of atmosphere and pressure. The Hydrofaction^{TM} oil used as feed for the experiments contained 4.2 wt.% ash. Data from publication H.

A HTL product separation system has to handle the reactor effluents consisting of oil, CO_2 rich gas and high inorganics content HTL process water (PW). On that basis, steady state PW, characterised by pH 8.1 and an ash content of 8.7 wt.% was included in the experiments with CO_2. Table 3.7 compares the ash contents after separation using either RO water or HTL PW as washing agent. Please note that PW refers to the HTL reactor effluent, whereas WP is the resulting aqueous phase after a given washing experiment. It is evident that additional ash removal (compared to the gravitational separation) can be obtained in a 1st phase separator, where HTL PW and process gas (mainly CO_2) is applied at 30 bar. This is advantageous, since more alkali metal catalyst can be recovered in the PW, and less demineralization have to be done in a 2nd phase separator that utilities e.g. RO water as washing agent. Table 3.7 also emphasizes the potential of a solvent. In particular MEK improves separation.

Exp.#	Agent	Diluent	Gas	P [bar]	T [°C]	pH WP [-]	Ash Oil[a] [ppm]
SA5	PW (2:1)	None	CO_2	30	150	7.4	21500
SA11	PW (4:1)	MEK (1:1)	CO_2	30	20	7.4	11400
SA1&2	RO (4:1)	MEK (1:1)	CO_2	30	20	6.9	1505
SA9	RO (4:1)	Lights (1:1)	CO_2	30	20	6.8	5448

[a] MEK free basis

Table 3.7: Effect of washing agent and solvent. Data from publication H.

As evident from Table 3.8 it was observed that demineralization was improved at a temperature of 150 °C compared to 20 °C. This can partly be explained using Stokes Equation (3.1), where separation is improved by lower viscosity of the oil phase and a larger density difference between the phases. Moreover, a higher temperature induces a higher collision rate, weakened adsorption equilibriums for inorganics and/or re-dissolving/melting of solid organic compounds. It is not related to any operational costs to do the separation at elevated temperatures, because the reactor effluent have to be cooled from around 400 °C.

Exp.#	Agent	Diluent	Gas	P [bar]	T [°C]	pH WP [-]	Ash Oil[a] [ppm]
SA1&2	RO (4:1)	MEK (1:1)	CO_2	30	20	6.9	1505
SA3&4	RO (4:1)	MEK (1:1)	CO_2	30	150	6.9	1019
SA9	RO (4:1)	Lights (1:1)	CO_2	30	20	6.8	5448
SA8	RO (4:1)	Lights (1:1)	CO_2	30	150	6.9	1581

[a] MEK free basis

Table 3.8: Effect of temperature using two different solvents and RO water. Data from publication H.

Table 3.9 indicates the effect of reducing the washing agent to oil ratio. pH and WP ash content increases when the agent to oil ratio is reduced. This reduces separation efficiency leading to a higher ash content of the resulting oil phase.

Exp.#	Agent	Diluent	Gas	P [bar]	T [°C]	pH WP [-]	Ash Oil[a] [ppm]
SA3&4	RO (4:1)	MEK (1:1)	CO_2	30	150	6.9	1019
SA16&17	RO (2:1)	MEK (1:1)	CO_2	30	150	7.2	2318

[a] MEK free basis

Table 3.9: Effect of washing agent to oil ratio. Data from publication H.

The CO_2 treatment presented in this section is not as effective as the acid wash, and the ash content after treatment is still above 1000 ppm. However,

the small pressure resistant separation vessels had to be positioned vertically during separation in order to collect the products separately. The vertical position reduces the contact area between the aqueous and organic phase significantly compared to horizontal positioning. This is believed to affect the result, and a more efficient separation should be possible in an improved design.

Development of a product separation and oil demineralization process has been a critical point in developing the Hydrofaction^{TM} platform. Techniques were presented in the above sections for biocrude demineralization by washing using either citric acid or CO_2 as pH reducing agent. In particular the use of carbonated water represents an elegant and novel solution, where the CO_2 rich gas product from the liquefaction process can be used in synergy to demineralize the biocrude.

4 Design of Separation System for Pilot

The previous sections present how inorganics in the Hydrofaction^{TM} oil can be reduced to ppm level by batchwise washing with carbonated water or a citric acid solution. Based on these findings, a new separation system was designed for the pilot in order to validate and demonstrate the techniques in continuous mode. The system hardware is being delivered at the time of writing. Thus no test results are available yet, but this section will present the design and features.

4.1 Integrated Process Design

The new system, given in Figure 3.13, will be installed as part of the existing CBS1 pilot. An existing valve system enables the products to be sent to either the new separation system, the product drum that is currently being applied, or to waste collection. Reactor effluents are in the current design cooled to 90-110 °C, fully depressurised, further cooled to 40-60 °C and then collected in a drum where gaseous products are flashed off to vent. Liquid products are then manually separated at ambient conditions. In the new design, the products will not be cooled further after depressurization, but instead reheated to 100-200 °C in a counter-current double tube heat exchanger, which is installed but currently not used.

3-Phase Separation Vessels

The separation system will consist of two horizontally mounted Ø200 mm ID separation vessels with a total volume of 30 liter. The vessels, depicted in Figure 3.14, consists of an outer shell in 16MO3 and an inner lining in

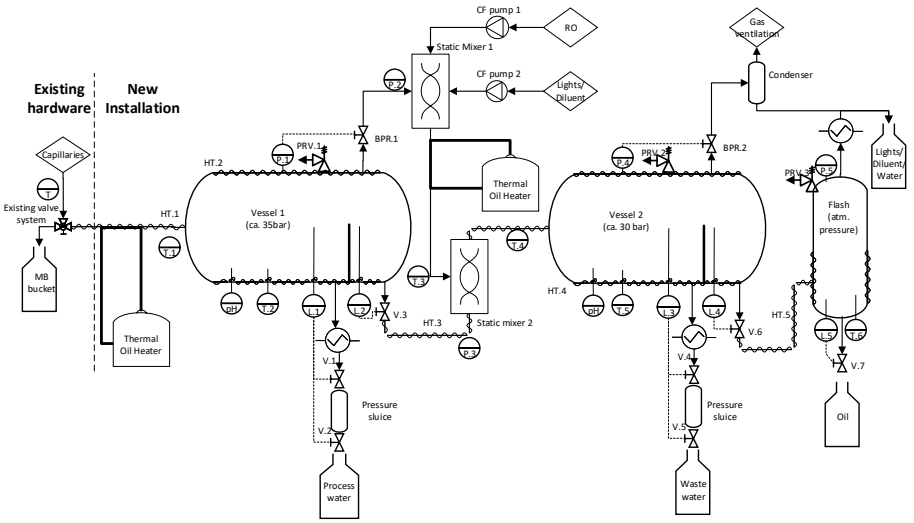

Fig. 3.13: PFD of new separation system designed for the CBS1 pilot plant.

SS316L. Further, the vessel consists of a large and a small chamber divided by an overflow plate (No. 4 in Figure 3.14). The aqueous product is discharged from the bottom of the large chamber, while the oil flows over the plate and is collected from the small chamber. Three different overflow plates with various heights are designed to vary the residence time between 15 and 30 min.

The separation vessels are designed for 50 bar and 200 °C. Pure CO_2 at 30 bar was used in Section 3.5, but since the CO_2 concentration of the liquefaction process gas is about 60 vol.% [Paper B,D], a higher design pressure is specified to allow a similar partial CO_2 pressure. The effect pressure and other parameters have on pH during separation can be evaluated using the pressure and temperature resistant pH probes that will be positioned in the aqueous phases of each tank.

The vessels and major product lines are heat traced to ensure accurate temperature control throughout the system. Elevated separation temperature reduces viscosity and density of the oil phase, which is beneficial for separation. On the other hand, a maximum separation temperature of 200 °C is chosen, because reduced water polarity makes phase separation less efficient at higher temperatures. E.g. the dielectric constant of water at 200 °C is halved compared to ambient conditions [Paper B]. [12] studied the separation of aqueous and organic phase after hydrothermal treatment of wood. A single phase appeared above 220 °C, the interface started to appear between

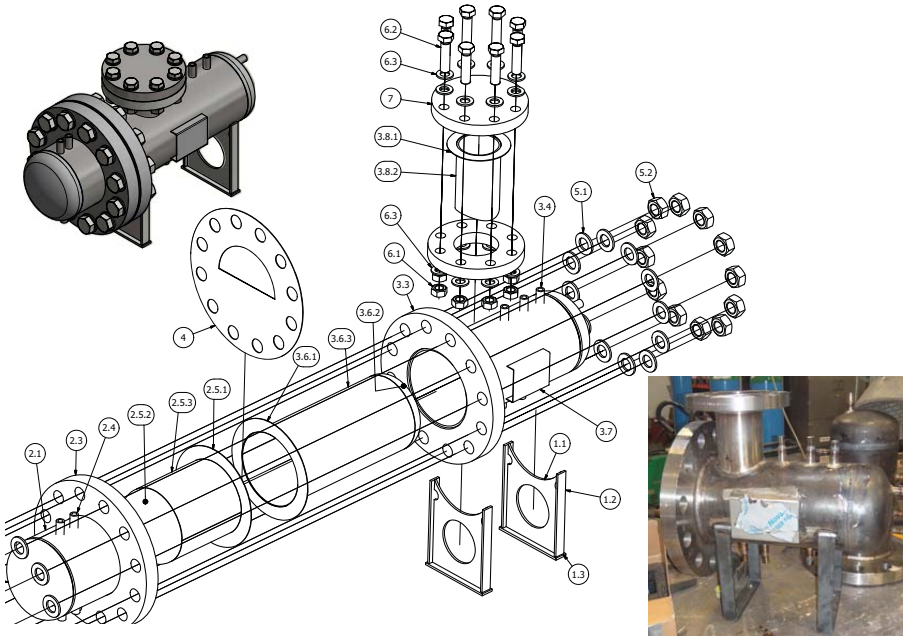

Fig. 3.14: CAD drawing of the 3-phase separation vessels and insert from fabrication.

180-220 °C, whereas clear phase separation occurred below 180 °C. [12] also observed a lighter color of the aqueous phase as separation temperature was reduced. This indicates that the separation temperature affects TOC of the process water, which is subject for evaluation when testing the new separation system.

Product Separation in 1st Separator

The 1st separator aims to separate off the aqueous product under reduced pH, obtained by the pressurized CO_2 rich gas. Separation at elevated temperature is beneficial because viscosity and density of the oil phase is reduced. A diluent would do the same, but it is undesirable to apply a diluent in the 1st separator, because some of it will end up in the process water. It is the hypothesis that the 1st separator will improve separation compared to gravimetric separation at ambient conditions, resulting in a lower inorganics and water content of the oil phase. The oil ash content was halved at similar conditions in SA5 in Table 3.7. Additionally, it is expected that the improved separation will result in a lower phenol and TOC content of the HTL PW, which in turn will improve the oil yield. Phenol is slightly acidic and forms salts with strong bases making the complex soluble in water. However, the phenol can be liberated from the salt using carbon dioxide at room tempera-

ture, which is why the CO_2 treatment is believed to reduce phenol content of the HTL PW [24].

Demineralization in 2nd Separator

The 2nd separator aims to demineralize the oil sufficiently to facilitate downstream upgrading, similar to the washing procedure that is currently applied. Though, the starting point is improved, due to the 1st separator that reduces inorganics content of the oil compared to gravimetric separation. Two static mixers are located upstream of the 2nd separator. The first mixes RO water with the process gas from the 1st separator, in order to obtain carbonated water with low pH. A diluent, such as MEK or lights, may potentially be added to the first mixer. Similarly, the RO water may be spiked with an acid or a deemulsifier to evaluate the performance of such. A 2nd mixer then mixes the carbonated water with potential additives, and the oil from the 1st separator. The mixture is then separated in the 2nd separator at conditions similar to the 1st separator, though obviously at a slightly lower pressure.

Oil Dehydration and Condensation of Lights

The process gas will depending on the operating temperature and pressure contain some water and lights. These are condensed and the remaining gas is analyzed with respect to volumetric flow rate and composition. The demineralised oil from the 2nd separator is depressurized and directed to a flash tank, where water, lights and a potential diluent are boiled off. The distillate is condensed, mixed with the gaseous product condensate and separated into an organic and aqueous phase in a phase separator. The two phases are expected to separate easily, similar to previous observations (Figure 3.8). The aqueous phase can be mixed with the washing water product, while the lights may be reintroduced into the oil and/or used as diluent in the 2nd separator.

Operation of Separation System

The numerous different product streams of the new separation system complicates establishment of overall process mass balances compared to the single product drum that is currently used at the pilot. However, constant volumetric flow rates of deionized washing water and potential diluent are ensured in order to easily subtract these from the final product yields. The relatively high pressure during separation results in a potential loss of dissolved gaseous products in both aqueous and oil phases. These gasses will appear as non condensates from both the flash unit and the process and waste water knock-out drums; and they are not quantified in the design of Figure 3.13.

Control of the water/oil interface is particularly important to e.g. avoid any carry-over of aqueous product to the oil chamber. The separation tanks of this system are too small to meet the specifications for any of the commercial interface level measures that are available. Thus, a pressure resistant, multi-point conductivity probe have been designed. The probe will be positioned vertically and provide 4 conductivity measurements around the oil/water interface, which can be used for automatic level monitoring.

The separation system provides high flexibility in terms of separation conditions, and the effect of different additives, acids, diluents, temperatures and pressures can be evaluated. The effect of recycling spent washing water from the 2nd separator can also be tested. Similarly, the use of lights as diluents can be tested, since these are readily available after the flash unit. Thereby, the system can be used to fine tune the separation technique and evaluate different process configurations that may potentially improve demineralization, reduce waste generation and operational costs of a commercial scale Hydrofaction^{TM} plant.

5 Conclusions on Demineralization

The HTL oil as produced from the CBS1 is a strong emulsion rich in inorganics and water. A continuous product separation and oil demineralization technique must be developed to allow subsequent catalytic hydrotreating. In the search for an effective approach the tests on filtering and centrifugation was found ineffective. Electrocoalescence improved speed of separation, but need to be combined with another demulsification approach such as pH reduction for effective demineralization. A successful washing procedure, using MEK as diluent and 0.1 M citric acid as washing agent, was developed for pilot scale, resulting in repeatable demineralization of Hydrofaction^{TM} oil to around 300 ppm ash and <50ppm metals. Use of the high pressure CO_2 rich HTL product gas as pH reducing agent represents a novel separation technique, which has been tested using carbonated water with promising results. The developments have been implemented in a flexible continuous separation and demineralization system that is to be commissioned at the CBS1 in Q3 2018.

References

[1] S. C. Blum, G. Sartori, M. L. Gorbaty, D. W. Savage, D. C. Dalrymple, and W. E. Wales, "Co2 treatment to remove organically bound metal ions from crude," Feb. 13 2001, US Patent 6187175.

[2] M. Chuang and M. Johannsen, "Characterization of pH in aqueous CO2-systems," in *9th international symposium on supercritical fluids (ISSF 2009), Arcachon, France*, 2009.

[3] J. Eastoe, *Microemulsions*. Colloid Science: Principles, Methods and Applications, John Wiley & Sons, 2010, ISBN: 9781444320190.

[4] D. C. Elliott, T. R. Hart, G. G. Neuenschwander, J. R. Oyler, L. J. Rotness, A. J. Schmidt, A. H. Zacher *et al.*, "System and process for efficient separation of biocrudes and water in a hydrothermal liquefaction system," Aug. 2 2016, US Patent 9404063 B2.

[5] J. S. Eow and M. Ghadiri, "Electrostatic enhancement of coalescence of water droplets in oil: a review of the technology," *Chemical Engineering Journal*, vol. 85, no. 2, pp. 357–368, 2002.

[6] J. S. Eow, M. Ghadiri, A. O. Sharif, and T. J. Williams, "Electrostatic enhancement of coalescence of water droplets in oil: a review of the current understanding," *Chemical engineering journal*, vol. 84, no. 3, pp. 173–192, 2001.

[7] E. Furimsky, "Selection of catalysts and reactors for hydroprocessing," *Applied Catalysis A: General*, vol. 171, no. 2, pp. 177–206, 1998.

[8] E. Furimsky and F. E. Massoth, "Deactivation of hydroprocessing catalysts," *Catalysis Today*, vol. 52, no. 4, pp. 381–495, 1999.

[9] J. H. Gary, G. E. Handwerk, and M. J. Kaiser, *Petroleum refining, Technology and economics, 5. Edition*. CRC Press, 2007, ISBN: 0-8493-7038-8.

[10] B. Gevert, P. Andersson, S. Jaeras, and S. Sandqvist, "Hydroprocessing of desalted directly liquefied biomass," *Prepr. Pap., Am. Chem. Soc., Div. Fuel Chem. (United States)*, vol. 33, no. CONF-8809228, 1988.

[11] J. M. Jarvis, N. M. Sudasinghe, K. O. Albrecht, A. J. Schmidt, R. T. Hallen, D. B. Anderson, J. M. Billing, and T. M. Schaub, "Impact of iron porphyrin complexes when hydroprocessing algal HTL biocrude," *Fuel*, vol. 182, pp. 411–418, 2016.

[12] D. Knezevic, "Hydrothermal conversion of biomass, PhD Thesis," http://dx.doi.org/10.3990/1.9789036528719, Enschede, Tech. Rep., 2009.

[13] F. S. Lupton and P. Edirisinghe, "Methods for removing contaminants from oils using base washing and acid washing," Jun. 2 2015, US Patent 9045698.

[14] Y. Mathieu, L. Sauvanaud, L. Humphreys, W. Rowlands, T. Maschmeyer, and A. Corma, "Opportunities in upgrading biomass crudes," *Faraday Discussions*, vol. 197, pp. 389–401, 2017.

[15] B. Meyssami, M. O. Balaban, and A. A. Teixeira, "Prediction of pH in model systems pressurized with carbon dioxide," *Biotechnology progress*, vol. 8, no. 2, pp. 149–154, 1992.

[16] J. G. Reynolds, "Demetalation of hydrocarbonaceous feedstocks using carbonic acid and salts thereof," Oct. 18 1988, US Patent 4778591.

[17] A. Schmidt, J. Billing, K. Albrecht, S. Fox, T. Hart, G. Maupin, L. Snowden-Swan, and R. Hallen, "Conversion of blended primary

and secondary sewage sludge into biofuels by hydrothermal liquefaction and catalytic hydrotreatment," http://www.gastechnology.org/tcbiomass/tcbiomass2017/Justin-Billing-Thu-tcbiomass2017-presentation.pdf, 2017, accessed: 03-11-17.

[18] L. J. Snowden-Swan, Y. Zhu, S. B. Jones, D. C. Elliott, A. J. Schmidt, R. T. Hallen, J. M. Billing, T. R. Hart, S. P. Fox, and G. D. Maupin, "Hydrothermal liquefaction and upgrading of municipal wastewater treatment plant sludge: A preliminary techno-economic analysis rev. 1," Pacific Northwest National Laboratory (PNNL), Richland, WA (US), Tech. Rep., 2016.

[19] J. G. Speight, *The refinery of the future*. William Andrew, 2010, ISBN: 978-0-81-552041-2.

[20] I. J. Stojkovic, O. S. Stamenkovic, D. S. Povrenovic, and V. B. Veljkovic, "Purification technologies for crude biodiesel obtained by alkali-catalyzed transesterification," *Renewable and Sustainable Energy Reviews*, vol. 32, pp. 1–15, 2014.

[21] S. J. Ubbels, "Methods for inhibiting naphthenate salt precipitates and naphthenate-stabilized emulsions," Aug. 17 2010, US Patent 7776930.

[22] L. Van de Beld, F. R. Boerefijn, G. M. Bos, F. Goudriaan, J. E. Naber, and J. A. Zeevalkink, "Process for the production of liquid fuels from biomass," Aug. 28 2007, US Patent 7262331 B2.

[23] V. B. Veljkovic, I. B. Bankovic-Ilic, and O. S. Stamenkovic, "Purification of crude biodiesel obtained by heterogeneously-catalyzed transesterification," *Renewable and Sustainable Energy Reviews*, vol. 49, pp. 500–516, 2015.

[24] M. Weber, M. Weber, and M. Kleine-Boymann, "Phenol ullmann's encyclopedia of industrial chemistry," 2000.

[25] J. J. Weers and S. Bieber, "Calcium removal from high TAN crudes," https://www.researchgate.net/file.PostFileLoader.html?id=55d4cec96307d905148b45a1&assetKey=AS%3A273835226533897%401442298813626, 2016, accessed: 04-10-17.

Chapter 4

Hydrotreating Hydrofaction^{TM} oil

Development of an upgrading technique for the Hydrofaction^{TM} platform targeting production of diesel, jet and/or marine drop-in fuels is a major research goal of the current project. The oxygenated and aromatic nature of liquefaction oil is detrimental to its compatibility with specifications of such fuels. Thus, the upgrading pathway need to facilitate deoxygenation and hydrogenation. In such application catalytic hydrotreating has been considered the obvious upgrading pathway to focus on.

Figure 4.1 illustrates the development progress of the PhD project, starting with parametric screening in microbatch reactors, over the first continuous tests in external facilities in Canada, to design, assembly and commissioning of a continuous multizone hydrotreater at AAU. Finally, the upgrading work include fractional distillation and collection of the first drop-in Hydrofaction^{TM} fuels.

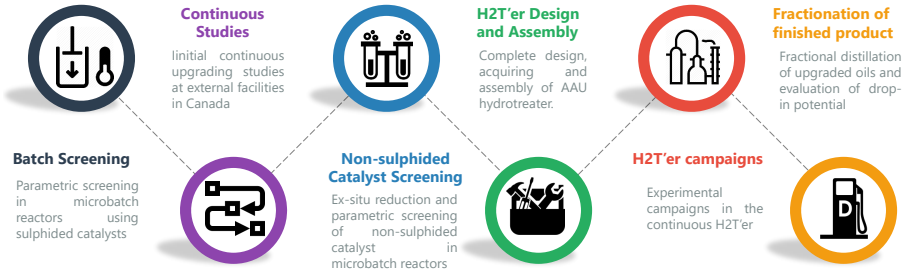

Fig. 4.1: Steps covered during development of a Hydrofaction^{TM} upgrading platform.

1 Literature Review on Hydrotreating

Hydrotreating is a widely-used process within conventional petroleum refining. The process applies heterogeneous catalysts, relatively high partial H_2 pressures (30-200 bar) and temperatures ranging from 300-450 °C. At the more severe temperatures the process is often referred to as hydroprocessing or hydrocracking. Hydrotreating is used for aromatic saturation and heteroatom removal, whereas hydroprocessing and hydrocracking aim to reduce the boiling point distribution by thermal and catalytic cracking respectively [17]. For the purpose of this thesis, hydrotreating is referred to as all catalytic processes involving HDO (hydrodeoxygenation), HYD (hydrogenation), HDM (hydrodemetallisation), HDS (hydrodesulphurisation), HDN (hydrodenitrogenation) and/or hydrocracking of an oil in the presence of hydrogen.

1.1 State of the Art on Continuous Hydrotreating of HTL Oil

Several review papers have pointed towards the lack of continuous upgrading studies as the barrier for further development of HTL oil upgrading [12, 20]. The following summarize state of the art on continuous hydrotreating of HTL oil.

In the early development years around 1980, Shell carried out initial upgrading of their biocrude in continuous microflow reactors. Due to limited amounts of oil only a few experiments with unknown duration were carried out [28]. Elliot and Baker presents both batch and continuous hydrotreating tests on model compounds and wood derived oils from the Albany facility [10]. The continuous hydrotreating studies were reported too short (<10 HoS) to be conclusive on steady state operation and catalyst deactivation. [2] observed catalyst deactivation due to sodium during continuous hydrotreating of a HTL oil with 3 wt.% sodium. Deoxygenation declined linearly during the 48 HoS. [18] compare hydroprocessing of a wood derived HTL oil versus iso-octane and xylene extractives. Higher deoxygenation and cracking conversion was observed for the entire oil compared to the extractives, and it was concluded that extraction before hydroprocessing is unnecessary.

More recently, a comprehensive study by Jarvis et al, [19] evaluates the impact of iron porphyrin complexes during continuous hydrotreating of algae derived biocrude. The algae biocrudes contains 700-1300 ppm iron, of which most was deposited in the catalyst inlet forcing a shutdown after 102 HoS in one experiment. ICP analysis of the catalyst bed after reaction show clear deposition of both iron, potassium and sodium at the very inlet of the catalyst bed. The iron was reported to be present as porphyrin complexes

before hydrotreating, whereas these complexes were absent after hydrotreating. An effect of catalyst bed packing was also reported. An extra length of extrudates at the inlet worked as demetalization guard bed and the experiment was run for 220 HoS without shutdown [19].

Additional continuous hydrotreating studies by PNNL include upgrading of HTL biocrude from waster water treatment sludge using a sulphided cobalt molybdenum (CoMo) catalyst for around 300 HoS without deactivation [4, 25]. [13] reports on continuous hydrocracking at 405 °C of 4 different algae derived HTL oils, all producing a low density (<800 kg/m^3) hydrocarbon product with about 80-85 % diesel range distillate. No details on upgrading duration or catalyst deactivation are provided [13]. [11] reports on upgrading of a wood derived HTL oil for more than 200 HoS without deactivation on a sulphided CoMo catalyst. Hydrogen consumption was 0.042 g H_2/g oil and mass and volumetric yields were 86 % and 107 % respectively. The 150-350 °C diesel equivalent fraction constitute 61 wt.% of the product and has a density of 900 kg/m^3 [11].

Mathieu et al. report on continuous hydrotreating of a wood derived biocrude provided by Licella [23]. More specifically, the heaviest 20-30 % are separated off by flashing and the distillate is hydrotreated. Complete deoxygenation and hydrocarbon recoveries around 87 wt.% are observed at relatively mild hydrotreating conditions (40 bar, 350 °C, 0.5 h^{-1}) on a sulphided nickel molybdenum (NiMo) catalyst. The resulting product with a density of 916 kg/m^3 is reported to contain around 60 wt.% aromatics as well as a large portion of polycyclic naphthenes [23].

The relatively dense upgrading products reported by [11] and [23], emphasize the need for deep hydrogenation and possibly ring-opening when targeting diesel production from a wood derived oil that is aromatic in nature. In comparison, the density is almost too low compared to disel specifications after upgrading algae derived HTL oils with high molecular linearity [13].

The upgrading work conducted as part of this PhD project advances state of the art on continuous hydrotreating by means of hours on stream and resulting product quality. Paper A presents stable hydrotreating of Hydrofaction^{TM} oil with 660 HoS, and similar unpublished hydrotreating campaigns resulting in state of the art product quality are presented later in this chapter.

1.2 Irregularities of Hydrotreating Liquefaction Oil

The differences between petroleum hydrotreater feeds and liquefaction oil need to be identified when adapting conventional hydrotreating processes to Hydrofaction^{TM} oil. [8] provides an excellent review on peculiarities regarding hydrotreating of Fischer-Tropsch (FT) syncrude. While FT syncrude and Hydrofaction^{TM} oil differ on molecular linearity, they are similar in the way in which they are different from petroleum crude. Both contain around 10 wt.% oxygen, a high TAN, a high number of C=C doublebonds and very low concentrations of nitrogen and sulphur. In relation to conventional hydrotreating, these characteristics induce several issues, which are discussed in the following.

Presence of Water

Wood derived Hydrofaction^{TM} oil contains around 10 wt.% oxygen, which will mostly be converted to water during HDO. Thus, there will be about 10 wt.% water in the liquid products after complete HDO, and the partial pressure of water during reaction is very high compared to conventional hydrotreating. The effect of water seems to be very catalyst and feedstock dependent, but several reviews state that water absorbs on the active catalyst sites, which reduces both activity and selectivity [15, 16]. Further, water causes irreversible deactivation through structure changes of conventional catalyst [8, 15, 16].

High Heat Release

Hydrogenation and in particular hydrodeoxygenation are often rapid and highly exothermic reactions resulting in significant heat release and high hydrogen consumption. In fact, the heat released per mass of heteroatom is about 2-4 times larger for oxygen removal compared to sulphur removal [8]. Meanwhile, the heteroatom content is 1-2 orders of magnitude higher for HTL oils compared to petroleum crude. As a result, the heat release during hydrotreating of HTL oil is around 20-200 times larger than during HDS of a petroleum feed. This is without considering the heat release from hydrogenation. Rapid temperature increase and hydrogen starvation around the active catalyst sites induce the risk of deactivation, coking and fouling of the catalyst beds, and pressure drop build up [9]. Thus, temperature control of the reactor is an extremely important aspect of the upgrading process design.

Coking Propensity

The aromaticity and in particular the PAH content of a hydrotreater feed relates to the risk of catalyst deactivation by coking. Additionally, oxygenates

and in particular methoxy- and diphenols are coke precursors [16]. Wood derived Hydrofaction^{TM} oil is rich in both aromatic and phenolic compounds, and the micro carbon residue (MCR) of 15-20 wt.% (Table 2.1) is high compared to conventional hydrotreating feeds. Thus, it is important to try and reduce the coking propensity during hydrotreatment. Coking proceed mainly via polymerization or polycondensation type reactions. Catalyst acidity, including that of the support, facilitate coking, and thus the choice of catalyst need to balance the activity of hydrocracking against the rate of coking [16]. Further, the presence of sulphur affects the availability of acidic sites, so these parameters are related.

Higher partial hydrogen pressures promote hydrogenation and conversion of coke precursors into stable products rather than coke. Further, a higher hydrogen availability inhibits coking by reducing hydrogen starvation around the active sites [16, 17]. Generally higher temperatures at around 400 °C favors dehydrogenation, which in turns increases coking. However, there are incidences with heavy feeds, where coke formation was reduced by increasing the temperature. [16] infers that the rate of conversion for heavy compounds can be increased by increasing the temperature. This reduces the time that the heavy compound is adsorbed to the catalyst surface, which in turn reduces the risk of polymerisation and coke formation. Precipitation issues have been observed in relation to upgrading of Hydrofaction^{TM} oil, where feed and upgraded product are insoluble. [16] states that coking from precipitation of heavies such as asphaltene-like compounds, can be reduced by a higher temperature that increases conversion and thus reduces precipitation of the heavy compounds. Finally, coking may be the result of local hot spots formed by exothermic reactions and insufficient heat transfer.

Hydrogen Dissolution

Reduced solubility of hydrogen in the polar oxygenated oil is considered a concern, as hydrogen availability around the active catalyst sites is important to suppress coke formation, especially considering the high reactivity and exothermicity of HDO type reactions. IFP has a pending patent application [24] that focus on pyrolysis oil, but is applicable to liquefaction oils. The method comprises mixing the biooil in a hydrocarbon type liquid with the aid of a dispersing agent, both preferably being recirculated streams of partially upgraded products. The major motivation for dispersing the biooil is improved hydrogen dissolution in a less polar mixture [24]. Simiarly, [21] by Korea Institute for Science and Technology, claims a method for co-processing fats or vegetable oils with a supercritical solvent such as CO_2, C_2-C_7 alkanes, dimethyl ether etc. The higher solubility of hydrogen is claimed to enable a lower operating pressure [21]. During upgrading of Hydrofaction^{TM} oil,

the presence of lights have been observed to reduce pressure drop build-up, which may relate to improved hydrogen dissolution.

Low Sulphur Concentration

The low sulphur content of wood derived HTL oils impose a catalyst stability issue for conventional sulphided catalysts, because catalyst sulphur is gradually desorbed from the active sites. As a consequence, it is widely used to add sulphur in form of dimethyl disulphide (DMDS), carbon disulphide (CS_2), hydrogen sulphide (H_2S), etc. to the biocrude subject for hydrotreating.

Similar to water, the effect of sulphur during HDO is catalyst and feed dependent [15]. [26] observed that increasing H_2S concentrations promoted HDO of aliphatic oxygenates, while it inhibited the HDO of phenol due to competitive adsorption. Further, different effects of H_2S were observed on a NiMo versus CoMo based catalyst in its sulphided state [26]. Likewise, the presence of sulphur during HDO on conventional catalysts has been reported to both counteract the negative effect of water, but also inhibit hydrogenation activity [15]. [22] studied the effect of sulphiding during HDO of vegetable oil on a sulphided CoMo based catalyst. Without addition of sulphur, the deoxygenation decreased steadily to 75 % after 144 HoS, whereas it remained above 95 % when 0.5 wt.% DMDS was added continuously. Addition of DMDS in pulses only partially restored deoxygenation activity. Further, [22] reports that the presence of sulphur primarily restored activity of the acidic sites, promoting the decarboxylation activity. Thus, it can be inferred that sulphidation affects mostly the acid sites that facilitates cracking and decarboxylation type reactions.

Presence of Carbon Oxides

CO and CO_2 are present in the gaseous products from hydrotreating of oxygenated oils. Since hydrotreating catalysts also are active for both reverse water gas shift and methanation reactions, it is difficult to deduct the origin of the carbon oxides. [9] observed that CO during hydrotreatment of light gas oil inhibit catalyst activity for the CoMo based catalyst, due to competitive adsorption. Addition of 1 % CO in 99 % H_2 reduced the HDS and HDN activity to 40 % and 60 % respectively. No or little effect was reported for the NiMo catalyst. The CO deactivation is reversible, so the activity is restored if the CO is removed.

[3] observed that CO_2 inhibits HDS, HDN and HYD conversion during hydrotreating of straight run gas oil on a CoMo based catalyst. The concentration of CH_4 increased, while CO and H_2O only appeared in the product gas, when CO_2 was present, indicating that reverse water gas shift and

methanation reactions occurred when CO_2 was co-fed [3]. Thus, the presence of carbon oxides during hydrotreatment of oxygenated oils will increase the hydrogen consumption through competing reactions, and it may reduce catalyst activity.

Effect of Inorganics

Iron is identified as the major trace metals in Hydrofaction^{TM} oil after washing (Figure 3.10). If demineralization efficiency for some reason decreases sodium and potassium are the most likely types of inorganics to appear. [16] provides a thorough review on deactivation of hydrotreating catalysts, including the effect of metals on catalyst activity. Iron has little effect on overall deactivation, though some inhibiting effect on hydrogenation activity. Sodium and alkali metals in general have a detrimental effect on catalyst activity and on hydrocracking in particular. This is because the alkalis inhibit the effect of acidic catalyst sites, which are important in cracking reactions [15, 16].

1.3 Reactor types and Catalyst Packing

Fixed bed, moving bed and ebullated (or expanded) bed are the three different hydrotreating reactor types that are commercially available. The continuous hydrotreating tests presented in this thesis are all conducted in co-current fixed-bed reactors. Firstly, it is by far the simplest configuration to test in laboratory scale. Secondly, it is the most common reactor type and the cheapest with respect to both installation and operational costs. Thus, it is commercially interesting to evaluate the fixed-bed approach. With that said, the moving and ebullated beds have interesting features in relation to hydrotreating of rather difficult feeds such as Hydrofaction^{TM} oil. Spent catalyst is continuously withdrawn and replaced with fresh catalyst from moving and ebullated beds. Thereby, they enable stable processing of feeds with higher metal contents, but at the cost of a higher catalyst consumption compared to fixed-bed hydrotreating. The reactor effluent from an ebullated bed is recycled and mixed with the feed to obtain sufficient velocity to keep the bed fluidised. The fluidisation improves mass transfer, and it allows small solid particles to exit the reactor, thereby avoiding accumulation and pressure drop build-up. The dilution of the feed reduces rates of reaction and the rate of heat release from exothermic reactions. On the other hand, the amount of catalyst required to reach the same conversion level is up to three times higher for ebullated beds compared to more plug-flow type fixed- and moving bed reactors. [14, 17]

Based on the take home messages of the previous section on irregularities

of hydrotreating HTL oil, it would be interesting to evaluate the potential of an ebullated bed configuration for the Hydrofaction^{TM} platform. Improved mass transfer, reduced reaction rates, better control of heat release, potential flushing of coke particles and improved hydrogen dissolution in the partially upgraded reactor effluent that is recycled. These are all features that make an ebullated bed interesting to evaluate in future work.

Packing of Fixed Catalyst Beds

Catalyst bed activity depends on catalyst wetting, flow distribution and liquid hold-up, which in turn depend on how the catalyst bed is initially packed. Catalyst bed packing is particularly important in relation to pilot reactors, because the ratio between bed volume and the catalyst extrudate is significantly smaller for a pilot reactor compared to a commercial scale reactor. Thus, the extrudates will not pack as densely in a pilot reactor, where the impact of e.g. reactor walls and a centered thermowell will be larger. Consequently, liquid channeling, incomplete catalyst wetting and limited mass transfer may deplete conversion of a pilot reactor compared to a large scale reactor [5].

Regarding packing of the catalyst bed it has been suggested to dilute the catalyst with small inert particles to fill up the void spaces and improve the flow pattern, contact time, mass transfer and heat distribution [1, 5, 6, 14, 29]. Further, [5] observed improved conversion by use of a graded bed with a higher catalyst dilution at the inlet (11% loading) compared to the remaining bed (44% loading). This is believed to be particularly important in relation to hydrotreating Hydrofaction^{TM} oil, due to temperature control of rapid exothermic reactions. Graded and diluted beds were used in Campaign 3-5 presented in Section 4.

2 Major Findings of Parametric Studies

Parametric hydrotreating studies of this project span from quick microbatch experiments to continuous hydrotreating campaigns in external facilities in Canada extending up to 660 hours on stream. It needs mentioning that the continuous tests in Canada were contracted externally, organised by J.K. Rodriguez and the PhD work in this regard comprise product analysis and data treatment only. Major findings of the parametric studies are gathered in this section.

Catalyst selection is an important aspect of hydrotreating development work, but it has not been in focus during the PhD project. Different catalysts are already being screened as part of other development projects in Steeper

Energy, but besides a few digressions, the same $NiMo/Al_2O_3$ catalyst has been used throughout the PhD project. The Criterion DN3630 catalyst is designed for severe HDN and HYD of fossil derived middle distillates for ultra low sulphur diesel production [7], and thus not at all designed for an oxygenated crude. Catalyst characteristics that are likely to be in focus during optimisation of the catalyst choice include: pore size distribution, water resistance, acidity, hydrogen dissociation, HDO selectivity, metal storage capacity etc. Unless otherwise is noted, the following results are all based on hydrotreating using the DN3630 catalyst in sulphided state. For the microbatch experiments, a preactivated and stabilised DN3630 trilobe extrudate catalyst from Criterion was supplied by Shell, Denmark. The same catalyst in regenerated form was used in the continuous studies and activated by in-situ sulphidation prior to feeding biocrude. Experimental procedures for the different reactor systems are described in Paper A and F.

2.1 Operating Parameters

Temperature affects reaction kinetics and below 300 °C kinetics are too slow to obtain any significant deoxygenation nor hydrogenation. Being dependent on other parameters too, complete deoxygenation has often been obtained at temperatures equal to or higher than 350 °C. A higher degree of cracking is observed at 370 °C, but at the cost of a reduced degree of hydrogenation (A and F). This observation matches the fact that the equilibrium is shifted, because cracking and hydrogenation reactions are endo- and exothermic respectively. Alternatively, the observation may also relate to kinetics being the rate limiting parameter at lower temperatures, versus hydrogen transfer to the active sites being rate determining at elevated temperatures, where reaction kinetics are faster, thus requiring a higher mass transfer to avoid hydrogen starvation. The latter induces risk of increased coking and deactivation.

Pressure affects the hydrogenation equilibrium, it improves dissolution of hydrogen in the liquid phase, and generally, a higher partial hydrogen pressure improves saturation reactions if temperature/kinetics is not the rate limiting parameter. Improved conversion by increasing pressure is evident from the microbatch results presented in F, but also from unpublished results from continuous studies where three different pressures were tested at 320 °C and a weight hourly space velocity (WHSV) of 0.5 h^{-1}. Selected product properties are listed in Table 4.1 and generally a higher pressure resulted in improved product quality. The continuous hydrotreater used in Canada had a maximum operating pressure of 66 bar. This is relatively low in relation to upgrading biocrude, and this limitation was some of the motivation behind designing a new hydrotreater at AAU.

Exp.#	Pressure [bar]	TAN [mg KOH/g]	Viscosity at 20 °C [cP]	Density at 15 °C [kg/m^3]	IBP-350 °C distillate [%]	H_2 cons. [g/g oil]
Feed	-	48.0	14429	1071	28.9	-
C3-HD14	34	0.0	618	1001	50.0	0.014
C3-HD13	55	0.0	399	995	51.4	0.016
C3-HD7	66	0.0	238	981	54.0	0.017

Table 4.1: Effect of operating pressure during continuous hydrotreating at 320 °C, 900 NL/L and a WHSV of 0.5 h^{-1}. Unpublished results from the S-spiked campaign partly presented in Paper A. The numbers reflect the average of two mass balances for each set of conditions.

Hydrogen availability reflects the ratio between feed rate of H_2 and oil, and it therefore relates directly to partial H_2 pressure. The hydrogen availability was varied from 150 to 550 normal liter (NL) per liter oil during microbatch reactor screening [Paper F]. An increasing H_2 availability was observed to improve both deoxygenation and hydrogenation. Effect of hydrogen availability is however not as straightforward when it comes to continuous fixed bed reactors, because a change of H_2 to oil ratio affects not only partial H_2 pressure, but also reactor residence time and mass and heat transfer. [6] studied the dynamic effects of a changed hydrogen feed rate in a fixed-bed pilot-plant hydrotreater used for hydrogenating partially stabilized light-coker naphtha. A decrease in volumetric H_2 feed rate, which corresponds to a decrease in partial H_2 pressure, increased the catalyst bed temperature. The observation was the effect of three dynamics; 1) lower heat diffusion out of the reactor with a lower gas flow; 2) increased reaction rate by increased concentration of olefins; and 3) increased conversion due to longer residence time of the liquid reactants [6]. Similar observations were done during continuous hydrotreating of Hydrofaction^{TM} oil. These are listed in Table 4.2, where an increase of H_2 availability decreased the product quality. Consequently, it is appealing to lower the H_2 availability, but it is a general guideline for fixed bed hydrotreating that a higher partial pressure reduces catalyst deactivation [16, 17, 27].

Exp.#	H_2 avail. [NL/L]	TAN [mg KOH/g]	Viscosity at 20 °C [cP]	Density at 15 °C [kg/m^3]	IBP-350 °C distillate [%]	H_2 cons. [g/g oil]
Feed	-	55.7	80432	1103	33.2	-
C1, cond. 2	600	0	89	969	55.7	0.029
C1, cond. 3	900	0	118	1013	54.4	0.022

Table 4.2: Effect of H_2 availability during continuous hydrotreating at 350 °C and a WHSV of 0.5 h^{-1}. Unpublished results from a non-spiked campaign conducted in the same experimental setup as that dexcribed in A.

Space velocity is inversely proportional to the time the oil is exposed

to the active catalyst and it is not surprising that a reduced space velocity improves conversion. Figure 4.2 presents product density and viscosity obtained at different space velocities during the S-spiked campaign, which is partly published in A. The space velocity was varied at two different temperatures, but a similar effect of WHSV is observed at both 300 °C and 350 °C.

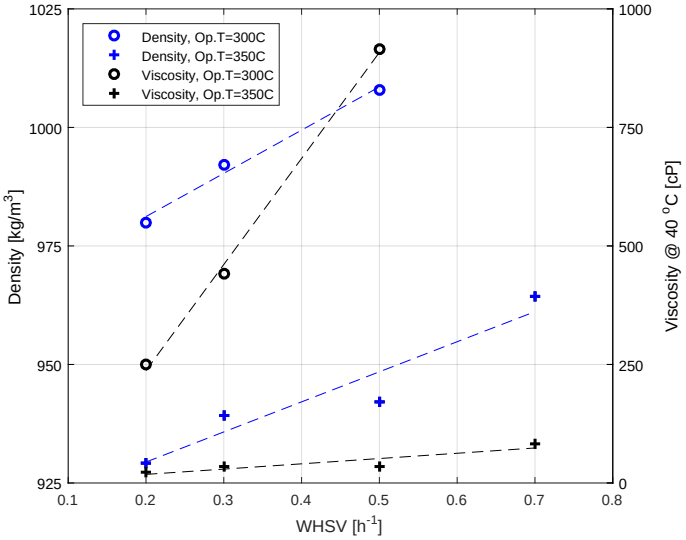

Fig. 4.2: Effect of WHSV during continuous hydrotreating. Unpublished results from the S-spiked campaign partly presented in A.

H2 consumption Hydrotreating of Hydrofaction^{TM} oil aims to maximise hydrogenation of the aromatic feedstock in order to obtain a high cetane, low density diesel and marine fuel. A deeper hydrogenation results in a lower product density, which in turn results in a higher volumetric yield. A high voluemtric yield is desirable, since fuel products are most often sold on a volumetric basis ($ per barrel, liter or gallon) Consequently and counter-intuitively, a high consumption of costly H_2 is desirable as long as it is not consumed in secondary reactions such as methanation and reverse water gas shift.

Figure 4.3 plots the hydrogen consumption as function of density for the partially upgraded products obtained during the S-spiked campaign described in Paper A. The linear relationship can be used to roughly estimate the H_2 consumption associated with fully upgraded / refined Hydrofaction^{TM} products. Observations indicate that the bulk oil density after hydrotreating has to approach 900-880 kg/m^3 in order for the diesel fraction to meet density specifications. According to the trendline in Figure 4.3, this would corre-

spond to a hydrogen consumption around 0.030-0.035 g/g oil.

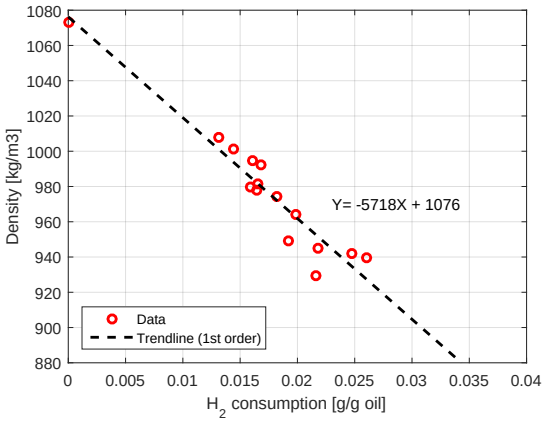

Fig. 4.3: Density of partially upgraded products as function of hydrogen consumption. Data are from the continuous S-spiked campaign described in A.

2.2 Heteroatom Removal and Catalyst Activity

Oxygen is the most abundant heteroatom in wood derived HTL oils, and it affects the physiochemical properties (density, viscosity, volatility, polarity, hydrophobicity), which determine its compatibility with petroleum equivalents. In fact, it is a main conclusion of Paper D that oxygen's effect on biocrude volatility need to be acknowledged in order not to underestimate the potential of a biocrude or the corresponding technology/feedstock. Deoxygenation by mild hydrotreating has been shown to reduce volatility and improve distillate yield by up to 75%. Thereby, distillation quality of the oil shifts from a heavy and troublesome crude, to one having a larger diesel fraction than the benchmark Brent crude oil. [Paper D]

Of the numerous different oxygenates present in wood derived HTL oil, the substituted phenolics are the most difficult compounds to deoxygenate [Paper C, D]. This is due to ring stabilistion, steric hindrance and adsorption phenomena [30]. Figure 4.4 compares qualitative Py-GCxGC-MS of the oil before and after hydrotreatment. While the biocrude contains mostly PAH's, phenolics and fatty acids, the remaining oxygenates after hydrotreatment are long chained alcohols and highly substituted phenolics.

Nitrogen is discussed in Paper D, which presents a study on the effect of using ammonia as alkaline agent during HTL instead of NaOH. The resulting biocrude was polluted with nitrogen, which seemed to have an ef-

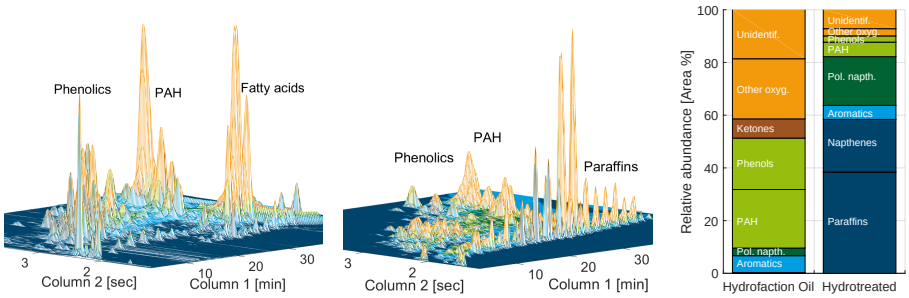

Fig. 4.4: Copied from poster presentation at EUBCE 2016, Amsterdam.

fect on conversion during hydrotreatment. Heteroatom removal, including both oxygen and nitrogen removal, was reduced compared to upgrading of a standard Hydrofaction^{TM} oil. Similarly, and possibly as a consequence of the lower deoxygenation, the improvement in boiling point volatility was also reduced. This is not surprising, as nitrogen is the most common catalyst poison wihtin petroleum hydrotreating, due to strong adsorption to especially the acid sites [16]. Ammonia was discarded as an option due to additional disadvantages and the nitrogen content of wood derived Hydrofaction^{TM} oil is around 0.1 wt.% [Paper A], which is below normal concentrations within petroleum refining. Though, the negative effect of nitrogen during upgrading is noteworthy in the light of other nitrogenous HTL feedstocks such as algae, manure, sewadge sludge, grass etc. that are often mentioned as suitable feedstocks for advanced biofuel production.

Sulphur removal is the main objective of hydrotreating within petroleum refining. In such process, use of sulphided bimetallic catalysts is common, and the catalyst stays active from the sulphur that is removed from the feed. Wood derived Hydrofaction^{TM} oils are characterised by a low sulphur content. This is an advantage in relation to meeting fuel specifications, but an issue in relation to hydrotreating on conventional sulphided catalysts. Paper A presents data from continuous hydrotreatment of a 309 ppm S Hydrofaction^{TM} oil versus a Hydrofaction^{TM} oil spiked to 1 wt.% S. The campaigns last for 380 and 660 HoS respectively. Figure 4.5 illustrates how the H_2S concentration is stable throughout the S-spiked campaign, whereas it drops to below detection level during the first 150 HoS in the non-spiked campaign. As a consequence, it was observed that the sulphided catalyst loses both hydrogenation and cracking activity resulting in a deoxygenated, but lower quality product.

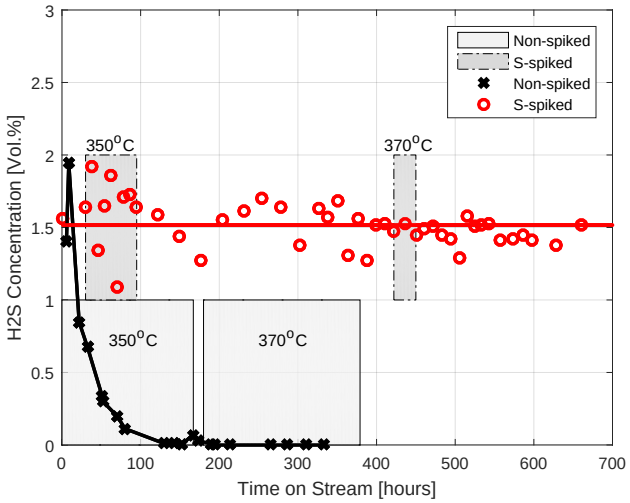

Fig. 4.5: H_2S concentration of the product gas during continuous hydrotreating of a spiked and non-spiked oil. [Paper A]

2.3 Non-sulphided Catalysts

The potential of non-sulphided catalysts is relevant due to the low-sulphur content indigenous to Hydrofaction^{TM} oil. Paper A reports on the initial screening of nickel wolfram (NiW) and palladium (Pd) based catalysts. The screening was carried out in microbatch reactors, and based on promising results a two-zone reactor configuration is suggested and claimed in Patent application G.

The stability and activity of the non-sulphided catalysts used in Paper A were recently evaluated in a continuous 2-zone test. The campaign was carried out in the continuous hydrotreating unit that will be presented in the following sections. The NiW and Pd based catalyst was loaded in reactor 1 (R1) and R2 respectively. Catalyst activation protocols and operating conditions were copied from the microbatch experiments, except that the catalysts were activated in-situ and not stabilised with 1 % O_2 in N_2 after reduction. A standard quality wood derived Hydrofaction^{TM} oil was used as feed, and during 100 hours of smooth operation, temperatures between 350 °C and 400 °C were tested in R1.

Deoxygenation and hydrogenation was very disappointing, with more or less no conversion, except a slight increase of the H/C ratio. Figure 4.6 shows the temperatures inside the catalyst bed as function of time at the very beginning of the non-sulphided test. When the first oil feed contacted

the catalyst, temperatures increased dramatically to 380 °C in the first part of the bed, indicating large exoterms. Consequently, the furnace setpoint was immediately reduced to avoid temperature runaway. Over the next 2 hours, the location of the highest temperature moved slowly down through the bed. After these 2 hours, temperatures were stable, the exoterms were gone and the furnace setpoint had to be increased again to keep the desired temperature.

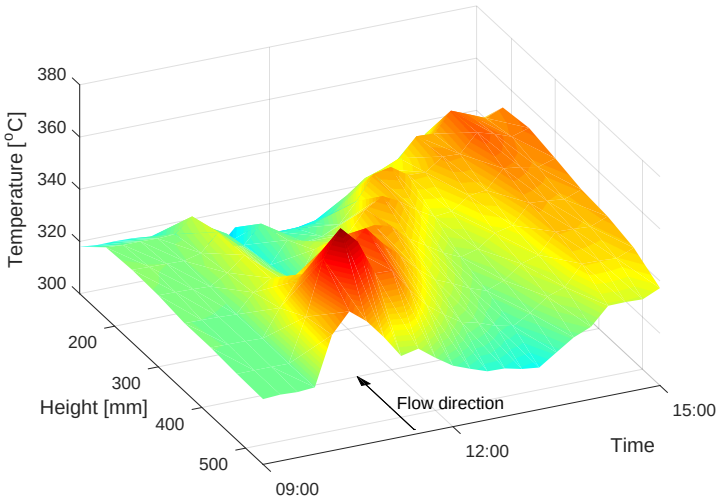

Fig. 4.6: Temperature dynamics in catalyst bed when the first oil enter the reduced catalyst. Reactor height = 500 mm is at the inlet of the catalyst bed, while 120 mm reflects the bed outlet.

[6] reports that the actual bed temperature may be up to 60 °C higher than that measured in a similar thermowell inside the reactor. The study was on a larger pilot reactor, and thus in the current test the difference between the actual bed and thermowell temperature may have been even higher. With that reasoning it is likely that the non-sulphided catalyst deactivated immediately due to poor control and resulting temperature runaway. No further tests of these non-sulphided catalysts have been prioritized, as focus shifted back to the conventional sulphided NiMo catalyst.

3 Considerations on H2T'er Design

A continuous hydrotreating unit (now H2T'er) was designed, assembled and commissioned as part of the industrial PhD project. The H2T'er was designed to solve some of the limitations that were identified for the external unit(s), used for the initial continuous studies. Features and design consid-

erations will be presented in this section, while a detailed description of the system is given in Appendix i. Figure 4.7 visualizes the time line of the entire project including application for funding, detailed engineering, assembling, commissioning and experimental testing. Except application for funding, the entire project was mainly done by the PhD candidate and Postdoc Daniele Castello, AAU. The H2T'er is funded by a hardware grant from the Obel Family Foundation. Although delayed several months by new laboratories that were not finished on time, the H2T'er was commissioned soon enough to complete 5 campaigns on Hydrofaction^{TM} oil and include the results in this thesis. Pictures of the unit are given in Figure 4.8.

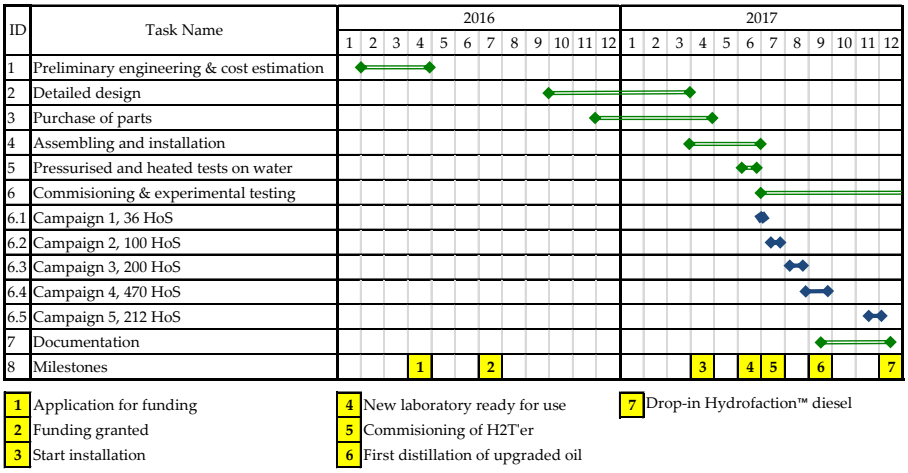

Fig. 4.7: Timeline of the AAU H2T'er project.

Fig. 4.8: The H2T'er unit during installation (left) and after commissioning (right).

3.1 Design and Features

The H2T'er is a dual reactor, continuous fixed-bed hydrotreating pilot unit, depicted by a PFD in Figure 4.9. The nominal oil feed flow rate is 30 $^{mL}/_{h}$, at a WHSV of 0.5 h^{-1} for each reactor and a H_2 availability of 1000 $^{NL}/_{L}$ oil. Though, the unit is flexible in terms of operating conditions and span at least 15-120 $^{mL}/_{h}$ oil feed, space velocities from 0.05-4 h^{-1}, and H_2 availabilities between 100-4000 $^{NL}/_{L}$. Further, the system is rated for 200 bar, and a maximum operating pressure of 150 bar. This is a significant advance relative to the limit of 66 bar for the unit used for initial studies in Canada. Table 4.3 lists additional differences between the two continuous hydrotreating units.

	External unit	H2T'er
Nominated oil flow	30 $^{mL}/_{h}$	30 $^{mL}/_{h}$
Operating pressure	Up to 66 bar	Up to 150 bar
Gas supply	N_2, H_2	N_2, H_2, CH_4, CO_2
Reactor heating	Heating cables	Tubular furnace
Reactors	1	2
Reactor mode	Up flow	Down flow
Monitoring of exoterms	No	Yes
Separation pressure	Operating pressure	Can be varied
Location	Calgary, Canada	Aalborg, Denmark
Results available in	Paper A	Thesis

Table 4.3: Comparison of the continuous hydrotreaters used in the PhD project.

Feeding of Reactants

Oil is pressurised and fed at a constant volumetric flow rate using a dual cylinder syring pump, which automatically refills from a 20L oil tank. The oil temperature and thus density is kept constant using a heating circulator. This is important in order to convert the volumetric flow rate to mass flow for mass balance closure. The oil is mixed with hydrogen before any further substantial heating to stabilise reactive compounds and reduce polymerization and condensation reactions during heating.

The gas supply includes nitrogen, hydrogen, carbon dioxide and methane, all being controlled by mass flow controllers. Nitrogen is used for various utilities and catalyst drying during activation protocols. Hydrogen is obviously a necessity during hydrotreating, and the flow control range span a wide range of hydrogen availabilities. CO_2 and CH_4 are produced during hydrotreating of oxygenated oils and will be present in the gaseous product together with excess hydrogen. Recirculation of the hydrogen rich gas product is common for H_2 recovery in commercial scale hydrotreaters. Based thereon, it is relevant to study the effect of these gases in minor concentrations during hydrotreating. Similarly, it is relevant in relation to recovery and

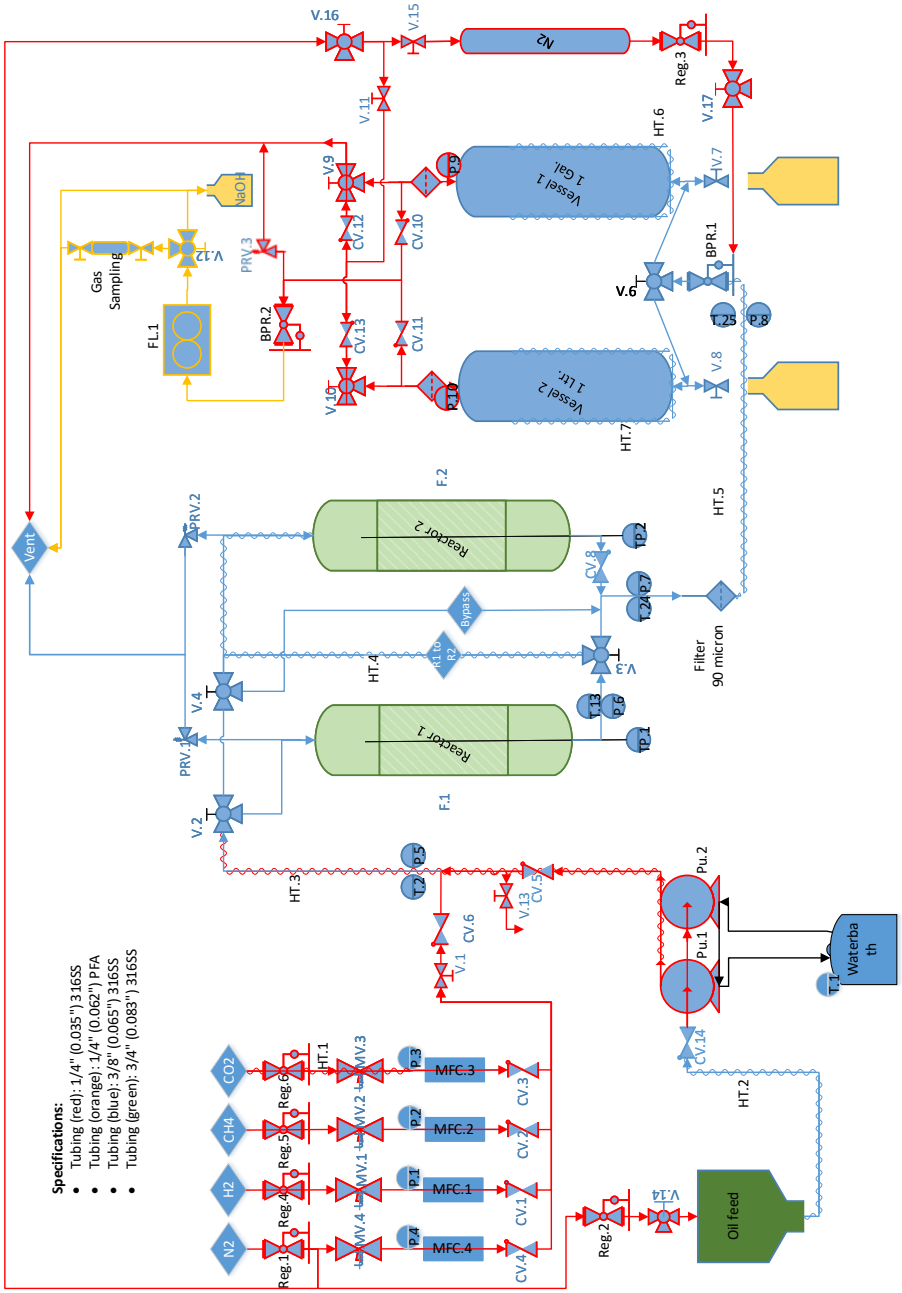

Fig. 4.9: PFD of multizone H2T'er.

use of the hydrogen produced during HTL. Such hydrogen stream, depending on the purification efficiency, will contain some CO_2 and CH_4, as they are the major compounds in liquefaction gaseous products. As mentioned previously, similar studies tested the effect of CO and CO_2 during hydrotreating of vegetable oil and light cycle oil [3, 9].

Multi Reactor Configuration

The H2T'er consists of two co-current down flow fixed bed reactors, each surrounded by tubular furnaces. A down flow configuration was chosen based on what is mostly used in commercial hydrotreaters, because the results reported in literature on the effect of down flow versus up flow mode are contradicting. [2] reports that plugging issues related to hydrotreating of wood derived HTL oil in a down flow trickle bed reactor, was solved by switching to up flow mode. It is likely that the observation by [2] was influenced by the relatively high inorganics content of the oil. The hydrotreater used for the relatively long (660 HoS) tests in Canada [Paper A] was operated in up flow mode, and it has been speculated that up flow mode results in improved catalyst wetting and liquid hold up. Though, [5] concluded that up and down flow mode resulted in the same operation and conversion after 5 days on stream.

The H2T'er is designed to enable operation in different reactor configurations, which is also apparent from Figure 4.9. The two reactors can be configured in series to test two-step conversion, where pressure and H_2 availability are rather constant in both reactors, while the type of catalysts, temperatures and/or space velocities can be different. Alternatively, each reactor can be run separately, while the other is off-line. This is useful during a two-step conversion campaign, where the second reactor can be taken off-line for a short period of time in order to get a sample of the intermediate product and/or perhaps tune the operating conditions of the first reactor. Thereby, each reactor in a two-step configuration can be tuned independently. Alternatively, the single reactor configuration can be beneficial during catalyst screening, where a catalyst can be tested in one reactor, while it is changed in the other reactor. In this regard, a specific Swagelok VCR®fitting is used at the disassembling point of the reactor, because it reassembles and seals reliably despite many sealing and heating cycles.

Monitoring of Temperature Increase from Exothermic Reactions

Control and monitoring of reactor temperatures is important during hydrotreating of Hydrofaction™ oil, due to excessive heat generation from exothermic reactions. The reactor of the Canadian hydrotreater [Paper A]

was supplied with heat through electrical heating cables, which were spun around the reactor tubing and covered by insulation. A 10 point thermowell was positioned along the center of the reactor. First of all, the use of heat cables and insulation makes this configuration troublesome and tedious to maintain and install after e.g. changing catalyst. Secondly, the operators concluded it impossible to observe temperature increase from exothermic reactions in that configuration. Based on these learnings, a 3-zone tubular, split type furnace were chosen for each H2T'er reactor in combination with a 10 point thermowell. The furnaces ability to split in half facilitates easy access for maintenance, while temperature increase from exothermic reactions have been clearly observable. In fact, thermowell temperatures 15-40 °C above the furnace set point have been normal in the inlet region of the first catalyst bed. In this context, [6] made the important observation that the temperature measured by the thermowell may be up to 60 °C lower than the actual temperature of the catalyst bed, which, if ignored, might cause significant errors in the interpretation of the pilot data. Consequently, the actual catalyst bed temperatures in the H2T'er could have been up to 100 °C higher than the furnace set point, and possibly up to 60 °C higher than the desired operating temperature? This is crucial information and therefore a potential master project has been proposed for the upcoming semester on modeling of mass and heat transfer in the fixed bed H2T'er reactor, similar to the study reported in [6].

4 Results from H2T'er

A total of 5 campaigns, or 1018 hours of operation on Hydrofaction^{TM} oil, have been completed as part of this project, since commissioning of the H2T'er on the 6th of July 2017. This has resulted in both extensive amounts of data, and improved understanding on how the irregular Hydrofaction^{TM} oil can be hydrotreated. These learnings provided in part the basis for Patent Application L.

This section summarize firstly the learnings from the first 3 campaigns, on how to obtain both high conversion and stable operation; followed by a detailed presentation of the successful Campaign 4 and 5. The same sulphided NiMo catalyst as used previously were used and activated with heavy gas oil spiked to 2.5 wt.% sulphur. The experimental work around Campaign 1-4 was conducted by the PhD candidate, while Campaign 5 was conducted by PhD J.K. Rodriguez and Postdoc D. Castello.

4.1 Learnings from Commissioning Campaigns

The H2T'er unit itself has been operating without any implications or safety hazards since commissioning. Minor modifications include taking the BPR.1 and the filter upstream of BPR.1 off-line, as pressure drops developed across both units during operation on Hydrofaction^{TM} oil.

Development of a stable hydrotreating process that can handle the irregular feedstock has been an iterative process. The critical reactor during hydrotreating of the reactive and oxygenated feed was soon found to be R1. Thus, most of the learnings from the first campaigns focus on tuning of R1 conditions. The preferred approach was balancing the conversion of R1 to avoid excessive reaction rates, while obtaining a partially upgraded oil that can be further upgraded in subsequent reactors at more severe conditions.

Monitoring of Heat Release

It was clear from the very first campaign that the H2T'er enables monitoring of temperature increases from exothermic heat release in the catalyst bed. Figure 4.10 visualize the development of catalyst bed temperatures in R1 as function of the very first hours of operation during the commissioning campaign. The furnace setpoint is also given, and a temperature difference is clear once operating temperatures has been reached. Particularly, the exotherms are evident in the inlet region of the catalyst bed, indicating rapid reaction rates in the inlet.

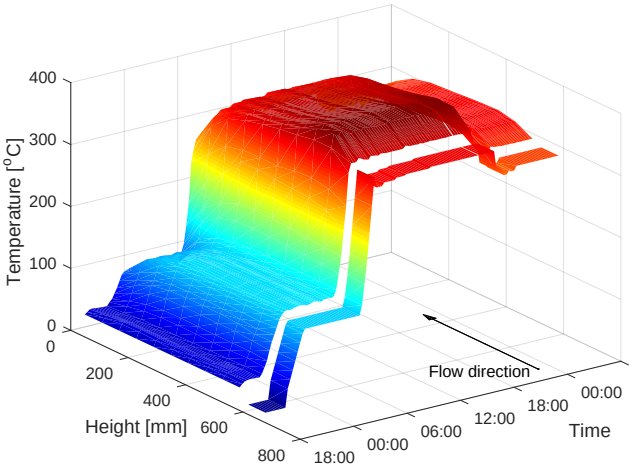

Fig. 4.10: Development of temperatures in R1. The furnace setpoint temperature is reflected by the strip. A reactor height of 0 mm equals the reactor outlet.

As a consequence of the rapid reactions around the inlet of the catalyst bed, a pressure drop of 5-10 bars developed quite rapidly during 10 hours of operation at 360 °C, 100 bar and 0.5 h^{-1}. To try and solve this issue, the operating temperature of R1 was reduced to 320 °C, which removed the pressure drop shortly after. But interestingly, the change of operating temperature in R1 affected the heat release in R2. This observation is elucidated in Figure 4.11. At an operating temperature of 360 °C, the ΔT is 40 °C in R1 and 10 °C in R2. Upon lowering the operating temperature of R1 to 320 °C, the ΔT of R1 decreased to 30 °C, whereas it started to increase in R2 after 1-2 hours. The lower temperature of R1 reduces the reaction rate and thus heat generation. Consequently, a lower conversion is obtained in R1 and a more reactive feedstock is entering R2, where the heat generation increases.

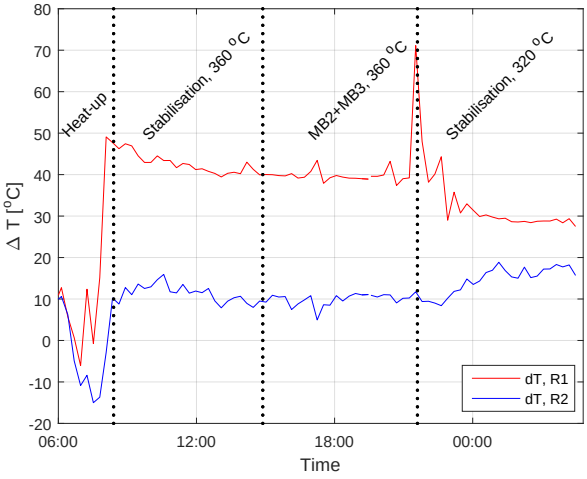

Fig. 4.11: Difference between furnace setpoint and actual temperature measured in the top part of the catalyst bed for both reactors.

Another interesting observation in relation to exothermicity was made after catalyst activation, when switching from sulphur spiked heavy gas oil to Hydrofaction^{TM} oil. After switching to the oxygenated feed, the furnace setpoint required to reach 350 °C in R1 had to be lowered from 340 °C to 295 °C. Roughly, this indicates a 5.5 times higher heat release. Meanwhile, the heavy gas oil was spiked from its initial concentration of 0.26 % sulphur to 2.5 % sulphur for activation purposes. In other words, the heteroatom content was increased by a factor 10. This indicates that the heat release during hydrotreating of Hydrofaction^{TM} oil at these conditions were at least 50 times higher than for conventional HDS of heavy gas oil.

The fact that the new system enable monitoring of exotherms to this degree was very satisfying as it was impossible in the setups applied previously in Canada. The difference is believed to be the use of furnaces for reactor heating, instead of electric heating cables as in the Canadian setup. Heating cables affect the wall temperature depending on how they are spun around the tubing, while a furnace provides a rather constant outer reactor wall temperature. The latter enables improved monitoring of heat release inside the reactor.

Graded Catalyst Bed and Temperature Control in R1

Processing issues such as exothermic heat release, rapid reaction rates and the resulting risk of coking and pressure drop build-up have been utmost in R1, where significant deoxygenation takes place. Stable operation of R1 was the focus of Campaign 3, which lasted for 270 HoS. Hydrofaction^{TM} oil was spiked to 0.5 wt.% sulphur by DMDS and different operating pressures and temperatures were tested for R1. A graded bed was prepared and tested against a non-graded bed of the sulphided NiMo based catalyst. Grading reflects a varying catalyst concentration through the bed, where the diluent is silica carbide (SiC), also comprising the in- and outlet packing. The bed packings are specified in Figure 4.12. The figure shows the temperature profiles in R1 at different operating conditions for the graded versus non-graded catalyst bed.

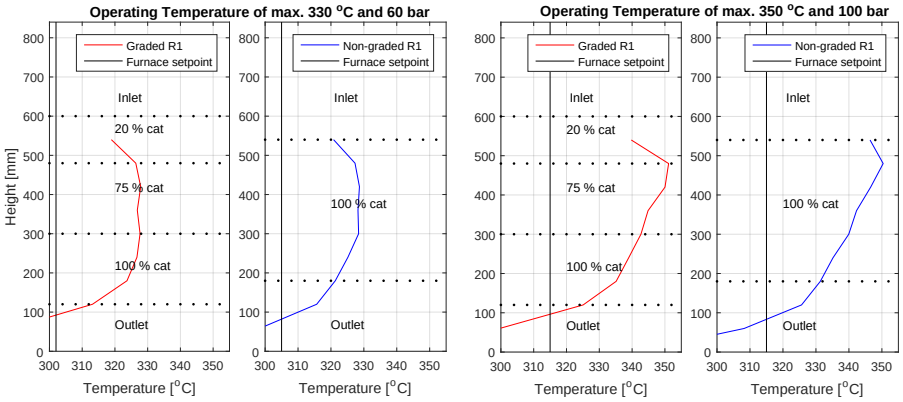

Fig. 4.12: Temperature profile in R1 for graded and non-graded sulphided NiMo catalyst packing at 330 °C, 60 bar, 0.5 h^{-1} and 350 °C, 100 bar, 0.5 h^{-1}.

Figure 4.12 does not indicate a significant difference between temperature control of the graded versus the non-graded bed, except a slightly more even temperature profile of the graded bed. It is evident how the furnaces are set

well below the operating temperatures due to significant heat release. In fact, the oil temperatures when entering the catalyst bed are above the furnace setpoints in all incidences. This shows that heat released in the bed distributes upstream into the inlet zone resulting in autothermal heating of the oil.

At operating conditions of 330 °C and 60 bar, the furnace setpoints are 20-25 °C below the maximum bed temperature, whereas it need to be 35 °C lower at 350 °C and 100 bar. This indicates how reaction rates and associated heat release are higher at the more severe conditions. Further and as evident from Figure 4.12, the temperature profile of the bed is poor at 350 °C and 100 bar, due to difficult temperature control. It is likely that a different grading with lower concentration at the inlet of the bed can improve the temperature control, but this is yet to be investigated. In Campaign 4, presented later, the entire catalyst bed of R1 was diluted with 50 % SiC and moved up to the inlet of the reactor. Thereby the reactive oil was in contact with the catalyst during heat-up from 100 °C to operating temperature. This comprise another method for a gradually increasing 'catalyst activity', as reaction kinetics increase with temperature.

In general, the use of a graded bed in R1 resulted in smoother operation, where the operating temperature could be higher without inducing a pressure drop across R1. Though, even with a graded bed temperatures above 340 °C were observed to induce slight pressure drops across R1, and the preferred operating temperature in R1 is generally in the range 300-330°C.

Operating pressures in R1 of 60 to 80 bar provide good temperature control, but at the expense of reduced hydrogenation. At pressures above 100 bar reaction rates are increased substantially leading to poor temperature control and steady development of pressure drops from coking and/or condensation reactions. This effect was obviously not observed during the microbatch experiments at 100-150 bar. Nor during the S-spiked continuous tests presented in Paper A, because the operating pressure was limited to maximum 66 bar.

Miscibility Issues of Feed and Partially Upgraded Oil

The critical temperature control could potentially be eased by recirculation of the partially upgraded reactor effluent, thereby reducing the oxygen and aromatics content and reactivity of the incoming feed. This would reduce the degree of heat release and also provide the advantage of improved mass transfer in the catalyst bed and improved hydrogen solubility of the reactor feed. Miscibility issues were however observed between the oxygenated Hydrofaction^{TM} oil feed and a deoxygenated product, as depicted in Figure 4.13. The polarity differences adds a limit to the ability of mixing upgraded

oil with Hydrofaction^{TM} oil. For such recirculation to work, the degree of partial upgrading has to be controlled in order to avoid miscibility issues.

Fig. 4.13: Incompatibility between feed and hydrotreated product.

It has been speculated whether similar precipitation may occur in the reactor if conversion is both too rapid and/or too high? Further, if such precipitation induced the pressure drop build-ups observed across R1? Intuitively it makes sense, but on the other hand the miscibility is believed to be much higher at operating temperature. The correct answer to these speculations is yet unknown.

Variation in Hydrofaction^{TM} Oil Quality

Physiochemical properties of different wood derived Hydrofaction^{TM} oils were compared in Paper A and concluded to be of very similar and consistent quality. Though, during H2T'er Campaign 4 the oil feed had to be changed from one batch of Hydrofaction^{TM} oil to another, as the first batch was emptied. The change of oil turned out to impact product quality, which was surprising, as the feeds were expected to have similar composition. Proton- and carbon NMR of the two different feeds show that the new feed contains slightly more PAH's, more methoxy carbon and seem to have a higher molecular weight compared to the first batch. The reason for an abnormal quality of the new feed was sought explained and it is likely that poor temperature control during HTL production has resulted in too high temperatures, which in turn affects oil composition.

Additionally, the new feed was more viscous, which could indicate a loss of lights (IBP-140 °C of HTL oil) during washing (Figure 3.9). Presence of lights have previously been observed to stabilise the oil from condensation type reactions during upgrading. Motivated by [21, 24] on improved hydrogen dissolution of oxygenated oils, the presence of lights may also improve

hydrogen dissolution and mass transfer of the oil, as the lights will be at supercritical state at upgrading conditions.

4.2 3-Zone Upgrading

After successful commissioning of the H2T'er unit, it became the ultimate goal of the remaining PhD project to develop a process design that enables upgrading of Hydrofaction^{TM} oil to advanced drop-in fuels. At the time, Campaign 4 resulted in the best product quality yet obtained, but fractional distillation indicated that the diesel equivalent fraction was not sufficiently hydrogenated to meet diesel fuel specifications. As a consequence, the partially upgraded oil from Campaign 4 was dehydrated and further hydrotreated in Campaign 5. Thus, the work of Campaign 4 and 5 reflect a triple-reactor configuration as visualised in Figure 4.14. The tests formed basis for Patent Application L and will be presented in this Section. Fractional distillation of both the partially upgraded oil (Campaign 4) and the upgraded oil (Campaign 5) is presented in Chapter 5.

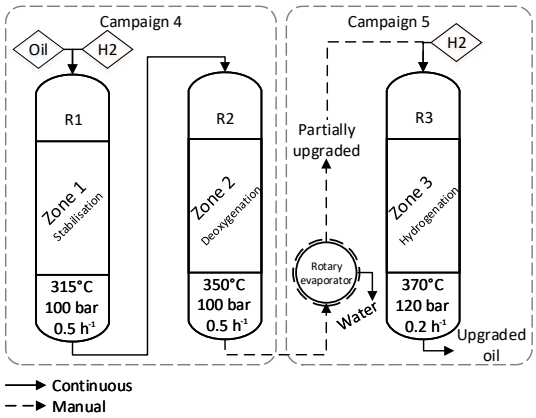

Fig. 4.14: Schematic of the 3-Zone configuration tested in Campaign 4 and 5. A range of operating conditions were tested, but those given were used during collection of product for fractional distillation.

Table 4.4 lists selected oil characteristics for the R2 and R3 products. Total liquid mass balance closures, oil yields and water yields are also provided for the operating conditions given in Figure 4.14. Due to lack of calibration of the gas chromatograph, analysis of the gaseous products cannot be provided, nor any hydrogen consumption figures.

Reactor 1 of the 3-Zone configuration in Figure 4.14 reflect a stabilization reactor at relatively mild conditions to convert the high reactivity oxygenates

Product	Liquid MB [wt.%]	Oil Yield [vol.%]	Water[a] [wt.%]	Density[b] [kg/m^3]	Arom. C[c] [mol.%]	C	H [wt.%]	O[d]	H/C [-]
Part. Upgr.	99.3	99.3	9.7	926	21.1	87.4	12.0	0.6	1.64
Upgr. Oil	101.6	103.2	0.1	903	17.7	87.3	12.7	0.0	1.73

[a]: as produced °C, [b]: at 15 °C, [c]: determined by C13-NMR, [d]: by difference

Table 4.4: Yield figures and product characteristics on dry basis for the partially upgraded and upgraded product of R2 and R3 at operating conditions given in Figure 4.14.

at a rate that does not cause poor temperature control from excessive reaction rates. Temperature profiles of the 3 different reactors are given at steady state operation in Figure 4.15. Note that the R1 catalyst bed temperatures span from 100 °C to 315 C. This is because the catalyst bed was moved up to the inlet of R1, as a way to control reaction rates. In other words, by contacting the reactive feed with catalyst at a lower temperature, the reaction rate is reduced, preventing local hotspots and making temperature control easier.

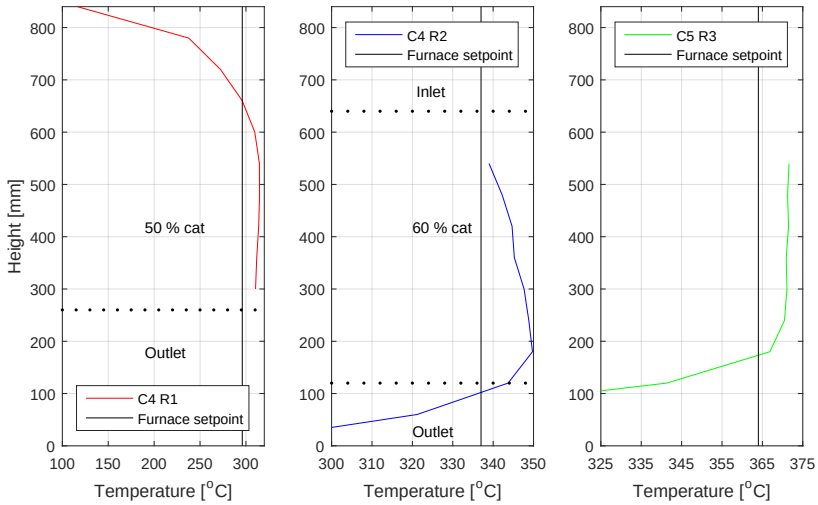

Fig. 4.15: Temperature profile in R1, R2 and R3 of Campaign 4 and 5. Operating conditions were R1: 315 °C, 100 bar, 0.5 h^{-1}; R2: 350 °C, 100 bar, 0.5 h^{-1}; and R3: 370 °C, 120 bar, 0.2 h^{-1};

Reactor 2 is the main HDO reactor operated at 100 bar, 0.5 h^{-1} and a maximum bed temperature of 350 °C. The R1 effluent is less reactive and thus the R2 bed is positioned in the middle of the reactor, allowing a more isothermal reactor at higher temperatures. A significant degree of hydrogenation is also obtained in R2. It seems from the R2 temperature profile in Figure 4.15 that the inlet temperature of the bed matches the furnace setpoint. Hereafter the oil is auto-thermally heated around 13 °C as it moves down through the bed.

The high concentration of water in the partially upgraded oil is believed to affect catalyst selectivity and activity, and the water was removed by rotary evaporation to simulate a dehydration flash step before a last hydrogenation pass. Reactor 3 serves primarily hydrogenation and the partially upgraded feed was very easy to process, causing no increase in pressure drop what so ever. As given in Figure 4.15, the temperature control of the R3 catalyst bed was also good, due to lower reactivity, coking propensity and heat release associated with the partially upgraded oil.

Catalyst Stability

Campaign 4 and 5 lasted for 470 and 212 HoS respectively. The oil feed to Campaign 4 was a standard Hydrofaction^{TM} oil spiked with DMDS to 0.5 wt.% sulphur. After 330 hours of operation the feed tank was empty and a new batch of Hydrofaction^{TM} oil was used. The change of oil turned out to affect product quality. No deactivation was observed during the first 330 hours, which is apparent from Figure 4.16 and Figure 4.17, where selected product quality parameters are plotted against time on stream. Note that different operating conditions were tested, resulting in some scatter of the results. No deactivation was obvious after 330 hours either, but it is difficult to compare as the new oil feed resulted in a different product quality. The partially upgraded oil that were used in Campaign 5 was collected during the first 330 HoS of Campaign 4.

A WHSV of 0.5 h^{-1} of R1 and R2 was used for the first 210 HoS after which it was lowered to try and improve conversion. A WHSV of 0.25 h^{-1} compared to 0.5 h^{-1} improved the H/C ratio from 1.64 to 1.70 and reduced density from 926 to 912 kg/m^3. Further, the loss of bottoms by centrifugation was reduced from 7 to 4 wt.%, thus increasing the overall mass and volume yield. This indicates that cracking and hydrogenation of heavies are the rate limiting steps in upgrading Hydrofaction^{TM} oil on this catalyst. Possibly, due to a relatively small catalyst pore size, which limits the active sites that are available for large and bulky, high molecular weight compounds.

Similarly, Figure 4.18 Figure 4.19 provide selected product quality parameters as function of time on stream for Campaign 5. Overall, relatively stable conversion is evident and product densities range from 897-914 kg/m^3. Again, a lower space velocity and a higher pressure improved hydrogenation, similar to previous findings.

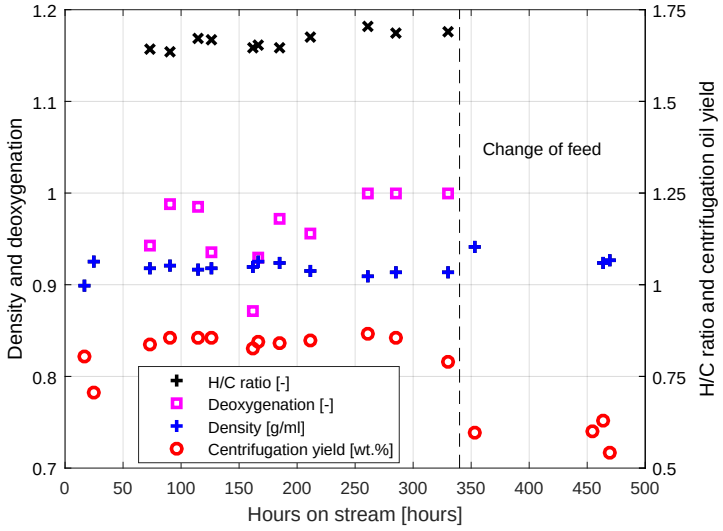

Fig. 4.16: Selected product properties as function of time on stream for Campaign 4. Change of feed affected the product significantly.

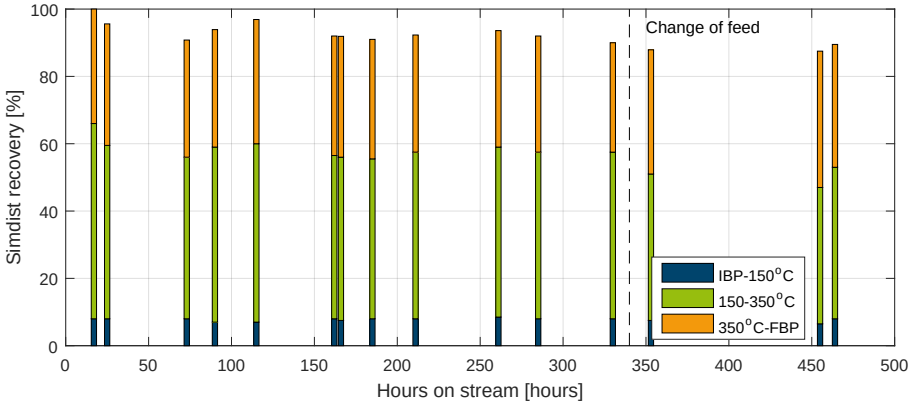

Fig. 4.17: Product distillation data as function of time on stream for Campaign 4. Change of feed affected the product significantly.

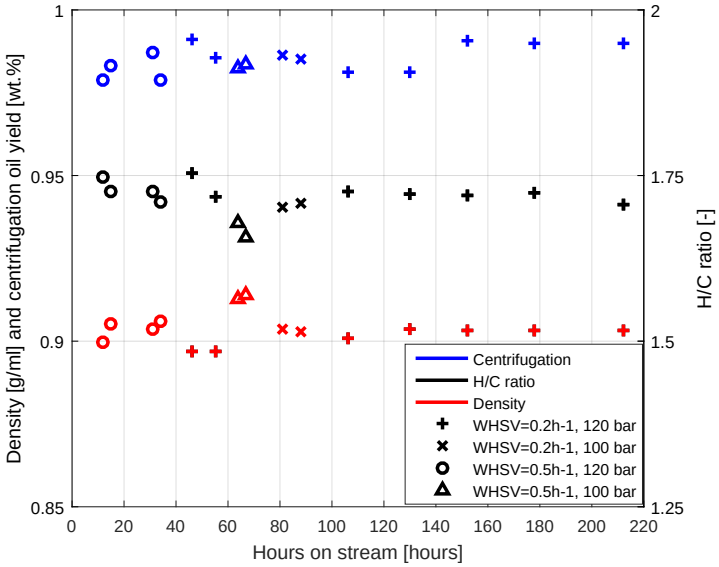

Fig. 4.18: Selected product properties as function of time on stream for Campaign 5. Operating temperature was 350 °C for the first 2 mass balances, and 370 °C for the remaining campaign.

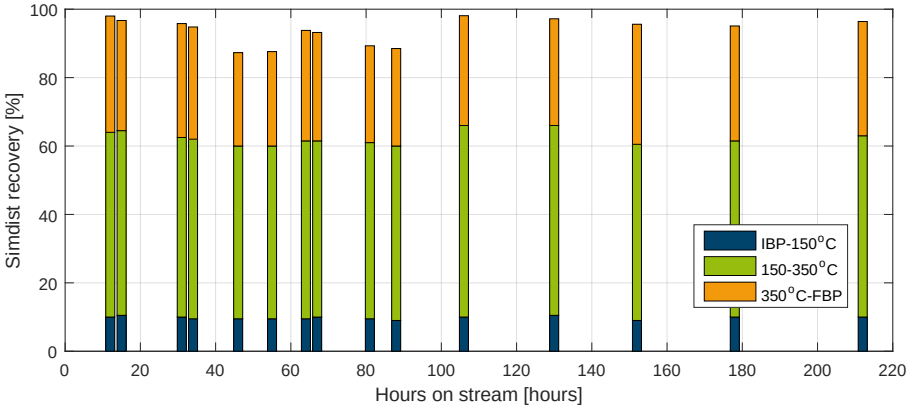

Fig. 4.19: Product distillation data as function of time on stream for Campaign 5.

4.3 Discussion of Future Work

To keep the discussion of future hydrotreating work on a practical and applicable level, it is presented as the authors suggestions to how the next H2T'er campaign can be improved compared to those presented above.

It would be interesting to evaluate to what degree a lower operating pressure in R1 and R2 will reduce the partially upgraded product quality. A lower pressure reflects a simpler process and with lower hydrogenation in R1 and R2, miscibility issues may be reduced. The hydrogen availability during hydrotreating should not be overdone. Too little hydrogen will obviously induce hydrogen starvation, but too much reduces the reactor residence time. In the H2T'er campaigns presented above the hydrogen to oil ratio has been around 10 wt.%. It is suggested to evaluate the effect of lowering the hydrogen to oil ratio to 7-8 wt.%.

Dehydration of the partially upgraded product was a promising approach of Campaign 5. It should be repeated in the next campaign, but with a slight modification. The gasoline fraction that will be co-distilled with water during evaporation should not be reintroduced to the partially upgraded oil. As concluded in the following chapter, additional hydrogenation of this fraction reduces its octane rating and consumes additional hydrogen.

A triple-reactor configuration with dehydration of the R2 effluent seems appropriate. Rather than hydrotreating the partially upgraded oil as a whole like in Campaign 5, it would be interesting to fractionate the partially upgraded oil into a distillate fraction and a residual heavy fraction. The distillate could then be hydrogenated on an isomerisation and ring-opening catalyst for improved diesel specifications. The heavy fraction could be hydrocracked at more severe conditions for maximisation of the distillate fuel products.

Catalyst bed packing may be improved compared to previous campaigns. [5] suggest to implement several glass or quartz wool plugs at the in- and outlet as well as in the middle of the catalyst bed to improve catalyst wetting. Further, removal of the longest extrudates result in a denser bed packing with less channeling effects [5].

Except a single trial with non-sulphided catalysts, the same sulphided NiMo catalyst has been applied for all upgrading work during the PhD project. Using this catalyst, a lot of knowledge has been gained on how to handle the irregular Hydrofaction^{TM} oil in a hydrotreating context. Though, at this stage of the learning curve, it may be time to optimise the choice of catalyst in the different reactor zones. The R1 catalyst should preferable be

a conventional sulphided HDM catalyst with low activity and high pore size distribution, whereas, the R3 may be improved if a suitable isomerisation and ring-opening catalyst can be identified.

Modeling of heat release and validation against experimental data from previous and upcoming campaigns has been proposed to AAU as a master student project. Motivated by [6], such study would provide valuable knowledge on heat release and heat transfer in the H2T'er reactors. This is valuable in terms of operation, but the information is also critical for the design of an up-scaled hydrotreater.

5 Conclusions on Hydrotreating

The oxygenated and aromatic nature of liquefaction oil limits its direct compatibility as advanced biofuel and upgrading is a necessity. Catalytic hydrotreating is often mentioned as the preferred upgrading pathway, but it needs to be adapted to the irregular properties of a liquefaction oil compared to conventional feeds. Presence of water from HDO, higher exothermic heat release, presence of carbon oxides, low sulphur content and high coking propensity represent the major peculiarities of hydrotreating HTL oil, and a lack of continuous studies in the open literature has detained development. On that basis, progression from microbatch to continuous hydrotreating has been a major research goal and a continuous dual-reactor hydrotreating pilot unit (H2T'er) has been designed, build and commissioned at AAU as part of the PhD project. Several campaigns with up to 660 HoS have been completed in the H2T'er and a unit at the UofC, Canada. Parametric studies have evaluated the effect of temperature, pressure, space velocity, H_2 availability, sulphur spiking and catalyst bed packing. A 3-Zone reactor configuration has been developed, proving the concept of upgrading Hydrofaction^{TM} oil to advanced transportation biofuels.

References

[1] S. A. Ali and M. A. Siddiqui, "Dearomatization, cetane improvement and deep desulfurization of diesel feedstock in a single-stage reactor," *Reaction Kinetics and Catalysis Letters*, vol. 61, no. 2, pp. 363–368, 1997.

[2] E. G. Baker and D. C. Elliott, "Catalytic hydrotreating of biomass-derived oils," https://web.anl.gov/PCS/acsfuel/preprint%20archive/Files/32_2_DENVER_04-87_0257.pdf, Pacific Northwest Lab., Richland, WA (USA), Tech. Rep., 1988.

[3] S. Bezergianni and V. Dagonikou, "Effect of co2 on catalytic hydrotreatment of gas-oil," *The Canadian Journal of Chemical Engineering*, vol. 93, no. 6, pp. 1017–1023, 2015.

[4] J. Billing, R. Hallen, A. Schmidt, and L. Snowden-Swan, "Hydrothermal processing of biomass," https://energy.gov/sites/prod/files/2017/05/f34/waste_to_energy_billing_222301.pdf, 2017, accessed: 29-09-17.

[5] J. D. Carruthers and D. J. DiCamillo, "Pilot plant testing of hydrotreating catalysts: Influence of catalyst condition, bed loading and dilution," *Applied Catalysis*, vol. 43, no. 2, pp. 253–276, 1988.

[6] J. Chen, Z. Ring, and T. Dabros, "Modeling and simulation of a fixed-bed pilot-plant hydrotreater," *Industrial & engineering chemistry research*, vol. 40, no. 15, pp. 3294–3300, 2001.

[7] Criterion Catalysts & Technologies, "Transforming ulsd economics," http://www.criterioncatalysts.com/products/product-applications/distillate-hydrotreating/_jcr_content/par/textimage.stream/1481634461635/482fba1bb8a6eb82d161497e4e9c696d3d75092131df51234dfd71d698c077b5/transform-ulsd-economics.pdf, 2017, accessed: 15-12-17.

[8] A. de Klerk, "Hydroprocessing peculiarities of fischer–tropsch syncrude," *Catalysis Today*, vol. 130, no. 2, pp. 439–445, 2008.

[9] R. Egeberg, N. Michaelsen, L. Skyum, and H. Topsoe, "Novel hydrotreating technology for production of green diesel," *ERTC, Nov*, pp. 9–11, 2009.

[10] D. Elliott and E. Baker, "Catalytic hydrotreating of biomass liquefaction products to produce hydrocarbon fuels: Interim report," https://www.osti.gov/scitech/servlets/purl/6912635, Pacific Northwest Lab., Richland, WA (USA), Tech. Rep., 1986.

[11] D. Elliott, R. Hallen, and A. Schmidt, "Hydrothermal processing of biomass," https://energy.gov/sites/prod/files/2015/04/f22/thermochemical_conversion_hallen_222301.pdf, 2015, accessed: 17-10-17.

[12] D. C. Elliott, "Historical developments in hydroprocessing bio-oils," *Energy & Fuels*, vol. 21, no. 3, pp. 1792–1815, 2007.

[13] D. C. Elliott, T. R. Hart, A. J. Schmidt, G. G. Neuenschwander, L. J. Rotness, M. V. Olarte, A. H. Zacher, K. O. Albrecht, R. T. Hallen, and J. E. Holladay, "Process development for hydrothermal liquefaction of algae feedstocks in a continuous-flow reactor," *Algal Research*, vol. 2, no. 4, pp. 445–454, 2013.

[14] E. Furimsky, "Selection of catalysts and reactors for hydroprocessing," *Applied Catalysis A: General*, vol. 171, no. 2, pp. 177–206, 1998.

[15] E. Furimsky, "Hydroprocessing challenges in biofuels production," *Catalysis Today*, vol. 217, pp. 13–56, 2013.

[16] E. Furimsky and F. E. Massoth, "Deactivation of hydroprocessing catalysts," *Catalysis Today*, vol. 52, no. 4, pp. 381–495, 1999.

[17] J. H. Gary, G. E. Handwerk, and M. J. Kaiser, *Petroleum refining, Technology and economics, 5. Edition*. CRC Press, 2007, ISBN: 0-8493-7038-8.

[18] B. Gevert, P. Andersson, S. Jaeras, and S. Sandqvist, "Hydroprocessing of desalted directly liquefied biomass," *Prepr. Pap., Am. Chem. Soc., Div. Fuel Chem. (United States)*, vol. 33, no. CONF-8809228, 1988.

[19] J. M. Jarvis, N. M. Sudasinghe, K. O. Albrecht, A. J. Schmidt, R. T. Hallen, D. B. Anderson, J. M. Billing, and T. M. Schaub, "Impact of iron porphyrin complexes when hydroprocessing algal HTL biocrude," *Fuel*, vol. 182, pp. 411–418, 2016.

[20] M. Kaltschmitt and U. Neuling, *Biokerosene: Status and Prospects*. Springer, 2017, ISBN: 978-3-662-53063-4.

[21] J. Kim, J. M. Park, J. Y. Han, and S. K. Kim, "Method for producing renewable fuel using supercritical fluid," Mar. 3 2015, US Patent 8968425.

[22] D. Kubička and J. Horáček, "Deactivation of hds catalysts in deoxygenation of vegetable oils," *Applied Catalysis A: General*, vol. 394, no. 1, pp. 9–17, 2011.

[23] Y. Mathieu, L. Sauvanaud, L. Humphreys, W. Rowlands, T. Maschmeyer, and A. Corma, "Opportunities in upgrading biomass crudes," *Faraday Discussions*, vol. 197, pp. 389–401, 2017.

[24] D. Radlein and A. Quignard, "Methods of upgrading biooil to transportation grade hydrocarbon fuels," Jun. 4 2014, US Patent App. 14295857.

[25] A. Schmidt, J. Billing, K. Albrecht, S. Fox, T. Hart, G. Maupin, L. Snowden-Swan, and R. Hallen, "Conversion of blended primary and secondary sewage sludge into biofuels by hydrothermal liquefaction and catalytic hydrotreatment," http://www.gastechnology.org/tcbiomass/tcbiomass2017/Justin-Billing-Thu-tcbiomass2017-presentation.pdf, 2017, accessed: 03-11-17.

[26] O. Şenol, E.-M. Ryymin, T.-R. Viljava, and A. Krause, "Effect of hydrogen sulphide on the hydrodeoxygenation of aromatic and aliphatic oxygenates on sulphided catalysts," *Journal of Molecular Catalysis A: Chemical*, vol. 277, no. 1, pp. 107–112, 2007.

[27] J. G. Speight, *The refinery of the future*. William Andrew, 2010, ISBN: 978-0-81-552041-2.

[28] W. P. van Swaaij, S. R. Kersten, and W. Palz, *Biomass power for the world*, Vienna ed. Pan Stanford Publishing, 2015, ISBN: 978-981-4669-24-5.

[29] A. H. Vivas, G. B. Larsen, R. G. Egeverg, and S. S. Enevoldsen, "Production of high quality diesel fuel and lubricant from high boiling aromatic carbonaceous material," Sep. 14 2015, US Patent App. 15504365.

[30] M. Weber, M. Weber, and M. Kleine-Boymann, "Phenol ullmann's encyclopedia of industrial chemistry," 2000.

Chapter 5

Fractionation and Fuel Blending

The ultimate objective of Hydrofaction^{TM} is to produce drop-in long-haul transportation fuels. Commodity transportation fuels are legislated by a stringent set of fuel specifications to ensure consistent quality and engine performance. There are no additional specifications related to HVO, GTL or biomass derived fuel alternatives such as Hydrofaction^{TM} products. These renewable liquids are allowed in any proportions in gasoline, diesel or marine fuel, as long as they comply with the fuel specifications [3–5]. In relation to jet fuel, BTL is not one of the 5 alternative jet fuel pathways that have yet been certified [12], but jet fuel is included in the evaluation below. Hydrotreated Hydrofaction^{TM} oil has been fractionated and analysed, and suitability as drop-in is assessed for the four main transportation fuel types: gasoline, jet, diesel and bunker.

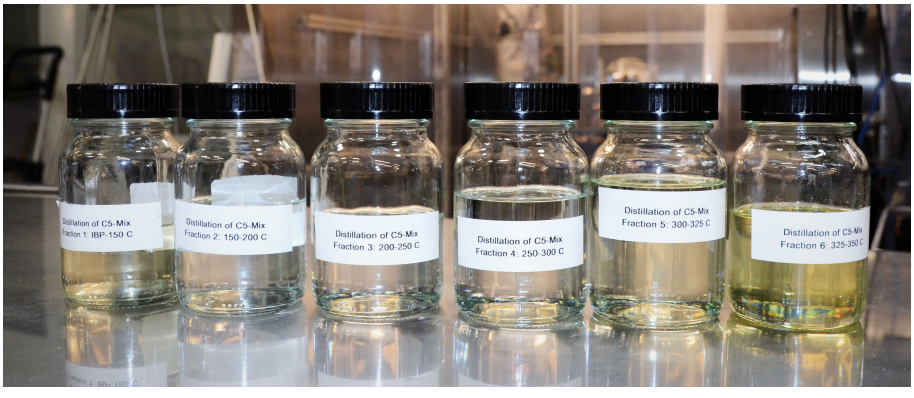

Fig. 5.1: Picture of C5,H2T fractions F1-F6 (IBP-350 °C) after distillation.

1 Fractionation of Upgraded Hydrofaction^{TM} oil

Three different upgraded oils were distilled during this PhD project, and will be referred to as follows. C3,UofC was upgraded at the UofC during the S-spiked campaign presented in Paper A. Distillation of this oil was carried out by Alberta Innovates Technology Futures, Edmonton. C4,H2T and C5,H2T were collected during H2T Campaign 4 and 5 respectively, and distilled at AAU by the PhD candidate. C4,H2T and C5,H2T were previously referred to as partially upgraded oil and upgraded oil respectively. Figure 5.1 depicts an example of the clear distillate fractions and Figure 5.2 provides the TBP distillation profiles. Characteristics of the fractions will be summarised in this section and discussed in a fuel context in the following sections.

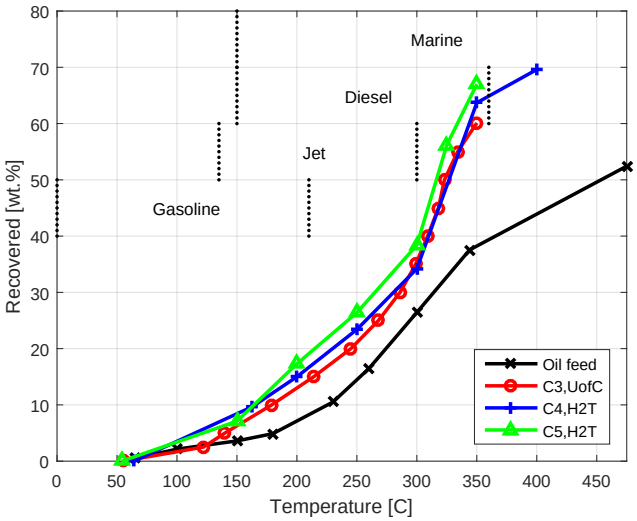

Fig. 5.2: True boiling point distillation curve of Hydrofaction^{TM} oil and the upgraded oils.

The non-upgraded liquefaction distillates are concluded inapplicable as drop-in fuel (Section 3.3 of Chapter 2), mostly due to oxygenates and their even distribution in all distillation fractions. The adverse fuel characteristics have been significantly improved during upgrading, which is evident from Table 5.1. Please note the slight variations in cut point for the three distillations. Deoxygenation and hydrogenation through hydrotreating reduces density, aromaticity and polarity, it improves the heating value, H/C ratio and eliminates the TAN. Additionally and quite importantly, hydrotreating improves volatility of the oil. Figure 5.2 visualizes how the yield of IBP-350°C distillates is almost doubled from 37 wt.% to 60-70 wt.%. The diesel fraction is the largest fraction after upgrading, comprising 50-6 0wt.% of the

oil. The additional hydrotreating of C5,H2T compared to C4,H2T is evident from the higher degree of hydrogenation and the improved properties as a heavy transportation fuel.

	Cut [°C]	Yield [wt.%]	Density[a] [kg/m3]	HHV[b] [MJ/kg]	Arom. C[c] [mol.%]	Flash [°C]	CCI[d] [-]	S[e] [ppm]	Elemental [wt.%] C	H	O[f]	H/C [-]
C3,UofC	-	-	941	43.3	-		-	-	88.3	11.2	0.5	1.52
F1	IBP-180	9.0	787	44.7	-	<20.5	-	212	84.1	13.6	2.3	1.93
F2	180-350	48.5	882	43.1	-	74	41	131	87.1	12.1	0.8	1.65
Residue	350+	42.6	1033	42.4	-	>200	-	-	90.5	9.6	0.0	1.26
C4,H2T	-	-	926	43.9	21.1	-	-	48	87.4	12.0	0.6	1.64
F1	64-163	9.7	776	46.3	3.3	<25	-	13	84.9	15.1	0.0	2.13
F2	163-200	5.3	828	44.7	11.3	54.5	29	14	85.8	14.2	0.0	1.97
F3	200-250	8.4	871	44.7	15.9	84.5	29	37	86.7	13.3	0.0	1.83
F4	250-300	10.9	879	44.7	13.8	120.5	41	45	86.6	13.4	0.0	1.84
F5	300-350	29.5	894	44.7	17.8	161.5	51	67	87.0	13.0	0.0	1.77
F6	350-400	5.9	970	43.4	25.1	NA	37	68	87.9	11.6	0.5	1.58
Residue	400+	29.3	1048	41.5	51.4	NA	NA	NA	88.6	9.6	1.9	1.29
C5,H2T	-	-	903	44.3	17.7	37.5	-	30	87.3	12.7	0.0	1.73
F1	54-150	7.1	770	44.8	3.4	<25	-	54	85.0	15.0	0.0	2.10
F2	150-200	10.2	814	45.1	8.2	44.5	35	19	85.5	14.5	0.0	2.02
F3	200-250	9.1	863	45.0	11.8	82	32	23	86.4	13.6	0.0	1.87
F4	250-300	12.0	872	45.2	12.8	117	44	10	86.5	13.5	0.0	1.86
F5	300-325	17.8	866	45.4	10.6	151	59	15	86.2	13.8	0.0	1.91
F6	325-350	10.8	921	44.3	19.6	169	46	34	87.3	12.7	0.0	1.73
Residue	350+	31.6	1023	43.1	33.0	NA	NA	NA	89.4	10.6	0.0	1.42

[a]: at 15 °C, [b]: dry basis [c]: by C13-NMR, [d]: estimated from density and distillation data, [e]: up to 50 ppm deviation, [f]: by difference

Table 5.1: Selected physio-chemical properties of different upgraded Hydrofaction^{TM} oils and their corresponding boiling point fractions.

Sulphur contents of the distillation fractions were measured using a Horiba x-ray fluorescence analyser, but the calibration curve was associated with up to 50 ppm inaccuracy. This is off course highly unfortunate as the sulphur specifications for gasoline and diesel is 10-15 ppm. Based on that, the sulphur measurements given in Table 5.1 can only be used for indicative purposes and need to be re-analysed in the near future.

Figure 5.3 shows relatively linear correlations of H/C ratio and density with TBP. For both the C4,H2T and C5,H2T a plateau is evident for F3-F5 and then a sudden increase to F6. The observations are emphasised by C-NMR and H-NMR of the C4,H2T and C5,H2T fractions, presented in Figure 5.4, where aromatic carbon increases from a plateau around 325 °C. As a result, F6 is more aromatic than F5 and the upper cut point of the diesel fraction may be lowered if density or aromaticity become constraining parameters. Generally, the concentration of aromatic carbon increases with TBP, while that of aliphatic carbon decreases. Similarly, the concentration of aromatic carbon bound to an oxygen, as in the case of phenolics or ethers, increases with TBP. The relatively high concentration of the latter is surprising, but it may be an effect from the integration and base line correction of the C-NMR spectra. The base line correction is particularly uncertain in the upper aromatic region (>140 ppm), where the aromatic C-O are found. The higher fractions

are also imposed by a lower signal to noise ratio, which increases uncertainty of the integration. It needs mentioning that the NMR analysis provides molar concentrations. Though, the molar concentration is somewhat indicative for the mass concentration, since a relatively even carbon number and molecular weight distribution can be expected in a hydrocarbon fraction that is separated by boiling point.

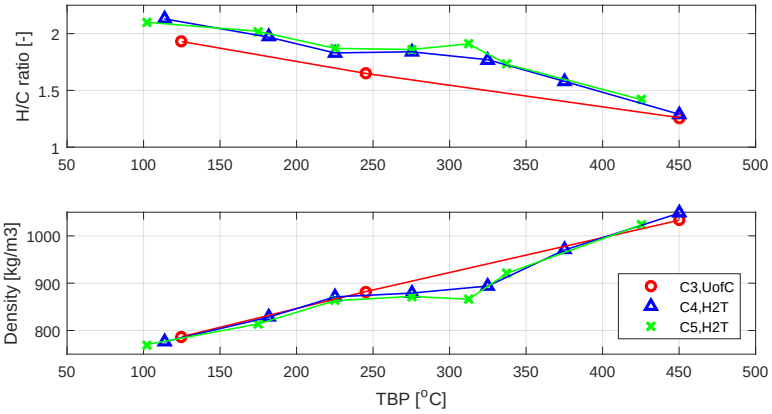

Fig. 5.3: Variation of selected properties with TBP for fractions in Table 5.1.

The H-NMR data given in Figure 5.4 also indicates that PAH's only appear in F6 and the distillation residue. The concentration of PAH's given does not reliably reflect the actual concentration, since it is only the so-called bay protons that are integrated, which is only a fraction of the protons associated with a PAH. However, the fact that they are only detected at TBP's higher than the diesel and jet fuel range is advantageous, as the specifications for these fuels are strict with respect to the presence of PAH's.

All distillate fractions were clear in color upon distillation, but only the C5,H2T distillates did not become darker upon exposure to air. The other sets of fractions became pink, red and darker in color. Colored distillates are normally related to minor concentrations of nitrogen, phenolics and active hydrocarbon colour precursors. Olefinic protons, given in the bottom of Figure 5.4, are completely absent in the C5,H2T fractions, whereas they are detected in minor concentrations of the C4,H2T fractions. Thus, the differences in olefin content may contribute to the differences in color change.

Overall, the properties of the upgraded fractions presented above indicate promising potential as drop-in transportation fuels. The following sections will discuss the suitability of upgraded Hydrofaction^{TM} products as trans-

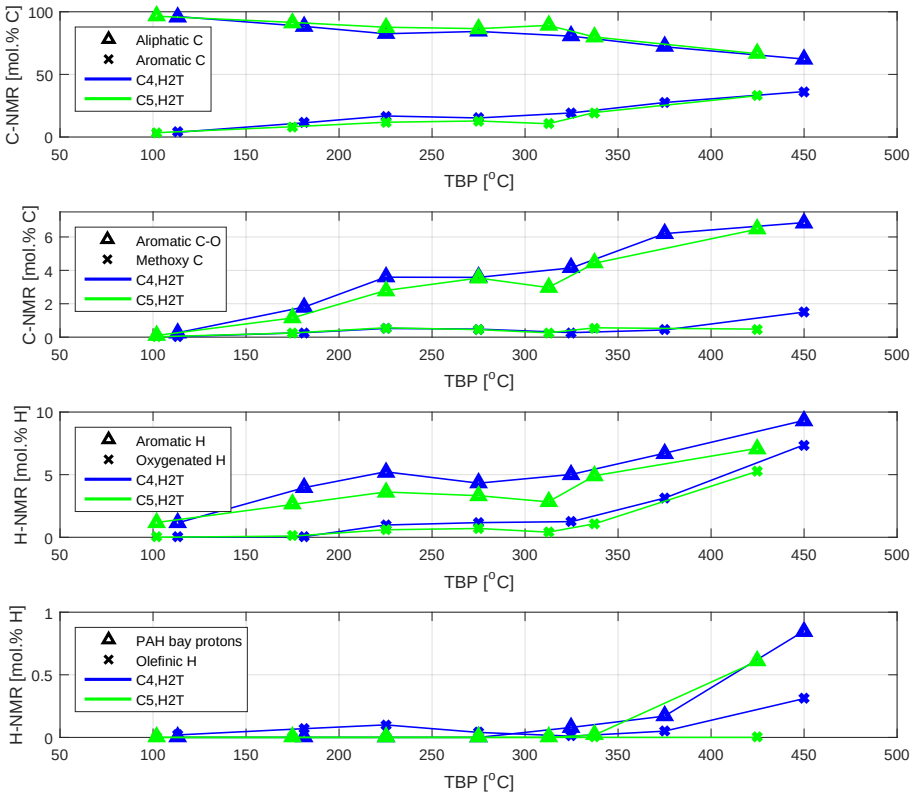

Fig. 5.4: Carbon and hydrogen NMR of the C4,H2T and C5,H2T fractions.

portation fuel by evaluating against current fuel specifications.

2 Gasoline Applicability

The Hydrofaction^{TM} platform is not designed to maximise gasoline production, as the demand for gasoline is expected to decline as a consequence of the introduction of efficient electric vehicles. But since a Hydrofaction^{TM} barrel does contain some gasoline range material, and the spark-ignition engines not will be replaced over night, gasoline is included in the evaluation.

In Europe gasoline is legislated by the EN228 standard, and a relevant selection of specifications from this standard is given in Table 5.2. Gasoline is the lowest boiling liquid transportation fuel with a final boiling point of 210 °C. As a consequence, it is only F1 and F2 of Table 5.1 that is in focus. The densities of these fractions are relatively high, partly due to a high IBP

around 60 °C and partly because the fractions are rich in napthenes. As a result, the gasoline equivalent fractions from upgraded Hydrofaction^{TM} oil cannot become a finished gasoline fuel, but must be blended with lighter and more volatile blendstocks to meet specifications.

Gasoline, Class A			
RON, Research octane number		min	95.0
MON, Motor octane number		min	85.0
Vapor Pressure	kPa	max	65-80
Density @ 15 °C	kg/m^3		720 - 775
E70, evaporated at 70 °C	Vol.%		22-50
E100, evaporated at 100 °C	Vol.%		46-72
E150, evaporated at 150 °C	Vol.%	min	75
Final boiling point	°C	max	210
Olefin content	Vol.%	max	18.0
Aromatic content	Vol.%	max	35.0
Benzene content	Vol.%	max	1.0
Oxygen content	wt.%	max	3.7
Other oxygenates content	Vol.%	max	15.0
Sulphur content	ppm	max	10
Oxidation stability	minutes	min	360
Copper strip corrosion	-	rating	Class 1

Table 5.2: Gasoline fuel specifications selected from the current EN228 standard [3].

Gasoline is used in spark-ignition engines, where the point of ignition is crucial. To prevent so-called knocking, the gasoline must resist the temperature and pressure increase during compression without igniting. The octane number quantifies this property to prevent auto-ignition or anti-knocking. In this light, aromatic hydrocarbons are desirable due to their high octane rating. Likewise, olefins have higher octane numbers than alkanes and cycloalkanes have octane numbers similar to the resulting acyclic alkene. The octane number of linear hydrocarbons increase with branching and a decreasing carbon number. Finally, oxygenates are often associated with high octane rating and sometimes used as octane improvers. [2, 10]

The octane rating of the light Hydrofaction^{TM} distillates depend on the degree of hydrotreating that they are exposed to. Table 5.3 lists the major compounds identified by GC-MS analysis in fraction 1 of three different oils exposed to no, single and dual reactor upgrading respectively. It is evident that the amount of oxygenates is significantly reduced by upgrading, and the amount of napthenes increases rapidly due to both deoxygenation and hydrogenation of aromatics. As a consequence, the octane rating will decrease with severity of upgrading from quite high for the non-upgraded fraction to poor for the severely hydrogenated fraction.

If gasoline is a desired product, the optimum path would perhaps be to

F1, from HDO0, Table 2.2, No upgrading			F1,C3UofC, Table 5.1, single reactor upgrading			F1, C4,H2T, Table 5.1, dual reactor upgrading		
Identified compound	Formula	Area%	Identified compound	Formula	Area%	Identified compound	Formula	Area%
2-Butanone	C4H8O	4.5	CyC5, 1,3-diMe	C7H14	2.3	Butane, 2,3-diMe	C6H14	0.8
2-Butanol	C4H10O	2.2	Heptane	C7H16	1.0	CyC6	C6H12	1.0
2-Butanone, 3-Me	C5H10O	1.5	CyC6, Me	C7H14	3.8	CyC5, 1,3-diMe	C7H14	2.9
1-Butanol	C4H10O	2.6	CyC5, Et	C7H14	1.2	Heptane	C7H16,	1.0
2-Pentanone	C5H10O	3.1	Toluene	C7H8	4.8	CyC6, Me	C7H14	4.4
3-Pentanone	C5H10O	1.7	CyC5, 1,2,4-triMe	C8H16	3.1	CyC5, Et	C7H14	1.0
1-Butanol, 2-Me	C5H12O	1.2	CyC5, 1-Et-3-Me	C8H16	5.9	CyC5, 1,2,4-triMe	C8H16	3.5
Toluene	C7H8	1.8	C6, 3-Et	C8H18	4.2	CyC6, 1,3-diMe	C8H16	4.9
3-Hexanone	C6H12O	2.4	CyC6, 1,3-diMe	C8H16,	1.9	CyC5, 1-Et-3-Me	C8H16	5.1
2-Hexanone	C6H12O	1.9	CyC6, 1,2-diMe	C8H16	4.2	CyC6, 1,3-diMe	C8H16	4.4
CyPentene, 1,2,3-triMe	C8H14	1.2	CyC6, Et	C8H16	6.0	CyC6, 1,4-diMe	C8H16	3.1
CyPentene, 1-Et, 5-Me	C8H14	2.9	CyC5, 1,2-DiEt	C9H18	4.3	CyC6, Et	C8H16,	5.7
CyPentanone, 2-Me	C6H10O	2.9	CyC6, 1,3,5-triMe	C9H18	1.1	CyC5, 1,2-DiEt	C9H18	4.8
CyPentanone, 2,5-diMe	C7H12O	6.0	Ethylbenzene	C8H10	1.9	p-Xylene	C8H10,	2.4
CyHexanone, 3-Me	C7H12O	4.1	p-Xylene	C8H10	5.3	CyC6, 1,2,4-triMe	C9H18	9.0
p-xylene	C8H10	3.9	CyC5, 1,3-DiEt	C9H18	1.2	CyC6, 1-Et-3-Me	C9H18	10.8
Nonane	C9H20	3.4	CyC6, 1,2,4-triMe	C9H18	1.3	CyC5, 1,3-DiEt	C9H18	1.8
CyC5, 2-Et, 1,1-diEt	C9H18	1.6	CyC6, 1-Et-3-Me	C9H18	5.7	Nonane	C9H20	3.2
CyHexanone, 2,6-diMe	C8H14O	2.2	Decane	C10H22	2.2	CyC6, 1,2,3-triMe	C9H18	1.3
CyHexanone, 2-Et	C8H14O	1.5	CyC6, 1-Et-4-Me	C9H18	1.3	CyC6, propyl	C9H18	4.9
Benzene, 1,4-diEt	C10H14	1.3	CyC6, propyl	C9H18	3.2	CyC6, 1,2 diEt	C10H20	0.9
O-Cymene	C10H14	1.1	Benzene, 1-Et-3-Me	C9H12	3.2	CyC6, 1,2-diEt	C10H20	3.9
Undecane	C11H24	2.8	Benzene, 1,4-diEt	C10H14	1.6	CyC6, 2-Et-1,3-diMe	C10H20	1.4
Total		57.8			70.9			82.1
Aromatics & olefins		8.2			16.8			2.4
Napthenes		1.6			46.5			74.7
Oxygenates		37.9			0.0			0.0

Table 5.3: Compounds identified by GC-MS of three potential gasoline fractions exposed to no, mild and severe upgrading.

collect the gasoline fraction after a mild upgrading, preferably milder than that of the C3,UofC. Thus, a fraction 1 with low oxygen content and relatively high aromaticity would be characterised by a high octane number, low vapor pressure and high density. Such fraction may serve as a valuable blendstock, allowing for addition of relatively cheap e.g. butane. Addition of such is most likely required, in order to achieve good cold start properties and fulfill the density and E70 specifications.

The sulphur contents are likely to become constraining parameters if the gasoline equivalent fraction is only exposed to mild upgrading. The sulphur content of F1,C3UofC in Table 5.1 is surprisingly high at 212 ppm. Though, this is most likely related to the fact that the oil prior to upgrading was spiked with high amounts (equivalent to 1 wt.% S) of DMDS (TBP=110 °C). It was found later that such degree of spiking is unnecessary and thus the sulphur levels are expected to be closer to that of the C4,H2T fractions, where F1 contains 13 ppm S.

An oxygen content above that specified in Table 5.2 is perhaps not an issue, when the gasoline fraction is to be used as blendstock. Instead, the type of oxygenates are of concern. Some oxygenates, e.g. ketones may cause problems with elastomeric seals and gaskets in the vehicle fuel system. Though ketones are highly reactive during upgrading and they are not expected to be present after mild deoxygenation. Along this line, [10] report that addition of

about 2 % oxygenates found in hydroprocessed pyrolysis oil had no negative impact on the gasoline specifications.

Summing up, the light distillates of Hydrofaction^{TM} oil may represent a valuable gasoline blendstock with relatively good octane and vapor pressure characteristics. However, it implies that the fraction is only exposed to mild hydrotreating in order to avoid deep hydrogenation and complete deoxygenation. This is however a plausible process design, as the gasoline equivalent fraction can be co-flashed with water during dehydration after a deoxygenation reaction zone. This procedure is suggested as near-future work in Chapter 4, Section 4.3.

3 Jet fuel Potential

Jet fuel has been given little attention as a potential market, because the distillation range overlaps with that of diesel, which is the main product target by Steeper Energy. Further, BTL pathways such as Hydrofaction^{TM} are yet not certified for jet fuel in any blending proportions [12]. Though, let us ignore the commercial agenda and evaluate the jet fuel potential for completeness.

The specifications for jet fuel are listed in Table 5.4. Based on the distillation specifications, fraction 2-4 (C4,H2T and C5,H2T) of Table 5.1 are within the jet fuel equivalent boiling range. In fact, based on the flash point of F2, the lower cut point can be reduced below 150 °C until the flash point specification become a constraining parameter. This will also reduce density a bit. Mixing F2-F4 plus the heaviest part of F1 correspond to around 25 wt.% of the upgraded oil. The net heating value of such blend should be just within specifications. Based on the molar concentration measured by NMR, the amount of aromatics is also within specification. The stringent napthalene specification is not of concern, because napthalene will be at least partly hydrogenated to tetralin during severe hydrotreating. The smoke point is related to PAH content, and this specification is also likely to be met based on the indicative H-NMR results in Figure 5.4.

Hydrofaction^{TM} oil is rich in phenolics that boil in the jet fuel equivalent range. Phenolics are quite resistant to deoxygenation during hydrotreatment [Paper C], and thus trace phenolics may be present. It is unknown how trace phenolics comply with the jet fuel specifications. Likewise, it need to be analysed how the Hydrofaction^{TM} distillates match the stability specification.

The density specification will be constrained if blending F2-F4. This may be solved by blending with conventional blendstocks, or by blending F2 and

Jet fuel, Jet A-1			
Freezing Point	°C	max	-47.0
Viscosity @ -20 °C	cSt	max	8.00
Density @ 15 °C	kg/m^3		775 - 840
T10 boiling point	°C	max	205.0
Final boiling point	°C	max	300.0
Flash point	°C	min	38.0
Smoke point	mm	min	25.0
Aromatic content	Vol.%	max	25
Napthalene content	Vol.%	max	3
Sulphur content	ppm	max	3000
Thiol content	ppm	max	30
TAN	mg KOH/g	max	0.1
Stability @ 260 °C	torr	max	25.0
Specific energy content	MJ/kg	min	42.80

Table 5.4: Jet A-1 Kerosine specifications.

F3 of C5,H2T only. Such blend is also expected to have good cold flow properties, because the calculated cetane index (CCI), NMR, density and elemental analysis indicate that these two fractions have an aromatic character. Further, a relatively high amount of alkylated napthenes have been identified in the fractions by GC-MS. Similar to aromatics, such compounds have good cold flow properties.

Despite uncertainty of sulphur measurements, the sulphur content is below the 3000 ppm specification. Further, the thiols specification is likely to be met as thiols (except H_2S) are easily converted during hydrotreating. H_2S is also a thiol, but it is removed through the gaseous products, not affecting the thiol content of the jet fuel fraction.

4 Hydrofaction^{TM} Diesel

Diesel has been the target fuel during development of Hydrofaction^{TM} . A wide boiling range of diesel (150-350 °C) match well with the distillation profile of an upgraded Hydrofaction^{TM} oil, where 50-60 wt.% is within the diesel equivalent range. For comparison, the benchmark Brent crude oil contains 35 wt.% diesel range distillates [11]. However, the aromatic and napthenic nature of a ligno-cellulosic derived Hydrofaction^{TM} oil is the limiting parameter in relation to production of drop-in diesel fuel, due to the low cetane number inherent to such compounds. Diesel engines are compression ignition engines that are based on auto-ignition of the diesel fuel. The cetane number is a measure of the ignition delay, and it is high for a fuel that easily oxidizes with air. Thus, suitable diesel compounds when looking at the cetane specification are linear parafinnic hydrocarbons with little branching, and not alkylated aromatics. A wood derived liquefaction oil is aromatic and

oxygenated by nature. Upon hydrotreating it is rich in napthenes, which are by default still quite dense and with a poor cetane rating. As a consequence, severe hydrogenation and some ring-opening are required during upgrading to improve the cetane number of the Hydrofaction^{TM} middle distillates.

Table 5.5 lists the European EN590 and North American D975 diesel fuel specifications. It is evident that the European specifications are significantly stricter than the North American. While the C4,H2T F2-F5, except for sulphur, is likely (cetane, viscosity, lubricity, copper corrosion etc. unknown) to fulfill the D975 specifications, it requires further hydrogenation and ring-opening to meet the EN590 density and cetane specifications. On that basis the objective of Campaign 5 was an additional hydrotreating to get a more hydrogenated product with better diesel fuel properties. As evident from Table 5.1, the C5,H2T is more hydrogenated compared to C4,H2T. The cetane number according to ASTM D613 has not been measured for any Hydrofaction^{TM} products, though the calculated cetane index (CCI) has been estimated based on ASTM D4737 [6]. The CCI of a C4,H2T F2-F5 blend is 33, while it is 36 for a C5,H2T F2-F6 blend. If F2 is left out of the blend, the CCI increases to around 40, but at the cost of an increased density.

Diesel			EN590	D975 No.2D
Density @ 15 °C	$^{kg}/_{m^3}$		820 - 845	-
Viscosity @ 40 °C	cSt		2-4.5	1.9-4.1
T90 boiling point	°C		-	282-338
T95 boiling point	°C	max	360	-
Flash point	°C	min	55	52
Cetane number		min	51.0	40.0
Cetane index		min	46	40[a]
Total aromatic content	vol.%	max	-	35[a]
Polycyclic aromatic content	wt.%	max	8.0	-
Sulphur content	ppm	max	10	15
Water content	ppm	max	200	500
TAN	$^{mg\ KOH}/_{g}$	max	0.08	-
Copper strip corrosion	-	rating	Class 1	No.3
Lubricity @ 60 °C	micron	max	460	520
Oxidation stability	h	min	20	
Conductivity	pS/m	min		25

[a] At least one of these specifications must be met

Table 5.5: Selected diesel fuel specifications in force in Europe (EN590) [4] and North America (D975) [7].

In Table 5.1 the oxygen content by elemental analysis (by difference) was below the detection level, but oxygenates where detected in the middle distillates by NMR as given in Figure 5.4. Trace oxygenates will affect some of the properties that are specified in Table 5.5. Firstly, some oxygenates have high and some have poor cetane numbers [1]. [10] reports that all oxygenates found in hydroprocessed pyrolysis oil have low cetane numbers. E.g. the

cetane of certified diesel was reduced from 43.0 to 41.6 by addition of 1 % phenol. Based on that, it is expected that the trace oxygenates present in Hydrofaction^{TM} diesel will have a sligtly negative impact on the cetane number. An impact that can only be quantified by real cetane determination and not by the CCI. Secondly, the lubricity of a fuel depends on the presence of surface active species, and in particular oxygenates have been reported to improve the lubricating properties [9]. In the study by [10], phenolic oxygenates were found to improve not only lubricity, but also conductivity and oxidation stability of the diesel fuel.

Cold flow properties such as the cold filter plugging point (CFPP) are also specified in the EN590 and D975 standards for different climates. The cold flow properties are expected to meet specifications due to the relatively low ratio of n-alkanes to cyclic structures. However, this has to be verified by actual measurements.

Summing up, blending seems to be necessary for Hydrofaction^{TM} diesel to meet the European specifications. Alternatively, a catalyst that enables ring-opening of napthenes can be applied during hydrotreating of either the bulk oil or perhaps the diesel distillate only. But the Hydrofaction^{TM} diesel fraction may, once the remaining analyses are validated, meet specifications in North America without blending. This is quite an achievement.

5 Low Sulphur Marine Fuel

Marine fuel is a broad term for various different fuel products with very different specifications. Table 5.6 lists examples of both a distillate marine fuel with a quality similar to D975 diesel, and a residual marine fuel. Obvious from the naming, the residual marine fuel is a heavier and more viscous product consisting of the 'bottoms of the barrel'. From an economic perspective, the Hydrofaction^{TM} process aims to maximise the production of higher value products such as diesel, gasoline and/or jet fuels, while ensuring that the remainder has a quality sufficient for use as marine fuel. Meanwhile, it is also advantageous to limit the amount of different products, as each product requires separate storage tanks, utilities, certification etc.

A recent decision by the International Maritime Organization reduces the global sulphur limit in marine fuel from 3.5 wt.% to 0.5 wt.% by 2020 [8]. In certain Sulphur Emission Control Areas (SECA), the specification was reduced to 0.1 wt.% by 2015. The change in sulphur specifications is quite drastic and it has, and will continue to change the marine fuel supply. The high sulphur residues can to a lesser extent be used, and the need for further

Marine Distillate Fuels (DMA)				Marine Residual Fuels (RMG)			
Viscosity @ 40 °C	cSt		2.0-6.0	Viscosity @ 50 °C	cSt		180-700
Density @ 15 °C	kg/m^3	max	890	Density @ 15 °C	kg/m^3	max	991
MCR	wt.%	max	0.3	MCR	wt.%	max	18
Flash point	°C	min	60.0	Flash point	°C	min	60.0
CCI		min	40.0	CCAI		max	870
Pour point, summer	°C	max	0	Pour point, summer	°C	max	30
Pour point, winter	°C	max	-6	Sodium	ppm	max	100
Sulphur content[a]	wt.%	max	0.1-0.5	Sulphur content[a]	wt.%	max	0.1-0.5
Ash content	wt.%	max	0.010	Ash content	wt.%	max	0.10
Oxidation stability	g/m^3	max	25	Water content	vol.%	max	0.50
H_2S content	ppm	max	2.0	H_2S content	ppm	max	2.0
TAN	$^{mg\ KOH}/_{g}$	max	0.5	TAN	$^{mg\ KOH}/_{g}$	max	2.5

[a] Sulphur specification varies with geografic location.

Table 5.6: Marine fuel specifications based on the ISO 8217 Fuel Standard [5]. The upper sulphur limit reflect the new global specification that will be in force from 2020 [8].

HDS processing adds to the cost of bunker fuel. In fact, severe desulphurisation of fossil residue is often infeasible and thus low sulphur marine fuels are often associated with density and viscosity 'give away'. This is a term for fuels that posses a quality higher than required by the fuel specification. A good example of this, is that vessels currently change their fuel supply from viscous bunker fuel to low sulphur marine distillate when entering a SECA region. The switching between fuels with very different viscosity, quality and solubility properties has induced engine performance problems such as filter clogging or sudden shutdown.

The Hydrofaction^{TM} residue fraction is characterised by a high density, high viscosity and a unique sulphur content below 100 ppm. This makes it a suitable blendstock for low sulpur residual marine fuel. The low sulphur content even allows for blending with relatively sulphur rich diluents such as straight run gas oils. Based on that, focus is on the specifications for residual marine fuel rather than for distillate marine fuel in Table 5.6.

A limited amount of analyses, such as calculated carbon aromaticity index (CCAI), pour point and viscosity, make it difficult to evaluate how the residue best fit into the bunker market. As described above it can certainly be used as a blendstock, but it may even be possible to make an ultra low sulfur Hydrofaction^{TM} bunker that meets specifications. Focusing on the C5,H2T fractions, F6 was concluded to be rather aromatic and dense for diesel applications above. Thus, if F6 is blended with the residue fraction, the density of this mixture will be 997 kg/m^3. This is very close to the upper limit of 991 kg/m^3 in Table 5.6, but the viscosity of such mixture will be out of range. In the lack of viscosity measurements, lets estimate that F6 and the residue fraction have viscosities at 50 °C around 5 and 2e5 cSt respectively. By addition

of 2.5 wt.% of F1 to a mixture with 95 wt.% F6+Residue, the viscosity can be reduced to roughly 700 cSt, which is within the specifications. This is based on the Refutas viscosity equation. Addition of 2.5 wt.% of F1 also reduces the density to 989 kg/m^3, which is just within specifications. This would be a beneficial as the F1 cannot be used as diesel, nor jet fuel. Though, the flash point specification will limit the amount of F1 that can be added and even 2.5 wt.% may be too much. Further, the sulphur content of such blend will be less than 100 ppm and it is very unlikely that such ultra low sulphur biobunker can be sold at a premium. Thus, the best option is probably to sell the low sulphur heavies as blendstock, possibly after addition of F1 to reduce viscosity.

If, in some potential setting, it makes sense to target the production of jet fuel, rather than diesel. Then, an ultra low sulphur marine residual fuel that meets all specifications can be produced by combining F5, F6 and the residue. Based on the previous estimations using the Refutas equation, such mixture will have a viscosity below 100 cSt and correspond to around 60 wt.% of the upgraded oil. The density will be 958 kg/m^3. In order not to have density, viscosity and sulphur give away and to improve the economic margin, a cheap high sulphur fossil residue can be blended in. E.g. close to 5 % fossil derived vacuum residue with 2 % sulphur and very high viscosity and density can be added without violating specifications. Overall, the accumulated product value of such process design is likely to be lower, since more of the upgraded oil is sold as marine fuel. On the other hand, operational costs may be reduced, as it is likely that the severity of hydrotreating can be eased as the strict cetane and density specifications of diesel are no longer constraining. The optimal configuration depends on the Hydrofaction^{TM} setting, but the Hydrofaction^{TM} fuel cuts seem to be rather flexible in terms of use.

6 Summing up on Drop-in Potential

Current legislation allows biomass derived fuels e.g. Hydrofaction^{TM} products in any proportion (except for jet fuel) as long as they meet specifications. On that basis, this chapter evaluated the drop-in potential of the fractions obtained from fractionation of upgraded Hydrofaction^{TM} oils. There has not been access to complete fuel assays, and thus the evaluation is not definitive. The gasoline equivalent fraction comprise around 10 wt.% of the upgraded oil. GC-MS analysis indicate that severe hydrogenation is detrimental to the octane rating of the gasoline fraction, and it should be exposed to mild deoxygenation only. Thereby a valuable Hydrofaction^{TM} gasoline blendstock with high octane rating, low vapor pressure and high density allow blending with relatively cheap butane to meet specifications for cold start, density and E70. Jet fuel is another potential fuel product that comprise up to 25 wt.%

of the upgraded Hydrofaction^{TM} oil. Despite limited analyses, the jet fuel equivalent fractions seem to be sufficiently hydrogenated to meet aromaticity and smoke point related specifications, yet sufficiently cyclic to have good cold flow properties. Density is however a constraint, suggesting blending as an option to introduce Hydrofaction^{TM} fuel in aviation. The diesel equivalent boiling fraction becomes the largest upon hydrotreating, comprising around 50-60 wt.% of the oil. The napthenic and aromatic nature affects density and cetane rating negatively, making blending a necessity for compliance with the European EN590 specification. Meanwhile, the current diesel cut is likely to comply with the North American D975 diesel specification as is. The residual heavy fraction fits perfectly into the bunker market, where new sulphur restrictions have sparked a demand for dense and viscous residues that avoid quality give-away without violating the sulphur specification.

References

[1] Advanced Motor Fuels (AMF) under IEA, "Oxygenates," http://www.iea-amf.org/content/fuel_information/oxygenatesfordiesel, 2017, accessed: 27-11-17.

[2] A. De Klerk, *Fischer-Tropsch Refining*. John Wiley & Sons, 2012, ISBN: 978-3-527-32605-1.

[3] E. C. for Standardization, "EN228:2012+A1 Automotive fuels - Unleaded petrol - Requirements and test methods," 2017.

[4] E. C. for Standardization, "EN590:2013+A1 Automotive fuels - Diesel - Requirements and test methods," 2017.

[5] I. O. for Standardization, "ISO8217:2017 Petroleum products - Fuels (class F) - Specifications of marine fuels," 2017.

[6] A. S. for Testing and M. (ASTM), "ASTM D4737-03, Standard Test Method for Calculated Cetane Index by Four Variable Equation," 2003.

[7] A. S. for Testing and M. (ASTM), "ASTM D975-16, Standard Specification for Diesel Fuel Oils," 2016.

[8] International Maritime Organization (IMO), "IMO sets 2020 date for ships to comply with low sulphur fuel oil requirement," http://www.imo.org/en/MediaCentre/PressBriefings/Pages/MEPC-70-2020sulphur.aspx, 2016, accessed: 27-11-17.

[9] G. Knothe and K. R. Steidley, "Lubricity of components of biodiesel and petrodiesel. the origin of biodiesel lubricity," *Energy & fuels*, vol. 19, no. 3, pp. 1192–1200, 2005.

[10] R. L. McCormick, M. A. Ratcliff, E. Christensen, L. Fouts, J. Luecke, G. M. Chupka, J. Yanowitz, M. Tian, and M. Boot, "Properties of oxygenates found in upgraded biomass pyrolysis oil as components of spark and compression ignition engine fuels," *Energy & Fuels*, vol. 29, no. 4, pp. 2453–2461, 2015.

[11] Totsa Total Oil Trading SA, "Crude Assays," https://www.totsa.com/pub/crude/index2.php?expand=3&iback=3&rub=11&image=europe#, 2017, accessed: 27-11-17.

[12] US Department of Energy, "Alternative aviation fuels: Overview of challenges, opportunities, and next steps," https://energy.gov/sites/prod/files/2017/03/f34/alternative_aviation_fuels_report.pdf, U.S. Department of Energy's Bioenergy Technologies Office (BETO), Tech. Rep., 2017.

Chapter 6

Conclusion

This work focuses on development and design of an integrated separation and upgrading platform for Steeper's Hydrofaction^{TM} technology that targets production of advanced biofuels for heavy transportation. Current transportation fuel legislations allow biomass derived fuels in any proportion (except for jet-fuel) as long as they meet specifications. But the oxygenated and aromatic character of a wood derived Hydrofaction^{TM} oil causes miscibility and non-compliance issues with commodity transportation fuels. Rather than partial upgrading to refinery biofeed quality, a standalone process configuration was selected, with complete upgrading of the entire liquefaction oil to drop-in fuel quality. This configuration optimizes potential product yield and value, and it enables Hydrofaction^{TM} to provide the undivided technology path from tree to tank.

The interface between the HTL process and the separation and upgrading platform was defined by analyzing the effect operating conditions and feedstock variations have on HTL oil quality and upgradability. Hydrofaction^{TM} HTL operates at temperatures in the supercritical water domain and at pressures above the pseudo critical pressure of water. Further characteristics include recirculation of aqueous and oil phases and use of homogenous alkali metal catalysts (K_2CO_3 and NaOH). Steady state operation at these conditions was resembled at the pilot, and potential replacement of NaOH with non-metal NH_3 was studied and then omitted. Presence of NH_3 induced severe coke formation and polluted the resulting biocrude with 2.7 wt.% nitrogen, which in turn inhibited subsequent hydrotreating. Variations in wood types were found to have negligible impact on the oil composition.

The organic product, as produced by gravimetric separation at the pilot, is a water in oil emulsion stabilised in part by amphiphilic carboxylate surfac-

tants. Demineralization tests showed that pH reduction is required to break the emulsion, and thus filtering, centrifugation and electrocoalescence were found ineffective. A washing procedure, using MEK as diluent and 0.1 M citric acid as washing agent, was developed for pilot scale, resulting in repeatable demineralization of Hydrofaction^{TM} oil to around 300 ppm ash or <50 ppm inorganics by ICP. Carbonated water was successfully tested as washing agent, reflecting a novel approach were the CO_2 rich gaseous HTL product is used as acidifying agent during demineralization. The developments have been implemented in a flexible continuous separation and demineralization system that is to be commissioned at the CBS1 in Q3 2018.

The present work advance state of the art on hydrotreating of HTL oil by parametric screening in continuous systems with up to 660 HoS. A continuous dual-reactor hydrotreating pilot unit (H2T'er) has been designed, built and commissioned at AAU as part of the PhD project. The irregular composition of liquefaction oil impose critical differences when conventional hydrotreating is adapted to Hydrofaction^{TM} . A critical step was configuration of the first reactor to keep reaction rates, exothermic heat release and pressure drop build up at a manageable level. A continuous 3-Zone hydrotreating process was developed upon several iterations, proving upgrading of Hydrofaction^{TM} oil to drop-in transportation fuel.

HTL oil volatility is significantly improved by deoxygenation and the diesel equivalent boiling fraction becomes the largest upon hydrotreating, comprising around 50-60 wt.% of the oil. The napthenic and aromatic nature affects density and cetane rating negatively, making blending a necessity for compliance with the European EN590 specification. Meanwhile, the current diesel cut is likely to comply with the North American D975 diesel specification as is. A valuable gasoline blendstock ($\approx$10 % of oil) can be collected if exposed to mild deoxygenation only, because severe hydrogenation is detrimental to the octane rating. Despite limited analyses, the jet fuel equivalent fractions ($\approx$25 % of oil) seem to be sufficiently hydrogenated to meet aromaticity and smoke point related specifications, yet sufficiently cyclic to have good cold flow properties. Density is however a constraint, suggesting blending as an option to introduce Hydrofaction^{TM} fuel in aviation. The low sulphur residual heavy fraction fits perfectly into the bunker market, where new sulphur restrictions have sparked a demand for dense and viscous residues that avoid quality give-away without violating the sulphur specification.

As a conclusion, an integrated separation, demineralization and upgrading technology platform has been developed for Hydrofaction^{TM} , enabling production of advanced biofuel blendstocks targeting heavy transportation.

Part II

Appendices

Chapter i

Documentation of AAU Continuous H2T'er

A continuous hydrotreating pilot unit, referred to as the H2T'er, have been designed, build and commisioned as part of this PhD project. Project timeline and pilot features are described in Section 3 of Chapter 4, while this appendix provide a technical review of the unit.

i Oil Feed Handling and Pressurization

Biocrude subject to hydrotreating is poured into a 20 liter feed tank, which is designed with a 250 mm ID flanged lid in order to ease filling and cleaning. The tank can be pressurized with a nitrogen blanket of up to 20 bar to displace air and ensure that also viscous oils can be fed to the pump. The feed line is made in 3/8" OD tubing to reduce pressure losses, and it is heat traced to reduce viscosity of the oil feed during filling.

The oil feed is pumped at constant volumetric flowrate using an ISCO A500HV continuous flow dual cylinder syringe pump, specifically suited for highly viscous fluids. Each cylinder, which has a capacity of 500ml, is maintained at constant temperature using a heating jacket connected to a Julabo waterbath. The constant temperature and volume flow ensures a constant mass flow rate, which is crucial to establish mass balances for the process.

ii Gas Supply

Table i lists the different gasses that are connected to the hydrotreating unit. Besides hydrogen, which is a necessity during hydrotreating, nitrogen is connected to dry catalysts during activation, and displace air or hydrogen before

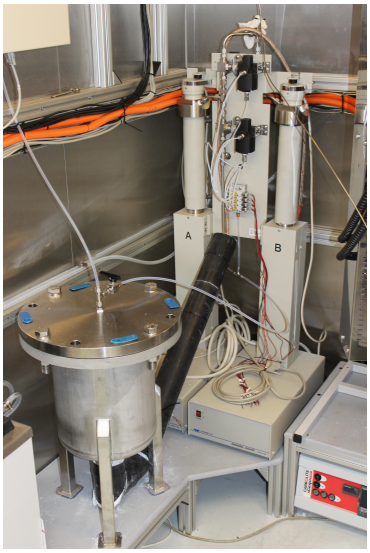

Fig. i: Feedtank and syring pump of the H2T'er.

or after a campaign. Additionally, nitrogen is used to purge separation vessels, the feed tank and it is used to define the setpoint of BPR.1. Similarly, air is used to drive the valve system of the oil pump.

Gas	Supply pressure [bar]	Minimum flow [NmL/min]	Maximum flow [NmL/min]
H_2	220	40	2000
CH_4	220	0.3	15
CO_2	55	0.1	5
N_2	220	2	100
Air	8	-	-

Table i: Details of the gas supply lines that are controlled by Bronkhorst high pressure mass flow controllers.

Methane and carbon dioxide are made available with mass flow controllers to simulate the effect of a polluted hydrogen feed, which becomes relevant in relation to e.g. hydrogen recirculation. Further reasoning is provided in Section 3. Bottled CO_2 can only be purchased at a pressure of 55 bar, which limits the operating pressure of the system when CO_2 is co-fed. This is related to the fact that at higher pressures CO_2 condenses to liquid phase at ambient temperature. The CO_2 gas supply line is heat traced to avoid any condensation around the mass flow controller (MFC.3).

The bottle pressure of each gas supply is digitally provided in the lab. This makes the operator aware of current gas levels and when to purchase a

Fig. ii: Each gas supply line consist of (from the top) a manual pressure reguator, a magnetic safety valve (normally closed), a pressure transducer and a mass flow controller.

refill of e.g. H_2.

iii Reactors and Heating

The oxygenated biocrude is relatively reactive at elevated temperatures and to reduce or stabilise polymerization reactions the biocrude is mixed with hydrogen prior to any noticeable heating. The oil-hydrogen mixture is then heated to 75-125 °C by heat tracing along the tubing to reduce viscosity and thereby improve reactant mixing and reduce the pressure drop.

Two vertical, tubular Carbolite Gero TVS12/900 furnaces with three-zone control surround the reactors to supply an even temperature. The two reactors each consists of an 800 mm, 3/4" OD SS-316L tubing packed with catalyst and inert silicon carbide (SiC). A multipoint thermocouple probe by Omega with 10 evenly distributed measurements are positioned inside each reactor to monitor the axial temperature distribution. This is particularly important in relation to processing an oxygenated biocrude, because both hydrodeoxygenation and hydrogenation are exotermic reactions that make temperature monitoring and control a necessity.

The reactors are designed to make the operators life easy, when changing catalyst beds. Firstly, the furnaces are easily opened by three clips to access the reactor tubing as pictured in Figure iii. Secondly, Swageloks VCR Metal Gasket Face Seal Fittings have been used to improve the lifetime of the reactors. The VCR®fittings reassemble reliably after maintenance and are

superior to the two-ferrule compression fittings when it comes to being leak tight after many sealing and heating cycles. Finally, the thermocouple is fixed in the bottom and continues through the reactor tube to the location of the VCR®fitting so it can be aligned in the tube center during catalyst filling. The reactor design is sketched to the right in Figure iii.

Fig. iii: Left and center: Two vertical three zone split type furnaces from Carbolite Gero provide easy access to the reactor tubing. Right: A sketch of the reactor design with VCR®fittings in the top, and a multipoint thermocouple positioned along the center and out of the bottom.

Reactor Configurations

The system is designed to enable operation in different reactor configurations, which is shown in Figure 4.9 and explained further in Section 3. The two reactors can be run one at a time, configured in series or bypassed. The bypass line is useful in the case of a blockage in one of the reactors, because the bypass line enables pressure relief and/or back flushing. This either removes the plug or ensures a smooth shutdown. The reactor configuration is changed manually using 3-way valves, rated for the high temperatures and pressures that may be present in the reactor zone.

iv Cooling, Pressure Reduction and Separation

Due to the relatively low flow rate, the conductive heat loss through the product line tubing provides sufficient cooling of the reactor products. In fact the

product line is heat traced and insulated in order to maintain a given temperature of the products entering the separation vessels.

The back pressure regulator, BPR.1 is a critical component of the H2T'er. It was included in the design based on the hypothesis that product separation at operating pressure will result in loss of the light hydrocarbons, which are condensed at high pressures but flashed off during sampling where the pressure is reduced to atmospheric. Loss of these would affect the overall mass balance negatively. By reducing the pressure to 2-10 bar prior to separation, this effect is reduced and the light hydrocarbons that was otherwise lost will be present in the gaseous product. However, the BPR.1 is exposed to a multiphase product flow including water, oil, gaseous and sometimes even solid products. Thus finding a regulator that enables stable operation despite such mixture is demanding. An Equilibar H3P regulator with kalrez o-rings was chosen, because it is specifically suited for multiphase flow applications with high resistance to chemicals.

Fig. iv: Left: BPR.1, 3-way valve and two high pressure separation vessels, which are 1 and 3.4 liter respectively. Right: BPR.2, wet gas meter, KOH trap and gas ventilation lines.

The H2T'er is designed with two gas/liquid separation vessels in order to strip off the hydrogen rich product gas. Liquid products are then collected in a separation vessel for a given time until the vessel is depressurized, vented and emptied, while the product flow is directed to the other vessel. The vessels have a volume of 1 and 3.4 liters and are heat traced and insulated to keep a constant separation temperature. After collecting samples, the vessels can be repressurised with nitrogen before being switched back on-line. The gaseous products are directed through another more standard back pressure

regulator, BPR.2, before the volume flow is quantified in a W-NKA-0.5B-Z wet gas meter by Shina Gawa. Finally, the gas is passed through either a collection vessel for compositional analysis or a through a KOH aqueous solution trap before being vented.

v Process Control

Process control and automation has been developed in LabVIEW by the PhD candidate. Figure v depicts the main user interface in which pressures, temperatures, flow rates and valve settings can be monitored and controlled. The user interface executes on a windows laptop and connects to a CompactRio which is located in the control box. The CompactRio represent the process connection and it runs independently of the laptop to avoid a process shutdown if the laptop e.g. freezes, restarts etc. The control box and the CompactRio is depicted in the upper right and bottom left of Figure v. The control box is made with different SubD9, SubD25 and thermocouple sockets for quick connection of instruments in case of maintenance. Acknowledgements to Walter Neumayr and Mads Lund, who wired the control and heat tracing boxes respectively.

The bottom right of Figure v depicts the graphical interface which is useful during operation to monitor temperatures, pressure and flow rates over time. In the far bottom right, the two reactor temperature profiles are given. They plot temperature on the x-axis against reactor depth on the y-axis, and are useful in relation to monitoring autothermal heating by exotermic reactions. As an example, the provided screenshot shows an even temperature profile in reactor 2 (right), whereas in reactor 1 (left) exothermic reactions make the inlet of the catalyst bed about 10 °C warmer than the remaining bed.

Datalogging implies writing all input and output values to a text file. A new text file is created every 24 hours. A log file is also automatically generated to log a history of all operational changes and alarms. As an example, if a heat tracing set point is changed, it is written in the log file. Similarly, if a valve is opened or an alarm is triggered. Finally, the operator can write observations or note weights of a mass balance in the log file.

vi Safety Precautions

Safety is a highly prioritized matter both during design and operation of the continous H2T'er. Processing of a highly flammable mixture of hydrogen and oil at relatively high temperatures and pressures is one aspect, the presence of hydrogen sulphide is another, unmanned operation and control of the unit

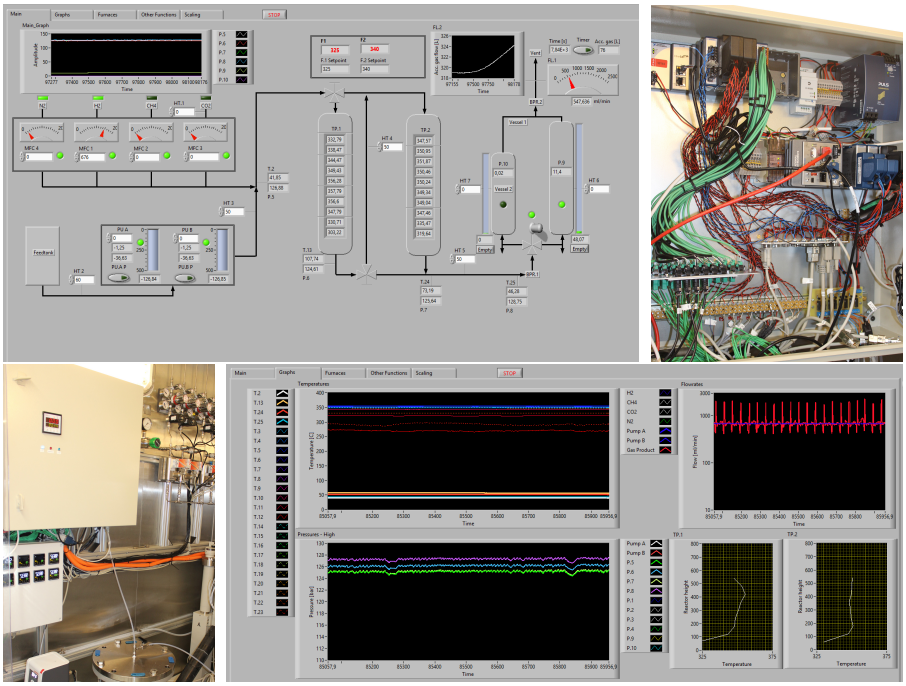

Fig. v: Top left: Main user interface. Top right: Wiring of CompactRio and control box. Bottom left: Control box and heat tracing controllers. Bottom right: Graphical user interface.

at these conditions is a third of many risks that need to be identified before commisioning the unit.

A rupture disc set to burst at 180 bar is installed at the entrance of each reactor. The outlets of both rupture discs are directed to a knock-out drum that is connected to the ventilation. Similarly, a pressure relief valve set to 130 bar is installed before BPR.2.

The H2T'er is installed in an ATEX walk-in fumehood. Five gas alarms (O_2, CO, H_2, CH_4, CO_2) are installed and connected to the alarm system. A so-called level 1 alarm warns the operator at a given threshold, while a level 2 alarm cuts all gas supplies at a more severe leakage. A H_2S alarm is being installed in the near future, but the H_2S concentration is also being monitored by personal detectors (O_2, H_2S, H_2 and flammable gasses).

Finally, the labview program is designed with different safety algorithms that warn the operator by email and potentially shut down the system in case of any abnormalities. System shutdown involves cutting all heat supply and

closing all gas and oil supply valves. Thereby the system cannot build up pressure, but the pressure remains rather constant, giving the operator time to respond. The alarms are as follows:

1. High pressure alarm (system shutdown)
2. Low pressure alarm (system shutdown)
3. High pressure alarm in separation vessels (system shutdown)
4. High temperature alarm in separation vessels (warning)
5. High temperature alarm in reactors (warning)
6. MFC flow rate alarm (warning)
7. Separation vessels are more than 75% full (warning)

The H2T'er unit was successfully commissioned in July 2017 and has been operated without safety remarks for the first 5 campaigns.

Part III

Publications

Paper A

Hydrofaction™ of Forestry Residues to Drop-in Renewable Transportation Fuels

Claus Uhrenholt Jensen, Julie Katerine Rodriguez Guerrero, Sergios Karatzos, Göran Olofsson, Steen Brummerstedt Iversen

The manuscript has been published as Chapter 10 in the book *Direct Thermochemical Liquefaction for Energy Applications* edited by Lasse A. Rosendahl, ISBN: 9780081010259, pp. 319-345, 2018.

The layout has been revised.

Hydrofaction™ of forestry residues to drop-in renewable transportation fuels

10

C.U. Jensen, J.K.R. Guerrero†, S. Karatzos†, G. Olofsson*, S.B. Iversen**
*Steeper Energy ApS, Hørsholm, Denmark, †Steeper Energy Canada Ltd, S.W. Calgary, AB, Canada

10.1 Introduction

On a global and unprecedented scale, climate change is threatening humanity through changing weather patterns and rising sea levels. An increasing frequency of catastrophic droughts and floodings affects essential food and water supply, forcing so-called climate migrants to move due to sudden or gradual changes in the natural environment [1,2]. The Paris agreement (in force November 2016, signed by 193 countries) addresses the urgent and potentially irreversible threat of climate change and the necessity to reduce greenhouse gas (GHG) emissions from the energy sector [2,3]. In the World Energy Outlook 2016 [3], IEA projects the future energy sector and how existing technologies for renewable heat and power generation will be deployed to approach emission targets. This includes a significant increase in electricity generation from, for example, solar and wind, which indirectly introduces renewables in the transportation sector, where electric cars are considered momentous for urban and short-distance transport [3]. However, the same report emphasises that the lack of renewable fuel alternatives for heavy transportation such as trucks and aviation will account for the continued growth in global consumption of fossil and carbon-intensive petroleum [3]. The European Commission also highlights the need for low-emission fuels for heavy transportation in order to meet the emission targets for the transportation sector, which currently represents about 25% of EU's total GHG emissions [4]. Steeper Energy is addressing this gap by commercializing its proprietary hydrothermal liquefaction (HTL) technology, Hydrofaction™, which facilitates the production of sustainable drop-in biofuels targeting heavy transportation.

The competitive strengths of HTL begin from the ability to process a wide range of wet and dry low-value nonfood biomass residues, thereby mitigating feedstock supply risks and interference with food supply. Secondly, HTL is currently considered a competitive and resource-effective thermochemical pathway to advanced biofuels, due to its high energy and carbon efficiency [5,6]. A 2014 study commissioned by the US DoE estimated a 70% GHG emission reduction from hydrotreated HTL biofuel compared with the 2005 petroleum baseline [5]. Finally, the hydrotreated HTL products are fully compatible with the existing petroleum infrastructure (pipelines, stations, and

Direct Thermochemical Liquefaction for Energy Applications. https://doi.org/10.1016/B978-0-08-101029-7.00009-6

engines) enabling drop-in without blend-wall limitations. This facilitates a gradual phase-in where production capacity and cost-efficiency can be balanced during the transition to fossil independence [7].

10.1.1 Forestry residues as feedstock

Steeper Energy is currently focused on forestry residues and mill wastes as Hydrofaction™ feedstock due to the global abundance of these resources and the industry's need for cost- and carbon-efficient utilisation of their wastes.

Forests cover around one-third (30.7% in 2010) [8] of the global land area and are an essential part of life. The significant amounts of carbon that is sequestered both below- and aboveground by photosynthesis also make forests essential for climate-change adaption and mitigation [8]. As an example, afforestation and reforestation were approved as GHG mitigating strategy under the Kyoto Protocol [9]. Carbon sequestration can be optimised by agroforestry and sustainable forest management, thus enhancing the rate of carbon absorption [8–11]. In other words, since a tree grows slower as it gets older, there is an optimum between the harvest rotation cycle and the rate of carbon uptake. In fact, [11] states that the shorter the harvest rotation age, the more favourable the carbon balance becomes over time. This however implies that the sequestered carbon (wood) is used to substitute fuel-intensive building materials such as steel or concrete, while the manufacturing residues (bark, branches, and sawdust) are used to substitute fossil fuels [11]. Such efficient use of the forestry residues is however not granted, as the industry currently wastes up to 40% of the harvested material [12].

The revenue from residuals is also crucial for the forest industry. This was concluded in a recent study on the biomass supply and utilisation chain in three Canadian provinces [13]. The study showed how sawmills were running at a small loss on their core process, the lumber output, but stayed in business due to revenue from residuals as inputs to, for example, electricity generation. Similarly, if the price of lumber would decrease, only the sawmills located close to residual offtakers (e.g. pulp mill) would stay in operation from the value of the residual products [13]. These residuals (wood chips, sawdust, planer shavings, and residual bark) are mainly produced at the mill during the primary processing. However, the major fraction of forestry residuals is the so-called slash, produced during the preliminary processing at the felling site. These have been estimated to account for more than 20% of the total harvested volume in Canada [12].

As mentioned previously, the forestry residuals need to be used as bioenergy to replace fossil fuels in order for agroforestry to be a carbon-efficient GHG mitigation strategy [11]. As such, the slash can be chipped and transported at a cost around US$ 30–60/ODT (oven-dried tonne) [12–14]. Due to the costs of processing and transportation, a significant amount of such slash is either disposed in stockpiles or burnt on site instead of being efficiently utilised. Wood waste stockpiles decompose over time releasing significant methane emissions from anaerobic digestion, which has a significant GHG footprint (1 kg CH_4 = 25 kg CO_2e) [15–17]. A portion of the forest residuals are currently used for electricity and heat types of bioenergy [3,13]. However, in the

longer run, this is unlikely to be a cost-competitive solution to alternative renewable sources such as solar PV and wind power, as IEA projects an average cost reduction on these by 2040 of 40%–70% and 10%–25%, respectively [3]. Furthermore, the pulp industry, which is a major offtaker of forestry residuals, is currently struggling in Europe and North America with a decreasing demand and increasing competition from Asian and South American mills [18,19]. This emphasises the need for finding alternative uses of forestry residuals, such as a feedstock for thermochemical production of biofuels. In fact, the transformation of pulp and paper mills into biorefineries in Europe and North America has been mentioned as a potential cornerstone of a green economy [20]. This is where the Hydrofaction™ technology becomes relevant by bridging the gap between a globally abundant waste product that needs to be cost-effectively and carbon effectively utilised and the heavy transportation sector that needs a renewable fuel alternative. A life-cycle GHG emission analysis of Hydrofaction™ products produced in Alberta, Canada, from forestry residuals (slash) as feedstock is presented later in Section 10.3.

10.2 The Hydrofaction™ process

Hydrofaction™ is a proprietary thermochemical technology platform that enables conversion of wet (as harvested) biomass residues directly to renewable drop-in biofuel indistinguishable from its petroleum equivalent. The reaction pathway includes two major subprocesses, which are supercritical HTL (first stage) and subsequent upgrading through hydrotreating (second stage). During the first stage, Hydrofaction™ utilises a combination of the following features to efficiently convert the biomass to an energy-dense renewable crude oil [21]:

- Operating pressures (300–350 bar) and temperatures (390–420°C) above the critical point of water
- Recirculation of water-soluble organics and Hydrofaction™ oil for improvements in feed characteristics, energy balance, oil quality, and yields
- Use of homogeneous alkali metal catalyst (K_2CO_3 and NaOH) for desired catalytic effects and control of pH to minimise corrosion
- Recovery and recycling of alkali metal catalysts for improved process economics and reduced footprint

The resulting biocrude is characterised by relatively high aromaticity and an oxygen content around 10 wt%, which strongly affects the physiochemical properties (density, viscosity, volatility, polarity, and hydrophobicity) that determine the biocrude compatibility with petroleum equivalents. Therefore, as any petroleum crude, the renewable crude oil needs further refining to meet the various fuel specifications. Whereas hydrodesulphurisation (HDS) and hydrodenitrogenation (HDN) are the major reaction steps in refining petroleum crudes, upgrading of wood-derived HTL crude oil is mostly focused on hydrodeoxygenation (HDO) and hydrodearomatisation (HDA). During Hydrofaction™, this is achieved by hydrotreating on commercial catalysts, which is a standard and widely used refinery operation [22]. Finally, the

hydrotreated product is fractionated by boiling point to renewable fuels for drop-in in the diesel and marine fuel pools. Thereby, forestry residues can be used to substitute fossil transportation fuels with a renewable alternative.

The Hydrofaction™ subprocesses are schematised in Fig. 10.1 including major interconnected operations, such as recirculation streams, water treatment, and utilisation of gaseous products in a fired heater. Fig. 10.1 is divided into an HTL and an upgrading part; accordingly, the description and presentation of experimental data for the first and second stage are divided into Sections 10.2.1 and 10.2.2, respectively.

10.2.1 Supercritical HTL (first stage)

Characteristics of Hydrofaction™ HTL are the use of high-density, supercritical water; homogenous alkali metal catalysts; and the recycling of aqueous and oil products back into the process. The Hydrofaction™ HTL stage applies operating conditions (300–350 bar and 390–420°C) that are above the critical point of water, which is higher than most other HTL processes reported in literature [23–28]. The chemical properties, such as the dielectric constant and ionic product, that make near-critical water an appealing reaction medium for HTL are a direct function of density [29]. Thus, by ensuring a high pressure, key thermodynamic properties of water can be maintained at the same order of magnitude as for the subcritical conditions while taking advantage of improved kinetics, mass, and heat transfer at higher temperatures. As an example, the ionic product of water is an important parameter within hydrothermal processing, because it reflects whether a medium favours ionic or radical reactions [30,31]. Due to the relatively high

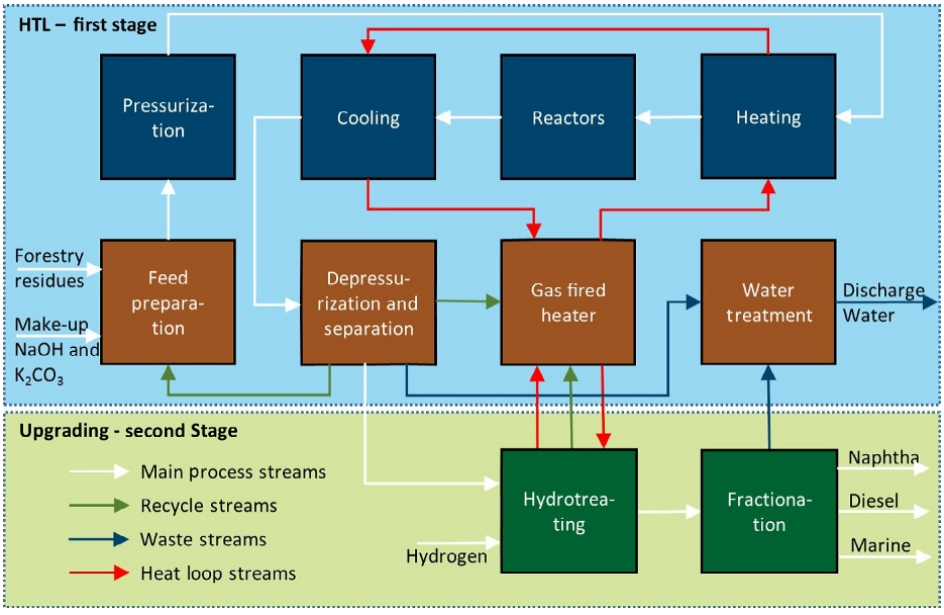

Fig. 10.1 Schematic of the Hydrofaction™ process consisting of supercritical HTL and subsequent hydrotreating. Besides the major heat loop streams indicated, the process utilises additional heat integration between the stages.

pressure, the ionic product of water at Hydrofaction™ conditions is up to several orders of magnitude higher than at the critical point. Similarly, the higher pressure ensures that density and derived properties are less dependent on temperature changes, which is beneficial during plant operations to ensure a smooth transition of process parameters such as fluid velocities, Reynolds numbers, specific heat capacity, heat-transfer coefficients, and retention times. Consequently, due to the supercritical temperature, it is crucial to maintain a high pressure during the Hydrofaction™ HTL stage.

At near-critical conditions, the dielectric constant of water is reduced more than 90% as compared with ambient conditions. Thereby, water dissolves nonpolar compounds, such as biomass and biocrude molecules that are hydrophobic at ambient conditions. This accelerates conversion through, for example, hydrolysis and solvolysis reactions by reducing mass-transfer limitations. Such ionic reactions are further promoted by water dissociation, which is maintained high in relatively high-density supercritical water [29].

The recirculation of produced organic compounds in the form of both water-soluble organics and oil has a number of benefits. It simplifies feed preparation and reduces the heat capacity of the process fluid, and it appears that the presence of water-soluble organics in the feed inhibits further formation of water-soluble organics, thereby increasing the relative amount of oil produced. Ref. [21] provides further details on the characteristics of Hydrofaction™ HTL, the reasoning behind the operating conditions, and the considerations around the major chemical reactions occurring during the HTL stage.

10.2.1.1 Feed preparation

The first step of the HTL stage in Fig. 10.1 is to prepare a pumpable feed of the different reactants including the forestry residues. The feed is prepared from size-reduced forestry residues, recycled oil, and aqueous products as well as make-up homogenous catalysts in the form of potassium carbonate and sodium hydroxide. Recirculation of both the aqueous and oil products is beneficial during feed preparation, because the water-soluble organics and phenolic oil compounds introduce a partial dissolution mechanism, which increases homogeneity and improves rheological properties of the feed. Similarly, the presence of alkali salts gives rise to carbonate/bicarbonate, which accelerates the depolymerisation by hydrolysis during pretreatment. The homogeneous catalyst in the form of potassium is mainly introduced by recirculation of the aqueous products, but make-up is required because a small fraction of the aqueous products are discharged to prevent build-up of trace compounds. Sodium hydroxide is added for control of the pH to alkaline conditions throughout the process.

A high biomass dry-matter loading in the feed is important to drive down both capital and operational expenses per fuel volume produced. Wood feeds with a dry-matter content of 17–25 wt% are used during pilot testing of Hydrofaction™ HTL [21,32,33].

10.2.1.2 Pressurization and heating

The feed mixture is pressurised to a pressure in the range of 300–350 bar and subsequently rapidly heated to a reaction temperature in the range of 390–420°C. The heating is to a large degree performed by heat recovered from the outgoing product stream.

This is performed by indirect heat exchange using high-pressure water as heat-transfer medium in a loop from the cooling section to the heating section.

It should be noted that several benefits are provided by the supercritical operating pressure and temperature applied in the Hydrofaction™ process. This is related to the fact that Hydrofaction™, despite being supercritical, is operating below the so-called pseudocritical line (PCL), which is defined as the temperature at a given pressure where the specific heat capacity of water is at a maximum [29]. This means, for example, that the enthalpy of water at, for example, 335 bar and 400°C is similar to the specific enthalpy at the critical point of water [29]. The specific enthalpy of the actual mixture is even lower as water typically only comprises around 50 wt% of the feed mixture due to the high dry-matter and organic content. Recirculation of organics through both the aqueous and oil product reduces the overall heat-transfer requirement, due to the lower specific heat capacity of organics compared with water. This reduces the overall heat requirement of the process, which is emphasised with Fig. 10.2 that shows how the power consumption of the two serially connected heaters in the pilot plant decrease once the process fluid is switched from water to feed at a constant mass flowrate. Note that the pilot does not facilitate heat exchange and thus it has a slightly different configuration than that given for the first stage in Fig. 10.1. The pilot plant is described in Section 10.2.1.6.

Heat exchange is an obvious feature that improves the cost and energy efficiency of a hydrothermal process that utilises near-critical water as a reaction medium. The relatively high pressure applied in Hydrofaction™ ensures that the heat-transfer coefficient of water does not drop above the critical point. Likewise, the higher temperature, compared with subcritical, results in a high thermal effusivity and a more favourable driving force for

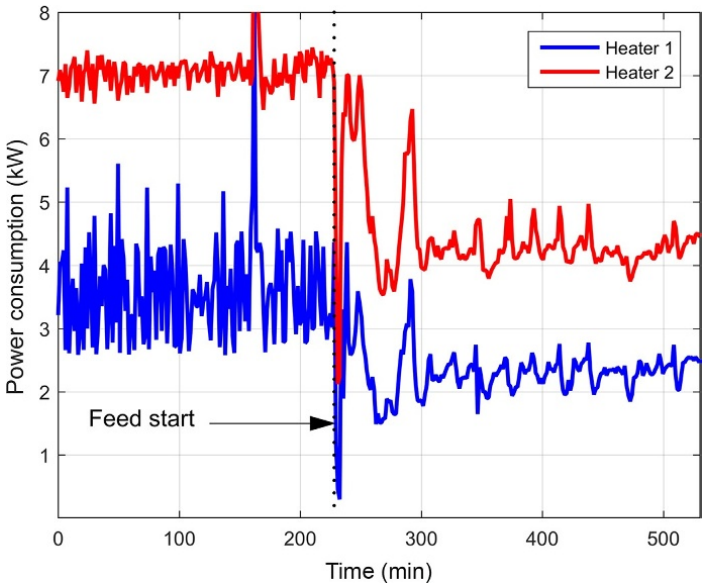

Fig. 10.2 The effect of switching from water to feed on power consumption of the pilot plant heaters.

heat exchange, which improves the heat recovery potential. Typically, 50%–75% of the heat required for heating to reactor temperature is recovered through heat exchange. The remaining heat load of the process is supplied by a fired heater, which at steady state is fired with gas from the process. This stream possesses more than sufficient calorific value, even if the hydrogen fraction is extracted (for upgrading use) before combustion. In fact, this makes the Hydrofaction™ process self-sustained with thermal energy at steady state.

10.2.1.3 Reactors

The heated feed/product intermediate enters the reactors, where it is maintained at reaction temperature and pressure for a certain period of time, typically 10–15 min. A proposed set of major chemical reactions occurring during Hydrofaction™ is presented in Ref. [21].

10.2.1.4 Cooling and pressure reduction

The product mixture from the reactors is cooled to about 150°C by heat exchange with the incoming feed via the high-pressure water loop described above, before the pressure is reduced to separation pressure in the pressure let-down system.

10.2.1.5 Separation and water treatment

In the separation part of the process, the cooled and depressurised products are separated into a gas stream, a water stream containing dissolved salts, a crude oil stream, and optionally a solid stream. This is performed by a combination of filtration and gravimetric phase separation.

The gas phase produced is mixed with product gas from the upgrading section and used to fuel the fired heater and heat the high-pressure water loop as described above. Optionally, the first-stage gas phase may be further separated to extract hydrogen and/or CO_2 before combustion (see Section 10.3 for details).

The aqueous phase is split into a concentrate and a distillate phase in a recovery unit. The distillate is purified to allow disposal and discharged in amounts that balances the water deducted from the feedstock biomass. The concentrate, which contains most of the total organic carbon (TOC) and alkali metal catalysts, is recycled back to the feed preparation step, except a bleed of 5%–15% that is withdrawn to prevent build-up of trace compounds such as chloride. A fraction of the oil phase is also recycled back to the feed preparation step, while the remainder is conditioned through desalting to recover potassium and sodium alkali catalysts and reduce the ash and water content prior to hydrotreating. The first-stage product is a renewable crude oil that similar to fossil equivalents requires further upgrading to meet transportation fuel specifications.

10.2.1.6 Summary of HTL pilot operation data (first stage)

A continuous pilot facility dedicated to supercritical HTL was commissioned at Aalborg University, Denmark, in 1Q2013. Since then, the pilot has completed >1600 oil production hours and constituted a centrepiece in the generation of data from the first stage (HTL) of Hydrofaction™.

The pilot is a semicontinuous HTL plant; feeds are prepared in 100 kg batches and then processed continuously at a flowrate around 20 kg/h. In standby mode between batches, the plant circulates pressurised deionised water, which is also the medium used for heat-up and cool-down of the plant. The batchwise processing of feeds complicates the recirculation of aqueous and oil products, that is, characteristic to Hydrofaction™ HTL. The recirculation is however demonstrated in the pilot by using a start-up oil and recycling the products a number of times until the start-up oil is sufficiently diluted/converted and a steady-state product is produced. Using this approach, it has been observed that recirculation of the aqueous product enhances oil yield, because the TOC content of the aqueous product is stable at steady state [21,33].

Table 10.1 lists key figures on the operating conditions, the feed characteristics, and the product yields observed during an extensive oil production campaign that is published in Ref. [21]. A 50:50 mix of spruce and pine wood chips was used as Hydrofaction™ feedstock to produce >150 kg of renewable Hydrofaction™ crude oil. The total mass balance at steady state was on average 100.3 wt%, with no detectable production of char or filter retentate products. The yield of renewable Hydrofaction™ crude oil from dry ash-free woody biomass was on average 45.3 wt%, and similarly, the gas yield was 41.2 wt%. Based on closure of the carbon, hydrogen, and oxygen elemental balances, the remaining product mass was suggested to be water synthetically produced during the biomass conversion.

10.2.1.7 Effect of feedstock on renewable crude oil quality (first stage)

Table 10.2 lists basic physiochemical properties, and Fig. 10.3 depicts distillation profiles of six different renewable Hydrofaction™ crude oils that were produced from three different woody biomass types and using two different start-up oils, crude tall oil (CTO) and distilled tall oil (DTO). The results indicate that the different Hydrofaction™ oils appear to have very similar key characteristics, which emphasises that the start-up oil has little effect on the final product quality because it seems to be diluted sufficiently after 4–6 recirculation cycles. It needs mentioning that the IBP-130°C volatiles were lost during the production of oil A, which increased the viscosity relative to the other oils. The H/C ratio of oil A and the volatility in Fig. 10.3 are also slightly affected by this.

The effect of hardwood (birch) versus softwood (pine/spruce) was also tested at the pilot at the same operating conditions as those given in Table 10.1, but Table 10.2 and Fig. 10.3 indicate only little noticeable difference between the key quality characteristics of the Hydrofaction™ oil produced from the two different types of woody biomass. Though it seems that birch wood results in a slightly higher nitrogen content compared with pine/spruce mixtures. A 10% bark in a pine/spruce feedstock was also tested, based on the motivations previously mentioned for using forestry residues in which bark will be a significant constituent. Again, the quality of the resulting crude oil is comparable, and thus, it could be suggested that a renewable Hydrofaction™ crude oil produced from woody biomass is expected to be relatively viscous; contains roughly 10 wt% oxygen, 1000–2000 ppm nitrogen, and 100–200 ppm sulphur; and possesses an HHV around 38 MJ/kg and a H/C ratio around 1.3–1.4.

Table 10.1 **Key figures on the first-stage Hydrofaction™ HTL are based on Ref. [21]**

Feed characteristics			**Operating conditions**			**Yield figures**		
Feedstock		50:50 Spruce/pine	Feed flowrate	kg/h	20–22	Mass balance	wt%	100.3
Dry-matter content	wt%	17–20	Reactor temperature	C	390–410	Oil yield	wt%	45.3
Oil-to-wood ratio	kg/kg	0.8–1.0	Reactor pressure	bar	300–320	Gas yield	wt%	41.2
Particle size	mm	<2	Heating rate	C/min	<350–450	Water yield	wt%	13.8

Table 10.2 Basic properties of renewable crude oils produced by Hydrofaction™ of various woody biomasses using different start-up oils

Oil	Cycle	Start-up oil	Feedstock	Viscosity[a] (cP)	HHV[b] (MJ/kg)	MCR[b,c] (wt%)	C[b] (wt%)	H[b] (wt%)	N[b] (ppm)	S[b] (ppm)	O[d] (wt%)	H/C
Oil A [21]	6	CTO	Pine/spruce	17,360	38.6	21.0	81.4	8.6	1124	100	9.8	1.26
Oil B	4	CTO	Pine/spruce	714	38.0	16.4	80.4	9.0	822	195	10.4	1.34
Oil C	5	CTO	Birch	813	38.0	15.6	80.8	9.1	2635	215	9.8	1.34
Oil D	5	DTO	Birch	2084	37.7	18.6	80.2	9.2	2201	159	10.4	1.37
Oil E	5	DTO	Pine/spruce	3313	37.2	19.7	80.0	9.0	1447	104	10.9	1.34
Oil F	5	DTO	10% Bark in pine/spruce	1954	37.9	18.1	81.4	9.7	973	100	8.8	1.42

[a] Viscosity at 40°C.
[b] On dry basis.
[c] Micro carbon residue (ASTM D4530).
[d] Oxygen by difference.

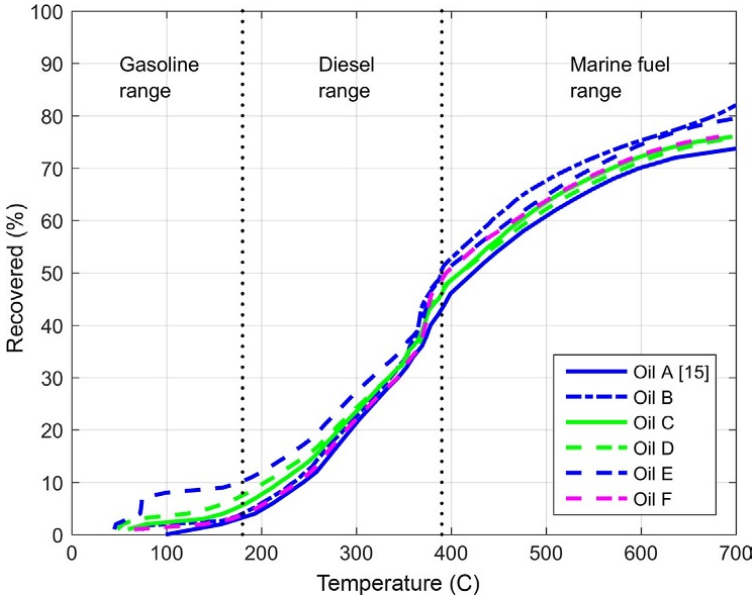

Fig. 10.3 Simulated distillation (ASTM D7169) of the oils given in Table 10.2 produced from pine/spruce *(blue)*, birch *(green)*, and 10% bark in pine/spruce *(purple)*.

10.2.2 Upgrading to drop-in biofuels (second stage)

A significant degree of biomass deoxygenation takes place during the first-stage Hydrofaction™ HTL, but the remaining oxygen content of the renewable crude oil affects the physiochemical properties that determine its compatibility with petroleum equivalents. In other words and similar to petroleum crude oils, the renewable crude oil can be referred to as an intermediate that requires further upgrading in order to gain transportation fuel value. Upgrading of the renewable Hydrofaction™ crude oil is done through catalytic hydrotreatment, which is a widely used process within conventional petroleum refining [22]. The process applies heterogeneous bimetallic catalysts and relatively high partial H_2 pressures to remove oxygen as mainly water through HDO and hydrogenate the renewable crude oil to remove aromatics and improve the diesel and marine fuel characteristics such as cetane number, density, and aromaticity. As indicated with a recirculation stream in Fig. 10.1, the hydrogen produced in situ during the HTL stage can be separated from the gaseous HTL product and utilised to cover part (~50%) of the hydrogen consumption in the second stage.

The current chapter presents hydrotreating experiments carried out in both continuous and batch reactor systems (BRS) and using both sulphided and nonsulphided catalysts. The objective is to show the product quality of wood-derived renewable oil after upgrading while also addressing catalyst activation and stability issues. Catalyst stability is crucial for the economic feasibility of hydrotreating; in petroleum refining, fixed-bed hydrotreating catalysts are generally in operation for several months or years before being regenerated or replaced. Most petroleum hydrotreaters apply sulphided bimetallic catalysts to remove sulphur and nitrogen in, for example,

a middle-distillate fraction. Such sulphided catalysts stay active from the sulphur that is indigenous to the petroleum-derived feed. Hydrofaction™ renewable crude oil contains only 100–200 ppm sulphur, and as shown in the experimental results below, this affects the activity of a sulphided $NiMo/Al_2O_3$ catalyst. Based on these observations, two additional approaches were tested in the current study to improve catalyst activity:

(1) The renewable crude oil was spiked with butanethiol to a total sulphur content of 1 wt% S and upgraded in a continuous fixed-bed reactor system to test if a higher sulphur concentration improved the catalyst activity.
(2) Alternatively, the use of nonsulphided hydrotreating catalysts was tested as a potential upgrading path that reduces/eliminates the need of expensive gas cleaning operations downstream of the hydrotreater.

The two approaches have been tested experimentally, and the results are presented in the following.

10.2.2.1 Experimental procedure, Hydrotreating studies (second stage)

Feedstocks for the upgrading experiments presented below were different samples of renewable Hydrofaction™ crude oils produced at the pilot described in Section 10.2.1.6. The oils originate from oil production campaigns similar to that presented in Ref. [21].

10.2.2.2 Continuous reactor system

The CRS consists of a dual-piston syringe pump that ensures constant volumetric flowrate of oil. The pistons were kept at 90°C to reduce the viscosity and ensure a constant density, which was used to estimate the mass flowrate of oil. Oil and hydrogen were mixed in-line, and pressurised hydrogen was fed at a rate corresponding to 900 NL/L oil in all experiments. The fixed-bed reactor was made of ¾ in. stainless steel tubing, was operated in upflow mode, and was heated by electric heat cables. A 1/8 in. multipoint thermocouple facilitated 10 measurements inside the reactor. The feed mixture was heated at the entrance of the reactor, and the entrance region ensured a constant temperature of the mixture when reaching the catalyst bed. Reactor products were separated at 60°C and operating pressure in a cylindrical vessel. Gases were either collected for compositional analysis or passed through a wet test meter for volumetric flowrate. A back-pressure regulator at the gas-line outlet was used to set the operating pressure of the system.

The experimental results below present two different upgrading campaigns where the CRS was used. Both campaigns used a $NiMo/Al_2CO_3$ catalyst (activated in situ by sulphidation), but in the so-called spiked campaign, the renewable crude oil was spiked with butanethiol to increase the total sulphur content to 1 wt% S. The nonspiked campaign was carried out over 16 days (380 h), while the spiked campaign was running for 28 days (660 h) and mass balances were taken at least two times daily.

10.2.2.3 Batch reactor system

The BRS consisted of two 25 mL microbatch reactors build from 316 L Swagelok fittings that enable pressure logging. The reactors were loaded with reactants, leak tested, and pressurised with H_2 prior to a rapid heat-up by introducing them into a preheated Techne SBL-2D fluidised sand bath with temperature control. Thorough mixing of the reactants was ensured by shaking the reactors at 450 Hz using a shaking device. All experiments were carried out in repeats to ensure accurate data. Gaseous products were quantified by weighing the mass loss during depressurisation into a gas sampling vessel for compositional analysis. Catalysts were filtered off the reactor liquid products, and the latter were centrifuged at 3800 g for 10 min to separate the aqueous and upgraded oil products. Additional details on the BRS upgrading methodology is given in Ref. [34].

Space velocity is a thought parameter in relation to microbatch reactors, but it is advantageous to adapt to the terminology of continuous systems to enable comparison with the CRS experiments. With that in mind, a WHSV equivalent (WHSV*) incorporating reaction time, oil, and catalyst loading for the BRS experiments was defined as $\text{WHSV}^* = m_{\text{oil}}/(m_{\text{catalyst}} \times t_{\text{reaction}})$. The hydrogen availability at initiation of the experiments was 525 NL/L oil.

10.2.2.4 Sulphided catalysts

A commercial $NiMo/Al_2O_3$ catalyst in the form of 3.2 mm extrudates was used for the sulphided catalyst tests. For the CRS, this catalyst was activated in situ using vacuum gas oil with 3.7 wt% dimethyl disulphide at a liquid hourly space velocity (LHSV) of $1.5\,h^{-1}$ and a pressure of 41 bar.

10.2.2.5 Nonsulphided catalysts

The nonsulphided catalysts have up until now only been screened in the BRS to evaluate the degree of deoxygenation and hydrogenation that these catalysts can provide. Two different catalyst types were tested, a $NiW/SiO_2/Al_2O_3$ catalyst and a Pd/Al_2O_3 hydrogenation type catalyst. The nonsulphided catalysts were activated by reduction ex situ. After reduction in H_2 atmosphere, the catalysts were stabilised using 1 vol% O_2 in N_2 for 5 h, in order to avoid reoxidation of the catalyst during loading into the BRS. The flowrate of different gases during activation was 225–250 mL/min.

10.2.2.6 Results: Hydrotreatment using a sulphided catalyst (second stage)

Continuous hydrotreatment of renewable Hydrofaction™ crude oil was successfully carried out on a sulphided $NiMo/Al_2O_3$ catalyst. Two different campaigns were carried out with 380 and 660 h on stream, respectively. A standard renewable Hydrofaction™ crude oil with a sulphur content of 309 ppm was used in the first campaign (non-spiked). Based on observations indicating potential desulphurisation of the catalyst (Fig. 10.4), a similar renewable crude oil (oil B) was spiked to 1 wt% sulphur in the

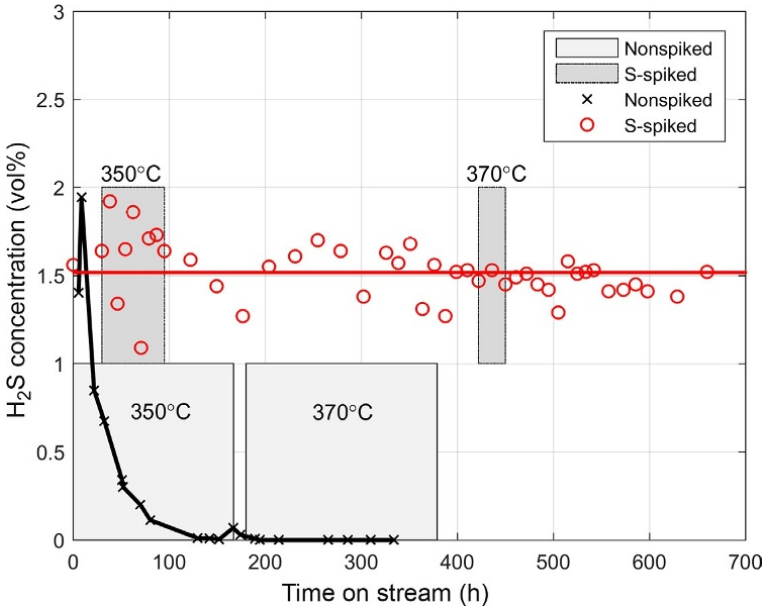

Fig. 10.4 H_2S concentration of the product gas during the two continuous hydrotreating campaigns.

second campaign (spiked). Additionally, data from two different hydrotreating temperatures will be presented for each campaign, adding up to four different datasets. In the spiked campaign, several other operating parameters were screened, but these are left out of the current study for simplicity.

Table 10.3 lists the hydrotreating conditions of the different experiments, together with mass balance data and the product gas composition. At first sight, the datasets appear rather similar with mass balances closing to 93%–96% and with volumetric oil yields between 96 and 100 vol%. However, it is worth focusing on the gas composition and in particular the concentration of H_2S, which is also pictured as a function of time on stream for the two campaigns in Fig. 10.4. It is clear that the H_2S concentration is stable throughout the *s*-spiked campaign, whereas it drops to below detection level during the first 150 h on stream in the nonspiked campaign. This depicts the reasoning behind testing the effect of crude oil sulphur content.

Table 10.4 lists physiochemical properties of the renewable crude oils used as feedstock for the two campaigns and the corresponding hydrotreated products. Complete deoxygenation and TAN elimination were achieved at both temperatures applied during both campaigns. Furthermore, the viscosity is reduced almost three orders of magnitude. Density, HHV, and H/C ratios indicate that the hydrogenation is improved during the spiked campaign. This observation is supported by the hydrogen consumptions (Table 10.3), which seem slightly higher for the spiked campaign as compared with the nonspiked campaign. This is an important finding, since a high degree of hydrogenation is desirable when producing diesel and marine drop-in fuels. Likewise, it is clear from both campaigns that the higher operating temperature (370°C) reduces

Table 10.3 Hydrotreating conditions, mass balance results, and product gas composition at two operating temperatures for both the nonspiked and sulphur-spiked upgrading campaign

	Unit	Nonspiked		Spiked	
Operational data					
Flowrate	(mL/min)	0.30	0.30	0.33	0.33
Temperature	(C)	350	370	350	370
Pressure	(bar)	62	62	66	66
LHSV	(h^{-1})	0.5	0.5	0.5	0.5
H_2 availability	(NL/L)	900	900	900	900
Mass balance	(wt%)	93.5	93.3	94.0	95.6
Gas yield	(wt%)	5.5	6.7	4.3	5.0
H_2 consumption	(wt%)	1.9	1.9	2.4	2.2
Water content	(wt%)	9.4	9.1	6.7	7.7
Hydrocarbon yield	(wt%)	81.0	80.0	85.5	84.6
Hydrocarbon yield	(vol%)	99.7	98.2	97.4	96.0
Gas composition					
H_2	(vol%)	94.6	93.0	96.1	93.9
H_2S	(vol%)	0.3	0.0	1.6	1.5
C_1	(vol%)	1.7	2.3	0.6	1.4
C_2	(vol%)	0.5	0.9	0.2	0.4
C_3	(vol%)	0.2	0.5	0.1	0.3
C_4	(vol%)	1.2	1.1	0.7	1.1
C_5	(vol%)	0.0	0.0	0.0	0.0
CO_2	(vol%)	1.3	1.3	0.7	1.4
CO	(vol%)	0.1	0.9	0.0	0.0

Table 10.4 Physiochemical properties of the products obtained at different conditions as compared with the renewable crude oils used as feedstock

	Unit	Oil G	Nonspiked		Oil B[c]	Spiked	
Op. temperature	(C)	—	350	370	—	350	370
Density at 15°C	(kg/m^3)	1103	989	989	1073	942	945
TAN	(mg/g)	55.7	<0.0	<0.0	48.0	<0.0	<0.0
Viscosity at 20°C	(cP)	80432	297	166	14429	34	33
HHV[a]	(MJ/kg)	37.2	42.1	42.2	38.0	43.3	43.2
Carbon[a]	(wt%)	80.6	88.1	88.4	80.4	88.6	87.4
Hydrogen[a]	(wt%)	9.1	11.9	11.6	9.0	13.4	12.6
Nitrogen[a]	(ppm)	1500	1175	986	822	424	402
Sulphur[a]	(ppm)	309	389	212	195	764	572
Oxygen[b]	(wt%)	10.1	0.0	0.0	10.4	0.0	0.0
H/C	(−)	1.34	1.61	1.57	1.34	1.84	1.71

[a] On dry basis.
[b] Oxygen by difference.
[c] Analysis before spiking with $C_4H_{10}S$.

hydrogenation as compared with 350°C. This is because hydrogenation is an exothermic reaction that is favoured by lower temperatures until reaction kinetics become rate limiting [22]. As a result, the continuous hydrotreating experiments suggest that the hydrogenation activity of the catalyst is reduced for a low-sulphur renewable crude oil compared with a sulphur-spiked equivalent.

HDN seems to be improved by both a higher operating temperature and a catalyst in its sulphided state (spiked campaign). Whereas the sulphur content is rather unchanged for products of the nonspiked campaign, it has increased in the products of the spiked campaign as compared with the biocrude. This is most likely due to H_2S trapped in the products, because the hydrotreating setup did not enable stripping of H_2S from the products.

Simulated distillation curves of the hydrotreated products are given in Fig. 10.5. True-boiling-point (TBP) distillation was also carried out and given in Fig. 10.5 of both the renewable crude oil and the 350°C samples from both the spiked and nonspiked campaigns.

The deoxygenation results in a significant degree of volatilisation and boiling-point reduction during hydrotreatment. In particular, products of the spiked campaign have been improved as compared with the simulated distillation of the renewable crude oil. The IBP-390°C distillate is improved with more than 30% in the spiked products compared with the renewable crude oil, whereas it is only around 10% for the nonspiked

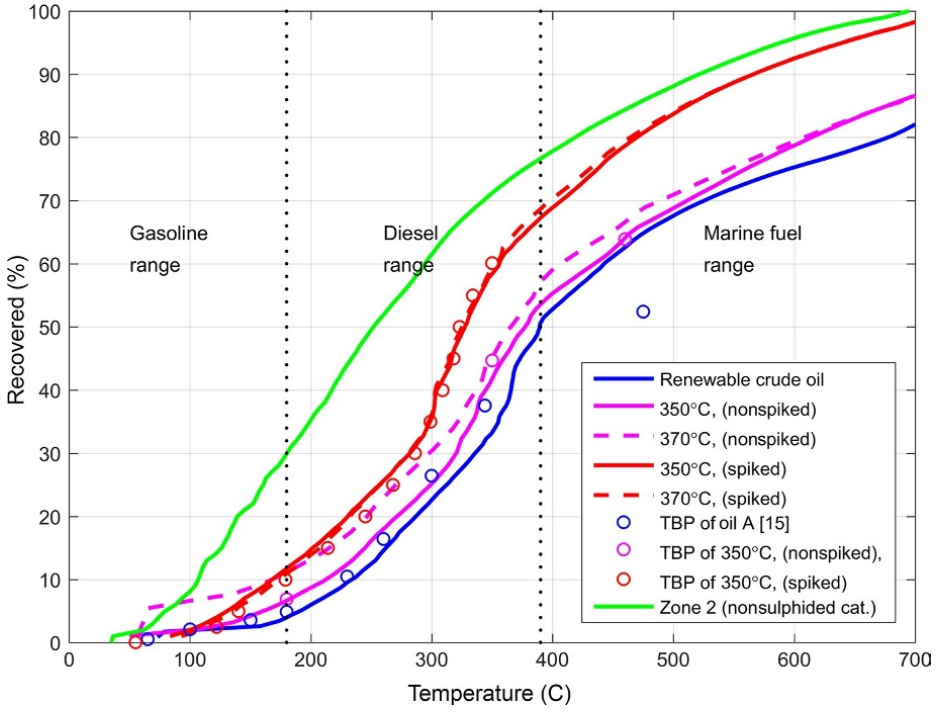

Fig. 10.5 Simulated distillation (ASTM D7169) profiles of the hydrotreated products compared with the renewable crude oil. TBP refers to a true-boiling-point distillation (ASTM D2892).

products. This indicates that cracking of heavy ends is improved when the catalyst is kept in sulphided state by sulphur spiking. The operating temperature of a specific campaign seems to have less effect on the boiling-point distribution. A higher degree of cracking is observed at 370°C for both campaigns but at the cost of a reduced degree of hydrogenation.

10.2.2.7 Results: Two-zone upgrading using nonsulphided catalyst (second stage)

The use of nonsulphided hydrotreating catalysts for upgrading of a low-sulphur renewable Hydrofaction™ crude oil may prove beneficial, because expensive gas cleaning equipment may be avoided when H_2S is reduced/avoided in the gaseous products. In Section 10.2.2.6, it was found that the hydrogenation and cracking activity of a sulphided catalyst is reduced when processing a low-sulphur renewable crude oil. Hydrogenation is however very important, when the objective is to produce diesel and marine fuel drop-in products. Based on a desire to improve the H/C ratio, a two-zone upgrading process was proposed, where deoxygenation and reduction of the boiling-point distribution is the objective of the first zone, while deep hydrogenation to improve the H/C ratio is the objective of the second zone. A schematic of such process is depicted in Fig. 10.6.

Initial screening of the nonsulphided catalysts was carried out to evaluate their ability to deoxygenate and hydrogenate the renewable crude oil. The screening included variation of temperature, pressure, and space velocity. The approach of the study was to initially screen the nonsulphided catalysts in microbatch reactors and

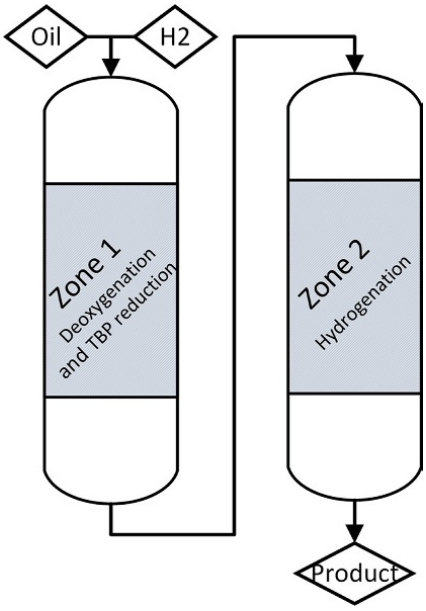

Fig. 10.6 Schematic of two-zone upgrading approach that is tested using nonsulphided catalysts.

then batchwise upgrade enough oil at the optimum conditions of zone 1 and zone 2 to analyse both the intermediate zone 1 product and the final zone 2 product from such two-zone upgrading. An initial parameter screening resulted in a preferred set of operating conditions for each catalyst shown in Table 10.5. Multiple zone 1 experiments at these conditions were carried out to obtain sufficient oil to enable analysis and have enough feedstock for the zone 2 experiments that were also carried out a number of times to get enough samples for analyses.

The amount of sample from the BRS limits the amount of possible analyses, but density, HHV, and elemental composition are given in Table 10.6 for the renewable crude oil, the intermediate zone 1 product, and the final zone 2 product. The oxygen content is reduced to 0.7 wt% in zone 1 and further reduced to below detection level in zone 2. The hydrogenation facilitates an overall increase in H/C molar ratio from 1.25 to 1.58, which indicates a noticeable degree of dearomatisation. This is less than the H/C ratios achieved during the spiked campaign in the CRS (Table 10.4). However, the noble metal loading of the Pd catalyst was only around 500 ppm, and the H/C ratio is likely improved further by increasing the metal loading of this catalyst. The purpose of each reaction zone or catalyst is effectively visualised by the FTIR spectra given in Fig. 10.7. The spectra show that absorption from oxygenated functional groups in the Hydrofaction™ oil is nearly eliminated during the zone 1 reaction. Likewise, the olefinic and aromatic absorption are reduced during the zone 2 reaction, which indicates hydrogenation reactions.

Additional quality improvements are reflected by a 16% increase in HHV and a 15% reduction of the bulk density. Both the HHV and especially the density are improved

Table 10.5 Preferred set of operating conditions based on the initial screening of the catalysts

	Catalyst	Temperature	Pressure	WHSV*
Zone 1	$NiW/SiO_2/Al_2O_3$	350°C	~100 bar	0.5 h^{-1}
Zone 2	Pd/Al_2O_3	300°C	~100 bar	1.0 h^{-1}

Table 10.6 Product quality before, between, and after the two reaction zones using nonsulphided catalysts

	Density[a] (kg/m^3)	HHV[b] (MJ/kg)	Elemental comp.[b] (wt%)					H/C (–)
			C	H	N (ppm)	S (ppm)	O[c]	
Oil A [21]	1051	38.6	81.4	8.6	1124	100	9.8	1.26
Zone 1 product	914	42.4	89.0	10.3	66	61	0.7	1.38
Zone 2 product	892	43.5	88.3	11.7	[d]	[d]	0.0	1.58

[a] Density at 15°C.
[b] On dry basis.
[c] Oxygen by difference.
[d] Insufficient sample.

compared with the products obtained using sulphided catalysts (Table 10.4). Finally and perhaps most importantly, the simulated distillation profile of the zone 2 product (Fig. 10.5) shows a remarkable improvement of the amount of distillates compared with the products obtained using the sulphided catalyst. More specifically, the IBP-390°C distillate fraction increased by 50% compared with the renewable crude oil. As a result, the initial screening of a two-zone upgrading process with nonsulphided catalyst appears as a promising route for upgrading of Hydrofaction™ crude oil. Though, long term catalyst activity and stability need to be studied in a continous reactor system.

10.3 Life cycle GHG emissions of Hydrofaction™

The sustainability of a renewable drop-in fuel is highly dependent on the energy efficiency of the production and the GHG emission reduction associated with use of the particular fuel. This section presents a calculation of the life-cycle GHG emission reductions associated with Hydrofaction™ products. The calculation is based on a 2000 barrel/day (BPD) Hydrofaction™ plant using forestry residues as feedstock and producing diesel and marine drop-in renewable fuels. Fig. 10.8 visualises the overall mass and energy flows for the 2000 BPD Hydrofaction™ plant assessed in the

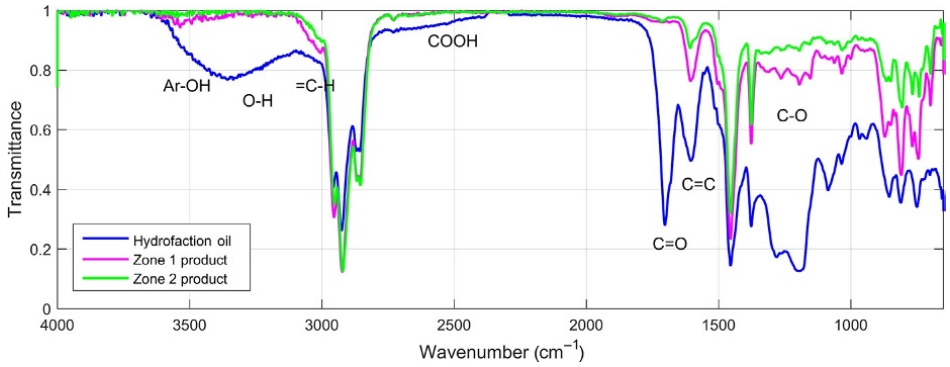

Fig. 10.7 Change in FTIR spectra during the two-zone upgrading process.

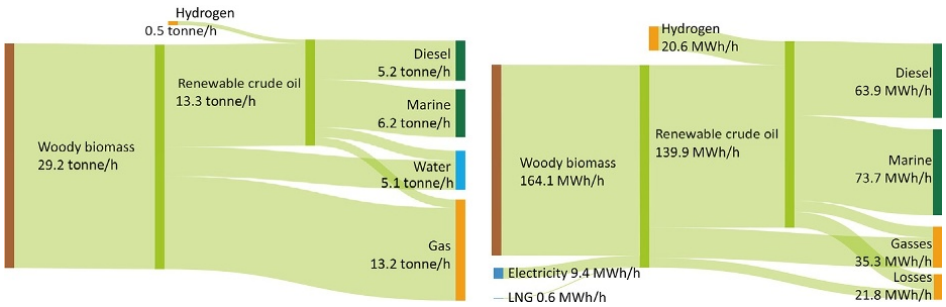

Fig. 10.8 Sankey diagrams of mass and energy balances in a potential 2000 BPD Hydrofaction™ plant.

GHG emission calculation. Mass and energy balances are based on the yield figures presented for the first and second Hydrofaction™ stage. More specifically, mass and energy balances for the first-stage Hydrofaction™ HTL are based on Ref. [21], while mass balances for the second stage are based on the *s*-spiked continuous upgrading experiment presented in Section 10.2.2.6. Fig. 10.8 illustrates the significant heating value that is available through the gaseous products from Hydrofaction™. In steady-state operation, combustion of these gaseous products is more than sufficient to make the overall process self-sustained with heat. However, an external LNG stream is included to cover start-up operations. Based on the energy balance in Fig. 10.8, the energy efficiency of the process can be calculated to 71%, which means that 71% of the energy added to the process is recovered in the drop-in fuels.

The location of the potential Hydrofaction™ plant assessed is the province of Alberta, Canada. Forestry residues are abundant in the region (Section 10.1.1), and fuel distribution infrastructure is widely available because extraction, refining, and distribution of oil sands and derived products is the largest industry in Alberta. Table 10.7 lists the emission intensities used in the GHG analysis of a Hydrofaction™ plant located in Alberta, Canada. Emission factors given in Ref. [15] by the government of Alberta have been used whenever possible. The plant applies forestry residues as feedstock that would have otherwise been disposed in permanent wood waste stockpiles. The methane emissions from decomposition of such wood waste stockpiles in the baseline scenario have been calculated based on the guidelines in Ref. [15]. It is assumed that the feedstock is transported on average 200 km from the harvesting site [16,35]. The gaseous Hydrofaction™ products are combusted to provide process heat, and the emission intensities of CH_4 and N_2O combustion products are assumed equal to that from combustion of liquefied natural gas (LNG). LNG is purchased to cover any additional heat requirements related to process start-up. The effect of using standard grid electricity versus renewable grid electricity has been tested. Heat, electricity, and make-up HTL catalyst requirements are based on design studies for a 2000 BPD Hydrofaction™ plant. Upgrading catalysts is assumed to be changed once every year, and transportation of all make-up catalysts to site is assumed to be on average 1000 km by heavy truck. Hydrogen consumption during upgrading is defined to a conservative 4 wt% (oil feed basis), higher than shown in Fig. 10.8, in order to accommodate for improved hydrogenation and losses from process gas recirculation. The upgraded Hydrofaction™ oil is fractionated into 50 vol% renewable drop-in diesel fuel used to displace petroleum diesel and 50 vol% drop-in marine fuel used to displace heavy fuel oil. Emissions related to distribution and dispensing of the finished fuels are left out of the calculation, because it is assumed to be the same and independent of the carbon origin of the fuel. Finally, GHG emissions related to construction of the plant are assumed negligible over the lifetime of the plant.

Table 10.8 lists the GHG emissions related to a 2000 BPD Hydrofaction™ plant producing diesel and marine fuel as compared with a baseline scenario where petroleum-derived diesel and heavy fuel oil products are refined and used in Alberta, Canada. The GHG emission reduction associated with using Hydrofaction™ products as compared with petroleum-derived products is 77%. This is comparable with the 70% GHG emission reduction determined for hydrotreated HTL fuel by Ref. [5], where emissions related to plant construction are also neglected.

Table 10.7 Emission intensities used in the GHG emission analysis of Hydrofaction™ products

Emission source	Unit	CO_2	CH_4	N_2O	CO_2e[a]	Reference
Feedstock harvesting and transportation (200 m), 15.9 L diesel/tonne	(kg/tonne)	4.2E+01	2.1E−03	6.4E−03		[15,16,35]
Combustion of liquefied natural gas (LNG)	(kg/m^3 LNG)	1.9E+00	3.7E−04	3.3E−05		[15]
Emission factor for grid electricity	(kg/kWh)	BNA			6.4E−01	[15]
Emission factor for renewable grid electricity	(kg/kWh)	BNA			0.0E+00	
Hydrogen emission intensity	(kg/kg H_2)	BNA			8.9E+00	[36]
K_2CO_3 emission intensity	(kg/kg)	BNA			2.7E−01	[37]
NaOH emission intensity	(kg/kg)	BNA			4.7E−01	[38]
Upgrading catalyst emission intensity	(kg/kg)	BNA			5.5E+00	[39]
Catalyst transportation by truck, 1000 km	(kg/kg)	BNA			4.9E−02	[40]
Emission intensity of fuel extraction and production	(kg/L)	1.4E−01	1.1E−02	4.0E−06		[15]
Combustion of diesel	(kg/L)	2.7E+00	1.3E−04	4.0E−04		[15]
Combustion of heavy fuel oil	(kg/L)	3.1E+00	3.4E−05	6.4E−05		[15]
Emission intensity from decomposition of wood waste stockpile	(kg/tonne)	Biogenic	2.0E+01			[15]

[a] 1 kg CH_4 = 25 kg CO_2e; 1 kg N_2O = 298 kg CO_2e; [15] BNA, breakdown not available.

Table 10.8 GHG emission reduction associated with displacement of diesel and heavy fuel oil by renewable Hydrofaction™ products

Emission source	Amount		CO_2 (kg/h)	CH_4 (kg/h)	N_2O (kg/h)	CO_2e* (kg/h)
2000 BPD Hydrofaction™ plant						
Feedstock collection and transport	29.2	tonne/h	1.2E+03	6.2E−02	1.9E−01	1295
Combustion of HTL process gas	3436	m^3 LNGe/h	Biogenic	1.3E+00	1.1E−01	66
Combustion of purchased LNG for heat	60.9	m^3/h	1.2E+02	2.3E−02	2.0E−03	118
Purchased electricity	9362	kWh/h	BNA	BNA	BNA	5992
Purchased hydrogen	530	kg/h	BNA	BNA	BNA	4717
Drop-in diesel fuel usage	6.5	m^3/h	Biogenic	8.6E−01	2.6E+00	791
Drop-in marine fuel usage	6.5	m^3/h	Biogenic	2.2E−01	4.1E−01	129
Make-up catalysts	1087	kg/h	BNA	BNA	BNA	443
CO2 sequestration	0	tonne/h	BNA	BNA	BNA	0
Hydrofaction™ GHG emission total						13550
Petroleum baseline						
Extraction and refining of petroleum diesel and fuel oil	12.9	m^3/h	1.8E+03	1.4E+02	5.2E−02	5313
Diesel combustion	6.5	m^3/h	1.7E+04	8.6E−01	2.6E+00	17974
Heavy fuel oil combustion	6.5	m^3/h	2.0E+04	2.2E−01	4.1E−01	20287
Wood waste stockpiling, decomposition	29.2	tonne/h	Biogenic	5.9E+02		14642
Baseline GHG emission total						58216
GHG emission reduction						44666
GHG emission reduction relative to baseline						77

Table 10.8 lists the details of a base-case scenario where the Hydrofaction™ process purchases all the hydrogen required for upgrading and uses standard grid electricity (coal-intensive in Alberta) and where the biogenic CO_2 from the HTL gaseous products is all emitted. It is clear that the major contributions to GHG emissions from Hydrofaction™ are related to the purchased electricity and hydrogen, covering 44% and 35% of the total emissions, respectively. Based on that, the following three additional scenarios were tested in the LCA.

Case 1: The base case is modified so hydrogen produced in situ during first-stage Hydrofaction™ is applied during upgrading of the renewable crude oil to lower the amount of hydrogen that need to be purchased. No additional LNG needs to be purchased, because there is sufficient heating value in the remaining gaseous products after hydrogen separation. Additional electricity demand is not accounted for.

Case 2: The base case is modified so renewable grid electricity is used to reduce the emission intensity of electricity but at the expense of a higher cost.

Case 3: The base case is modified so all the biogenic CO_2 from the HTL gaseous products is extracted (before combusting the gaseous products with air) and sequestered. Additional electricity demand is not accounted for.

Case 4: The base case is modified to include all of the above.

Fig. 10.9 compares the GHG emissions from the different scenarios and the resulting emission reduction. The effect of utilising in situ produced hydrogen in case

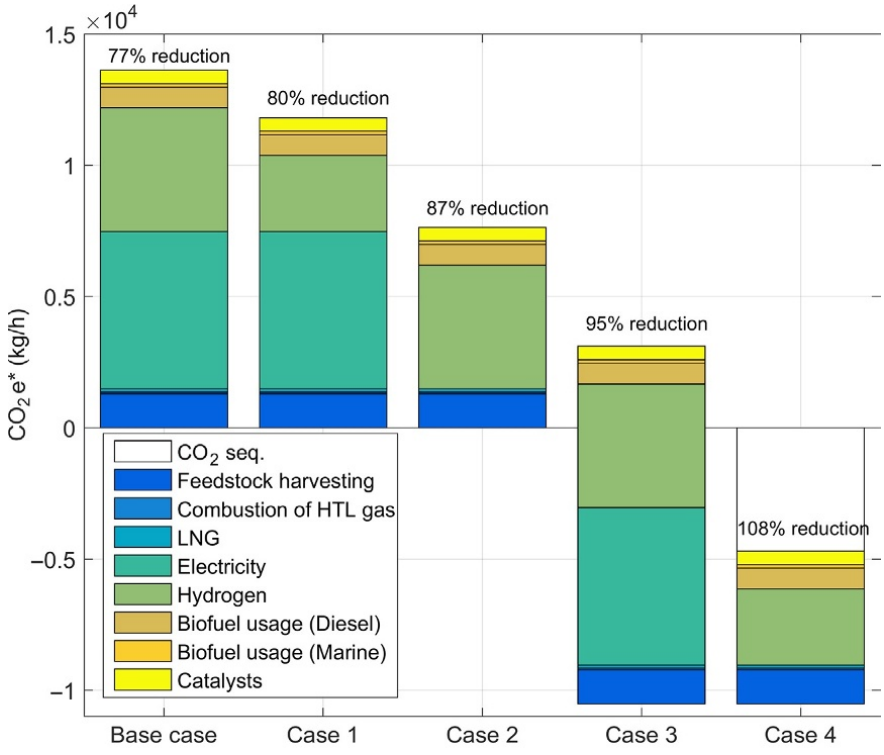

Fig. 10.9 GHG emission intensity of different Hydrofaction™ cases.

1 is minor, but this process modification is likely to be cost-efficient, since hydrogen is an expensive utility. The use of renewable electricity instead of standard grid electricity in case 2 has a major effect on the GHG emissions, which is because power generation in Alberta is relatively carbon-intensive due to coal-fired power plants. The cost-efficiency of case 2 depends on carbon legislation and the additional price of renewable electricity. The possibility of sequestering CO_2 from the HTL gaseous products is also worth considering as illustrated with case 3, since CO_2 is a major product from the first-stage Hydrofaction™ HTL and sequestration can significantly enhance the project's GHG emission savings. The rightmost column of Fig. 10.9 includes all the modifications to show the potential GHG emission reduction associated with Hydrofaction™ products. The result is a 108% GHG emission reduction, which implies a process that is not only CO_2 neutral but actually CO_2 negative.

10.4 Conclusion

Hydrofaction™ aims to fill the need for renewable heavy-transport fuels by converting forestry residues into drop-in renewable diesel and marine fuel using supercritical HTL and subsequent hydrotreating. Process descriptions and details are provided and supported by experimental data from continuous pilot operations. A comparison of six renewable Hydrofaction™ crude oils produced by supercritical HTL from different pine, spruce, birch, and bark mixtures shows similar quality independent of the woody feedstock. The characteristic fuel properties of these oils were significantly improved during two continuous hydrotreating campaigns with 300 and 700 h on stream. The low sulphur content (100–200 ppm S) of the crude oils was however found to inhibit the activity of the sulphided catalyst. A two-zone deoxygenation and hydrogenation reactor system using nonsulphided catalysts was screened in batch reactors, and improved devolatilisation relative to the sulphided catalysts was observed. Finally, mass and energy balances for a 2000 BPD Hydrofaction™ plant indicate that 1 tonne forestry residues can be converted to more than 400 L renewable diesel and marine fuels with an energy recovery of 71% and a GHG emission reduction of 77%–108%, reflecting an energy- and resource-efficient technology for the production of renewable fuels for heavy transportation.

Acknowledgements

The authors are thankful for the collaboration with Professor Lasse A. Rosendahl, Aalborg University, Denmark, and Professor Pedro Pereira Almao and his team at University of Calgary, Canada. The authors acknowledge the funding provided by EASME Horizon 2020 (Grant No. 666712), Danish Energy Technology Development and Demonstration Program (Grant No. 64013-0513), and Innovation Fund Denmark (Grant No. 4135-00126B).

References

[1] IPCC (2014), Climate Change 2014: Synthesis Report. Contribution of Working Groups I, II and III to the Fifth Assessment Report of the Intergovernmental Panel on Climate Change, (Core Writing Team: R.K. Pachauri and L.A. Meyer (eds.)). IPCC, Geneva, 151 pp.

[2] United Nations/Framework Convention on Climate Change (2015) Adoption of the Paris Agreement, 21st Conference of the Parties, Paris, France, United Nations.

[3] IEA (2016), World energy outlook 2016, Executive summary, Tech. rep., International Energy Agency. Paris.

[4] European Commission. Communication from the commission to the european parliament, the council, the european economic and social committee and the committee of the regions. A european strategy for low-emission mobility; 2016. SWD(2016), 244 final, Brussels, Belgium.

[5] I. Tews, Y. Zhu, C. Drennan, D. Elliott, L. Snowden-Swan, K. Onarheim, Y. Solantausta, D. Beckman (2014), Biomass direct liquefaction options: Technoeconomic and life cycle assessment, Tech. Rep., Prepared for U.S. Department of Energy, Springfield.

[6] De Jong S, Faaij A, Slade R, Mawhood R, Junginger M. The feasibility of short-term production strategies for renewable jet fuels is—a comprehensive techno-economic comparison. Biofuels Bioprod Biorefin 2015;9(6):778–800.

[7] Jensen CU, Hoffmann J, Rosendahl LA. Co-processing potential of HTL bio-crude at petroleum refineries. Part 2: A parametric hydrotreating study. Fuel 2016;165:536–43.

[8] FAO (2016), State of the World's Forests 2016. Forests and Agriculture: Land-Use Challenges and Opportunities. Food and Agriculture Organization of the United Nations, Rome.

[9] Ramachandran Nair PK, Mohan KB, Nair VD. Agroforestry as a strategy for carbon sequestration. J Plant Nutr Soil Sci 2009;172(1):10–23.

[10] Millar CI, Stephenson NL, Stephens SL. Climate change and forests of the future: managing in the face of uncertainty. Ecol Appl 2007;17(8):2145–51.

[11] O'Laughlin, Jay, and Mahoney, Ron (2008), Forests and Carbon. From University of Idaho Extension's 'Woodland notes', 19, 2.

[12] Bradley, D. (2007), Canada- Sustainable forest biomass supply chains. Prepared for IEA Task 40 by Climate change solution. Ottawa, Canada.

[13] Peter B, Niquidet K. Estimates of residual fibre supply and the impacts of new bioenergy capacity from a forest sector transportation model of the Canadian Prairie Provinces. Forest Policy Econ 2016;69:62–72.

[14] U.S. Department of Energy (2016), 2016 Billion-Ton Report: Advancing Domestic Resources for a Thriving Bioeconomy, Volume 1: Economic availability of feedstocks. M. H. Langholtz, B. J. Stokes, and L. M. Eaton (Leads), ORNL/TM-2016/160. Oak Ridge National Laboratory, Oak Ridge, TN. 448p.

[15] Government of Alberta (2015), Carbon offset emission factors handbook, ESRD Climate Change 2015, No. 1, Alberta Carbon Offset Program. Edmonton, Canada.

[16] Cambero C, Alexandre MH, Sowlati T. Life cycle greenhouse gas analysis of bioenergy generation alternatives using forest and wood residues in remote locations: a case study in British Columbia, Canada. Resour Conserv Recycl 2015;105:59–72.

[17] BTG BV (2002), Methane and nitrous oxide emissions from biomass waste stockpiles. Technical Report no. 12, Prepared for Worldbank PCFplus Research by Biomass Technology Group BV, Washington, DC.

[18] Macdonald C. Market pulp:overcapacity on the way. Pulp & Paper-Canada 2016; 117(3):9–11.
[19] RISI. China, Brazil paper and pulp production advances, even as growth slows globally, http://www.risiinfo.com/press-release/china-brazil-paper-pulp-production-advances-even-growth-slows-globally/; 2017. Accessed January 24, 2017.
[20] FAO (2009), State of the World's Forests 2009. Food and Agriculture Organization of the United Nations, Rome, Italy.
[21] Jensen CU, Guerrero JKR, Karatzos S, Olofsson G, Iversen SB. Fundamentals of Hydrofaction™: renewable crude oil from woody biomass. Biomass Convers Biorefin 2017; https://doi.org/10.1007/s13399-017-0248-8.
[22] Gary JH, Handwerk GE, Kaiser MJ. Petroleum refining, technology and economics. 5th ed. CRC Press; 2007, ISBN: 0-8493-7038-8.
[23] Lane, J. (2015), 4 minutes with… Taner Onoglu, Vice President, Altaca Energy. Biofuels Digest. http://www.biofuelsdigest.com/bdigest/2015/06/04/4-minutes-with-taner-onoglu-vice-president-altaca-energy/. [Accessed 21 February 2017].
[24] Genifuel 2015. Genifuel corporation closeout report for NAABB program, DE-FOA-0000123 http://www.energy.gov/sites/prod/files/2016/01/f28/naabb_genifuel_pilot_system_final_report.pdf. [Accessed 21 February 2017].
[25] Muradel Pty Ltd. (2017), Technology http://www.muradel.com/aboutus.asp#tech. [Accessed 21 February 2017].
[26] Licella Pty Ltd. Cat-HTR, http://www.licella.com.au/cat-htr/; 2017.
[27] Elliott DC, Biller P, Ross AB, Schmidt AJ, Jones SB. Hydrothermal liquefaction of biomass: developments from batch to continuous process. Bioresour Technol 2015;178:147–56.
[28] Elliott DC. In: Process development for biomass liquefaction. Volume 25:4, Conference 180, Report no. CONF-800814-P3, Pacific Northwest Lab., American Chemical Society, Division of Fuel Chemistry, Richland, USA; 1980.
[29] Harvey AH, Peskin AP, Klein SA. NIST/ASME Steam properties database, Software Version 3.0. In: Standard Reference Database. National Institute of Standards and Technology (NIST), US Department of Commerce; 2013.
[30] Akiya N, Savage PE. Roles of water for chemical reactions in high-temperature water. Chem Rev 2002;102:2725–50.
[31] Kruse A, Dinjus E. Hot compressed water as reaction medium and reactant properties and synthesis reactions. J Supercritical Fluid 2007;39:362–80.
[32] Sintamarean IM, Grigoras IF, Jensen CU, Toor SS, Pedersen TH, Rosendahl LA. Two-stage alkaline hydrothermal liquefaction of wood to biocrude in a continuous bench scale system. Biomass Convers Biorefin 2017; https://doi.org/10.1007/s13399-017-0247-9.
[33] Jensen CU, Olofsson G, Rosendahl LA. Impact of Nitrogenous Alkaline Agent on Continuous HTL of Lignocellulosic Biomass and Biocrude Upgrading. Fuel Process Technol 2017;159:376–85.
[34] Hoffmann J, Jensen CU, Rosendahl LA. Co-processing potential of HTL bio-crude at petroleum refineries. Part 1: Fractional distillation and characterization. Fuel 2016;165:526–35.
[35] McKechnie J, Chen J, Vakalis D, MacLean H. Energy use and greenhouse gas inventory model for harvested wood product manufacture in Ontario; 2014. Climate change research report, CCRR-39, Ontario, Canada.
[36] Ruether J, Ramezan M, Grol E. Life-cycle analysis of greenhouse gas emissions for hydrogen fuel production in the United States from LNG and coal. DOE/NETL-2006/1227; 2005.

[37] Pendolovska, V., Fernandez, R., Mandl, N., Gugele, B., and Ritter, M. (2014), Annual European Union Greenhouse Gas Inventory 1990–2012 and Inventory Report 2014. Technical report no. 09/2014 by European Environment Agency. Copenhagen.
[38] Biograce. Harmonised calculations of biofuel greenhouse gas emissions in Europe, list of standard values, http://www.biograce.net/content/ghgcalculationtools/standardvalues; 2017.
[39] Snowden-Swan LJ, Spies KA, Lee GJ, Zhu Y. Life cycle greenhouse gas emissions analysis of catalysts for hydrotreating of fast pyrolysis bio-oil. Biomass Bioenergy 2016;86:136–45.
[40] Railway association of Canada. Rail Freight Greenhouse Gas Calculator, http://www.railcan.ca/environment/calculator; 2017.

Paper B

Fundamentals of Hydrofaction^{TM} : Renewable crude oil from woody biomass

Claus Uhrenholt Jensen, Julie Katerine Rodriguez Guerrero, Sergios Karatzos, Göran Olofsson, Steen Brummerstedt Iversen

The manuscript has been published in the
Journal of Biomass Conversion and Biorefinery, vol. 7, no. 4, pp. 495–509, 2017.

The layout has been revised.

Biomass Conv. Bioref. (2017) 7:495–509
DOI 10.1007/s13399-017-0248-8

ORIGINAL ARTICLE

Fundamentals of Hydrofaction™: Renewable crude oil from woody biomass

Claus Uhrenholt Jensen[1] · **Julie Katerine Rodriguez Guerrero**[2] · **Sergios Karatzos**[2] · **Göran Olofsson**[1] · **Steen Brummerstedt Iversen**[1]

Received: 10 October 2016 / Revised: 2 February 2017 / Accepted: 8 February 2017 / Published online: 23 February 2017

Abstract As a response to the global requirement for renewable transportation fuels that are economically viable and fungible with existing petroleum infrastructure, Steeper Energy is commercializing its proprietary hydrothermal liquefaction (HTL) technology as a potential path to sustainable lignocellulosic-derived transport fuels. Hydrofaction™ utilizes high-density, supercritical water chemistry at distinctly higher pressures and temperatures than most literature on HTL. The paper presents a direct relation between density and the chemical properties that make near-critical water an appealing HTL reaction medium. Further, the fundamentals of Hydrofaction™ and how these are carefully chosen to favor certain chemical reaction paths are explained, including the use of high-density supercritical water, homogenous alkaline metal catalysts at alkaline conditions and recycling of aqueous and oil products. Steady state operational data from a campaign producing 1 barrel (>150 kg) of oil at a dedicated pilot plant is presented, including closure of mass, energy, and three elemental balances. A detailed oil assay specifying the oil quality as well as mass and energy recoveries from wood to oil of 45.3 wt.% and 85.6%, respectively, reflect that Hydrofaction™ is an energy-efficient technology for sourcing renewable biofuels in tangible volumes.

Keywords Hydrofaction™ · Hydrothermal liquefaction · Supercritical water · Biofuel · Renewable oil

✉ Steen Brummerstedt Iversen
si@steeperenergy.com

[1] Steeper Energy ApS, Sandbjergvej 11, 2970 Hørsholm, Denmark

[2] Steeper Energy Canada Ltd, Suite 200, 1210 11th Avenue S.W., Calgary T3C 0M4, Canada

1 Introduction

Petroleum is currently the lifeblood of technologically advanced civilization, and it is consumed at a rate of 94 million barrels a day globally [1]. The oil industry is sourcing these significant volumes of crude oil and refining them into transportation fuels and petrochemicals for solvents, polymers, and other higher-value materials. However, petroleum is finite and its consumption generates greenhouse gasses (GHGs) that raise climate change concerns. Industry is constantly extracting fossil carbon that is later combusted and becoming a net contributor of CO_2 and other GHGs into the Earth's atmosphere. Moreover, global reserves of good quality light sweet crude are diminishing and are mainly located in politically unstable areas. As such, the oil and gas industry, arguably the biggest industry in the world, is currently facing political, environmental, and economic challenges.

To counter these challenges, the world is turning towards new technologies that help reduce dependency on petroleum. Such alternatives include renewable transportation fuels. Vehicles fueled with electricity from renewable energy are one of these alternatives, but it requires new fuel distribution infrastructure and is mostly applicable to urban and short-distance transportation. Long-distance transportation sectors such as marine, heavy trucking, rail, and aviation cannot be readily electrified and thus have a unique dependency on liquid biofuels that are fungible with bunker, diesel, and jet fuels.

Ethanol and biodiesel are the two most widely available commercial biofuels, but they are highly oxygenated and are mostly blended in small percentages (except modified engines such as E85 in the USA and Sweden or E100 in Brazil) in gasoline and diesel road transport fuels. These oxygenates are not suitable for long-distance transportation such as aviation, heavy road freight, and marine, which require energy-dense biofuels that are functionally indistinguishable ("drop-in") to

the fossil equivalents. For example, in commercial airplanes, the total weight of fuel at takeoff is higher than the total weight of the payload (e.g., cargo and passengers) [2], which make high-energy density fuels indispensable.

Hydrotreated vegetable oils and animal fats (collectively known as hydrogenation-derived esters and fatty acids or HEFAs) are a recent non-oxygenated biofuel addition to the two main commercial biofuels. However, HEFAs are derived from fatty acid raw materials that are costly and can compete with food end uses [3]. Thermochemical biomass conversion technologies such as gasification, pyrolysis, and hydrothermal liquefaction (HTL) are being developed in order to produce advanced drop-in biofuel blendstock from non-food and lower-cost lignocellulosic biomass.

HTL is currently viewed with the potential to become a competitive and resource effective pathway to advanced biofuels from lignocellulosic biomass, mainly due to its high-energy efficiency. For example, a 2014 US DOE-commissioned study has determined that hydrotreated HTL biofuel is cheaper than the fast pyrolysis equivalent on both mass and energy bases. Additionally, the study estimates 70% GHG emission savings on HTL biofuel from wood compared to the 2005 petroleum baseline [4].

Hydrofaction™ utilizes a unique combination of supercritical water chemistry and homogenous catalysts to efficiently convert biomass residues directly to a high-energy density renewable crude oil. The present article presents the fundamentals of the Hydrofaction™ process and the reasoning behind each parameter. This includes the use of water at supercritical, high-density conditions; the use of homogenous alkaline metal catalysts; and recycling of aqueous and oil products back into the process. Furthermore, the major chemical reaction paths and their contribution during conversion are discussed.

While most HTL results in the public domain come from small-scale batch experiments, Hydrofaction™ has been proven in a continuous pilot facility. The second part of the article presents mass, energy, and elemental balances from operating this pilot plant as well as characterization data of the produced energy-dense and free-flowing oil.

1.1 Subcritical or supercritical HTL and the importance of density

The critical point of water, which is given in the phase diagram of Fig. 1, is often used to distinguish between liquefaction and gasification hydrothermal processes. HTL is often considered to take place mainly via ionic type of reactions near or below the critical point at temperatures of approximately 280–374 °C and at a pressure of at least the saturation pressure of water to avoid boiling. In contrast, hydrothermal gasification or supercritical water gasification is considered to occur mainly via radical type of reactions at supercritical temperatures or above, typically in the range of 450–600 °C and at pressures in the range of 50 to 250 bar [5, 6]. Contrary to most HTL processes, Hydrofaction™ is carried out above the critical point of water at 300–350 bar and 390–420 °C, in the transition between liquefaction and supercritical water gasification according to the general perception described above. However, due to the higher pressure of Hydrofaction™, key thermodynamic properties of water such as density and derived properties can be maintained at the same order of magnitude as for the subcritical conditions, while taking advantage of faster kinetics at higher temperatures.

Numerous HTL studies have been published on either the effect of operating temperature or pressure on product yields, coking propensity, oil quality, etc. [5, 6, 8, 9]. However, the chemical properties that make near-critical water an appealing reaction medium for HTL is a direct function of density and only indirectly of pressure and temperature. This is visualized in Fig. 2, where the ionic product and dielectric constant of water are given as a function of density for different isobars. A certain density can be obtained at different combinations of both subcritical and supercritical temperatures and pressures; however, the chemical kinetics and relative reaction rates may be very different at different temperatures. Thus, the different reaction regimes are better represented by density and temperature than the commonly used pressure and temperature. Finally, the transition from liquefaction to gasification regime is not instantaneous but occurs via a gradual transition, and this phenomenon is utilized in Hydrofaction™.

The rationale behind the relatively high operating pressures applied in Hydrofaction™ is thus to ensure a certain relatively

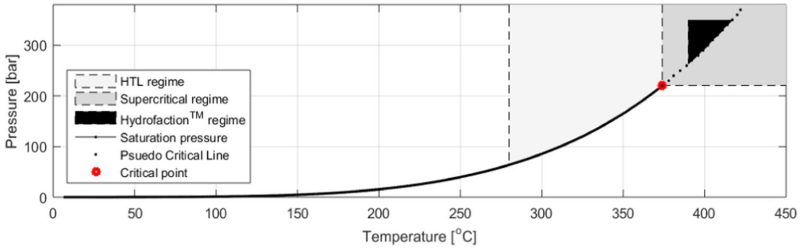

Fig. 1 Phase diagram of water to visualize the different operating regimes. Data source [7]

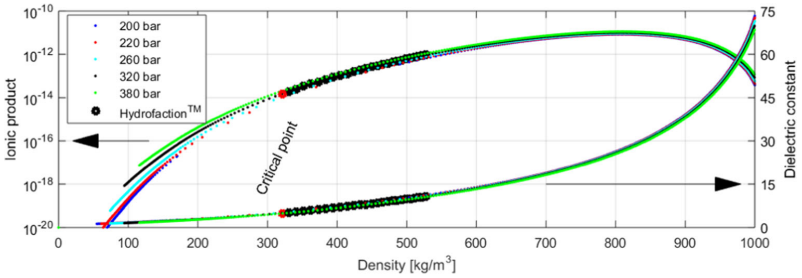

Fig. 2 Ionic product and dielectric constant of water as function of density for different isobars. Data source [7]

high density, while taking advantage of the benefits of higher temperatures. Further details on the specific choice of operating conditions are based on the changes several thermophysical properties undergo around the critical point of water.

2 Fundamentals of Hydrofaction™

The Hydrofaction™ technology platform is rooted in the generic field of hydrothermal liquefaction and is based on catalytic supercritical water chemistry. The technology applies a number of features [10]:

- Operation above the critical point of water at relatively high pressures (300–350 bar) and temperatures (390–420 °C);
- Recirculation of produced organic compounds in the form of water-soluble organics and oil for improved feed characteristics, improved energy balance, desired chemical kinetics, and improved oil yields;
- Use of homogeneous catalyst in the form of potassium carbonate (K_2CO_3) for desired catalytic effects;
- Control of pH to alkaline conditions for desired catalytic effects and minimization of corrosion;
- Recovery and recycling of homogeneous catalysts for improved process economics;
- Self-sustaining with process heat when in steady state.

The reasoning behind each of the fundamentals listed above will be specified in detail in the following.

2.1 How does Hydrofaction™ take advantage of supercritical water chemistry?

Water near its critical point obtains thermophysical properties which are very different from those at ambient conditions. The

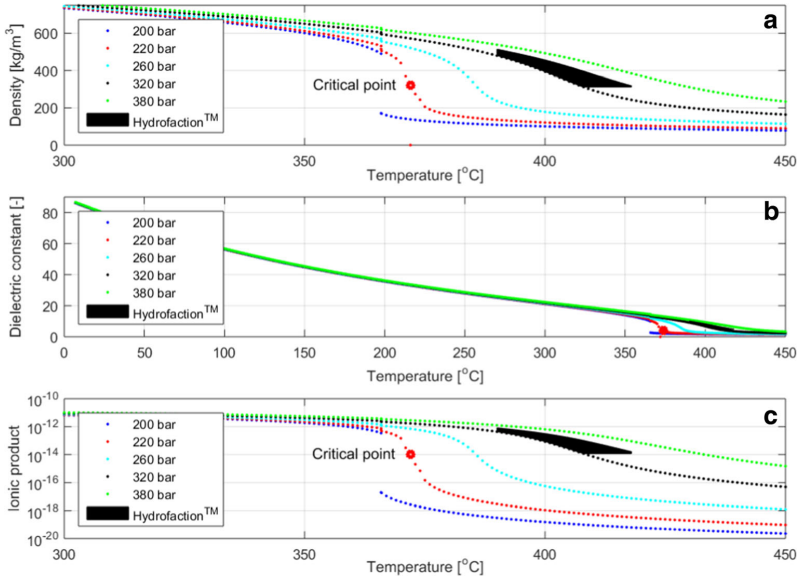

Fig. 3 Thermophysical properties of water behavior at temperatures and pressures above the critical point of water. **a** Density. **b** Dielectric constant. **c** Ionic product. Data source [7]

dielectric constant is significantly reduced making near-critical water a non-polar solvent. Additionally, the ionic product of water is very dependent on pressure around the critical temperature, and supercritical water can facilitate both ionic and radical reactions. Finally, interphase mass and heat transfer resistances are significantly reduced and mass and heat transfer rates are enhanced. The exploitation of these properties is being maximized by carefully selecting the operating conditions and configuration of the process.

Hydrofaction™ is applying a relatively high operating pressure to ensure a certain, relatively high density, while taking advantage of the benefits of supercritical temperatures. In Fig. 3a, it is clear that the relatively high-pressure range, although supercritical, sustains a high-density as compared to most HTL processes that operate near the critical point of water. Figure 3a also reveals how higher pressures reduce the gradient of density change with temperature. Considering the direct influence density has on key properties, a smoother transition is beneficial since small-temperature deviations during plant operations thereby have less impact on the important properties. For example, the 220-bar isobar in Fig. 3a reveals how density is reduced by 50% with a 5–10 °C temperature increase around the critical point. This would be undesirable from a plant operation standpoint as it would significantly alter process parameters such as retention times, fluid velocities, Reynolds numbers, and heat transfer coefficients.

The polarity of water also diminishes as water gets closer to its supercritical state as shown by the dielectric constant plotted against temperature at different pressures in Fig. 3b. The dielectric constant drops from around 85 at ambient water conditions to below 10 at and around the supercritical point of water. This allows water to dissolve biomass and biocrude molecules that are hydrophobic at ambient conditions. Such molecules include phenolics and polyaromatic hydrocarbons derived from lignin. The higher pressure applied in Hydrofaction™ slightly elevates the dielectric constant compared to the critical point. Although, it is still reduced by more than 90% as compared to ambient conditions, which facilitate solubility of non-polar compounds.

Self-ionization of water, expressed as the ionic product in Fig. 3c, is a crucial parameter within HTL because it reflects whether the reaction medium favors ionic ($>10^{-14}$) or radical ($<10^{-14}$) reactions [11, 12]. Radical reactions are in most cases undesirable due to the risk of extensive coke formation. These radical reactions are minimized below the critical point, where the ionic product is relatively high regardless of pressure. Further, the isobars are more or less identical below the critical point as seen in Fig. 3a–c, whereas a sudden drop in the ionic product is observed at lower pressures around the critical point of water. However, as shown in Fig. 3c, the high pressures of the process sustain a high ionic product despite the supercritical temperatures, thus minimizing radical reactions. In fact, the ionic product of water at Hydrofaction™ conditions can be an order of magnitude higher than for ambient water and up to several orders of magnitude higher than at the critical point.

The specific heat capacity and heat transfer properties of water change dramatically around the critical point, or more specifically around the pseudo-critical line (PCL), which influence the energy requirements of the process. The effect of operating pressure on heat requirement for an isobaric temperature increase from ambient water is visualized with specific enthalpy in Fig. 4a. At near-critical pressures, the specific enthalpy of water increases sharply around the critical point. This increase is less distinct at higher pressures, which is because the maximum specific heat capacity (PCL) is significantly reduced at higher pressures [7]. In fact, the energy required to heat water to 400 °C at 300 bar is lower than that required to heat water to the critical point at the saturation pressure. In other words, due to the elevated pressure, the additional energy required to operate at supercritical conditions compared to subcritical is insubstantial.

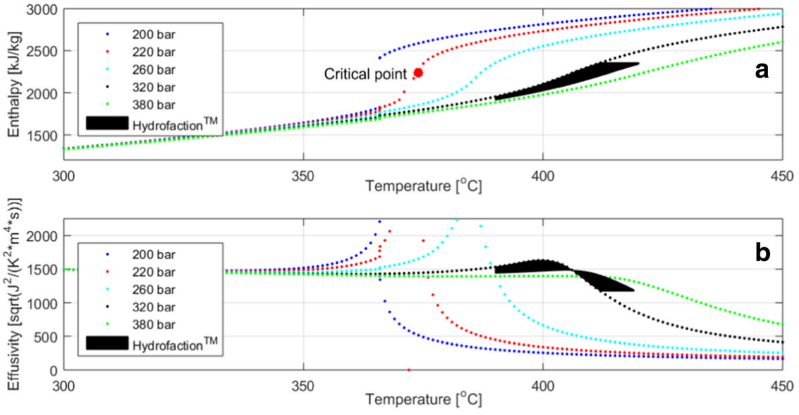

Fig. 4 Water's heat capacity and effusivity as function of temperature and pressure. **a** Enthalpy. **b** Effusivity. Data source [7]

Finally, a higher operating temperature results in a higher driving force during heat exchange, which both improves the economics of heat recovery as well as the overall energy efficiency.

The heat transfer properties of water are known to deteriorate at supercritical conditions. Figure 4b visualizes this characteristic through thermal effusivity, which reflects the ability of a substance to exchange heat with its surroundings. It is a direct function of density, specific heat capacity, and thermal conductivity. The peak at each isobar in Fig. 4b represents the PCL at which the specific heat capacity is highest. At near-critical pressures, the thermal effusivity of water sharply decreases at the critical temperature. However, at higher supercritical pressures, the thermal effusivity is sustained higher and suggests that the thermal resistance of the boundary layer is reduced at pressures above the critical [13]. At Hydrofaction™ conditions, the thermal effusivity of water is close to a maximum, exploiting a synergetic effect of the PCL, a higher density, and thermal conductivity. Theoretically, a much higher maximum can be obtained at lower pressures, but such peaks are difficult to take advantage of due to the drastic changes within a very narrow temperature range. This emphasizes how the process conditions are carefully chosen to also improve energy and heat transfer efficiency.

The above discussion is largely focused around the properties of supercritical water. Although supercritical water constitutes an important part of the process, it will typically only make up about 50 wt.% of the fluid; hence, the critical point of water is only partially relevant. The remaining 50 wt.% consists of biomass, recycled organics, Hydrofaction™ oil, and gas, depending on location in the process. The presence and recirculation of these components have several beneficial effects, which will be specified in the following sections.

2.2 Benefits of aqueous phase recirculation

The aqueous product consists of water, water-soluble organics, dissolved homogeneous catalyst, and dissolved salts from the biomass feedstock. Recirculation of this mixture reduces the makeup of the homogeneous catalyst, and the water-soluble organics are beneficial during pre-treatment and conversion. In Hydrofaction™, aqueous phase recirculation is performed by extraction and purification of the same amount of water as deducted from the feedstock biomass, while concentrating and recycling the remainder of the aqueous product. A bleed of 5–15% of the water phase is required to prevent buildup of trace components such as chloride. The bleed is further treated and purified to dischargeable or recyclable water quality.

The recycled water-soluble organics are mainly C_1–C_4 alcohols, ketones, phenols, catechols, and smaller organic acids produced by the process. They are beneficial for the pre-treatment to produce a pumpable slurry, as a dissolution mechanism is introduced in parallel with the hydrothermal depolymerization mechanism. It is believed that this effect proceeds via reactions such as solvolysis and acidolysis. The presence of recovered water-soluble organics during the heat-up and conversion is critical to the outcome of Hydrofaction™. They are believed to act as radical scavengers or stabilizers of intermediate products as well as hydrogen donors during heat-up and conversion, thereby inhibiting the formation of undesired char products and promoting the deoxygenation reactions via hydrogenolysis. For example, it is known that phenol can reduce or inhibit coke formation during lignin degradation [14]. The depolymerization of lignin by hydrolysis is promoted by the presence of phenols. An additional beneficial effect appears to be that the presence of water-soluble organics in the feed inhibits further formation of water-soluble organics, thereby increasing the relative amount of oil produced.

2.3 Benefits of oil recirculation

The addition of recycled oil into the feedstock slurry increases the homogeneity of the feed mixture by facilitating partial dissolution of the biomass. This improves the rheological properties of the incoming slurry, making it more pumpable. The significant fraction of organics, especially recycled oil, reduces the energy required for heat-up due to the lower specific heat capacity of organics compared with water. Finally, the recycled oil is believed to act as radical scavenger or stabilizer of intermediate products during heat-up and conversion, similarly to the water-soluble organics in the aqueous phase.

2.4 How do homogenous alkali metal catalysts benefit the process?

Homogeneous catalysts in the form of potassium, and to lesser degree sodium, are well known to catalyze the degradation of macromolecules by hydrolysis, decarboxylation, and depolymerization type of reactions, as well as inhibit formation of tar, char, and coke. At alkaline conditions, potassium in near-critical and supercritical water is further known to promote water gas shift (WGS) and steam reforming reactions as well as gasification [5, 6, 15].

Carbonate is the preferred form of the potassium salt as CO_2 is an important reaction product from the decarboxylation and gasification reactions. The presence of carbonate/bicarbonate is believed to increase hydrogen production due to changes in the gaseous equilibrium and accelerate WGS as well as steam-reforming reactions. Further, the presence of carbonate/bicarbonate appears to accelerate the depolymerization by hydrolysis during pre-treatment and improve the rheological properties of the slurry.

The pH is important for the reactions to proceed as desired, particularly the production of in situ produced hydrogen via WGS reactions. Hence, the pH is controlled so that sufficient buffer capacity is present in the feed to maintain the pH

alkaline throughout the process. At low pH, the H_2/CO ratio may be close to 1, whereas the ratio is typically in the range of 20–100 at alkaline conditions, indicating both that CO is consumed and that more hydrogen is produced. Additionally, significant amounts of char are observed at acid conditions, whereas no or only small amounts are detected at alkaline conditions.

The reasoning behind the characteristics of the Hydrofaction™ process is discussed above, whereas the following will focus on biomass composition and the chemistry during decomposition and conversion.

3 Biomass composition and conversion

Biomass is biological material derived from recently living organisms; in the context of the energy industry, it mostly refers to plant materials such as wood, straw, seeds, and leaves, as well as animal manures and the organic fraction of municipal solid and sewage wastes. Hydrofaction™ can process most types of biomass, although at present time, mostly focuses on lignocellulosic forest biomass, which is readily and commercially accessible in large aggregated volumes and derived from wood harvest and processing residues including tree branches, bark, leaves and limbs, non-merchantable wood, wood pulp wastes, and sawdust [16]. Lignocellulosic biomass is a complex structural material found in the cell walls of woody plants and consists of cellulose and hemicellulose polysaccharides as well the lignin aromatic polymer (Fig. 5). Proteins, resins, and inorganic matter are also present in minor concentrations. The exact proportion of each component varies among plant genotypes and even among phenotypes, as indicated in Table 1.

Cellulose is an unbranched homopolysaccharide consisting of repeat cellobiose (glucose dimer) units, which are connected to each other with β (1 → 4) glycosidic bonds. A large proportion of cellulose is crystalline due to a characteristic configuration in which cellulose chains are aligned in parallel to each other to allow a very tight network of intermolecular and intramolecular hydrogen bonds [17, 18]. This makes crystalline cellulose very resistant to chemical or biological decomposition. However, this crystallinity is not expected to interfere with biomass decomposition at supercritical conditions, as it has been reported that cellulose undergoes crystalline-to-amorphous transformation in water at around 320 °C and 250 bar [19]. Likewise, alkaline aqueous solutions are known to interfere with cellulose crystallinity, thus making cellulose chains more accessible to degradation [20].

Hemicelluloses, as opposed to cellulose, are a collection of fully amorphous, branched heteropolysaccharides with shorter

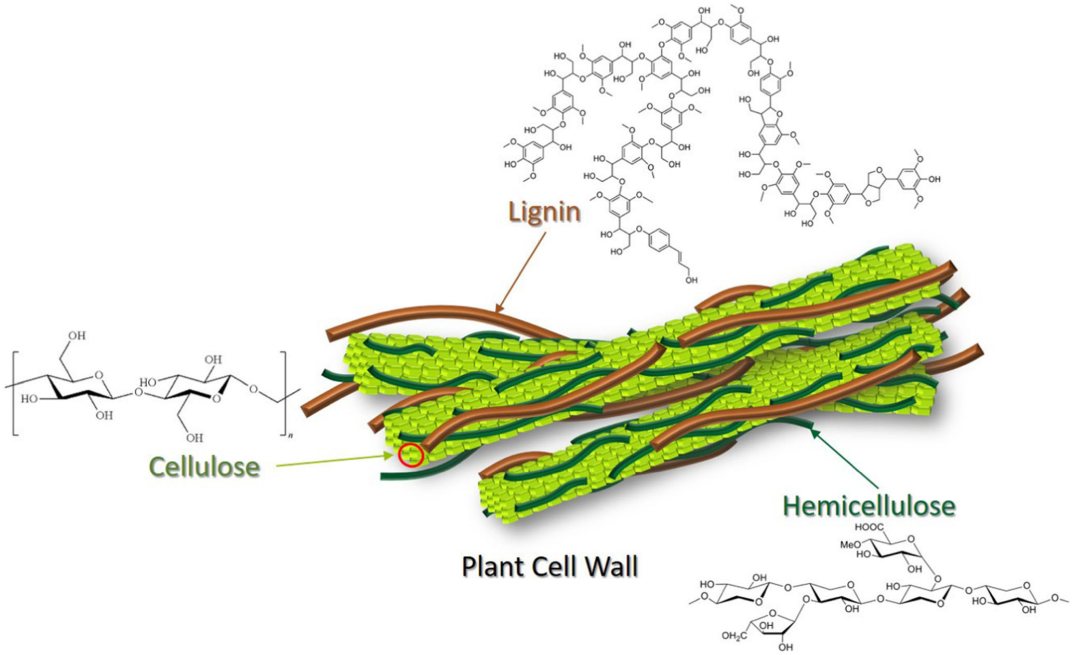

Fig. 5 Structure of lignocellulosic biomass

Table 1 Typical biomass and waste compositions (wt.% dry mass, average) [23]

Lignocellulosic materials	Cellulose	Hemicellulose	Lignin	Ash
Hard woods				
Poplar	46.2	24.4	24.5	1.1
Birch	40.6	29.6	20.2	0.6
Willow	60.5	29.9	25.6	2.2
Eucalyptus	43.2	22.5	25.0	1.6
Soft woods				
Spruce	44.1	21.2	26.9	0.9
Pine	43.6	24.9	25.6	0.7
Coniferous wood	57.5	22.5	30.0	0.4
Douglas fir	45.4	20.9	26.1	1.3
Forest residues				
Bark, pine	23.7	24.9	50.0	3.8
Wood stems	42.6	22.3	37.7	
General residues	45.5	21.0	27.3	
Other lignocellulosics				
Corn stover	38.3	25.2	14.8	6.1
Sugarcane bagasse	37.3	35.8	20.1	5.7
Wheat straw	37.9	26.8	18.3	6.2
Miscanthus	44.6	23.9	21.3	3.7
Switch grass	37.1	31.2	8.5	6.3

chain lengths. They consist of combinations of hexoses (C_6) and pentoses (C_5) as well as uronic acids and acetyl groups, and the combinations vary characteristically between plant species or even plant tissues [21]. Finally, lignin is a complex non-linear macromolecule resulting from the polymerization/cross-linking (via C–C and C–O–C ether bonds) of the following three phenypropanoid units: *p*-coumaryl, coniferyl, and sinapyl alcohols. Similar to hemicellulose, the proportion of these lignin monomers depends on the plant species and tissues [22].

At the plant cell wall structural level, cellulose molecules align in parallel to form the rod-like cellulose microfibrils (Fig. 5). These microfibrils intertwine (to form macrofibrils), leaving some spaces in between which are filled with lignin and hemicelluloses [24]. Lignin and hemicellulose form co-valent bonds (ester and ether) with each other but not with cellulose. Adhesion between cellulose and hemicelluloses is provided by hydrogen and van der Waals forces [22].

From an elemental composition viewpoint, lignocellulosic biomass is mainly comprised of carbon, hydrogen, and oxygen. As an example, Table 2 lists the composition of the sawdust blend that was processed at the pilot plant to produce the oil results discussed in the present article. The oxygen content in lignocellulosic biomass is high, and as mentioned above, this is undesirable for the production of transport biofuels that are functionally indistinguishable to their petroleum counterparts. Oxygen content is also responsible for the low energy density of biomass. More specifically, the 50/50 mix of spruce and pine wood given in Table 2 has the empirical stoichiometric formula $CH_{1,47}O_{0,65}$, whereas liquid hydrocarbon transportation fuels may be represented by the formula $CH_{1,8–2,0}$. Therefore, production of liquid hydrocarbon transportation fuels from lignocellulosics like wood is fundamentally about deoxygenating the biomass, while increasing the H/C ratio.

3.1 Reaction chemistry

The reaction chemistry of hydrothermal liquefaction is complex, and a plethora of chemical reactions may proceed depending of the specific operating conditions. A proposed scheme for the major reactions at Hydrofaction™ conditions is visualized in Fig. 6. The reaction scheme will be used to explain the decomposition and deoxygenation of biomass to renewable oil in an alkaline supercritical water-organic reaction media. It is important to acknowledge that different transition stages, such as heating and cooling, occur along the conversion from biomass to renewable oil. The rate of the individual reactions and the extent to which conversion proceeds via specific reaction pathways differ between these transition stages. Figure 7 provides a conceptual depiction of which major reactions (given in Fig. 6) are favored at the different reaction regimes during the conversion from biomass to renewable oil.

3.2 The heat-up transition stage

During biomass slurry pre-treatment, alkaline conditions and organic solvents facilitate dissolution of the lignocellulosic to its major macromolecules, which are hemicellulose, cellulose, and lignin.

In the initial heat-up transition stage at temperatures up to the critical point, the ionic product of water is high above 10^{-12} and the reaction medium can be considered as completely ionic. The macromolecules depolymerize to oligomers and

Table 2 Elemental composition and higher heating value of spruce and pine on a DAF basis

	Spruce	Pine	50/50 mix	Standard
Carbon (wt.%)	50.4	50.2	50.3	ASTM D 5291
Hydrogen (wt.%)	6.1	6.2	6.2	ASTM D 5291
Oxygen (wt.%)	43.1	43.4	43.3	Balance
Sulfur (wt.%)	0	0	0	ASTM D 1552
Nitrogen (wt.%)	0.2	0.1	0.2	ASTM D 5291
Chloride (wt.%)	0.008	0.007	0.008	ASTM D 808 (mod.)
HHV (MJ/kg)	20.2	20.1	20.2	ASTM D 240

All analyses were performed at the certified laboratory at Uniper, Karlshamn, Sweden

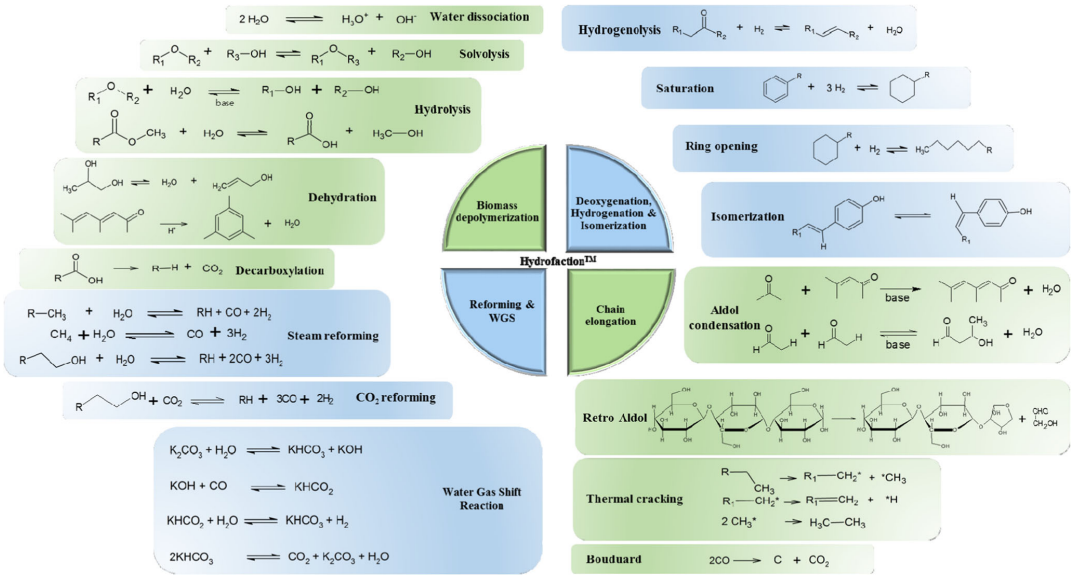

Fig. 6 Major chemical reactions occurring during Hydrofaction™

eventually monomers through alkaline hydrolysis and solvolysis type of reactions. The hydrolysis and solvolysis reactions cleave the glycosidic bonds in hemicellulose and cellulose and the intermolecular ether bonds in lignin.

Hemicellulose depolymerizes first due to its amorphous structure. Cellulose and crystalline cellulose in particular are more resilient to depolymerization, and depolymerization occurs at more severe temperatures. The oligomers and monomers formed from hydrolysis and solvolysis further dehydrate and isomerize to carboxylic acids, aldehydes, and enols, which may further react via decarboxylation and repolymerize via aldol condensation reactions.

The hydrolysis and solvolysis in this region are mainly of heterogeneous nature and therefore associated with a relatively

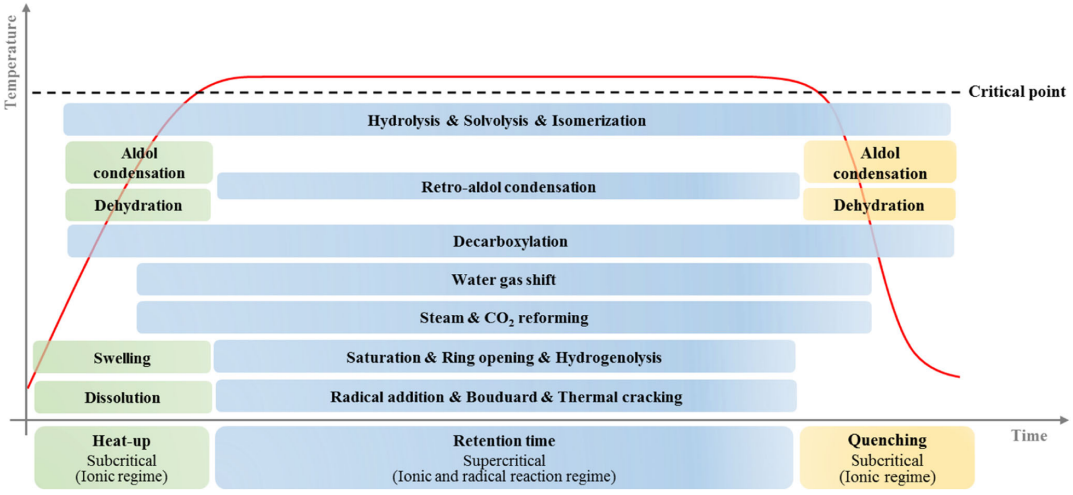

Fig. 7 Visualization of the major reactions occurring in different transition stages of Hydrofaction™

slow dissolution rate in water. Hence, a slow heat-up stage (e.g., <10 °C/min) as for most batch autoclave experiments [5, 6, 8, 9] means that the macromolecules will eventually be depolymerized to monomers. As limited competing reaction options are present in this region, a risk of significant dehydration and condensation reactions similar to caramelization of sugars exists due to the long residence time.

Lignin depolymerization can also take two main pathways, an ionic pathway through the hydrolysis/solvolysis of intermolecular ether bonds leading to the formation of low molecular weight phenolics and a radical pathway through the thermolytical cleavage of both ether and C–C bonds. The high-density water, presence of alkali metal catalysts under alkaline conditions, and perhaps most importantly the recycled organics favor the ionic pathway through hydrolysis/solvolysis of cleaving the ether bond, thereby minimizing the formation of char or high molecular weight compounds through radical addition reactions. Similar findings have been observed by Roberts, Saisu, Okuda, and Pedersen [15, 17, 18, 25].

Hydrofaction™ applies a rapid heat-up (>450 °C/min), whereby the initial heat-up phase is completed within seconds compared to hours for batch reactors [26]. Thereby, undesired reactions such as dehydration and aldol condensation proceeds to a lesser extent until more reaction options are available.

As temperature increases and approaches the critical point of water, rapid dissolution of cellulose occurs and its hydrolysis is greatly accelerated by overcoming mass transfer limitations. This homogeneous type of hydrolysis favors the formation of cellulose oligomers as opposed to monomers [27]. Further alternative reaction options in the form of an alkali metal and base-induced ionic type water gas shift and reforming reactions with water and CO_2 become increasingly important.

Thus, with a rapid heat-up, the effect of the heat-up transition stage is reduced, and the major conversion is occurring at the supercritical reaction regime, in which water gas shift, reforming, and homogenous hydrolysis and solvolysis reactions are favored.

3.3 The supercritical reaction regime

The high-density, alkaline supercritical water applied in Hydrofaction™ promotes further depolymerization of macromolecules through homogeneous hydrolysis and solvolysis rather than pyrolytic cleavage and retro-aldol reactions [15, 27, 28]. Water dissociation catalyzes additional ionic reactions such as isomerization, saturation, and hydrogenolysis. However, due to the relatively severe temperature exploited, radical reactions should also be considered in the supercritical regime. Radical reactions may potentially propagate into coke formation or shift the selectivity towards high molecular weight species, which induces the risk of reactor fouling. With that in mind, Hydrofaction™ utilizes radical scavengers in various forms to participate in chain-terminating reactions. Water acts as a radical scavenger due to its hydrogen-donating ability [11, 12]. Reducing gasses produced in situ such as H_2 and CO are also known to stabilize fragmented radicals and improve biocrude quality during HTL [11, 29, 30]. Additionally, recirculation of organics is believed to improve the impact of free-radical chemistry for two reasons. Firstly, the organics act as radical scavengers with their polar and often reactive carbonyl, carboxyl, and hydroxyl functional groups [30]. Secondly, it is beneficial to increase the concentration of low molecular weight species in relation to radical addition reactions, because they limit the possible chain length of the obtained product [17, 28]. A similar method, though using a heterogenous metal catalyst, is utilized in petrochemical hydroprocessing of heavy residues, where thermal cracking is stabilized by immediate hydrogenation in the presence of hydrogen [31].

The high-density supercritical water appears to provide sufficient solubility of the alkali metal catalysts, and it promotes ionic WGS and reforming reactions, which are considered crucial [11]. To enable the benefits of hydrogen produced in situ, the WGS reactions are promoted by alkaline conditions and in particular by the presence of potassium carbonate. At these conditions, the WGS equilibrium is shifted in the desired direction of a high H_2/CO ratio [32]. This statement is supported by the steady state product gas composition presented later in Table 4, in which the H_2/CO ratio is around 80 and the CO concentration is low at 0.29 wt.%. CO is a prerequisite for WGS reactions, and the CO intermediate is formed by steam and CO_2 reforming that are favored over, e.g., aldol condensation in the supercritical transition stage. Steam reforming facilitates an appealing compromise between gaining hydrogen from the water by sacrificing a carbon and often removing oxygen from the biomass.

Based on the above, reforming reactions followed by WGS are also considered the main pathway for formation of CO_2, which is the most abundant compound in the gaseous product. Decarboxylation is another potential pathway to CO_2 formation, but the effect of decarboxylation is suppressed by the rapid heat-up.

Hydrogen produced from the reforming and water gas shift reactions reacts further through hydrogenolysis of functional groups and hydrogenation type of reactions.

The reactions characteristic to the supercritical operating regime are quenched during subsequent cooling from supercritical conditions to ambient. As indicated in Fig. 7, the reaction products are passing through the purely ionic reaction regime, where dehydration and condensation reactions are favored. Like the initial heat-up transition stage, the cooling is preferably fast to avoid exothermic polymerization and condensation reactions that impose the risk of forming high molecular weight compounds.

The above describes how a complex plethora of reactions need to be carefully controlled to proceed in synergy in the reaction media to liquefy and deoxygenate the biomass into renewable oil.

Fig. 8 Photos from the Pilot at Aalborg University

4 Pilot plant production of Hydrofaction™ oil

The experimental campaign presented in this section resulted in roughly 1 barrel (>150 kg) of steady state oil produced in a continuous pilot facility (the "Pilot") located at the campus of Aalborg University, Denmark. The Pilot has demonstrated the Hydrofaction™ technology since 2013 and is designed to operate at supercritical water conditions up to 450 °C and 350 bar with a capacity of 30-kg/h slurry throughput. The Pilot was commissioned in 1Q2013, and since then, it has completed more than 4000 h of hot operation, including 1200 oil production hours. The plant has constituted a centerpiece for both the experimental work on Hydrofaction™ oil production and academic research activities [33]. Pictures of the Pilot are given in Fig. 8.

4.1 Experimental procedure

A process flow diagram of the Pilot is given in Fig. 9 and described in the following. The pilot is heated up by circulating pressurized deionized water until the system has reached desired temperatures [34]. When the desired process conditions have been established, the feed is switched to biomass slurry. Pressurization of the slurry is done by a high-pressure feed pump and subsequently heated in two serially connected heaters before

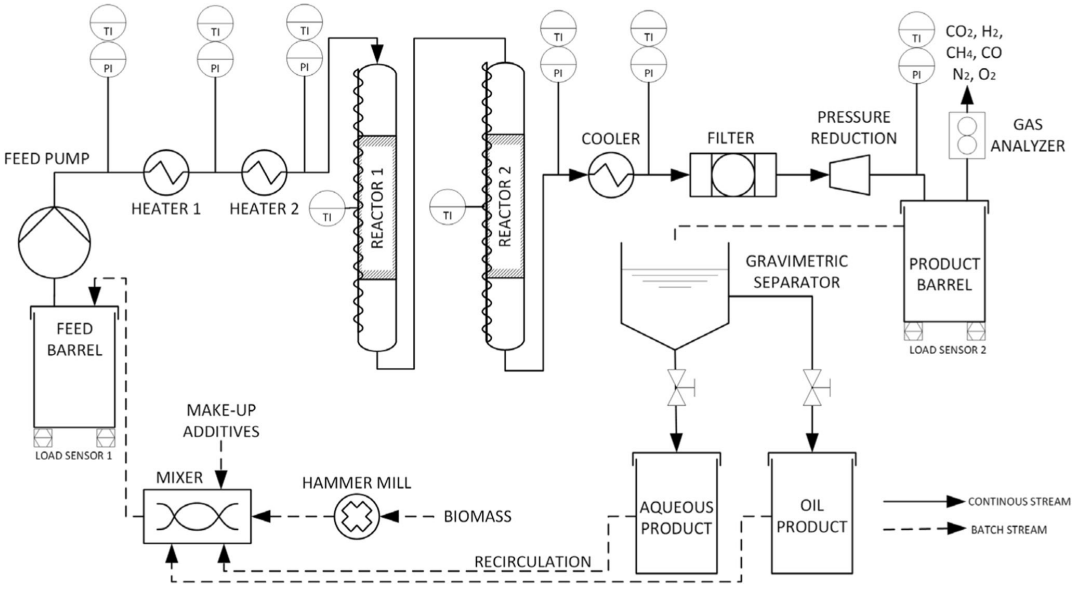

Fig. 9 Process flow diagram of the Pilot

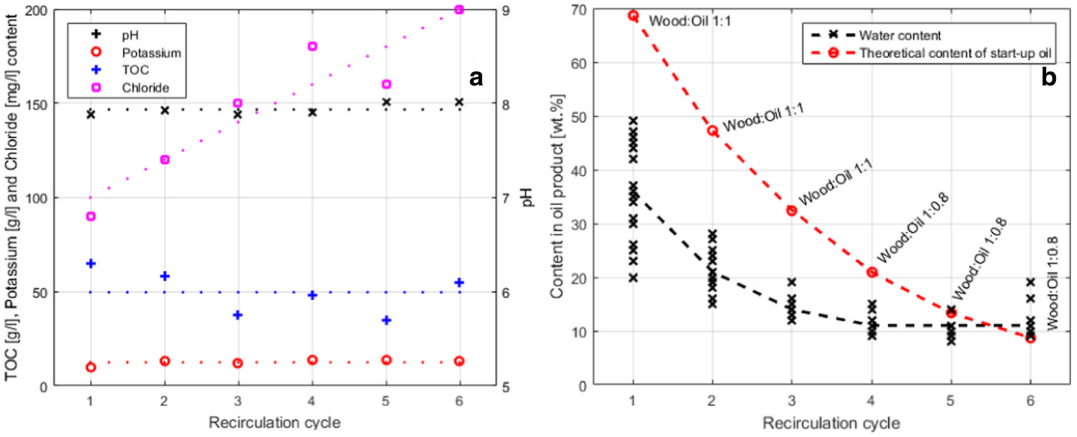

Fig. 10 **a** pH and concentration of potassium, TOC, and chloride in aqueous product as function of recirculation cycle. The analyses are based on Hach-Lange kits for TOC (LCK385), potassium (LCK328), and chloride (LCK311). **b** Water content and theoretical start-up oil content in oil product as function of recirculation cycle. The content of start-up oil is calculated based on the wood to oil ratio in the slurry, the wood to oil yield, and a conservative assumption that the start-up oil does not convert

entering the two 5-L reactors that are kept at 390–420 °C. Reactor effluents are cooled before entering a filtration unit and depressurized in a capillary system [35] prior to degassing the product. The volume flow of gaseous products is measured in an online gas flow meter along with the concentrations of CO_2, H_2, CH_4, CO, N_2, and O_2. Detailed gas compositions are analyzed by SP Technical Research Institute of Sweden by sampling in dedicated gas bags. Liquid products are sampled every 60 min to obtain three to four mass balances per run. An aqueous and an oil product phase are collected and weighed after gravimetric separation in a funnel for 60–90 min at ambient temperature. Prior to recirculation, the aqueous product is analyzed for potassium, ash, total organic carbon (TOC) content, and pH, while the oil product is analyzed for water and ash content. Thereby, the amount of makeup catalyst required in the feed slurry for the consecutive cycle can be determined, and oil can be recirculated on a dry ash-free (DAF) basis.

A homogenous and pumpable slurry is prepared batchwise (100 kg) by mixing wood, milled to a particle size of less than about 2 mm, with recycled aqueous phase, recycled oil, and makeup catalyst. Each slurry batch comprises 17–20 wt.% of wood and 17–20 wt.% of recycled oil on a dry ash-free basis. The balance is made of aqueous effluent from the previous pilot run containing water-soluble organics and alkali metal catalysts. Makeup K_2CO_3 is added as homogeneous catalyst to a slurry concentration of 2.5 wt.% by balancing with the concentration in

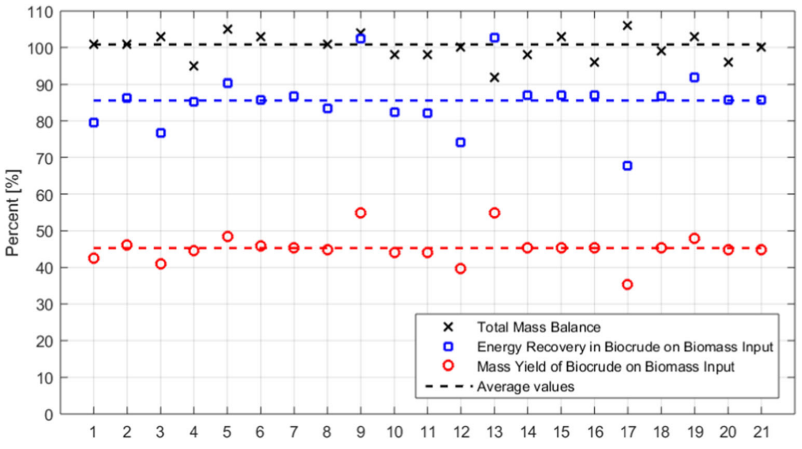

Fig. 11 Key numbers on efficiency for steady state production of biocrude. Total mass balance reflects overall mass balance closure of input and output streams. Energy recovery expresses how much of the energy in the incoming wood is recovered in the biocrude and does not include external utilities. Note that the mass balances presented do not include runs with less than five consecutive recycling of oil and water

the recirculated water product. The pH is adjusted by adding sodium hydroxide to ensure a pH >8.0 in the aqueous product. Stable pH and potassium levels as well as a rather stable TOC content are shown in Fig. 10a as a function of recirculation cycles. At initiation of a new pilot demonstration campaign, the oil and aqueous effluent of the previous run is not available so crude tall oil is used as start-up oil, while 4.5 wt.% ethanol is added to deionized water to emulate water-soluble organics. As such, each run recycles portion of the oil and the water product of the previous run. Figure 10b depicts that the water content of the oil product reaches a steady level after four recirculation cycles. Likewise, the figure shows that the theoretical content of start-up oil in the oil product is <15 wt.% after five recirculation cycles. Based on this, five consecutive cycles have been defined as a minimum to reach steady state, and unless stated otherwise, the results presented are from mass balances collected during fifth- and sixth-cycle runs only.

4.2 Mass, energy, and elemental balances

All mass and energy balances reported in this document are based on data garnered from the steady state operation of the pilot at conditions described above and using the 50/50 wt.% wood mixture listed in Table 2. Figure 11 depicts oil yield, energy recovery, and mass balance closure for a number of mass balances collected during fifth- or sixth-cycle runs. The average values are given in Table 3 together with elemental balances for carbon, oxygen, and hydrogen. Mass yields and elemental composition of raw material and products were used in the determination of elemental balances. The yield of water is based on complete closure of the oxygen balance, assuming that all oxygen from the fed biomass that is not embraced in the oil or forming gaseous species is converted to water. The hydrogen balance is derived from the oxygen balance, and any errors in the previous assumption accumulate in the hydrogen balance. On that basis, an elemental hydrogen balance closure of 114% is considered acceptable.

The overall mass balance is determined to be on average 100.3 wt.%, showing that no mass is accumulated within the plant. The filter, depicted in Fig. 9, is only in place to protect the capillaries from particles, and it did not affect the mass balances. No significant amounts of char or other retentate products were collected in the filter, and any potential char or coke particles must be dispersed in the oil product. This supports the hypothesis that char formation is inhibited by the Hydrofaction™ conditions. The oil yield, defined as the mass of dry ash-free oil produced per mass of dry ash-free biomass fed, is on average 45.3 wt.%. Note that in the presented oil yield, the recycled oil is accounted for and subtracted from the produced oil. The average energy recovery of 85.6% is defined to be energy in the dry ash-free wood that is recovered in dry ash-free produced oil. The gas has a heating value of 7.73 MJ/kg (Table 4), which corresponds to an energy recovery of 15.8%. Extrapolations on a system with heat exchange indicate that if this energy is utilized for energy production (heat), it will release more than enough to make the process self-sustained with heat.

Table 3 Mass, energy, and elemental balance of Hydrofaction™ oil production, based on average values of the runs presented in Fig. 11

		Feed (wood)	Oil	Off gas	Water[a]	Total out
Mass and energy balance						
Mass	wt.%	100	45.3	41.2	13.8	100.3
Energy	%	100	85.6	15.8	0	101.4
Elemental balance						
C	wt.%	100	73.7	26.2	0	99.9
O	wt.%	100	10.5	61.1	28.4	100.0
H	wt.%	100	63.8	25.4	25.1	114.3

Elemental balances reflect the distribution of feedstock elements in the products

[a] Determined based on 100% oxygen balance

Elemental balances of carbon, oxygen, and hydrogen at steady state conditions are listed in Table 3. The products of the Hydrofaction™ process are oil, gas, and water, of which just oil and gas contain biomass carbon. The aqueous phase that is recycled does contain carbon, but the carbon content is rather constant as function of recirculation cycle as shown in Fig. 10a. This indicates that an even amount of carbon is lost to and gained from the aqueous phase, emphasizing how the aqueous phase

Table 4 Steady state gas composition for the product gas

Component	vol.%[a]	wt.%[a]	HHV (MJ/kg)	Standards
H_2	25.79	1.69	2.40	SS-ISO 6974
CO_2	61.14	87.27	0.00	SS-ISO 6974
CO	0.32	0.29	0.03	SS-ISO 6974
CH_4	7.20	3.75	2.08	SS-ISO 6974
Ethene	0.17	0.16	0.08	SS-ISO 6974
Ethane	2.36	2.31	1.20	SS-ISO 6974
Propene	0.29	0.40	0.19	SS-ISO 6974
Propane	1.02	1.46	0.74	SS-ISO 6974
Sum C_4	0.68	1.25	0.62	SS-ISO 6974
Methanol	0.44	0.46	0.10	SS-ISO 6974
Ethanol	0.29	0.43	0.13	SS-ISO 6974
Acetone	0.28	0.53	0.17	SS-ISO 6974
Total	100	100	7.73	

The gas analyses were performed by the certified analysis laboratory at SP Technical Research Institute of Sweden, Sweden. The gas samples were supplied to the laboratory in special designed sample bags dedicated for gas samples. Based on the given composition, the elemental content of the gaseous product is 32 wt.% C, 3.8 wt.% H, 0.0 wt.% N, and 64.1 wt.% O

[a] Air free

Table 5 Hydrofaction™ oil characteristics

Test	Unit	Hydrofaction™ oil	Standard
Elemental analysis (DAF)	wt.%		
C		81.4	ASTM D5291
H		8.7	ASTM D5291
N		0.095	ASTM D5291
S		0.01	ASTM D2622
O		9.8	By difference
H/C mole ratio (DAF)	–	1.28	Calculated
HHV (DAF)	MJ/kg	38.6	ASTM D4809
Water content	wt.%	0.8	ASTM D6304
Density	kg m^{-3}		
At 40 °C		1,057.2	ASTM D4052
At 50 °C		1,050.3	ASTM D4052
At 60 °C		1,043.5	ASTM D4052
At 70 °C		1,036.8	ASTM D4052
Kinematic viscosity at 40 °C	mm^2/s	17,360	ASTM D445
Kinematic viscosity at 60 °C	mm^2/s	1,545	ASTM D445
Total acid number	mg KOH/g	8.8	ASTM D664
Strong acid number	mg KOH/g	<0.01	ASTM D664
Pour point	°C	24	ASTM D97
Flash point	°C	59	ASTM D97

All analyses of the oil were performed by the certified oil laboratory at Saybolt Nederland B.V. Dehydration of the oil by distillation (ASTM D2892) was also done by Saybolt Nederland B.V., and the oil characteristics reflect the dehydrated oil

recirculation improves the mass, energy, and carbon efficiencies by avoiding carbon loss to the aqueous phase. Although, as mentioned in Sect. 2.2, water needs to be purged from the process, because water is added both as biomass moisture and by the water generated during conversion. Thus, in a fully continuous scaled-up system, an aqueous purge stream will be purified to TOC levels low enough to allow disposal, while the majority of the TOC is recycled back into the process through a concentrated aqueous product. Additionally, a purge of the concentrate is required to avoid buildup of wood impurities such as chloride, which is given in Fig. 10a. The loss of TOC through this purge depends on the water treatment technology but is expected to be 1–3 wt.% of the feedstock carbon. This provides some background on the assumption that no or negligible quantities of carbon are lost to the water effluent.

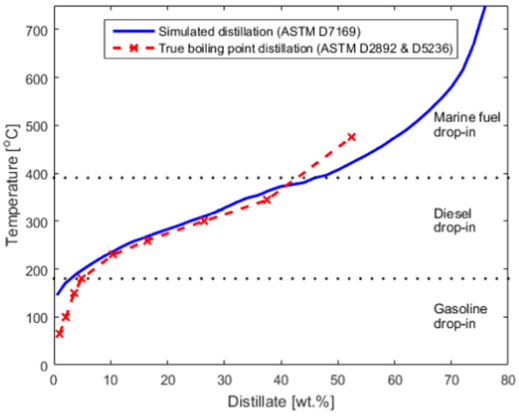

Fig. 12 True and simulated boiling point distribution of dehydrated Hydrofaction™ oil

The oil has a carbon content of 81.9 wt.%, which with the given yield corresponds to a wood to oil carbon recovery of 73.7 wt.%. Likewise, 26.2 wt.% of the feedstock carbon is recovered as gaseous products, resulting in a carbon balance closure of 99.9 wt.%.

The oxygen balance in Table 3 shows that 10.5 wt.% of the biomass elemental oxygen is traced in the oil and 61 wt.% in the gaseous products. This complies with the overall objective of maximizing deoxygenation of the biomass to improve energy density with minimal loss of carbon and hydrogen. The molecular gas composition listed in Table 4 shows that CO_2 is the major gas product. This result indicates that almost two thirds of the oxygen is removed via reforming and WGS reactions and to a lesser extent through decarboxylation, whereas about one third is removed as water. Methane and other light hydrocarbons are products of methanation and cracking reactions. The gas

product composition in Table 4 also shows a significant concentration of H_2 (26 vol.%) and a comparably low CO concentration (0.32 vol.%). This highlights that the presence of potassium carbonate in an alkaline supercritical water medium accelerates the water gas shift reaction towards consuming CO and thus favoring in situ H_2 production.

The significant yield of gaseous products with a higher heating value of 7.73 MJ/kg enables the Hydrofaction™ process to be self-sustained with heat when in steady state. Alternatively, the significant hydrogen production that is characteristic to the technology can be utilized in the downstream oil upgrading, where costly hydrogen is used to upgrade the biocrude to biofuel blendstock. On a biocrude mass basis, 1.5 wt.% H_2 is produced in situ during conversion of wood, which constitutes a significant share (~50%) of the overall H_2 required during upgrading of the Hydrofaction™ oil.

4.3 Hydrofaction™ oil

The oil produced from the continuous steady state pilot plant operations described above has been analyzed by the certified oil laboratory at Saybolt Nederland B.V. for thermophysical properties (Table 5) and distillation properties (Fig. 12). Generally, the oil has properties (oxygen content, H/C ratio, HHV, acid numbers) that make it at least as amenable to upgrading as state-of-the-art, wood-derived HTL oils reported in the literature [5, 6, 8, 9]. It is worth noting that the oil produced from wood is intrinsically low in sulfur (<80 ppm) due to the very low sulfur content in the biomass feedstock. Thus, besides a low carbon footprint, the low sulfur content of Hydrofaction™ oil is a key feature that advances it from petroleum crudes in relation to ultralow sulfur diesel and marine fuel production.

5 Conclusions

The present article covers the characteristics of the Hydrofaction™ technology, from the fundamentals on high-density, supercritical water chemistry with recirculation of organics to operational data from production of 1 barrel of oil in a dedicated pilot plant. The distinctly higher pressures and temperatures applied during Hydrofaction™, relative to the critical point of water and most literature on HTL, maintain a high-water density, thereby enhancing the properties of supercritical water as reaction medium for biomass conversion to renewable oil. Mass, energy, and three elemental balances have been closed for steady state operation, and the reported mass and energy recoveries from wood to oil are 45.3 wt.% and 85.6%, respectively. The oil quality indicates that it is amenable to upgrading to transportation fuel blendstock and can thus contribute to society's imminent challenge of sourcing renewable biofuels that are functionally indistinguishable to existing and carbon-intensive petroleum fuels.

Acknowledgements The authors are thankful for the collaboration with Professor Lasse A. Rosendahl, Aalborg University, Denmark, and the funding provided by EASME Horizon 2020 (Grant No. 666712), Danish Energy Technology Development and Demonstration Program (Grant No. 64013-0513), and Innovation Fund Denmark (Grant No. 4135-00126B).

References

1. US EIA (2016) Short-term energy outlook. Technical report by U.S. Energy Information Administration. https://www.eia.gov/forecasts/steo/report/global_oil.cfm.
2. Ackert S (2013) Aircraft payload-range analysis for financiers. Technical report by Aircraft Monitor.
3. Karatzos S, McMillan JD, Saddler JN (2014) The potential and challenges of drop-in biofuels. Report for IEA Bioenergy Task 39
4. Tews IJ, Zhu Y, Drennan CV, Elliott DC, Snowden-swan LJ, Onarheim K, Solantausta Y, Beckman D (2014) Biomass direct liquefaction options: technoeconomic and life cycle assessment. Technical report 25379 by Pacific Northwest National Laboratory
5. Peterson AA, Vogel F, Lachance RP, Fröling M, Antal MJ Jr, Tester JW (2008) Thermochemical biofuel production in hydrothermal media: a review of sub- and supercritical water technologies. Energy Environ Sci 1:32–65
6. Xue Y, Chen H, Zhao W et al (2016) A review on the operating conditions of producing bio-oil from hydrothermal liquefaction of biomass. Int J Energy Res 40(7):865–877
7. Harvey AH, Peskin AP, Klein SA (2013) NIST/ASME Steam Properties Database, software version 3.0. Standard Reference Database, NIST.
8. Zheng J-L, Zhu M-Q, Wu H-t (2015) Alkaline hydrothermal liquefaction of swine carcasses to bio-oil. Waste Manag 43:230–238
9. Toor SS, Rosendahl LA, Hoffmann J, et al. (2014) Chapter 9, Hydrothermal liquefaction of biomass, 189–217. Book by Springer: Jin F (ed) Application of hydrothermal reactions to biomass conversion, ISBN 9783642544576.
10. Iversen SB (2015) Process and apparatus for producing liquid hydrocarbon. Patent WO2012/167794, issued 21 Apr 2015.
11. Akiya N, Savage PE (2002) Roles of water for chemical reactions in high-temperature water. Chem Rev 102:2725–2750
12. Kruse A, Dinjus E (2007) Hot compressed water as reaction medium and reactant properties and synthesis reactions. J Supercrit Fluid 39:362–380
13. Rutin SB, Skripov PV (2016) Controlled high-power heat release as a tool to selecting working pressure for supercritical water. J Eng Thermophys 25(2):166–173
14. Fang Z, Sato T, Smith RL et al (2008) Reaction chemistry and phase behavior of lignin in high-temperature and supercritical water. Bioresour Technol 99:3424–3430
15. Roberts VM, Knapp RT, Li X, Lercher JA (2010) Selective hydrolysis of diphenyl ether in supercritical water catalyzed by alkaline carbonates. Chem Cat Chem 2:1407–1410
16. Eisentraut A (2010) Sustainable production of second-generation biofuels: potential and perspectives in major economies and developing countries. Technical report by IEA
17. Okuda K, Man X, Umetsu M et al (2004) Efficient conversion of lignin into single chemical species by solvothermal reaction in water–p-cresol solvent. J. Of physics. Condens Matter 16:S1325–S1330
18. Saisu M, Sato T, Watanabe M et al (2003) Conversion of lignin with supercritical water-phenol mixtures. Energy Fuel 17:922–928
19. Deguchi S, Tsujii K, Horikoshi K (2006) Cooking cellulose in hot and compressed water. Chem Commu 31:3293–3295

20. Bali G, Meng X, Deneff JI et al (2015) The effect of alkaline pretreatment methods on cellulose structure and accessibility. Chem Sus Chem 8(2):275–279
21. Klemn D, Philipp B, Heinze T, Heinze U, Wagenknecht W (1998) Comprehensive cellulose chemistry. In: Fundamentals and analytical methods, vol Vol. 1. Wiley-VCH, Weinheim ISBN 9783527294138
22. Sjöström E (1993) Wood chemistry: fundamentals and applications, 2nd edn. Academic press, San Diego ISBN 9780080925899
23. Phyllis2 ECN (2012) Database for biomass and waste. Energy Research Centre of the Netherlands. https://www.ecn.nl/phyllis2/. Accessed 20 Oct 2016
24. Evert RF, Eichhorn SE (2006) Esau's plant anatomy: meristems, cells, and tissues of the plant body: their structure, function, and development, 3rd edn. John Wiley & Sons, Hoboken
25. Pedersen T H, Hydrothermal liquefaction of biomass and model compounds. PhD thesis (2016), Aalborg Universitetsforlag, DK, ISBN 9788771124972
26. Iversen SB (2011) Process and apparatus for producing liquid hydrocarbon. Patent application WO2012/167789, filed 10 Jun 2011
27. Matsumura Y, Sasaki M, Okuda K et al (2006) Supercritical water treatment of biomass for energy and material recovery. Combust Sci Technol 178:509–536
28. Sasaki M, Fang Z, Fukushima Y et al (2000) Dissolution and hydrolysis of cellulose in subcritical and supercritical water. Ind Eng Chem Res 39:2883–2890
29. Davis H, Figueroa C, Schaleger L (1982) Hydrogen or carbon monoxide in the liquefaction of biomass. Paper submitted for the World Hydrogen Energy Conference IV, Pasadena, Ca, US, 13–17 June 1982
30. He BJ, Zhang, Y, Yin Y, Funk TL, Riskowski GL (2001) Effects of alternative process gases on the thermochemical conversion process of swine manure. Trans ASAE 44, 6, 1873–1880
31. Gary JH, Handwerk GE, Kaiser MJ (2007) Petroleum refining: technology and economics, 5th edn. Book by CRC press, ISBN 9780849370380.
32. Kruse A (2011) Behandlung von Biomasse mit überkritischem Wasser. Chem Ing Tech 83(9):1381–1389
33. Pedersen TH et al (2016) Continuous hydrothermal co-liquefaction of aspen wood and glycerol with water phase recirculation. Appl Energy 162:1034–1041
34. Iversen SB (2015) Improved method for preparing shut down of process and equipment for producing liquid hydrocarbons. Patent WO2014/032669, issued 22 Dec 2015.
35. Iversen SB (2014) Pressure reduction device and method. Patent application WO2014/181283, filed 08 May 2014.

Paper C

Full characterization of compounds obtained from fractional distillation and upgrading of a HTL biocrude

Thomas H. Pedersen, Claus Uhrenholt Jensen, Linda Sandström, Lasse A. Rosendahl

The manuscript has been published in the
Journal of Applied Energy, vol. 202, pp. 408–419, 2017.

The layout has been revised.

Applied Energy 202 (2017) 408–419

Contents lists available at ScienceDirect

Applied Energy

journal homepage: www.elsevier.com/locate/apenergy

Full characterization of compounds obtained from fractional distillation and upgrading of a HTL biocrude

T.H. Pedersen [a], C.U. Jensen [b], L. Sandström [c], L.A. Rosendahl [a,*]

[a] Department of Energy Technology, Aalborg University, Pontoppidanstræde 111, 9220 Aalborg Øst, Denmark
[b] Steeper Energy ApS, Sandbjergvej 11, 2970 Hørsholm, Denmark
[c] SP Energy Technology Center AB, Box 726, SE-941 28 Piteå, Sweden

HIGHLIGHTS

- Fractional distillation has been performed successfully.
- Detailed characterization of the distillate fractions has been carried out.
- Similar chemical compounds arrange according to their boiling points.
- Upgrading of a distillate mixture was carried out.
- Reaction scheme through intermediates to biocrude is proposed.

ARTICLE INFO

Article history:
Received 22 November 2016
Received in revised form 24 May 2017
Accepted 26 May 2017
Available online 3 June 2017

Keywords:
Biofuels
Biochemicals
Fractionation
Hydrotreatment
Biorefinery

ABSTRACT

Biocrude from hydrothermal liquefaction of biomass provides a sustainable source from which to produce chemicals and fuels. However, just as for fossil crude, the chemical complexity of the biocrude impedes the characterization and hence identification of market potentials for both biocrude and individual fractions. Here, we reveal how fractional distillation of a biocrude can leverage biocrude characterization beyond state-of-the-art and uncover the full biocrude potential. By distillation combined with detailed individual analysis of the distillate fractions and distillation residue, more than 85% of the total biocrude composition is determined. It is demonstrated that a total mass fraction of 48.2% of the biocrude is volatile below 350 °C, comprising mainly value-added marketable ketones, oxygenated aromatics and prospective liquid fuel candidates, which are easily fractionated according to boiling points. Novel, high resolution pyr-GCxGC-MS analysis of the residue indicates a high molecular weight aromatic structure, valuable for bio-materials production or for further processing into fuels. The distillate fractions are mildly hydrotreated to show the fuel and chemical precursor potential of the volatile components. This results in the formation of mainly hydrocarbons and added-value phenolics. This work takes a significant step by going beyond the biocrude as an intermediate bulk energy product and addressing actual applications and pathways to these.

1. Introduction

Biomass will become the major sustainable source of carbon for future mass production of commodity chemicals and transport fuels, due to the environmental concerns caused by petroleum consumption. The roadmap for biomass conversion into platform chemicals, able to substitute petroleum-derived equivalents, is complex and ranges from biological to severe catalytic thermochemical processes. Commercial mass production of chemical and energy commodities from biomass relies on scalable, energy and resource efficient, and feedstock flexible processes able to produce renewable bulk platform chemicals sustainably and economically. Hydrothermal liquefaction of biomass is a thermochemical process carried out in a near-critical water environment capable of disintegrating and decomposing biomass macromolecules into lower molecular weight compounds, which are substantially deoxygenated compared to the original macromolecules [1–6]. Compound deoxygenation results in a spontaneous and distinct compound separation; polar compounds (usually termed water-soluble organics (WSO)) are contained in the effluent aqueous phase, whereas non-polar compounds are contained in a nearly

* Corresponding author.
E-mail address: lar@et.aau.dk (L.A. Rosendahl).

http://dx.doi.org/10.1016/j.apenergy.2017.05.167
0306-2619/

water-free liquid bulk fraction termed biocrude. Biocrude is an energy dense, transportable value-added liquid, but also a chemically complex mixture consisting of numerous chemical compounds. The spontaneous phase separation of the process effluent provides an inexpensive means of biocrude recovery, and fractional distillation provides an attractive method of grouping chemically similar compounds based on their volatility. The less complex fractions, compared to the biocrude, may then be further separated or processed into commodity chemicals or fuels resembling existing petroleum operations. Zhang et al. demonstrated the benefits of fractional distillation of a pyrolysis biooil [7]. Using a single stage, atmospheric pressure distillation procedure, they traced 13 major compounds in six different distillate fractions ranging from ambient temperature to 240 °C. A total mass fraction of 52% was recovered from the biooil of which nearly 60% was water. Although separation efficiencies of the major compounds were generally high (for some around 90%), most compounds were still distributed in all distillate fractions. Cheng et al. distilled a biocrude obtained from glycerol-assisted liquefaction of manure [8]. The distillation procedure was carried out at atmospheric pressure from ambient to 500 °C. A volume fraction of only 10 % of the biocrude was distilled at 359 °C, whereas 90% was distilled at 500 °C. Thermophysical and chemical properties of the distillate fractions clearly indicated thermal degradation and deoxygenation during distillation. This was evident from the fact that the energy contents of the fractions on a mass basis all were observed greater than that of the crude biooil. Furthermore, alkanes and alkenes having number of carbon atoms in the range of C_5—C_{14} were only identified in the heavier distillate fractions above a distillation temperature of 420 °C. Therefore, atmospheric pressure distillation seems inadequate in obtaining distillate fractions truly presenting the original biocrude. Capunitan et al. fractionated a biooil obtained from pyrolysis of corn stover at atmospheric and slightly reduced pressure (0.5 bar) [9]. A *heavy distillate* mass fraction of 45% was collected in the 180–250 °C temperature range, a fraction consisting mostly of phenolic compounds. The properties of the fractions were improved in terms of moisture content, TAN number, and heating value as compared to the crude biooil. Hoffmann et al. fractionated a HTL biocrude with 53.4% mass recovery at 375 °C (atmospheric equivalent), of which the equivalent gasoline, diesel and jet-fuel mass fractions comprised of 12.5%, 25.3% and 16.6%, respectively. An oxygen distribution was established showing that all distillate fractions still contained oxygenates [10]. Only details on the distillation residue included elemental composition and heating value, leaving yet almost 50% of obtained product uncharacterized. Eboibi et al. investigated vacuum distillation of algae derived biocrude [11]. Due to the high lipid and protein content of the micro algae as compared to a lignocellulosic feedstock, up to 73% could be distilled at 360 °C. Furthermore, the vacuum distillation greatly improved the quality and metal content of the biocrude.

Hydrotreatment of the biocrude provides another means of reducing the biocrude complexity by chemically altering the many oxygen-containing chemical functionalities mainly via deoxygenation and saturation by hydrogen addition. Hydrotreatment of biocrude has been investigated and reviewed in many aspects and in order to obtain drop-in fuels from biocrude, oxygen removal by hydrotreatment is to some extent regarded as a necessary step [12–18]. In a parametric hydrotreating study, Jensen et al. showed that complete deoxygenation of a HTL biocrude can be achieved [12]. Complete deoxygenation transforms biocrude oxygenates into their corresponding hydrocarbon backbones. Therefore, if a pool of oxygenates of identical hydrocarbon backbones are hydrotreated, a resulting fraction of identical hydrocarbons can be obtained.

The objective of this study is to demonstrate that multistage vacuum fractional distillation of a wood-derived biocrude, obtained from continuous hydrothermal liquefaction, provides a viable route for detailed analysis of a biocrude. Furthermore, characterization of the distillation residue is performed for a full closure on the biocrude chemical characteristics.

2. Materials and methods

2.1. Biocrude from aspen wood hydrothermal liquefaction

The biocrude used in the present study was obtained from glycerol-assisted aspen wood liquefaction represented in a previous study [19]. In brief, the biocrude was produced under continuous conditions at 400 °C, 300 bar, and a mass flow rate of approximately 14 kg/h. Wood flour and glycerol was mixed in a 50/50 mass ratio amounting to a mass fraction of 30% of the total feed slurry. Wood flour and glycerol were slurried in process water together with a potassium carbonate catalyst. The catalyst amounted to 4% of the total mass of the feed slurries. Based on total organic input (aspen wood + glycerol) yields in the order of 20–30% were obtained. After processing, the biocrude and aqueous phase were separated gravimetrically. The as-received biocrude was dewatered by distillation according to ASTM D2892 (Appendix X 1) [20]. Light organics distilled during dewatering were reintroduced into the biocrude prior to distillation. Therefore, no moisture is expected to be present in any of the obtained distillate fractions. Table 1 presents the ultimate and proximate analyses of the aspen wood used in the study.

2.2. Fractional distillation

Fractional distillation of the biocrude was carried out in accordance to the ASTM D2892 in a two liter 15:5 distillation column [20]. More information on the distillation equipment was published by Hoffmann et al. [10]. In order to avoid thermal degradation of the biocrude during distillation the vacuum was lowered stepwise to 100 (13332), 15 (2000), and 1 (133) torr (Pa). A similar procedure was used by Lavanya et al. [21]. The distillate was divided into six liquid fractions; first fraction was obtained from an initial boiling point (IBP) of 73–100 °C, the subsequent 5 distillation fractions were obtained with 50 °C cuts to a maximum atmospheric equivalent temperature (AET) of 350 °C. The initial boiling point was determined based on visual inspection for when the first reflux was observed. The residue represents non-volatile compounds with boiling points above 350 °C. The ash content of the residue is 0.88 wt.%. The AET is based on the formulas that are applied in the ASTM D2892 and derived by Maxwell & Bonnel [22].

2.3. Catalytic hydrotreatment

A distillate mix of the six obtained distillation fractions, excluding the residue, was catalytically hydrotreated. The distillate fractions were mixed in accordance to their respective ratios obtained from the biocrude distillation. The catalytic hydrotreatment was carried out using a pre-activated and stabilized NiMo/

Table 1
Ultimately and proximate analysis of the aspen wood on a dry basis.

Elemental analysis	[wt.%][a]	Proximate analysis	[wt.%]
C	50.39	Volatiles	77.04
H	6.19	Fixed Carbon	20.61
O[a]	43.23	Ash	2.35
N	0.19		

[a] Oxygen calculated by difference. No sulfur was detected. Data reported from [19].

Al_2O_3 hydrotreating catalyst in 25 mL micro-batch reactors enabling time resolved pressure logging. A fluidized sand bath at 360 °C facilitated instant heating. Experiments were conducted in duplicates to ensure reproducibility. The catalyst loading equaled 20% of the biocrude mass, and hydrogen was introduced to 77.5 bar corresponding to 540 NL/L of biocrude. After 1.5 h of reaction time, reactors were quenched in a water bath prior to gas venting and product separation. The hydrotreated products (HTP) were collected and centrifuged prior to analysis. The liquid recovery and yield of upgraded oil were 85 wt.% and 77 wt.%, respectively, which is calculated according to the equations given in [23]. No solid products were observed and the gaseous products were not quantified.

2.4. Characterization of biocrude and distillate fractions

Elemental composition was measured using a Perkin Elmer 2400 Series II system (ASTM D5291). Sulfur content of the aspen wood was below detection level and is therefore not reported. For the distillate fractions, nitrogen and sulfur were both below detection limits and therefore not reported. Functional group identification was done by IR spectroscopy carried out at room temperature on a Thermo Scientific Nicolet 380. Spectrum resolution was 1 cm^{-1} and recorded in the range of 4000–650 cm^{-1}. GC–MS analyses of all samples were carried out on a Thermo Scientific Trace 1300 ISQ GC–MS system (Length: 30 m., i.d.: 0.25 mm., Film: 0.25 μm, HP-5MS column). Higher boiling fractions (Fraction 5 and 6) were derivatized using a BSTFA reagent prior to analysis. Samples were then diluted in diethyl ether (DEE) and subjected to the following oven temperature profile; ramped from 40 °C to 300 °C at 10 °C/min. Injector and ion source temperatures were 300 °C, split ratio was 1:20, and flow rate of the carrier gas (helium) was 1.0 mL/min. The distillation residue was analyzed by pyrolysis-GCxGC-MS, using a GC–MS QP-2010 Ultra (Shimadzu) equipped with a PY-3030S Single Shot pyrolyzer (Frontier Laboratories) and liquid nitrogen modulation (ZOEX). About 0.2 mg of sample was used and the pyrolysis temperature was set to 600 °C. The column set was an Agilent DB-5 (length: 60 m, i.d.: 0.25 mm, film: 0.1 μm) on the first dimension and an Agilent DB-17 (length: 1 m, i.d.: 0.18 mm, film: 0.18 μm) on the second dimension. The column oven was ramped from 50 °C to 280 °C at 4 °C/min. and the modulation time was six seconds. In pyrolysis-GC the sample is thermally degraded by rapid heating in an inert atmosphere prior to entering the GC column, and this method was chosen due to the high boiling point range of the residue. Thermogravimetric analysis of the residue was performed on a TA Instuments Discovery TGA. The sample was heated to 600 °C with 100 °C/min ramp, and held isothermal for one hour to mimic the pyrolysis-GCxGC-MS temperature profile. Calorific values were measured using a IKA C2000 oxygen combustion calorimeter (ASTM D2015). Total acid number (TAN) was measured by color-indicating titration. A sample of approximately 0.1 g was diluted in a 50 mL 50/50 solution of isopropanol and toluene. Phenolphtalein was used as color indicator and a 0.1 M KOH/ethanol solution was used for titration. Measurements were carried out in duplicates to ensure reproducibility.

3. Results and discussion

3.1. Distillation yields

Table 2 summaries the distillation yields within each distillate cut. Fractional distillation of the biocrude resulted in a distillate mass recovery of 47% at an AET of 350 °C. The IBP of the biocrude was 73 °C and only a mass fraction of 1.6% was distilled in the light naptha range below 100 °C. Fraction 2, 3 and 4 are also minor mass fractions accounting for 4.1%, 6.3%, and 6.0%, respectively. Fraction 5 represents the largest fraction representing 15.3% of the bulk biocrude mass, with Fraction 6 being the second largest fraction accounting for 10.3%.

The distillation residue boiling above 350 °C accounts for 51.8 % of the total mass. The residue is solid at room temperature, but becomes liquid upon heat-up to approximately 100–150 °C. Based on the high boiling point range, only pyrolysis-GCxGC-MS analysis could be carried out for the residue. Apart from water bound in the biocrude due to compound polarities, which may not have been entirely removed during initial dewatering, additional reaction water may have been formed during distillation. Chemically formed water by thermally induced condensation reactions of reactive compounds at elevated temperatures have previously been observed in other studies [24–26]. At a vacuum of 15 torr and below, such reaction water will not condense in the condenser, but it will condense in the cold trap. By Karl Fischer titration it was determined that 59.7% of this fraction was water. In addition to the fraction collected in the cold trap, an additional distillation mass loss of 1.2% is observed from Table 2. This mass loss is above the ASTM D2892 guidelines (0.4 %) but the procedure is considered adequate for the current study [20].

Fig. 1 display the distillation curve and Table 2 also summaries elemental composition, higher heating value (HHV) and TAN for both the bulk biocrude, distillate fractions, and the distillation residue. An elemental and HHV balance is included in the table in order to verify the results obtained from fractional distillation. The weighted sum of HHV and the carbon contents of the fractions are within a satisfactory range of the original biocrude. A 3.9% hydrogen discrepancy indicates that the hydrogen content of the fractions have been slightly underestimated resulting in an equally

Table 2
Properties of the biocrude, distillation fractions, and distillation residue.

Sample	TBP [°C]	Yield		HHV [MJ/kg]	Elemental analysis [wt.%]					TAN
		[wt.%]	[vol.%]		C	H	O[a]	H/C [–]	O/C [–]	[mg KOH/g]
Biocrude	–	–	–	34.3	76.4	8.4	15.2	1.31	0.15	50
F1	<100	1.6%	2.2%	33.8	67.7	13.5	18.9	2.37	0.21	7
F2	100–150	4.1%	5.3%	36.0	74.2	12.8	13.1	2.05	0.13	29
F3	150–200	6.3%	7.4%	35.5	75.7	11.0	13.3	1.74	0.13	16
F4	200–250	6.0%	6.9%	37.1	78.8	10.5	10.7	1.59	0.10	14
F5	250–300	15.3%	16.2%	34.0	73.6	9.0	17.4	1.46	0.18	33
F6	300–350	10.3%	10.8%	35.5	77.8	9.2	13.0	1.41	0.13	71
Res	>350	51.8%	–	35.2	81.0	6.3	12.8	0.92	0.12	66[b]
Cold trap	–	3.4%	3.5%	12.5	14.0	9.9	76.1	8.42	4.08	59
Balance	–	98.8%	–	0.3%	−0.3%	−3.9%	3.6%	–	–	–

[a] Oxygen by difference.
[b] Estimated based on a weighted average calculation.

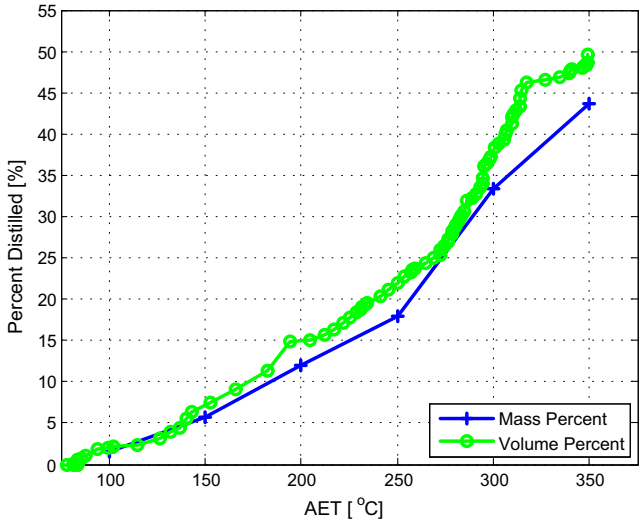

Fig. 1. Distillation profile from 15:5 fractional distillation of the biocrude.

higher oxygen content that is calculated by difference. Generally, the balances indicate smooth distillation, where thermal degradation of the biocrude has been avoided.

3.2. Properties of distillation fractions

FTIR spectra of the distillate fractions are presented in Fig. 2. Major absorptions in the 1700 cm^{-1} and 3300 cm^{-1} range indicate the presence of carbonyl and hydroxy groups throughout the fractions. More specifically, carbonyl absorption at 1715 cm^{-1} and 1745 cm^{-1} reflects six-membered and five-membered cyclic ketones, respectively, which seem to be mostly present in Fraction 1, 2 and 3 [27]. The sharp absorption around 1685 cm^{-1} in Fraction 4, 5 and 6 is likely to be α,β-unsaturated ketones or carbonyl absorption on aromatic structures. By comparing the hydroxy absorption in the range from 3650 cm^{-1} to 3000 cm^{-1}, hydroxy groups seem to be mostly present in Fraction 5 and 6, which is very likely related to the presence of phenolics and glycerol identified by GC–MS. Aromatic structures, identified by absorptions around 1600 cm^{-1} and slight absorptions between 3000 and 3050 cm^{-1}, are observed in all fractions but most pronounced in Fraction 6.

The elemental composition of the fractions are generally patterned in the way that increasing boiling points are correlated with decreasing H/C ratios, indicating a decreasing saturation of the compounds at higher boiling points. Oxygen is distributed in all distillate fractions and no general pattern in the oxygen content is observed. The HHV of the dewatered biocrude was 34.3 MJ/kg, whereas the fractions ranged from 33.8 MJ/kg for Fraction 1 to 37.1 MJ/kg for Fraction 4. The HHV of the fraction collected in the cold trap was 12.5 MJ/kg, which supports the significant share of water measured by Karl Fisher titration. The oxygen weight percent above 18% combined with a H/C atomic ratio of 2.37 indicates that the chemical compounds obtained in Fraction 1 are mainly volatile oxygenated compounds having low number of carbon atoms. Based on elemental composition, Fraction 2 and 3 are chemically similar with Fraction 3 being slightly more oxygenated, which is also emphasized by HHV and FTIR observations. Of all the fractions, Fraction 4 exhibits the lowest oxygen content and so the highest HHV. In terms of elemental composition, Fraction 5 is chemically different from the other fractions. The boiling point range of Fraction 5 includes the boiling point of glycerol (290 °C), which was a major constituent in the feedstock used for the biocrude production. Hence, the high oxygen content observed is likely related to the recovery of unconverted glycerol in this fraction. GC–MS analysis showed that glycerol is in fact present in Fraction 5. The H/C atomic ratio of Fraction 6 indicates that aromatic structures are dominating. The residue displays a HHV close to that of Fraction 6, but with a H/C ratio below unity. This fact points in the direction of high molecular weight and unsaturated oxygenates probably of multi-ring structures.

The elemental composition of the distillate fractions can be summarized by plotting the H/C and O/C atomic ratios in a Van Krevelen chart as shown in Fig. 3. All fractions but the residue show H/C ratios higher than that of the biocrude. Furthermore, all fractions but Fraction 1 and 5 show O/C ratios lower than that of the biocrude. For transport fuel production the ideal position in the Van Krevelen chart is at the H/C axis, resulting in pure hydrocarbon structures. However, in terms of HHV and elemental composition it appears that none of the fractions obtained from distillation have chemical properties significantly improved from those of the biocrude. If the ultimate objective is to produce transport fuels further chemical processing of all distillate fractions is necessary.

3.3. Compound identification in distillation fractions

Fractionation of the biocrude by fractional distillation allows for the separation of the many chemical compounds present in the biocrude due to differences in volatilities. The fractions obtained contain fewer chemical species, as compared to the biocrude, and are therefore chemically less complex, which in turn facilitates the identification of the chemical compounds. The compound identification is valuable and important in order to understand the underlying chemical pathways responsible for the formation of specific chemicals. Understanding such reactions permits one to direct the composition of the biocrude by controlling the feedstock composition and process conditions for favorable chemical reactions.

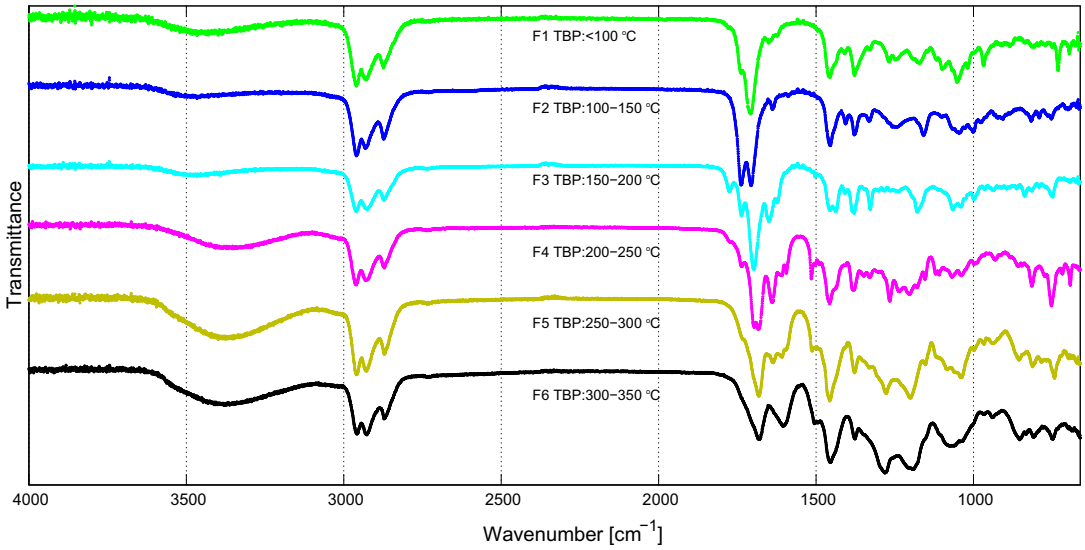

Fig. 2. Infrared spectra of the distillate fractions obtained from the fractional distillation.

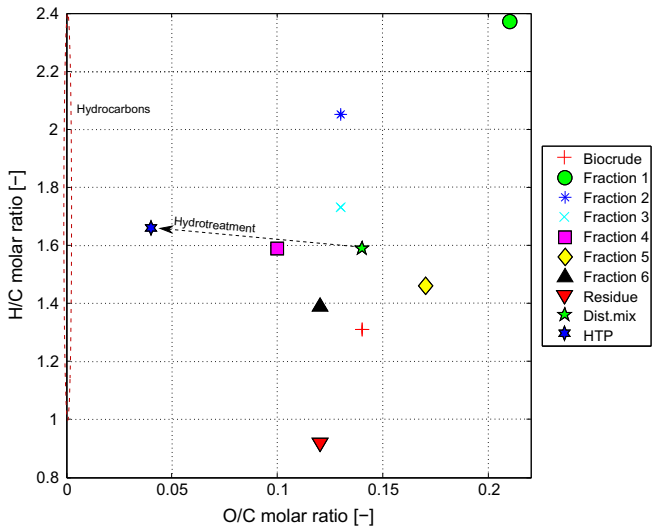

Fig. 3. Van Krevelen diagram of the biocrude, distillation fractions, distillation mix and HTP.

GC–MS analysis of the distillate fractions enables a visual inspection of the compound separation efficiency and furthermore indicates the chemical complexity of the fractions compared to the biocrude. Fig. 4 shows the normalized chromatograms of the six distillate fractions analyzed. It is clear that compound overlapping is a fact between preceding and proceeding distillate fractions as a result of imperfect distillation. However, an overlap must be expected; according to the ASTM D2892, the overlap is 15–20 °C when running a 15:5 vacuum distillation. In addition, it must be kept in mind that for the derivatized samples (Fraction 5 and 6) some bias is inevitably introduced due to shifts in volatility for certain compounds obscuring the separation efficiency interpretation. In Table 3 the 15 most abundant (by GC–MS peak area interpretation) chemical compounds identified in each distillate fraction are presented. From the table it appears that in Fraction 1 mainly short chained commodity chemicals are collected such as acetaldehyde, ethanol, and propanol alongside various ketones and hydrocarbons like toluene ranging from C^2—C_8 in number of carbon atoms [28]. Except from a few alcohols, Fraction 2 contains almost exclusively saturated ketones ranging from C_4—C_7 in number of carbon atoms, mainly in the form of cyclopentanones. This observation is consistent with the elemental composition and the FTIR interpretation. A

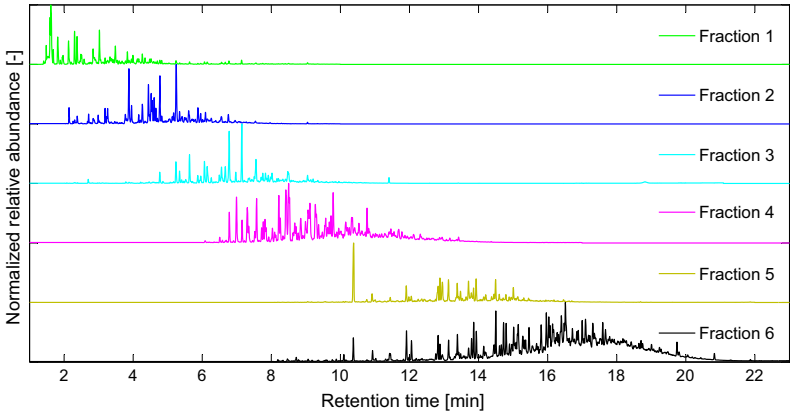

Fig. 4. GC–MS chromatograms of the distillate fractions. Chromatograms have been normalized to highest peak.

less pronounced overlap is observed between Fraction 2 and Fraction 3. From Table 3 it follows that substituted saturated and unsaturated cycloketones are dominating Fraction 3, such as mono- and dimethylated cyclopentenones and cyclohexanones. Here a rather successful separation is observed from the fact that only a few of the major compounds are identified in both distillate fractions. Ketones of C_5- and C_6-membered napthenic ring backbones are potential hydrocarbon precursors. The ease of hydrotreating these ketones is demonstrated later. Like in Fraction 3, Fraction 4 is also dominated by cycloketones. Different from Fraction 3, the cycloketones in Fraction 4 are heavilier substituted in the form of ethylation and trimethylation. Nevertheless, the potential of these heavier substituted ketones as hydrocarbon fuel is equivalent to those in Fraction 2 and 3, and thus Fraction 2–4 are dominated by chemical candidates for fuel production. Oxygenated aromatics in the form of substituted phenolics are also present in Fraction 4. The separation of compounds between Fraction 4 and 5 is concluded successful. The major peak in Fraction 5, interfering the compound range of Fraction 4, is identified as glycerol. As mentioned, the chemical derivatization of for instance glycerol decreases the boiling point causing interpretation bias. Except from a significant share of glycerol, Fraction 5 consists predominately of phenolic derivatives. The identification of compounds in Fraction 5 and 6 by NIST library search was poor compared to the lighter fractions, resulting in the identification of many identical or isomeric compounds. The presence of hydroxy, alcoholic, and carboxylic functionalities were evident from mass spectra interpretation by the observation of trimethylsilylation ($m/z = 73$) as a result of derivatization. The chemical potential of oxygenated aromatics is ranging widely [29]. In a lignin context, which is the most abundant source of aromatics, it has previously been concluded that high volume production of low molecular weight aromatic molecules is an attractive and very desirable goal, but perhaps also the most challenging and complex barrier for turning lignin into high valuable chemicals [29]. Due to the presence of the different monomeric aromatics, Fraction 4–6 are evidently sources of such high valuable aromatics with a summed distillate mass fraction over 30%, which are likely to originate mainly from the lignin fraction.

The findings of the compound identification by GC–MS is summarized by lumping the compounds into four major classifications; *hydrocarbons*, *ketones*, *other non-aromatic oxygenates*, and *aromatic oxygenates* and presented in Fig. 5. Fig. 5 also indicates the average number of carbon atoms of the compounds of each fractions. The average is based on the identified compounds and the relative peak area obtained from GC–MS analysis. The trend increases almost linearly with increasing boiling point. Fraction 5 diverges from the trend, which is most likely due to the presence of glycerol.

3.4. Compound identification in the distillation residue

The distillation residue was analyzed by pyrolysis-GCxGC-MS. The most abundant (by peak area interpretation) identified chemical compounds are shown in Table 4. Note that these compounds are pyrolysis products of the residue fraction. The use of GCxGC-MS generally improves both the peak separation and the sensitivity compared to 1D GC–MS. As a result, the number of detected components can be very large for complex samples, which is also the present case. Thermogravimetric analysis of the residue has shown that approximately 70% of the residue is volatilized at 600 °C. Hence, the pyrolysis-GCxGC-MS results serve as an almost complete indication of the residue chemical structure. The identified components of the residue fraction are mainly aromatics, as also indicated by the low H/C ratio in Table 1 as discussed earlier. Many of the components are oxygenated (several phenols and benzenediols are for instance detected), but some are not. This differs from the analyses of the six distillate fractions, where almost all identified compounds were oxygenated. The presence of non-oxygenated compounds in the chromatogram of the distillation residue can at least partly be explained by the formation of oxygen containing pyrolysis products such as carbon dioxide and water. Overall, the great similarity between the compounds obtained from the residue pyrolysis and the compounds obtained from distillation illustrates that by cracking of the residue this can contribute to increase the yield of the volatile fractions on a chemically similar basis. Ultimately, as will be explained later, the obtained cracking products can likewise be hydrotreated to yields drop-in fuels.

3.5. Proposed reaction mechanisms

In the following, a reduced reaction mechanism is proposed based on the general observations in the compound structures with each distillate fraction, and the fact that the biocrude was obtained by co-liquefaction of aspen wood and glycerol. Such a reduced reaction mechanism will not be conclusive but will serve as explanatory indicators of the formation of the specific compounds observed.

Table 3
List of major compounds identified in the distillate fractions including their relative abundance.

		Peak area (%)						
RT (min)	Identified compound	Fraction 1	Fraction 2	Fraction 3	Fraction 4	Fraction 5	Fraction 6	C#
1.41	Acetaldehyde	0.9%						2
1.49	Ethanol	10.6%						2
1.69	1-Propanol	2.8%						3
1.82	2-Butanone	11.4%	9.0%					4
1.89	Ethyl Acetate	1.2%						4
1.96	1-Propanol, 2-methyl-	3.9%	3.9%					4
2.14	2-Butanone, 3-methyl-	9.2%						5
2.15	1-Butanol		4.0%					4
2.31	2-Pentanone	11.10%						5
2.38	3-Pentanone	1.60%						5
2.51	n-Propyl acetate	2.70%						5
2.58	Butanoic acid, methyl ester	0.90%						5
2.7	1,2-propanediol			9.00%				3
2.71	1-Butanol, 2-methyl-		2.40%					5
2.85	3-Pentanone, 2-methyl-	4.70%						6
2.99	1-Pentanol		2.10%					5
3.03	Toluene	1.70%						7
3.19	3-Hexanone	1.00%	2.90%					6
3.26	Cyclopentanone		3.70%					5
3.49	Cyclopentene, 1,2,3-trimethyl-	1.00%						8
3.88	Cyclopentanone, 2-methyl-		11.80%					6
3.96	Cyclopentanone, 3-methyl-		3.10%					7
4.45	Cyclopentanone, 2,5-dimethyl-		8.10%					7
4.53	Cyclopentanone, 2,5-dimethyl-		9.20%					7
4.61	Cyclopentanone, 2,3-dimethyl-		1.90%					7
4.66	Cyclohexanone, 3-methyl-		2.20%					
4.78	2-Cyclopenten-1-one, 2-methyl-		4.50%	3.90%				6
5.25	2-Cyclopenten-1-one, 3,4-dimethyl-		6.50%	4.00%				7
5.35	2-Cyclopenten-1-one, 3,4-dimethyl-			2.40%				7
5.41	Cyclopentanone, 2,3-dimethyl-			2.10%				7
5.64	2-Cyclopenten-1-one, 3-methyl-			2.90%				6
5.85	Phenol				3.60%			6
5.87	Cyclohexanone, 2,6-dimethyl-			3.70%				8
5.96	Cyclohexanone, 2-ethyl-			11.80%				8
6.07	2-Cyclopenten-1-one, 3,4-dimethyl-			3.10%				7
6.15	2-Cyclopenten-1-one, 2,3-dimethyl-			8.10%				7
6.56	1-Isopropylcyclohex-1-ene			9.20%				9
6.67	1-Methylcyclooctene			1.90%				9
6.78	2-Cyclopenten-1-one, 2,3-dimethyl-			2.20%	3.50%			7
6.99	Phenol, 2-methyl-				3.20%			7
7.15	2-Cyclopenten-1-one, 2,3,4-trimethyl-			4.50%	2.10%			8
7.31	Phenol, 3-methyl-				4.30%			7
7.56	2-Cyclopenten-1-one, 3,3,4-trimethyl-			6.50%				8
7.57	2-Cyclopenten-1-one, 2,3,4-trimethyl-				6.20%			8
7.77	2-Cyclopenten-1-one, 3-(1-methylethyl)-				1.80%			8
8.22	2-Cyclopenten-1-one, 3-(1-methylethyl)-				5.20%			8
8.43	Phenol, 3,5-dimethyl-				4.20%			8
8.5	2-Cyclopenten-1-one, 2,3,4,5-tetramethyl-				8.60%			9
8.85	Phenol, 2,3-dimethyl-				2.10%			8
8.99	Phenol, 2-ethyl-5-methyl-				2.00%			9
9.12	2-Cyclopenten-1-one, 2,3,4,5-tetramethyl-				8.40%			9
9.3	1-Cyclohexene-1-carboxaldehyde, 2,6,6-trimethyl-				5.00%			10
9.79	3-Cyclohexene-1-carboxaldehyde, 1,3,4-trimethyl-				3.10%			10
10.39	Glycerol					9.57%		3
11.43	Nonanoic acid						1.43%	11
11.45	3,5-Dimethylphenol					0.80%		8
11.91	4-Methylcatechol					3.99%	1.11%	7
12.83	4-Hydroxyphenethyl alcohol					5.57%	1.21%	8
12.89	2-Hydroxyphenethyl alcohol					5.20%		8
12.96	4-Isopropylphenol					6.03%		9
13.14	2-Hydroxyphenethyl alcohol					5.31%		8
13.39	3-Hydroxyphenethyl alcohol					5.39%	1.40%	8
13.49	3-Hydroxy-benzeneacetic acid					2.38%		8
13.72	3-methyl-4-Hydroxy-benzeneacetic acid					4.11%		9
13.8	2-Hydroxy-2-phenylacetic acid					2.44%		8
13.86	3-Hydroxy-benzeneacetic acid					2.44%	1.04%	8
13.94	2-Hydroxy-4-methylbenzoic acid					4.35%	0.92%	8
14.5	3-Hydroxy-benzeneacetic acid					5.55%		8
14.73	1-Hydroxypentene, 1,3-diphenyl						0.92%	19
14.8	5-Isopropyl-2-methylphenoxy						0.96%	10
15.02	3-Hydroxy-benzeneacetic acid					3.05%	1.53%	8
15.15	tert-Butylhydroquinone						1.80%	14
15.29	1,3-Benzenedicarboxylic acid						1.34%	12

Table 3 (*continued*)

RT (min)	Identified compound	Peak area (%) Fraction 1	Fraction 2	Fraction 3	Fraction 4	Fraction 5	Fraction 6	C#
16.15	3-Hydroxyphenylpropionic acid, ethyl ester						0.94%	11
16.4	3,5-di-tert-Butyl-4-hydroxyacetophenone						1.10%	16
16.52	3-Hydroxyphenylpropionic acid, ethyl ester						2.32%	11
17.31	Phenol, 2,4,6-tris(1,1-dimethylethyl)-						1.26%	18
Total		64.41%	75.29%	75.29%	63.41%	66.18%	19.28	

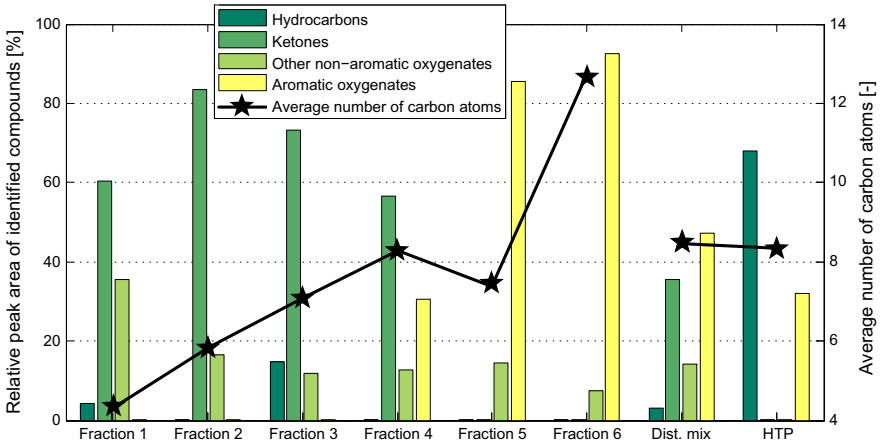

Fig. 5. Relative distribution of hydrocarbons, ketones, other non-aromatic oxygenates and aromatic oxygenates in the distillation fractions and the HTP.

The formation of short chained compounds primarily observed in Fraction 1, but to some extent also in Fraction 2, indicates the occurrence of C—C bond cleavage reactions. Glycerol conversion under near- and supercritical water conditions has been proposed to undergo C—C splitting through an ionic and a radical pathway forming acetaldehyde, formaldehyde, formic acid, ethanol and others [30,31]. Under alkaline hydrothermal conditions, high selectivity towards lactic acid formation has been observed when processing glycerol. 1,2-propandiol has been detected as a minor reaction compound [32]. 1,2-propandiol, which is detected in Fraction 3, is proposed to be derived from hydrogen-abstraction of glycerol to a glyceraldehyde intermediate, followed by dehydration and hydrogenation with in situ generated hydrogen [32–34]. The occurrence of hydrogenation reactions may then also explain the formation of propanol, ethanol, and pentanol probably from the reduction of carbonyl functionalities.

Ketones observed throughout Fraction 1–4 range from butanone observed in the light fractions to heavily substituted pentanones and hexanones observed at higher boiling points. The abundance of ketones suggests a more global pathway for ketonization of intermediates of similar chemical characteristics. Under supercritical, alkaline water conditions, carbohydrates are known to form carboxylic acids such as formic, acetic, propionic, and lactic acid through Retro-Aldol reactions. These may then undergo homogeneous and heterogeneous ketonic decarboxylation forming a variety of different ketones. Zhang et al. claim that the observation of these ketones in the distillate of a pyrolysis biooil is the result of *reactive* distillation, since no carboxylic acids were detected in the biooil [7]. However, ketonic decarboxylation of carboxylic acids proceeds at temperatures well above the boiling points of the precursor acids and in the presence of a base catalyst [35,36]. In the present study ketones were in fact observed in the biocrude but no carboxylic acids were detected, leading to the conclusion that ketones are more likely formed a priori distillation and hence not as a result of reactive distillation. The observation of a variety of different substituted ketones indicates that formed ketones further react with other compounds present. Ketonic decarboxylation of carboxylic acid like acetic and propionic acid with lactic acid can also explain the observation of ethyl and propyl acetate. Another potential pathway to ketone formation is base-catalyzed dimerization of acetone yielding diacetone alcohol. Acetone is the product of ketonic decarboxylation of acetic acid. Self-condensation of diacetone alcohol yields a cyclohexanone or methyl-cyclopentanone. More complex ketones, such as methyl- and ethyl-substituted pentanones and hexanones, cannot be explained simply as products of ketonic carboxylation reaction but involves further substitution and condensation reactions. Hu et al. investigated polymerization reactions of a model biooil and found that pentanone reacts with carboxylic acids, such as formic and acetic acid, upon heating [24]. As an example, ethylated hydroxy-pentenone was found as a condensation product, which points in the direction of a condensation reaction between cyclopentanone and acetic acid. Furthermore, Hu et al. also found that cyclopentanone in the model biooil was stable when the model biooil was blended in methanol and hence does not react with alcohols when heated. For more reduced compounds such

Table 4
List of major compounds identified in the distillate residue including their relative abundance.

RT (min)	Identified compound	Peak area (%)	C#
3.43	1-Butanol	3	4
3.62	Butanal, 3-methyl-	4.75	5
3.82	1-Hexene	1.8	6
4.42	(Z)-2-Heptene	0.94	7
4.83	1,3,5-Heptatriene, (E,E)-	1.01	7
5.03	Toluene	1.74	7
5.32	1-Octene	0.59	8
9.63	Pentanoic acid	0.48	5
9.63	3-Hexenoic acid (E)-	0.73	6
9.64	Phenol	0.67	6
11.15	2-Cyclopenten-1-one, 2,3-dimethyl-	0.51	7
11.74	Phenol, 2-methyl-	0.94	7
11.94	2-Cyclopenten-1-one, 3,4,4-trimethyl-	0.49	8
12.34	Phenol, 3-methyl-	1.27	7
14.84	Phenol, 2,3-dimethyl-	1.73	8
15.44	Phenol, 3,4-dimethyl-	1.17	8
16.35	Phenol, 3,5-dimethyl-	0.51	8
18.55	Phenol, 2-ethyl-4-methyl-	0.51	9
18.65	1,2-Benzenediol, 3-methyl-	0.84	7
18.95	Phenol, 2,3,6-trimethyl-	0.68	9
19.55	1,2-Benzenediol, 4-methyl-	1.1	7
21.65	1,4-Benzenediol, 2,6-dimethyl-	0.98	8
22.55	1,3-Benzenediol, 4,5-dimethyl-	1.8	8
23.35	1,3-Benzenediol, 2,5-dimethyl-	0.53	8
24.15	1,4-Benzenediol, 2,3,5-trimethyl-	1.06	9
24.45	Benzene, 1,4-dimethoxy-2-methyl-	0.68	9
25.45	1,3-Benzenediol, 4-propyl-	0.56	9
25.95	Phenol, 4-ethyl-2-methoxy-	0.69	9
26.45	Phenol, 5-methoxy-2,3-dimethyl-	0.84	9
28.55	1,4-benzenediol, 2-(1-methylpropyl)-	0.53	10
29.75	Naphtalene, 1,2,3,4-tetrahydro-1,5,7-trimethyl-	0.7	13
30.55	Benzene, 1,2,3,4-tetramethyl-4-(1-methylethenyl)-	1.35	13
31.85	Benzene, 1,3-diethyl-2,4,5,6-tetramethyl-	0.54	14
33.66	Benzene, 1,2,3-trimethoxy-5-(1-propenyl)-, (E)-	0.67	12
35.56	1-Naphthol, 2,5,8-trimethyl-	0.53	13
38.44	n-Hexadecanoic acid	1.93	16
38.56	5-Isopropyl-3,8-dimethyl-1,2-dihydronaphtalene	0.88	15
40.46	Phenanthrene, 2,5-dimethyl-	1.55	16
42.54	Octadecanoic acid	1.78	18
43.04	Eicosanoic acid	0.68	20
44.26	Retene	2.21	18
45.47	Benzene, 1,3-dimethoxy-5-[(1E)-2-phenylethenyl]-	0.74	16
50.67	Anthraquinone, 1,2,4-trimethyl-	0.99	17
Total		47.68%	

as dimethyl-hexanone and ethyl-hexanone, condensation reactions must have been necessitated by hydrogen-transfer reactions.

In the higher boiling fractions a dominance of aromatics is observed. The formation of oxygenated aromatics from lignocellulose processing is well-known. The three monolignols of lignin are the precursors of many aromatic compounds [37], alongside dehydration reactions of carbohydrates [38]. In contrast to the monofunctional ketones, the oxygenated aromatics generally show multiple functionalities resulting in far more complex compounds derived from the complex and heterogeneous structure of lignin. Formation of monomers proceeds mainly through thermal degradation and hydrolysis of ether bonds. The proposed reactions are summarized in Fig. 6.

3.6. Hydrotreating

Hydrotreating is tested as a way to decrease the chemical complexity of the biocrude. The distillate fractions are previously found to contain hydrocarbon derived compounds with various oxygen functional groups and various aromatic substitutions. For the biocrude or fractions to be used as drop-in biofuels or bio-chemicals, deoxygenation and purification is required. Due to a high degree of similarity in the hydrocarbon backbones of the compounds, observed from GC–MS analysis, deoxygenation may also result in a product mixture consisting of highly similar compounds.

Table 5 lists and compares the elemental analysis, TAN and HHV of the distillate mix before and after hydrotreating. The HHV is increased by 22% during hydrotreating, which is favorable in a biofuel context. The improved HHV is mainly the result of a 68% reduction in oxygen content from 14.5% to 4.6%. Likewise, the H/C ratio has increased slightly from 1.59 to 1.66 indicating some saturation of double bonds. The TAN value is decreased from 36 to 7 mg KOH/g. Although these parameters reveal a significant quality improvement from a fuel perspective, the oxygen content and acid number indicate incomplete deoxygenation under the given processing conditions. This is also emphasized by the FTIR spectra in Fig. 7, where slight hydroxy and carbonyl absorptions still appear. Without being conclusive on a quantitative basis, the HTP spectra suggests that carbonyl absorption has been reduced to a greater extent than the hydroxy absorption. This is not surprising considering the relatively higher deoxygenation reactivity expected for ketones compared to e.g. phenols [13,14]. Furthermore, the conditions applied, (residence time and catalyst:feedstock mass ratio) corresponding to an equivalent WHSV of 3.3, are considered as rather mild conditions, where more severe conditions would likely be beneficial for complete deoxygenation [12,23].

3.7. Compound identification of HTP

Fig. 5 shows the relative distribution of compound classes within the distillate mix and the HTP. It appears that after hydrotreatment the rather complex distillate mix has been converted into HTP containing solely hydrocarbons and aromatic oxygenates. Table 6 lists the most abundant (by GC–MS peak area interpretation) compounds found in the HTP. Approximately two thirds of the identified compounds are hydrocarbons of which the majority are five- and six-membered napthenic rings with different substitutions. It is expected that these hydrocarbons are mainly the counterparts to the broad range of ketones identified in the Fraction 2, 3, and 4, but also to a minor extent derivatives of the oxygenated aromatics. Compounds like propyl-phenol, 2-methyl-phenol, and 4-hydroxyphenethyl alcohol observed in Fraction 5 and 6, could potentially be the oxygenated phenolic counterparts of propyl-cyclohexane, 2-ethyl-5-methyl-hexane, ethyl-cyclohexane, respectively, observed in the HTP. Generally, the hydrocarbons in this table are chemically very similar, indicating that the chemical complexity of the distillate mix has been significantly reduced. From a biofuel perspective, such deoxygenated compounds will serve as a high quality bio drop-in e.g. in a gasoline pool due to high octane numbers or in jet-fuel due to good cold flow properties.

Table 6 also indicates that the high share of oxygenated aromatics in the distillate mix is still present in the HTP. These are expected to originate from the compounds found in Fraction 5 and 6. Whereas the oxygenated aromatics in Fraction 5 and 6 demonstrated many different oxygenated functional groups, such as phenolics, carboxylic acids, esters e.g., the only oxygenated functional group identified in the HTP is phenolics. Therefore, it is expected that the oxygenated aromatics in Fraction 5 and 6 will undergo incomplete deoxygenation and end up as phenolics with different degrees of hydrocarbon substitution under the given processing conditions. I.e. the oxygenated functional groups such as e.g. acetic acids, and ethyl alcohols will be deoxygenated to an ethyl substitution on a stable phenol. Phenols are known to be rel-

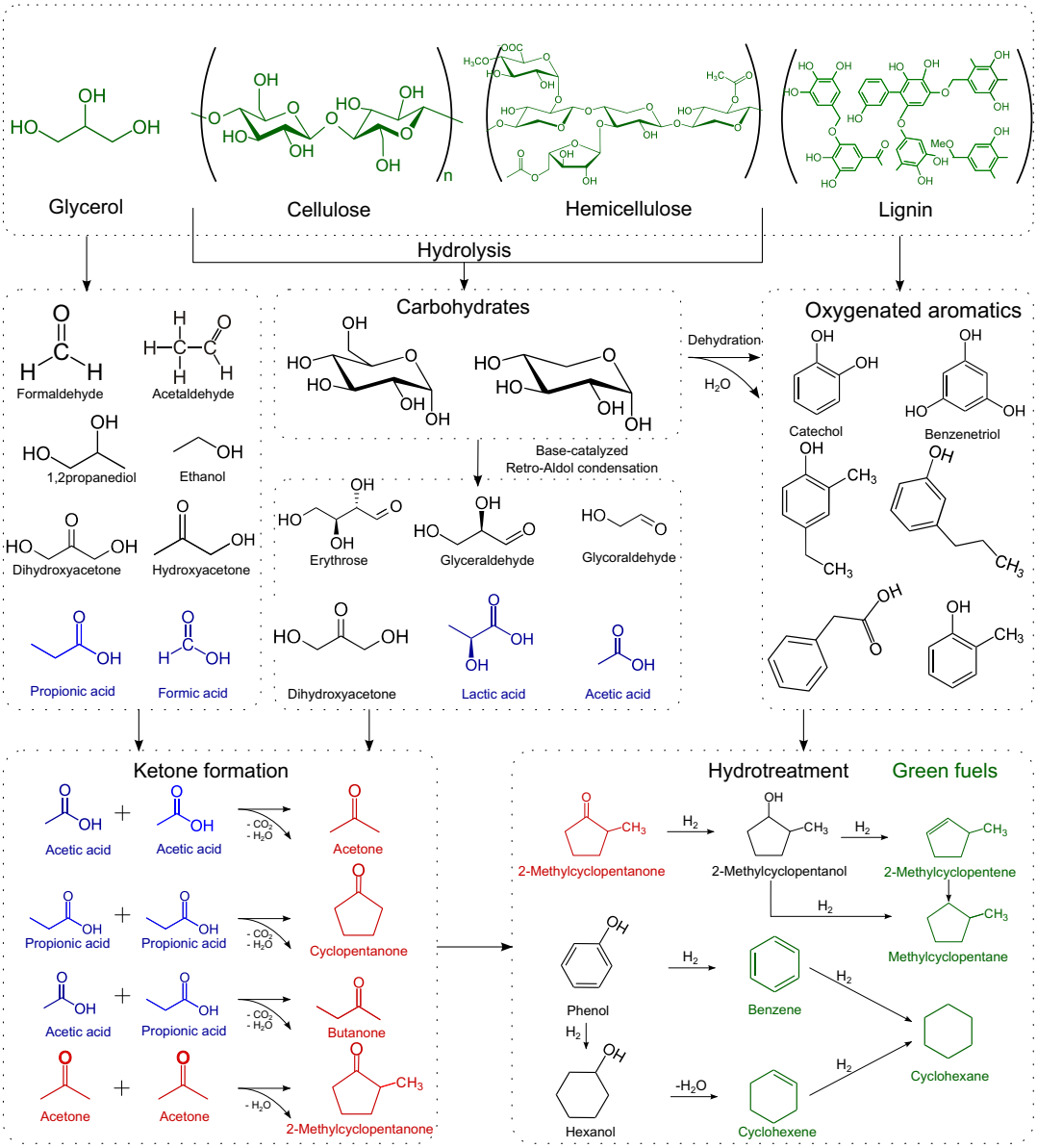

Fig. 6. Proposed reaction pathways for the formation of chemicals and fuels.

Table 5
Properties of the distillate mix and HTP.

	HHV	Elemental analysis [wt.%]					TAN
Sample	[MJ/kg]	C	H	O[a]	H/C [–]	O/C [–]	[mg KOH/g]
Dist. mix	35.2	75.4	10.1	14.5	1.59	0.14	35.58
HTP	42.9	83.7	11.7	4.6	1.66	0.04	7.00

[a] Oxygen by difference.

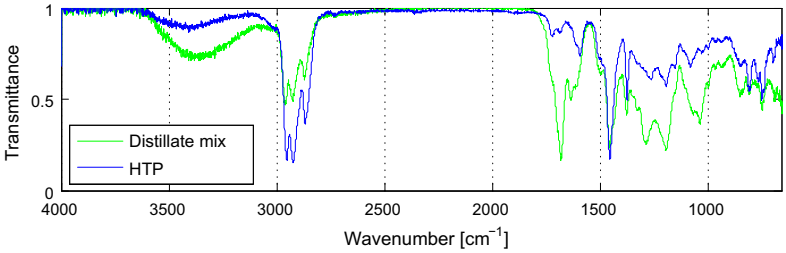

Fig. 7. FTIR spectra of the distillate mix before and after hydrotreating.

Table 6
List of major chemical compounds identified in the hydrotreated sample including their relative abundance.

RT (min)	Identified compound	Chemical Formula	Peak area (%)	C#
2.17	Cyclohexane	C_6H_{12}	1.70	6
2.31	Cyclopentane, 1,3-dimethyl-	C_7H_{14}	4.30	7
2.4	Hexane, 3-methyl-	C_7H_{16}	1.37	7
2.62	Cyclohexane, methyl-	C_7H_{14}	2.94	7
2.72	Cyclopentane, ethyl-	C_7H_{15}	1.56	7
2.76	Cyclopentane, 1,2,4-trimethyl-	C_8H_{16}	1.29	8
3.1	Cyclopentane, 1,2,4-trimethyl-	C_8H_{17}	1.93	8
3.26	Cyclopentane, 1-ethyl-3-methyl-	C_8H_{16}	4.84	8
3.81	Cyclohexane, ethyl-	C_8H_{16}	3.10	8
3.9	1,3-Diethylcyclopentane	C_9H_{18}	3.36	9
4.49	Cyclopentane, 1-methyl-2-propyl-	C_9H_{18}	2.21	9
4.81	Cyclohexane, 1-ethyl-2-methyl-	C_9H_{18}	1.95	9
5.15	Cyclohexane, propyl-	C_9H_{18}	2.98	9
5.27	Cyclopentane, 1,2-dipropyl-	$C_{11}H_{22}$	1.42	11
5.83	1,2-Dihydrocatechol	$C_6H_8O_2$	1.91	6
9.37	Phenol, 3,4-dimethyl-	$C_8H_{10}O$	1.61	8
10.02	Phenol, 2,3-dimethyl-	$C_8H_{10}O$	0.95	8
10.92	2-Methyl-1-phenyl-1-butanol	$C_{11}H_{16}O$	0.95	11
12.48	Phenol, 4-ethyl-3-methyl-	$C_9H_{12}O$	0.85	9
13.1	Phenol, 3-ethyl-5-methyl-	$C_9H_{12}O$	0.95	9
13.3	Phenol, 2,4,6-trimethyl-	$C_9H_{12}O$	1.23	9
13.42	Phenol, 2,3,6-trimethyl-	$C_9H_{12}O$	1.17	9
13.61	2,5-Diethylphenol	$C_{10}H_{14}O$	0.71	10
14.16	Phenol, 2,4,6-trimethyl-	$C_9H_{12}O$	0.55	9
15.14	Phenol, 2,3,5,6-tetramethyl-	$C_{10}H_{14}O$	0.89	10
15.38	Phenol, 2,3,5,6-tetramethyl-	$C_{10}H_{14}O$	0.69	10
15.49	Phenol, 2,3,5,6-tetramethyl-	$C_{10}H_{14}O$	3.16	10
16.74	Phenol, 2,3,5,6-tetramethyl-	$C_{10}H_{14}O$	0.78	10
30.63	Retene	$C_{18}H_{18}$	0.06	18
Total area			51.43	

atively resistant to deoxygenation due to aromatic stabilization [14].

Hydrotreating has deoxygenated and chemically simplified the distillate mix to mostly substituted cyclopentanes and cyclohexanes as well as substituted phenols. The present experiment demonstrated the easiness of hydrotreating ketones. This was also demonstrated by Kong et al., who investigated deoxygenation of various aliphatic ketones over nickel-based catalysts [16]. Even at low temperatures (160 °C) they found that all the ketones investigated were easily reduced to corresponding alkanes. For cyclohexanone they proposed that the catalytic hydrogenation proceeds effectively to cyclohexanol, which then may undergo dehydration to cyclohexene that is then quickly reduced to cyclohexane. Considering the HTP product distribution in Table 6, this reaction mechanism seems very likely for deoxygenation of the cyclic ketones together with similar mechanisms for the substituted equivalents.

The effects of hydrogenation on the various methyl-substitutions of phenolics were investigated by Massoth et al. [39]. Generally they found high resistance towards hydrogenation resulting in conversion efficiencies less than 50% for both phenol and all mono-, di-, and trimethyl-substituted phenols investigated. Moreover, they suggested that the dependency on the conversion rates of the various substituted phenols was an adsorption phenomenon due electrostatic potentials rather than a matter of steric effects. They proposed two reaction pathways; one involving ring saturation followed by dehydration to cyclohexenes, and one leading to the formation of aromatics. They found that when the number of methyl-substitutions were increased, the pathway for aromatics formation became more favorable. This may explain why hardly any phenolics are saturated in the present results. Although oxygenated aromatics are still present in the HTP, it is expected that the degree of deoxygenation and saturation can easily be tuned with catalyst development and in particular optimization of the hydrotreating conditions such as residence time [12]. In order to chemically simplify the products even more, separate hydrotreating of Fraction 1–4, 5–6 and the residue may also prove as a successful method to produce deoxygenated napthenes and substituted phenols, respectively.

4. Conclusion

Fractional distillation of a biocrude obtained from hydrothermal liquefaction was performed, resulting in six distillate fractions and

a distillate residue. It was found that fractional distillation is a viable means for separating the complex biocrude mixture into fractions containing compounds of similar chemical structures. Light oxygenates holding the potential of fine chemical production were identified in the lighter distillate fractions. A significant share of different ketones were obtained, which proved to be prospective precursors for liquid transport fuels. In the heavier distillate fractions, phenolics were found the most abundant group of compounds. Reaction pathways for the formation of compounds observed in the distillate fractions were proposed. The pool of monomeric and low molecular weight oxygenated aromatics of various functionalities holds particular potential as precursors for a variety of commodity bio-products. The distillation residue comprised a mass fraction of 51.8% of the biocrude. Pyrolysis-GCxGC-MS analysis revealed that this residue is mainly of aromatic character. Hydrotreatment of the distillate mixture displayed the amenability of removing certain oxygen functionalities. Ketones were completely converted into saturated hydrocarbons, whereas the various oxygenated aromatics were mainly converted into high-valuable substituted phenolics. In conclusion, hydrothermal liquefaction of biomass coupled with fractional distillation and hydrotreatment could potentially represent a bio-refinery concept for renewable fuel and chemical production.

Acknowledgements

This work is part of the Flexifuel Project, a Sino-Danish collaboration, and C3BO (Center for BioOil) at the Department of Energy Technology, Aalborg University. The research was financially supported by The Danish Agency for Science, Technology and Innovation (Grant No. 10-094552), The Danish Council for Strategic Research (Grant No. 1305-00030B), the Innovation Fund Denmark (Grant No. 4135-00126B), and the Swedish Energy Agency.

References

[1] Biller P, Ross A. Potential yields and properties of oil from the hydrothermal liquefaction of microalgae with different biochemical content. Bioresour Technol 2011;102:215–25.
[2] Leow S, Witter JR, Vardon DR, Sharma BK, Guest JS, Strathmann TJ. Prediction of microalgae hydrothermal liquefaction products from feedstock biochemical composition. Green Chem 2015;17:3584–99.
[3] Pedersen TH, Rosendahl LA. Production of fuel range oxygenates by supercritical hydrothermal liquefaction of lignocellulosic model systems. Biomass Bioenergy 2015;83:206–15.
[4] Elliott DC, Biller P, Ross AB, Schmidt AJ, Jones SB. Hydrothermal liquefaction of biomass: developments from batch to continuous process. Bioresour Technol 2015;178:147–56.
[5] Jensen CU, Rodriguez Guerrero JK, Karatzos S, Olofsson G, Iversen SB. Fundamentals of hydrofaction™: renewable crude oil from woody biomass. Biomass Convers Biorefin 2017:1–15. http://dx.doi.org/10.1007/s13399-017-0248-8.
[6] Sintamarean IM, Grigoras IF, Jensen CU, Toor SS, Pedersen TH, Rosendahl LA. Two-stage alkaline hydrothermal liquefaction of wood to biocrude in a continuous bench-scale system. Biomass Convers Biorefin 2017:1–11.
[7] Zhang XS, Yang GX, Jiang H, Liu WJ, Ding HS. Mass production of chemicals from biomass-derived oil by directly atmospheric distillation coupled with co-pyrolysis. Scient Rep 2013;3:1–7.
[8] Cheng D, Wang L, Shahbazi A, Xiu S, Zhang B. Characterization of the physical and chemical properties of the distillate fractions of crude bio-oil produced by the glycerol-assisted liquefaction of swine manure. Fuel 2014;130:251–6.
[9] Capunitan JA, Capareda SC. Characterization and separation of corn stover bio-oil by fractional distillation. Fuel 2013;112:60–73.
[10] Hoffmann J, Jensen CU, Rosendahl LA. Co-processing potential of HTL bio-crude at petroleum refineries - part 1: fractional distillation and characterization. Fuel 2016;165:526–35.
[11] Eboibi BEO, Lewis DM, Ashman PJ, Chinnasamy S. Hydrothermal liquefaction of microalgae for biocrude production: improving the biocrude properties with vacuum distillation. Bioresour Technol 2014;174:212–21.
[12] Jensen CU, Hoffmann J, Rosendahl LA. Co-processing potential of HTL bio-crude at petroleum refineries - part 2: a parametric hydrotreating study. Fuel 2016;165:536–43.
[13] Hoffmann J, Pedersen T, Rosendahl L. Near-critical and supercritical water and their applications for biorefineries; chap. hydrothermal conversion in near-critical water - a sustainable way of producing renewable fuels. Netherlands: Springer; 2008. p. 373–400. ISBN 978-94-017-8922-6.
[14] Furimsky E. Catalytic hydrodeoxygenation. Appl Catal A: Gen 2000;199:147–90.
[15] Mortensen P, Grunwaldt JD, Jensen P, Knudsen K, Jensen A. A review of catalytic upgrading of bio-oil to engine fuels. Appl Catal A: Gen 2011;407:1–19.
[16] Kong X, Lai W, Tian J, Li Y, Yan X, Chen L. Efficient hydrodeoxygenation of aliphatic ketones over an alkali-treated ni/hzsm-5 catalyst. ChemCatChem 2013;5:2009–14.
[17] Furimsky E. Hydroprocessing challenges in biofuels production. Catal Today 2013;217:13–56.
[18] Tews I, Zhu Y, Drennan C, Elliott D, Snowden-Swan L, Onarheim K, et al. Biomass direct liquefaction options: technoeconomic and life cycle assessment. Tech. Rep.; Prepared for U.S. Department of Energy; 2014.
[19] Pedersen T, Grigoras I, Hoffmann J, Toor S, Daraban I, Jensen C, et al. Continuous hydrothermal co-liquefaction of aspen wood and glycerol with water phase recirculation. Appl Energy 2016;162:1034–41.
[20] ASTM D2892. Standard test method for distillation of crude petroleum (15-theoretical plate column). Tech. Rep.; ASTM International; 2005.
[21] Lavanya M, Meenakshisundaram A, Renganathan S, Chinnasamy S, Lewis DM, Nallasivam J, et al. Hydrothermal liquefaction of freshwater and marine algal biomass: a novel approach to produce distillate fuel fractions through blending and of biocrude with petrocrude. Bioresour Technol 2016;203:228–35.
[22] Maxwell JB, Bonnell LS. Indust Eng Chem 1957;49:1187–96.
[23] Jensen CU, Rosendahl LA, Olofsson G. Impact of nitrogenous alkaline agent on continuous HTL of lignocellulosic biomass and biocrude upgrading. Fuel Process Technol 2017;159:376–85.
[24] Hu X, Wang Y, Mourant D, Gunawan R, Lievens C, Chaiwat W, et al. Polymerization on heating up of bio-oil: a model compound study. AIChE J 2013;59:888–900.
[25] Zhang Q, Chang J, Wang T, Xu Y. Review of biomass pyrolysis oil properties and upgrading research. Energy Convers Manage 2007;48:87–92.
[26] Diebold JP. A review of the chemical and physical mechanisms of the storage stability of fast pyrolysis bio-oils. Tech. Rep.; National Renewable Energy Laboratory; Golden, Colorado; 2000.
[27] Nakanishi K. Infrared absorption spectroscopy, practical. San Francisco: Holden-Day; 1962.
[28] Werpy T, Petersen G. Top value added chemicals from biomass. volume i: Results of screening for potential candidates from sugars and synthesis gas (pnnl-14804). Tech. Rep.; Pacific Northwest National Laboratory and the National Renewable Energy Laboratory; 2004.
[29] Bozell J.J, Holladay J.E, Johnson D, White J.F. Top value added chemicals from biomass. volume ii: Results of screening for potential candidates from biorefinery lignin (pnnl-16983). Tech. Rep.; Pacific Northwest National Laboratory and the National Renewable Energy Laboratory; 2007.
[30] Bühler W, Dinjus E, Ederer H, Kruse A, Mas C. Ionic reactions and pyrolysis of glycerol as competing reaction pathways in near- and supercritical water. J Supercrit Fluids 2002;22:37–53.
[31] Müller JB, Vogel F. Tar and coke formation during hydrothermal processing of glycerol and glucose. influence of temperature, residence time and feed concentration. J Supercrit Fluids 2012;70:126–36.
[32] Chen L, Ren S, Ye XP. Lactic acid production from glycerol using CaO as solid base catalyst. Fuel Process Technol 2014;120:40–7.
[33] Martin A, Armbruster U, Gandarias I, Arias PL. Glycerol hydrogenolysis into propanediols using in situ generated hydrogen a critical review. Euro J Lipid Sci Technol 2013;115:9–27.
[34] Pedersen TH, Jasinas L, Casamassima L, Singh S, Jensen T, Rosendahl LA. Synergetic hydrothermal co-liquefaction of crude glycerol and aspen wood. Energy Convers Manage 2015;106:886–91.
[35] Renz M. Ketonization of carboxylic acids by decarboxylation: Mechanism and scope. Euro J Organ Chem 2005;2005:979–88.
[36] Deng L, Fu Y, Guo QX. Upgraded acidic components of bio-oil through catalytic ketonic condensation. Energy Fuels 2009;23:564–8.
[37] Patwardhan PR, Brown RC, Shanks BH. Understanding the fast pyrolysis of lignin. ChemSusChem 2011;4:1629–36.
[38] Tompsett GA, Li N, Huber GW. Catalytic conversion of sugars to fuels. John Wiley & Sons, Ltd; 2011. p. 273–9. ISBN 9781119990840.
[39] Massoth FE, Politzer P, Concha MC, Murray JS, Jakowski J, Simons J. Catalytic hydrodeoxygenation of methyl-substituted phenols: correlations of kinetic parameters with molecular properties. J Phys Chem B 2006;110:14283–91.

Paper D

Impact of nitrogenous alkaline agent on continuous HTL of lignocellulosic biomass and biocrude upgrading

Claus Uhrenholt Jensen, Lasse A. Rosendahl, Göran Olofsson

The manuscript has been published in the
Journal of Fuel Processing Technology, vol. 159, pp. 376–385, 2017.

The layout has been revised.

Fuel Processing Technology 159 (2017) 376–385

Contents lists available at ScienceDirect

Fuel Processing Technology

journal homepage: www.elsevier.com/locate/fuproc

Impact of nitrogenous alkaline agent on continuous HTL of lignocellulosic biomass and biocrude upgrading

Claus Uhrenholt Jensen[a], Lasse A. Rosendahl[b,*], Göran Olofsson[a]

[a] Steeper Energy ApS, Sandbjergvej 11, Hørsholm DK-2970, Denmark
[b] Aalborg University, Department of Energy Technology, Pontoppidanstræde 111, Aalborg Ø DK-9220, Denmark

ARTICLE INFO

Article history:
Received 17 October 2016
Received in revised form 7 December 2016
Accepted 30 December 2016
Available online xxxx

Keywords:
Biofuel
Hydrotreating
GCxGC–MS
Distillation
Hydrofaction

ABSTRACT

Continuous hydrothermal liquefaction (CHTL) of lignocellulosic biomass with subsequent hydrotreating is carried out to study the effect of NH_3 versus NaOH as alkaline HTL catalyst. Product analysis include Py-GCxGC–MS, simulated distillation and fractional distillation. Ammonia enhances biocrude quality slightly in terms of H/C ratio, density and HHV, but a significant coke formation of 11 wt.% is observed. Furthermore, ammonia pollutes the biocrude with 2.7 wt.% nitrogen, which is observed to inhibit hydrotreating conversion. In comparison, CHTL with NaOH is associated with a 43 wt.% yield of a hydrotreatable biocrude, stable TOC levels during aqueous phase recirculation and mass, carbon and energy balance closure. Hydrotreating eliminates the TAN, reduces oxygen to 2–3 wt.% and produces a promising fuel bio-blendstock with ultra-low sulphur and a diesel fraction equal to 43%.

1. Introduction

Hydrothermal liquefaction (HTL) and pyrolysis are thermochemical processes capable of converting biomass into liquid energy carriers. In particular, HTL enables a feedstock-flexible conversion of non-food biomass to a liquid biocrude intermediate [1–5] that can be hydrotreated to produce drop-in biofuel [6–8]. The greenhouse gas emission savings on a HTL biofuel from wood is estimated to be 70% [9] to 84% [10] relative to the 2005 petroleum baseline. However, with the recent collapse of benchmark oil prices, there is little economic incentive to keep pursuing pathways to biofuel blendstocks or alternatives to fossil resources. The skepticism seems justified, as HTL biocrude production costs around $70 per barrel were reported in a thorough techno-economic assessment prepared for the U.S. Department of Energy by Tews et al. [9]. But is the price of biofuel equal to that of commodity fuels? And is it fair to determine a price just based on energy content, when the source of this energy has significant impact on the cost to society of using it?

During the last decade the price of liquid biofuels have been dictated by the price of their fossil equivalent and thus crude oil [11]. A margin between fossil and bio has facilitated a business case for e.g. production of hydrogenation derived renewable diesel by major players such as Neste, Preem, UPM biofuels and Dynamic Fuels [12]. However, hydrogenation of fatty acids and vegetable oils comprise a simpler process relative to thermochemical conversion of solid biomass into biofuels, and the additional complexity of the latter may need incorporation into the price margin before such technologies will be commercial. Contained in the production cost of biofuels is also the cost of curbing CO_2 emissions. In the case of fossil fuels, it is not, yet it is likely that the additional cost associated with removing resulting CO_2 from the atmosphere or dealing with climate changes (or both) will be significantly higher than the additional price tag on biofuels. Recognizing this and acknowledging the recent calls for action [13,14], it is very likely that near future society through legislative framework will create a market for biocrudes that is independent of benchmark crude oil prices. As a result, the price of biofuel will be less affected by the price of benchmark petroleum, but instead regulated by the biocrude availability and the cost competitiveness of the individual biocrude production technologies such as HTL. Significant players on the international political agenda are indirectly supporting the improved incitements for biofuel production by raising awareness to the heavy subsidisation of fossil fuels. In 2009, the G20 nations and APEC called for an end to fossil fuel subsidies. But since then the consumption subsidies to fossil fuels has increased from $390 billion in 2009 (in 2014 dollars) to $493 billion in 2014 [13]. Continuing these subsidies adds to the undermining of the competitiveness of renewables, and discourages necessary investments into energy efficiency and

* Corresponding author.
E-mail address: lar@et.aau.dk (L. Rosendahl).

http://dx.doi.org/10.1016/j.fuproc.2016.12.022
0378-3820/

renewable technology [13–15]. IEA calls for a progressively stronger commitment in the conclusive remarks of their 2015 World Energy Outlook [13]. In support of this and recognizing that even though the competitiveness will not be relative to the cost of fossil energy, there will still be strong motivations to drive down production costs for biofuel technologies in competition with each other, the present study contributes to the development of cost-competitive HTL of biomass for bio-crude production.

1.1. Aspects on ammonia as alkaline HTL catalyst

Based on the above reasoning, the effect of using ammonia instead of sodium hydroxide as HTL catalyst in continuous conversion of wood is studied. The catalyst comprises around 15% of the fixed HTL operating costs in the economic assessment by Tews et al. [9], which motivates the study of NH_3 as a potentially cheaper and/or more effective catalyst compared to NaOH. Secondly, ammonia may potentially act as both hydrogen donor to improve the H/C ratio of the biocrude, and as radical scavenger to reduce polymerization reactions or coke formation. Finally, the dielectric constant of water decreases significantly when entering the supercritical state, which introduces the risk of precipitation of inorganic salts such as NaOH [16,17]. This can be avoided by using ammonia as the alkaline catalyst, since it is completely soluble in supercritical water [18]. A potential downside associated with the use of ammonia during HTL of lignocellulosics is the risk of polluting the biocrude by introducing a nitrogenous reagent into a feed very low on nitrogen. The intended product is a pure hydrocarbon biofuel, and nitrogen removal through hydrotreating requires severer conditions and more stoichiometric hydrogen relative to sulphur and oxygen removal [19,20]. The risk of polluting the biocrude with nitrogen may however be of less importance considering the nitrogen that is indigenous to HTL biocrudes from protein rich feedstocks such as algae, manure and municipal waste [2,3,5]. Thus, the findings of this study may also contribute to the knowledge on HTL of such feedstocks.

In a recent study by Albrecht et al. [8] on CHTL and hydrotreating of algae, more than 50 vol.% of ammonia was detected in the gaseous hydrotreating products. From circularity and efficiency considerations, this introduces the potential of applying the ammonia produced during hydrotreatment of nitrogenous biocrudes as alkaline HTL catalyst during production of these. On the other hand Albrecht et al.[8] state that ammonia was observed to pollute the Brønsted acid sites of the presulphided $CoMo/Al_2O_3$ hydrotreating catalyst and thereby inhibit cracking activity. Thus, numerous aspects including the effect on HTL process stability, biocrude quality and downstream hydrotreatability are to be considered when evaluating the effect of using ammonia versus sodium hydroxide as HTL catalyst in the production of biofuels. In support of this, the current study investigates the effects discovered during the entire path from tree to tank.

1.2. Effect of hydrotreatment on biocrude volatility

Hydrotreating of biocrudes result in severe heteroatom removal and this is expected to affect the volatility of the biocrude significantly, which describes an additional hypothesis challenged in this study. Generally, oxygenates are characterized by a higher boiling point than the corresponding hydrocarbon due to the changes oxygen does to intermolecular forces such as hydrogen bonding and van der Waals attractions. To give an example, phenol has a boiling point of 182 °C, whereas the boiling point of benzene is 80 °C [21].

The distillation profile of a particular crude mineral oil is a crucial parameter in order to evaluate its suitability in a given petrochemical process such as e.g. a petroleum refinery that simply put is designed around the distillation profile of a particular group of crude oils [22]. Since biocrude is mostly proposed as a potential route towards petroleum crude oil substitution, it is beneficial to adopt crude oil characterization and evaluation tools. Meanwhile, it is important that the different composition of a biocrude compared to a mineral crude is acknowledged. Within commodity petroleum fuel production, distillation residue is associated with a higher degree of processing and thus costs to produce final products compared to the straight run distillates [19]. Thus, it is extremely important to acknowledge the effect heteroatoms have on a biocrude distillation profile when evaluating the corresponding technology for biofuel production.

Table 1
List of equipment used for product analysis.

Analysis	Equipment
Simulated distillation	ASTM D7169 (Cert. Lab.)
Elemental analysis	ASTM D5291 (Cert. Lab.)
Heating value	IKA C2000 Basic
FT-IR	Thermo Sc. Nicolet 380
Density	Anton Paar DMA500
CCR	Perkin Elmer STA 6000
Py-GCxGC–MS	Shimadzu QP-2010
GCxGC columns	DB-5 & DB-17
Gas analysis	Shimadzu GC2010
TAN	Manual titration
TBP distillation	BR Instruments, ASTM D2892

2. Experimental section

The experimental work includes CHTL at a continuous bench scale unit and subsequent hydrotreating in microbatch reactors. Microbatch HTL was also carried out to further evaluate certain observations, but the microbatch HTL is of minor importance and it is carefully outlined whenever microbatch HTL results are discussed. The methodologies applied are described for each reactor system below. Table 1 comprises the list of equipment used for the various analysis carried out. A 15:5 fractional distillation of the CHTL biocrudes were carried out according to ASTM D2892. 15:5 refers to a 15 theoretical plate, 5:1 reflux distillation. Hoffmann et al. [23] provides more information on the set-up and fractional distillation of HTL biocrudes in general.

2.1. Continuous hydrothermal liquefaction

CHTL at a state of the art research facility have been carried out during two campaigns with a total of more than 100 hours of operation. The two campaigns deviate with respect to HTL catalyst, which were aqueous ammonia (ammonia hydroxide) and sodium hydroxide applied in 1 wt.% and 2.5 wt.% slurry concentrations respectively. Potassium carbonate was added and adjusted to stable concentrations around 15 g /l in both campaigns.

Two biocrudes were produced during the continuous campaigns by processing aspen wood with supercritical water in a 17.5% dry matter content slurry at approximately 400 °C, 310 bar and 20–23 kg/h. Briefly described, the semi-continuous HTL bench scale unit CBS1 consists of a high pressure piston pump, two serially connected induction heaters, two 5 L serial reactors, a cooler, a capillary depressurisation system and a 3-phase funnel separator. Further details on the system can be found in Refs. [4,24-26]. Biocrude and aqueous phase products were recycled during production. Recycling of the biocrude phase enhance homogeneity and thus pumpability of the slurry, it improves oil quality and yield, and it reduces the overall heat capacity of the slurry [4]. Likewise, recycling of the aqueous phase improves process stability, biocrude quality and yield, and it reflects an up-scaled process design, in which water phase recycling is a necessity in order to reduce water treatment expenses [4]. Crude

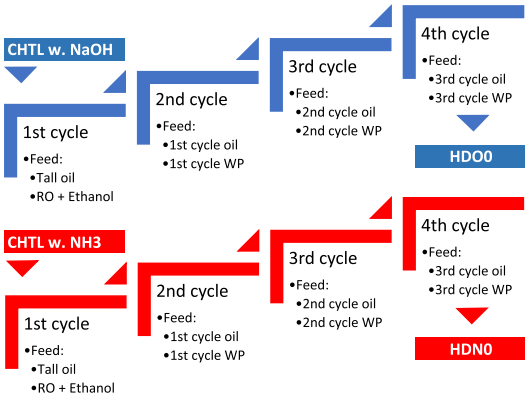

Fig. 1. Schematic of the product recirculation carried out during semi-continuous HTL to resemble a steady state biocrude. The 4th cycle feedstock slurry was also applied in microbatch reactors.

tall oil was used as start-up oil in a wood:oil ratio of 1:1. Distilled water with 4.5 wt.% ethanol was used as start-up aqueous phase to simulate the water soluble organics. As visualised in Fig. 1, products were recycled for 4 consecutive cycles each processing 80–100 kg of feed in order to resemble a steady state biocrude. The two different biocrudes produced during continuous HTL using NH_3 and NaOH are referred to as HDN0 and HDO0, respectively and it is these biocrudes that have been both fractionated and hydrotreated.

2.2. Microbatch hydrothermal liquefaction

The HTL feedstocks prepared for the 4th cycles pictured in Fig. 1 have also been processed in 10 mL microbatch reactors. The reason is mainly that microbatch reactors facilitate a better recovery of solids compared to continuous systems. Secondly, the scalability between microbatch and continuous systems is a key aspect that has gained surprisingly little attention in literature. Products from the microbatch reactors are recovered using 2-butanone and slightly acidified water. Biocrude is defined as 2-butanone soluble, water insoluble and recovered by rotary evaporation. Solids are defined as being water and 2-butanone insoluble, collected on 5–13 μ m filter paper and oven dried at 105 °C. The biocrudes produced from microbatch HTL are referred to as $HDO0_{batch}$ and $HDN0_{batch}$, but they will not be used for anything else than yield figures.

Yields of *i*, representing biocrude, solids or gas, are calculated by Eq. (1), where Δm_i represents the increase of mass during reaction after subtracting recycled products. Everything is given on dry ash free (DAF) basis. Carbon balances and energy recoveries are calculated similarly to Eq. (1).

$$Yield_i = \frac{\Delta m_{i,DAF}}{m_{biomass,DAF}} \quad [\text{wt.\%}] \qquad (1)$$

2.3. Hydrotreatment

Hydrotreatment experiments of both CHTL biocrudes have been carried out to investigate any effect the difference in HTL catalyst may have on hydrotreatability of the produced biocrude. Hydrotreating experiments are carried out using 25 mL microbatch reactors featuring pressure logging, a Techne SBL-2D fluidised sandbath and a purposely designed shaking device to enable mixing of the reactants. All experiments were carried out in repeats to ensure accurate data. Further details on the upgrading methodology is given in Ref. [7]. Table 2 summarises the experimental procedure.

2.3.1. Hydrotreating catalyst and conditions

A preactivated and stabilised conventional $NiMo/Al_2O_3$ hydrotreating catalyst in the form of 1.3 mm spherical pellets has been used. Pre-sulphided $NiMo/Al_2O_3$ catalysts are associated with good deoxygenation and denitrogenation activities based on a review by Furimsky [6].

The operating temperature is chosen to be 360 °C based on findings in Ref. [7] that suggest a minimum of 350 °C for good deoxygenation conversion of HTL biocrude. Additionally, this choice is below the hydroprocessing regime, where thermal cracking will affect the boiling point distribution to some extent [19]. 360 °C is considered appropriate considering both the need for minimising thermal cracking, while maintaining a good degree of deoxygenation of a crude that is expected to be rather phenolic. Previous experiments have indicated that deoxygenation of phenols on the given catalyst are associated with relatively slow kinetics [27], which is why hydrotreatment at a lower operating temperature than 360 °C is opted out. Identifying an optimal compromise between temperature and reaction time is left for a future study.

Eq. (2) describes how yield of deoxygenated bio-oil is estimated from *Liquid Recovery* and deoxygenation, ΔO. Besides oil,

Table 2
Experimental hydrotreating procedure.

Prior to experiment					
Catalyst	Catalyst loading (g/g oil)	Reactor volume (mL)	Leak test (bar N_2)	H_2 flush (bar H_2)	H_2 purge (bar H_2)
$NiMo/Al_2O_3$	0.2	2×25	100	3×80	80
Experimental conditions					
Temperature (° C)	Heating & cooling rate (° C/min)	Pressure (bar)	H_2/oil ratio (NL/L)	Reaction time (hours)	Shaking frequency (min^{-1})
360	>100	100–160	525	4	450

Table 3
Mass, energy and carbon balances for continuous versus microbatch HTL processing of the two 4th cycle feedstocks.

		Mass balance (wt.%)				Carbon balance (wt.%)				Energy recovery (%)		
		Gas	Biocrude	Solids	Total	Gas	Biocrude	Solids	Total	Gas	Biocrude	Total
Continuous	HDO0	54	43	–	97	34	69	NA	104	20	80	100
	HDN0	45	29	–	74	33	50	NA	84	18	55	73
Microbatch	HDO0	43	45	2	90	24	73	3	100	4	NA	NA
	HDN0	40	23	11	74	24	36	20	80	6	NA	NA

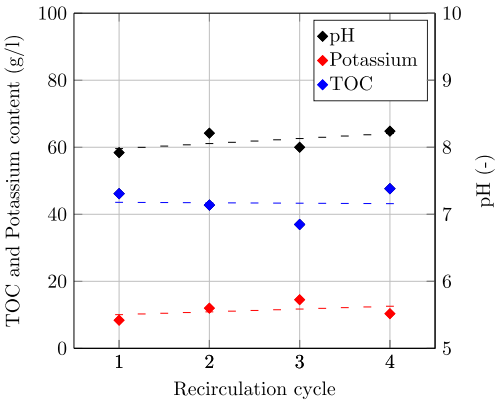

Fig. 2. Development in water phase pH, TOC and potassium content after recirculation of the aqueous product in the HDO0 experiments.

Liquid Recovery includes water which is the main deoxygenation biproduct. The water has to be subtracted to estimate the organic yield and this is done by assuming that all removed oxygen is converted to water. The yield calculation ignores potential coke formation or loss through CO and CO_2 formation. On the other hand, losses from catalyst and reactor wetting overestimates the losses. As a result, yield figures can only be used as a rough estimate.

$$\Delta O = O_{biocrude} - O_{upgr.\ oil} \quad [\ \text{wt.\%}]$$
$$Liq.Rec. = \frac{m_{liq.\ prod.}}{m_{biocrude}} \quad [\ \text{wt.\%}]$$
$$\text{Yield} = Liq.Rec. \cdot (1 - \Delta O) \quad [\ \text{wt.\%}] \qquad (2)$$

3. Results

3.1. Hydrothermal liquefaction

Continuous hydrothermal liquefaction of aspen wood under supercritical conditions and using either NH_3 or NaOH were successfully carried out with more than 100 h of hot operation. Scalable process conditions with aqueous phase recycling were resembled and two steady state biocrudes produced under enhanced conditions were obtained. Microbatch HTL of the same (4th cycle) feedstocks were also carried out for comparison and Table 3 lists mass, carbon and energy balances for both the continuous and microbatch HTL. The CHTL data is based on a set of representable steady state data.

Biocrude yields around 43–45 wt.% is observed in the presence of NaOH, whereas the yields are significantly lower in the presence of NH_3. Processing issues such as increasing pressure drops, and lack of mass balance closure were encountered during the experiments using ammonia as catalyst. This is most likely related to the severe formation of solids that is apparent from the microbatch experiments of this feedstock. 11.1 wt.% solids were recovered from the NH_3 experiments, whereas the NaOH experiments only produced 1.8 wt.% solids. Elemental analysis, CCR and ash analysis emphasize that these solids contain >80 wt.% carbon and <2 wt.% hydrogen. The carbon and energy balances are close to unity for the HDO0 experiments, whereas the HDN0 experiments have been affected by lack of mass balance closure. The HDO0 biocrude has an energy recovery of 80% and a carbon recovery of 69% relative to the input biomass. Appropriate utilisation of the product gas, such as combustion and subsequent CO_2 capture, will ensure even higher carbon and energy recoveries for the overall CHTL process. In literature HTL is often associated with carbon losses to the aqueous phase [24,28]. Madsen et al. [28] found that the aqueous phase TOC content increased with 3 water phase recirculations during CHTL of DDGS. A different approach was used in the current study, where water soluble organics were simulated with ethanol in the first cycle feed slurry in order to reflect steady state processing conditions at which there is an equilibrium between addition and removal of carbon from the aqueous phase. The HDO0 carbon balances in Table 3 indicate that this equilibrium has been reached during the 4 consecutive runs. The actual development in TOC content measured in the aqueous products are given for each recirculation cycle in Fig. 2 together with pH and potassium content. The results clearly emphasize that the TOC content is rather constant around the 45 g/l. Potassium content and pH is also rather constant during the recirculation.

Table 3 also touches upon the scalability between microbatch and the semi-continuous bench scale unit, and yield figures seem comparable. However, as given in Table 4, the composition of the product gas seems to differ. Generally, the CHTL product gas contains a higher concentration of hydrogen and light hydrocarbons, whereas a higher

Table 4
Gas composition (vol.%) for continuous versus microbatch HTL processing of the two 4th cycle feedstocks.

		H_2	CO	CH_4	CO_2	C_2H_4	C_2H_6	C_3	C_4	Others	Total
Continuous	HDO0	25.8	0.3	7.2	61.1	0.2	2.4	1.3	0.7	1.0	100.0
	HDN0	19.5	0.6	5.5	62.5	1.0	3.5	2.3	0.8	1.4	97.2
Microbatch	HDO0	7.7	0.9	2.2	88.8	0.3	1.3	–	–	–	101.2
	HDN0	9.9	10.7	2.5	70.1	0.2	1.7	–	–	–	95.1

Table 5
Physiochemical properties of HDN0 biocrude and the corresponding fractionation cuts.

	Cut (° C)	Yield (vol.%)	Acc. yield (vol.%)	CCR (wt.%)	Density[a] (kg/m³)	HHV[b] (MJ/kg)	TAN (mg/g)	Elemental (wt.%) C	H	N	O[c]	H/C (–)	O/C (–)
HDN0	–	–	–	20.5	1036	38.6	33.6	79.8	9.3	2.7	8.2	1.39	0.08
F1	IBP–180	8.4	8.4	–	857	37.6	0.4	66.2	9.3	2.6	21.9	1.67	0.25
F2	180–260	6.6	15.0	–	945	39.0	6.7	78.3	10.6	1.2	9.9	1.61	0.10
F3	260–375	26.7	41.7	–	1009	39.1	21.8	81.7	10.1	0.1	8.0	1.48	0.07
Residue	375+	53.8	95.5	33.6	1093	37.8	–	82.2	8.4	2.1	7.4	1.22	0.07
Balance	–	95.5	–	–	1044	38.2	–	80.7	9.1	1.5	8.7	1.34	0.08

[a] At 15.0 ° C.
[b] Dry basis.
[c] By difference.

Table 6
Physiochemical properties of HDO0 biocrude and the corresponding fractionation cuts.

	Cut (° C)	Yield (vol.%)	Acc. yield (vol.%)	CCR (wt.%)	Density[a] (kg/m^3)	HHV[b] (MJ/kg)	TAN (mg/g)	Elemental (wt.%) C	H	N	O[c]	H/C (–)	O/C (–)
HDO0	–	–	–	19.5	1051	37.6	55.7	81.4	8.5	0.1	10.1	1.25	0.09
F1	IBP–180	5.0	5.0	–	842	41.3	6.02	80.5	11.9	[d]	7.6	1.76	0.07
F2	180–260	13.2	18.2	–	943	39.0	3.75	80.3	10.3	[d]	9.4	1.53	0.09
F3	260–344	22.1	40.3	–	1024	37.8	8.15	82.3	9.5	[d]	8.2	1.38	0.08
Residue	344+	58.1	98.3	34.4	1154	37.5	–	84.8	8.0	[d]	7.2	1.12	0.06
Balance	–	98.3	–	–	1089	37.9	–	83.6	8.7	–	7.7	1.25	0.07

[a] At 15.0 ° C.
[b] Dry basis.
[c] By difference.
[d] Below detection level.

CO_2 and CO concentration in the microbatch products indicate inhibition of the water gas shift reaction. This difference in composition affects the energy recovery of the gaseous products given in Table 3. Comparative analysis of data from different reactor systems is still not well understood, but while the present microbatch experiments ensures rapid heating and mixing, it is possible that variations in data are due to different pressures during heating. While an isobaric heating is characteristic for continuous systems, the pressure during heating in microbatch reactors are dictated by the saturation pressure. Differences in pressure will facilitate different reaction pathways as described by Jensen et al. [4]. From this point it is only the continuously produced biocrudes that are discussed.

3.2. CHTL biocrude analysis

Physiochemical properties of the two continuously produced biocrudes are listed in Tables 5 and 6, respectively. First of all, with oxygen contents around 10 wt.% and HHV around 38 MJ/kg, both biocrudes possess state of the art quality relative to woody HTL oils found in literature [1-3,5,24,29]. The HDN0 seems to be of a slightly higher quality relative to the HDO0 in terms of density, HHV, H/C ratio, O/C ratio and especially total acid number (TAN). This supports the hypothesis suggesting that NH_3 may act as a hydrogen donor during HTL conversion improving especially density and H/C ratio. However, based on the relatively high nitrogen content of 2.7 wt.%, the concern about potential nitrogen pollution of the HDN0 biocrude when using ammonia is justified. The lower nitrogen content around 0.1 wt.% of the HDO0 may prove advantageous in relation to hydrotreating, since nitrogen can be a rather difficult heteroatom to remove. Fig. 3 illustrates a modified Van Krevelen diagram. Starting from the same biomass composition, it is clear that the ammonia improves the H/C ratio of the biocrude relative to NaOH during HTL. The (N +O)/ C ratio illustrates that the accumulated heteroatom content is about equal for the two biocrudes after liquefaction, but with significantly more nitrogen and less oxygen in HDN0. The hydrotreating data of Fig. 3 will be commented on later.

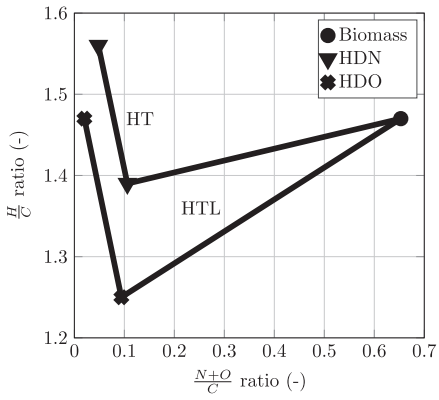

Fig. 3. Modified Van Krevelen diagram showing molar ratios of hydrogen to carbon as function of oxygen and nitrogen to carbon.

3.2.1. Fractional distillation

The HDN0 and HDO0 biocrudes were exposed to a 15:5 fractional distillation that was carried out according to the ASTM D2892. As pictured in Fig. 4, the biocrudes were each divided in 3 distillate cuts and a so-called atmospheric residue fraction.

The distillations were carried out under vacuum to protect the biocrudes from thermal degradation. ASTM D2892 is suited for distillation to an atmospheric equivalent temperature (AET) of 400 °C or until thermal cracking is observed. Distillation of the HDO0 biocrude was terminated at an AET of 344 °C due to unstable vacuum indicating thermal cracking. The HDN0 biocrude showed better thermal stability, since the distillation could be continued to an AET of 375 °C. Tables 5 and 6 compares the properties of the fractions obtained from fractional distillation of the HDN0 and HDO0 biocrudes respectively. For the linear blending properties such as density and HHV, a weighted average referred to as ' balance' is given to validate the distillation yields against the physiochemical properties measured for each product. Except for the elemental oxygen, which has a higher uncertainty because it is based on difference, the balanced properties show good agreement with those of the original biocrude. In terms of boiling point distribution, the simulated and TBP distillation profile in Fig. 5 are also similar.

The atmospheric residue fraction is the largest of both biocrudes. The residue fractions have similar and high coking potentials relative to petroleum crudes [19] as listed with the CCR in Tables 5 and 6. On the other hand, both residue fractions have relatively high HHV and according to Fig. 5, they contain 28–35 wt.% of fuel oil distillate. The presence of a significant amount of heavy distillate is also clear

Fig. 4. Visual appearance of HDN0 fractions with lights through heavies from left to right. No visual difference between the fractions from HDN0 and HDO0 were observed.

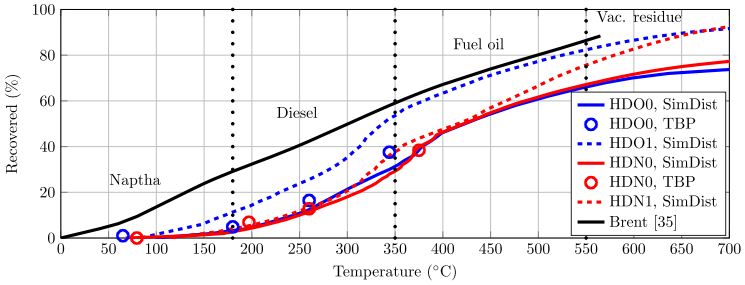

Fig. 5. Simulated versus TBP distillation of the biocrudes and the effect hydrotreating has on the distillation profile. The fossil benchmark Brent crude is given for comparison.

from Fig. 6 that presents TGA curves of the residue fractions. The fact that the fractional distillations were terminated at different temperatures is also clear from Fig. 6, where the HDN0 residue has a higher IBP compared to the HDO0 residue. Otherwise, the residues as well as the biocrudes seem very similar with respect to volatility when examining both TGA curves, simulated and TBP distillation profiles. This indicates that the choice of HTL catalyst has very little effect on the distillation profile.

3.2.2. Composition of the fractions

In petroleum crude oils heteroatoms are generally distributed as an increasing function of boiling point with the majority of sulphur and nitrogen located in the residue fractions [19]. Previous studies on HTL biocrudes have concluded a different tendency with a rather even distribution of heteroatoms throughout the different fractions [23,27]. The same pattern applies for the HDO0 biocrude, whereas the HDN0 seem to have more heteroatoms in the lighter fractions compared to the heavy ends. For both biocrudes, there is an increase in density and TAN with TBP, whereas the H/C ratio is steadily decreasing indicating a higher degree of aromatic and polyaromatic compounds in the heavier fractions. The fact that oxygen is present in significant concentrations throughout all fractions is also clear from the FT-IR spectra presented in Fig. 8. All spectra suggest significant carbonyl absorption and the broad peak around 3300 cm^{-1} suggests the presence of O–H functional groups, such as phenolics. Fraction 3 of the HDN0 has a broad absorption overlapping 3000 cm^{-1} indicating the presence of acids, which correlates well with the relatively high TAN number of this particular fraction. Finally, the IR spectra of Fig. 8 show an increasing degree of aromatic stretching around 1600 cm^{-1} for the heavier fractions [30]

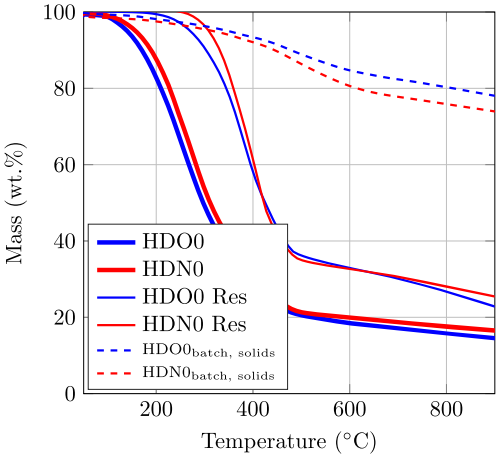

Fig. 6. TGA of the biocrudes and their corresponding fractionation residues. TGA curves of the solids formed during microbatch HTL is also given to emphasize the carbon nature.

3.3. Hydrotreating

Heteroatom removal and biocrude hydrogenation through hydrotreating were carried out in microbatch reactors using presulphided and stabilised $NiMo/Al_2O_3$ catalyst. HDN0 and HDO0 were both hydrotreated and Table 7 lists the outcome with respect to yield figures and physiochemical properties of the upgraded biooil that are referred to as HDN1 and HDO1 respectively.

The modified Van Krevelen diagram in Fig. 3 reflects heteroatom removal through decreasing *x*-values and hydrogenation by increasing *y*-values. Particularly nitrogen removal and relative hydrogenation is poorer for the HDN1. The heteroatom removal is also reflected in a lower density and an improved HHV and again the relative improvement is largest for the HDO1, where the HHV is improved from 37.6 MJ/kg to 42.3 MJ/kg. The CCR is reduced indicating a more thermally stable product and the TAN is completely neutralised for both biocrudes during hydrotreatment. All values indicate significant quality improvements.

Fig. 7 presents FT-IR spectra of the biocrudes before and after hydrotreatment. It is clear how especially the carbonyl absorptions around 1700 cm^{-1} are removed and the O–H stretches reduced during hydrotreatment. Remaining absorption around

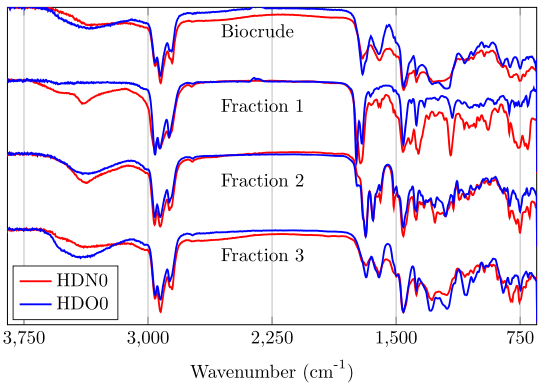

Fig. 7. FT-IR of the biocrudes before and after hydrotreating.

Table 7
Physiochemical properties of the different biocrudes before and after hydrotreating.

	Liq. Rec (wt.%)	Yield (wt.%)	Water (wt.%)	Ash (wt.%)	CCR (wt.%)	Density[a] (kg/m^3)	HHV[b] (MJ/kg)	TAN (mg/g)	Elemental (wt.%) C	H	N	O[c]	H/C (−)
HDN0	–	–	2.2	0.04	20.5	1036	38.6	33.6	79.8	9.3	2.7	8.2	1.39
HDO0	–	–	2.3	0.03	19.5	1051	37.6	55.7	81.4	8.5	0.1	10.1	1.25
HDN1	88.0	83.0	9.3	–	13.4	983	41.1	0.0	84.0	11.0	2.0	3.1	1.56
HDO1	87.0	79.0	11.4	–	11.0	975	42.3	0.0	87.0	10.7	[d]	2.3	1.47

[a] At 15.0 ° C.
[b] Dry basis.
[c] By difference.
[d] Below detection level.

3500 cm^{-1} suggests that the trace oxygen left in the HDO1 could be phenolic compounds. These observations match previous findings and literature statements about carbonyls being reactive towards deoxygenation, whereas phenolics are more resistant due to ring stabilisation [7,27,31]. Interpretation of the remaining non-hydrocarbon absorption of the HDN1 spectra is more difficult. But the broad peak overlapping 3000 cm^{-1}, could possibly indicate saturated amines. This absorption is commonly called the ammonium band, and it is described in further details in Ref. [30].

Table 8 lists the composition of the product gases from the two upgrading experiments. The yield of gaseous products are around 3–6 wt.% on a hydrogen free basis and relative to the input oil. Acknowledging a high uncertainty on these numbers, the hydrogen consumption on an oil input basis is around 1.5–2 wt.%. The compositions are similar with respect to hydrogen, CO and light hydrocarbons. However, it is noteworthy that the CO_2 is completely absent in the HDN1 product gas and relatively concentrated in the HDO1 products. The reduction in TAN of the HDN1 indicates that the acids have indeed been removed or neutralised. Absence of CO_2 despite TAN elimination is also the case in Refs. [8,32] during hydrotreatment of nitrogenous HTL biocrudes originating from algae. The observation could be related to ammonium neutralisation of the acid functionalities as suggested in Ref. [32], but more likely it is due to CO_2 absorption in aqueous ammonia, which is a CO_2 sequestration process [33].

3.3.1. Two dimensional gas chromatography

GCxGC–MS is a strong tool within biocrude analysis, since the numerous compounds in the biocrude are separated based on differences in both boiling point (column 1) and polarity (column 2). Furthermore, for relatively heavy oils with significant amounts of residue the combination of GCxGC–MS with pyrolysis enables volatilization and thus characterization of also the high boiling compounds. Both methods have been applied on different samples in the present study and Fig. 9 pictures the 2D chromatogram obtained from Py-GCxGC–MS of the HDN0 biocrude. The major peaks can be grouped into polyaromatic hydrocarbons (PAH), phenolics and fatty acids. The PAH's are mainly identified with a phenantrene or anthracene backbone. The fatty acids are identified as e.g. oleic acid, while the phenolics cover a range of mono- and di-phenols with different degrees of substitution. Especially the oleic acid may be traced back to the crude tall oil that was used as a start-up oil in CHTL campaigns. Similarly, some of the PAH's may be decarboxylated products of rosin acids, which is also a major compound in crude tall oil [34]. However, crude tall oil originates from wood just like the woody biocrude and thus a similar variety of compounds are expected. [35] carried out 2D NMR and FT-ICR MS on a pine wood HTL biocrude before and after hydrotreament. Substituted phenantrenes was detected together with various phenolics, aliphatics, cyclopentenones and polycyclic compounds.

Fig. 10 shows the chromatogram of the corresponding HDN1 after hydrotreatment. Comparing the two chromatograms gives a clear picture of the effect hydrotreating has on polarity and aromaticity. The relative abundance of paraffins has increased from insignificant to being the major group, which is related to the complete removal of fatty acids. Likewise, the PAH's have been partly or completely hydrogenated into polycyclic napthenes. The GCxGC was coupled with an FID detector to get an idea about the relationship between actual concentration and abundance in the MS chromatogram. The chromatograms showed high similarity, though paraffins showed slightly higher abundance in the chromatogram from MS detection compared to the FID, which should be kept in mind during interpretation.

Details on the relative abundance of different groups of compounds are given in Fig. 11 for both the two biocrudes and the corresponding hydrotreatment products. Fig. 11 is based on GCxGC-MS without pyrolysis, since pyrolysis degradation products will distort the relative abundance of light versus heavier compounds. The

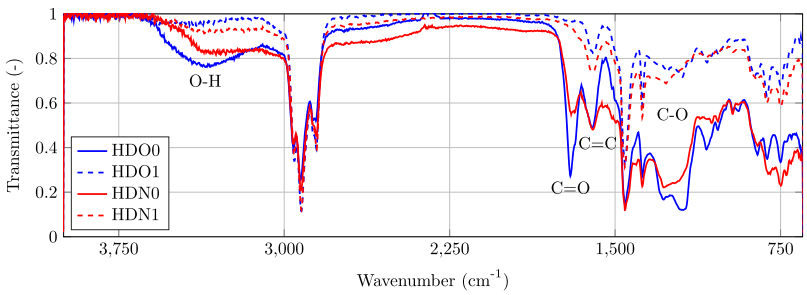

Fig. 8. FT-IR spectra of the two biocrudes and their respective fractions.

Table 8
The composition (vol.%) of gaseous products from HDO1 and HDN1 upgrading experiments.

Reaction	H_2	CO	CO_2	CH_4	C_2H_6
HDO1	92.5 ± 0.6	0.3 ± 0.0	2.8 ± 0.1	3.2 ± 0.1	1.2 ± 0.1
HDN1	94.8 ± 4.2	0.3 ± 0.0	0.0 ± 0.0	3.4 ± 0.2	1.5 ± 0.3

amount of pure hydrocarbons in the HTL biocrudes comprise around 30–40 area% of the chromatogram, whereas it is between 80–90 area% after hydrotreatment.

Remaining oxygenates identified in the hydrotreated products are mainly long chain alcohols and highly substituted phenols. This indicates that steric hindrance may be the reason for incomplete deoxygenation and relatively slow kinetics. It is especially the abundance of napthenes and parrafins that have improved, which is also visual from Figs. 9 and 10. Ketones are completely removed to napthenes during hydrotreatment and the phenols and PAH's are significantly reduced to mono and polycyclic napthenes. Biocrude complexity was also reduced significantly during hydrotreatment in the study by Sudasinghe et al. [35], but the polycyclic aromatic functionality was found to increase using a CoMoS/F-Al_2O_3 catalyst at 400 °C and 1500 psig. The low degree of hydrogenation contradicts the findings of the current study, but it is probably both due to the use of a different catalyst and especially a higher hydrotreating temperature, at which dehydrogenation is favored.

3.3.2. Effect on biocrude volatility

Fig. 5 presents the effect of hydrotreatment on biocrude volatility through simulated distillation profiles. The HDN1 has improved the final recovery with around 15 percentage points, whereas the improvement in distillate yield is minor. In a recent study by Albrecht et al. [8] on continuous hydrotreating of algae HTL biocrude, ammonia was stated to inhibit activity of the Brønsted acid sites of a CoMo/Al_2O_3 catalyst. This could very likely be one of the explanations to less conversion during hydrotreatment of the HDN0 biocrude, since nitrogen is removed as ammonia during hydrodenitrogenation. Another reason could be the lesser degree of heteroatom removal encountered for the HDN1 relative to the HDO1.

Hydrotreatment of the HDO0 biocrude has improved the distillation profile significantly. The bar plot in Fig. 12 illustrates the change in product distribution during hydrotreatment. The naptha yield is improved from 3 to 11% and the diesel from 29 to 43%. From the distillation curve of HDO0 in Fig. 5 it seems that the boiling point distribution is suppressed around 50–150 °C over the major part of the curve. In fact, this conclusion supports the hypothesis presented previously about deoxygenation having a significant effect on the TBP distribution. One could argue that the molybdenum sites of the catalyst facilitate cracking, and thus the effect on volatility cannot be assigned deoxygenation alone. This is correct, although the hydrotreating temperature is kept at 360 °C in order to operate below the regime where the kinetics of cracking become significant. As a result, the suppression of boiling point is believed to be mainly related to the reduced intermolecular bonding, which is the direct effect of deoxygenation and saturation. The largest fraction of the HDO0 biocrude is the so-called ' bottom-of-the-barrel', comprising the fuel oil cut and that boiling above 550 °C, which by difference each represents 33 wt.%. Based on this, the HDO0 is characterized as a relatively heavy crude that for commodity fuel production is less valuable due to the processing that is needed to obtain final products. However, deoxygenation affects these characteristics significantly, since the largest fraction of the hydrotreated products are the diesel fraction comprising 43 wt.% for HDO1. Since biocrudes often are presented as potential substitutes for fossil fuel production, it is crucial to acknowledge the effect of deoxygenation when evaluating the potential of a certain biocrude for fuel production. The current results clearly show how the potential of a biocrude is underestimated if the effect oxygen has on the TBP distribution is not accounted for.

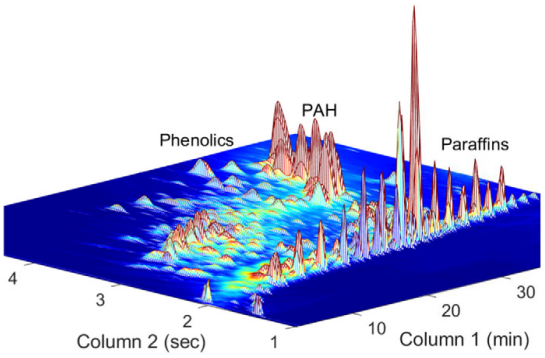

Fig. 10. 2D chromatogram obtained from Py-GCxGC–MS of HDN1.

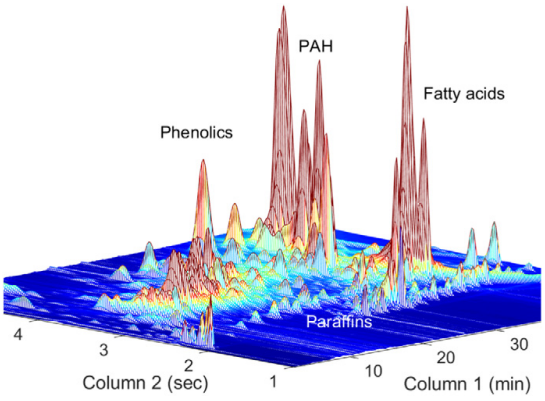

Fig. 9. 2D chromatogram obtained from Py-GCxGC–MS of the HDN0 biocrude.

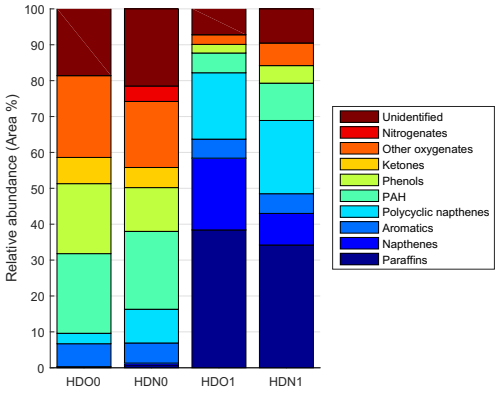

Fig. 11. The GCxGC–MS identifications grouped into families.

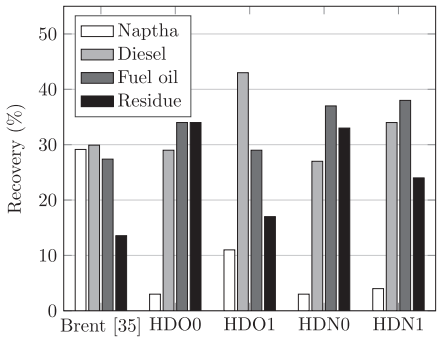

Fig. 12. Product distribution based on simulated distillation.

The distillation profile of the fossil benchmark Brent crude oil is given for comparison in Fig. 5. Comparing the HDO1 with this benchmark crude is of interest in order to indicate the value of the bio-product. Note how the amount of vacuum residue and fuel oil is similar. The diesel fraction of the hydrotreated biooil is 13 percentage points larger than that of the Brent crude, which indicates that the HDO1 is a high value biofeed particularly suitable for diesel and jet fuel substitution. Additionally, Table 7 reveals sulphur and nitrogen contents in the ppm range, which are both beneficial properties from a downstream refining or blending perspective. Finally, the carbon credits associated with a low carbon footprint is a value adding characteristic.

4. Discussion

The current study emphasizes the importance of complete studies, where the effect of changing a process parameter is investigated along the entire path from biomass to fuel. For example, it turned out that the choice of alkaline catalyst during HTL had an effect on the downstream hydrotreating process, this despite the many similarities between HDO0 and HDN0 biocrude composition. Such consequences must be considered when evaluating the change of a particular process parameter. Moreover, fractional distillation showed that both biocrudes consist of a significant share of high boiling compounds. Thus conventional GC–MS, which is a widely used analysis in HTL literature, only provides the composition of a fraction of the biocrude. Complete evaluation requires complete analysis and Py-GCxGC–MS proved useful in the characterization of the entire biocrude. However, quantitative characterization of biocrudes is still a topic for further development involving the techniques employed here as well as others.

Ammonia is an indigenous bi-product from hydrodenitrogenation of e.g. a nitrogenous biocrude [20]. Thus, it is appealing to recirculate ammonia from upgrading products as alkaline additive during HTL of nitrogenous feedstock such as grass, micro-algae, DDGS, sewage sludge and manure. In such trials, the learnings of this study should be considered, since ammonia was associated with nitrogen pollution of the biocrude and significant coke formation during HTL of wood, resulting in low energy and carbon recoveries.

Experiments with continuous hydrotreating of the NaOH biocrude on the same conventional catalyst are being carried out at the time of writing and the outcome shows good agreement with both the HDO1 product characteristics and yield figures presented above from hydrotreating in microbatch reactors. Thus, the prospects presented in the current study seem scalable and future work include tests of the long term catalytic stability.

5. Conclusions

Ammonia as HTL catalyst was observed to pollute the biocrude with 2.7 wt.% nitrogen, which seemed to inhibit hydrotreating conversion. Furthermore, ammonia resulted in severe coke formation, whereas NaOH was associated with high yields (43 wt.%) of hydrotreatable biocrude. Mass, carbon and energy balances were closed and stable pH, TOC and potassium levels were observed during HTL aqueous phase recirculation. GCxGC–MS revealed the relative abundance of pure hydrocarbons was improved to 80–90 % during hydrotreatment. The NaOH biocrude had a diesel cut comprising 43% after hydrotreatment making it a high value bio-blendstock particularly useful for substitution of low sulphur diesel and jet fuel.

Acknowledgments

The authors acknowledge the support for this research provided by EASME Horizon 2020 and Innovation Fund Denmark[4135-00126B].

References

[1] A.A. Peterson, F. Vogel, R.P. Lachance, M. Fröling, M.J. Antal, Jr, J.W. Tester, Thermochemical biofuel production in hydrothermal media: a review of sub- -and supercritical water technologies, Energ. Environ. Sci. 1 (1) (2008) 32–65.
[2] Y. Xue, H. Chen, W. Zhao, C. Yang, P. Ma, S. Han, A review on the operating conditions of producing bio-oil from hydrothermal liquefaction of biomass, Int. J. Energy Res. (2016)
[3] S. Toor, L. Rosendahl, A. Rudolf, Hydrothermal liquefaction of biomass: a review of subcritical water technologies, Energy 36 (5) (2011) 2328–2342.
[4] C.U. Jensen, J.K.R. Guerrero, S. Karatzos, G. Olofsson, S.B. Iversen, Fundamentals of Hydrofaction™: renewable crude oil from woody biomass, Biomass Conversion and Biorefinery (2017) In Press.
[5] D.C. Elliott, P. Biller, A.B. Ross, A.J. Schmidt, S.B. Jones, Hydrothermal liquefaction of biomass: developments from batch to continuous process, Bioresour. Technol. 178 (2015) 147–156.
[6] E. Furimsky, Hydroprocessing challenges in biofuels production, Catal. Today 217 (2013) 13–56.
[7] C.U. Jensen, J. Hoffmann, L.A. Rosendahl, Co-processing potential of HTL bio-crude at petroleum refineries. Part 2: a parametric hydrotreating study, Fuel 165 (2016) 536–543.
[8] K.O. Albrecht, Y. Zhu, A.J. Schmidt, J.M. Billing, T.R. Hart, S.B. Jones, G. Maupin, R. Hallen, T. Ahrens, D. Anderson, Impact of heterotrophically stressed algae for biofuel production via hydrothermal liquefaction and catalytic hydrotreating in continuous-flow reactors, Algal Res. 14 (2016) 17–27.
[9] I. Tews, Y. Zhu, C. Drennan, D. Elliott, L. Snowden-Swan, K. Onarheim, Y. Solantausta, D. Beckman, Biomass Direct Liquefaction Options: TechnoEconomic and Life Cycle Assessment, Tech. rep., Prepared for U.S. Department of Energy. 2014,
[10] Steeper Energy, Milestones & Activities, Q3 2015, 2016. www.steeperenergy.com/news/milestones-and-activities (accessed Aug. 31 2016)
[11] U.S.D.O.E. Clean Cities, Alternative Fuel Price Report, Tech. rep., U.S. Department of Energy. 2016,
[12] N. Lambert, Study of Hydrogenation Derived Renewable Diesel as a Renewable Fuel Option in North America, Tech. rep., Natural Resources Canada. 2012,
[13] IEA, World Energy Outlook 2015, Executive Summary, Tech. rep., International Energy Agency. Paris: IEA. 2015,
[14] D.P. Coady, I. Parry, L. Sears, B. Shang, How Large Are Global Energy Subsidies? 2015, International Monetary Fund. (IMF Working Paper).
[15] D. Clark, Phasing out fossil fuel subsidies 'could provide half of global carbon target', The Guardian 19 (Jan 2012)
[16] N. Akiya, P.E. Savage, Roles of water for chemical reactions in high-temperature water, Chem. Rev. 102 (8) (2001) 2725–2750.
[17] A. Kruse, E. Dinjus, Hot compressed water as reaction medium and reactant — properties and synthesis reactions, J. Supercrit. Fluids 39 (2007) 362–380.
[18] M. Schubert, J.W. Regler, F. Vogel, Continuous salt precipitation and separation from supercritical water. Part 1: type 1 salts, J. Supercrit. Fluids 52 (2010) 99–112.
[19] J.H. Gary, G.E. Handwerk, M.J. Kaiser, Petroleum Refining, Technology and Economics, 5. Edition, CRC Press. 2007. (ISBN 0-8493-7038-8)
[20] P. Biller, B.K. Sharma, B. Kunwar, A.B. Ross, Hydroprocessing of bio-crude from continuous hydrothermal liquefaction of microalgae, Fuel 159 (2015) 197–205.
[21] P. Linstrom, E.W.G. Mallard, NIST Chemistry WebBook, NIST Standard Reference Database Number, 69. National Institute of Standards and Technology. 2015. (accessed Aug. 31 2016), http://webbook.nist.gov
[22] R.G. Montemayor, Distillation and Vapor Pressure Measurement in Petroleum Products, Tech. rep., ASTM International. 2008,

[23] J. Hoffmann, C.U. Jensen, L.A. Rosendahl, Co-processing potential of HTL bio-crude at petroleum refineries. Part 1: fractional distillation and characterization, Fuel 165 (2016) 526–535.
[24] T. Pedersen, I. Grigoras, J. Hoffmann, S. Toor, I. Daraban, C.U. Jensen, S. Iversen, R. Madsen, M. Glasius, K. Arturi, R. Nielsen, E. Søgaard, L. Rosendahl, Continuous hydrothermal co-liquefaction of aspen wood and glycerol with water phase recirculation, Appl. Energy 162 (2016) 1034–1041.
[25] S.B. Iversen, Conversion of organic matter into oil, Dec. 15 2015. (Patent WO2011/069510)
[26] S.B. Iversen, Improved method for preparing shut down of process and equipment for producing liquid hydrocarbons, Dec. 22 2015. (Patent WO2014/032669)
[27] T.H. Pedersen, C.U. Jensen, L. Sandström, L.A. Rosendahl, Production of commodity chemicals and drop-in fuels from biomass by biocrude distillation and upgrading, 2017. (under review)
[28] R.B. Madsen, M.M. Jensen, A.J. Mørup, K. Houlberg, P.S. Christensen, M. Klemmer, J. Becker, B.B. Iversen, M. Glasius, Using design of experiments to optimize derivatization with methyl chloroformate for quantitative analysis of the aqueous phase from hydrothermal liquefaction of biomass, Anal. Bioanal. Chem. 408 (8) (2016) 2171–2183.
[29] D.C. Elliott, Process Development for Biomass Liquefaction, U.S. Department of Energy's Biomass Liquefaction Experimental Facility at Albany, Oregon, 1980, 257–263.
[30] K. Nakanishi, Infrared absorption spectroscopy, practical, Holden-Day, San Francisco, 1962.
[31] E. Furimsky, Catalytic hydrodeoxygenation, Appl. Catal. A Gen. 199 (2) (2000) 147–190.
[32] D.C. Elliott, T.R. Hart, A.J. Schmidt, G.G. Neuenschwander, L.J. Rotness, M.V. Olarte, A.H. Zacher, K.O. Albrecht, R.T. Hallen, J.E. Holladay, Process development for hydrothermal liquefaction of algae feedstocks in a continuous-flow reactor, Algal Res. 2 (2013) 445–454.
[33] J.T. Yeh, K.P. Resnik, K. Rygle, H.W. Pennline, Semi-batch absorption and regeneration studies for CO_2 capture by aqueous ammonia, Fuel Process. Technol. 86 (14) (2005) 1533–1546.
[34] L.-H. Norlin, Tall Oil, Ullmann's Encyclopedia of Industrial Chemistry.
[35] N. Sudasinghe, J.R. Cort, R. Hallen, M. Olarte, A. Schmidt, T. Schaub, Hydrothermal liquefaction oil and hydrotreated product from pine feedstock characterized by heteronuclear two-dimensional NMR spectroscopy and FT-ICR mass spectrometry, Fuel 137 (2014) 60–69.

Paper E

Co-processing potential of HTL bio-crude at petroleum refineries - Part 1: Fractional distillation and characterization

Jessica Hoffmann, Claus Uhrenholt Jensen, Lasse A. Rosendahl

The manuscript has been published in the
Journal of Fuel, vol.165, pp. 526–535, 2016.

The layout has been revised.

Fuel 165 (2016) 526–535

Contents lists available at ScienceDirect

Fuel

journal homepage: www.elsevier.com/locate/fuel

Co-processing potential of HTL bio-crude at petroleum refineries – Part 1: Fractional distillation and characterization

Jessica Hoffmann [a,*], Claus Uhrenholt Jensen [a,b], Lasse A. Rosendahl [a]

[a] Department of Energy Technology, Aalborg University, Pontoppidanstræde 101, 9220 Aalborg, Denmark
[b] Steeper Energy ApS, Sandbjergvej 11, 2970 Hørsholm, Denmark

ARTICLE INFO

Article history:
Received 16 March 2015
Received in revised form 18 October 2015
Accepted 22 October 2015
Available online 29 October 2015

Keywords:
Hydrothermal liquefaction
Fractional distillation
Co-processing
Biomass
Bio-crude

ABSTRACT

This study presents detailed chemical and thermophysical analysis of bio-crude from a continuous hydrothermal liquefaction research plant. Current research on bio-crude focuses mainly on specific biomass feedstocks and conversion process conditions and resulting yields rather than on bio-crude properties for downstream processing. This study contributes to the next level of research, where HTL bio-crude is evaluated as a potential refinery co-processing feedstock with regard to bulk and fractional properties.

The bio-crude used in the current work has been produced from a hardwood feedstock. Bio-crude assays, adapted from conventional crude oil assays, have been obtained, including fractionation of the bio-crude through 15:5 vacuum distillation. The bio-crude and its fractions have been analyzed with respect to heating value, elemental composition, density and oxygen-containing functional groups. Results show a highly promising bio-crude quality, with a higher heating value of 40.4 MJ/kg, elemental oxygen content of 5.3 wt.%, a specific gravity of 0.97 and a distillation recovery of ~53.4 wt.% at an atmospheric equivalent temperature (AET) of 375 °C, . Results show that only minor upgrading is needed to achieve co-processing properties and to obtain a refinery bio-feed. This forms the basis for subsequent assessment of drop-in and co-processing potential and parametric upgrading trials of the bio-crude presented in part 2 of this work.

1. Introduction

The concurrent increase in global primary energy consumption by an annual 2.3% (2013) [1] and depletion of conventional resources, combined with climate issues and the desire for national/regional energy independence, has led to an urgent need for renewable as well as sustainable energy sources and processes. Due to their potential carbon neutrality, liquid fuels from non-food biomass are essential to meet the imposing challenges of energy supply and climate impact [2]. In 2013, fossil fuels still accounted for 87% of global and 77% of EU primary energy consumption [1]. Since biomass will also become primary feedstock for chemicals, nutritional and pharmaceutical products, it will in future become a high-cost commodity. Therefore it is of great importance to develop a sustainable and cost-effective process for the conversion of biomass, which is feedstock flexible, energy efficient and offers high conversion efficiency. Whereas some processes need specialized feedstocks, processes that run on multiple low value feed streams such as agricultural and forestry waste and other non-food biomass are of significant interest. Only a process covering these attributes has the ability to produce a drop-in or refinery co-processing feed that is commercially competitive to conventional fuels and therefore has the capability to endure on the market.

Hydrothermal liquefaction (HTL) is one such promising feedstock flexible thermochemical conversion processes converting low-value, high moisture or wet biomass feedstock to a high value bio-crude. It works at near critical water conditions with temperatures of 360–450 °C and pressure from 250 to 400 bars. HTL offers numerous advantages compared to other thermochemical conversion processes: high moisture feedstock, conversion efficiency and product quality in terms of delivering a bio-crude with high refinery biofeed and co-processing potential. Such co-processing offers a number of advantages, the first of which is the opportunity to reuse existing refinery and downstream infrastructure and thus significantly shortening implementation time scales and reducing CAPEX. Secondly, it contributes to cost-effectiveness in terms of processing to synthetic, chemically equivalent drop-in products with a reduced environmental food print.

* Corresponding author. Tel.: +45 21370482; fax: +45 9815 141.
E-mail address: jho@et.aau.dk (J. Hoffmann).

http://dx.doi.org/10.1016/j.fuel.2015.10.094
0016-2361/

Naturally, data on individual bio-crudes must be available for refineries to consider introducing these into the processing stream. Just as is true for fossil crudes of different origins, HTL bio-crudes will differ depending on feedstock and process parameters. Individual bio-crude assays allow a direct comparison between petroleum and bio-crude and thus evaluation of co-processing feasibility and market value.

Bio-crudes like conventional petroleum crudes are highly complex hydrocarbon mixtures, with the challenging difference of containing oxygenated hydrocarbons to a higher degree. It is virtually impossible to identify every single molecule in crudes. Hence for conventional petroleum refineries, standardized crude oil assays have been developed to get an understanding of the chemical and thermophysical properties of the crude. This information enables modern refineries to characterize crude oils, simulate the refining process and get insights to the refining process and end products respective to the crude feed. For bio-crude such standard methods for an assay characterization have not yet been developed, which makes it hard to compare and assess the bio-crude quality. The lack of analytical knowledge on bio-crudes is mainly due to the high diversity of bio-oil and crudes and the lack of focus on the downstream side of the conversion process. This work will address this and try to initiate a procedure for bio-crude assays for refining operations.

1.1. Crude oil assays

A typical crude oil assay contains two types of information for an oil sample; bulk properties and fractional properties [3]. These properties are determined according to standardized methods, e.g. ASTM (American Society for Testing and Materials).

Bulk properties give an understanding of the overall crude oil sample, whereas fractional properties specify characteristics of the different fractions obtained by distillation [4]. As part of this research paper, selected conventional crude oil assay parameters are determined to facilitate evaluation of the bio-crude. Bulk and fractional properties include elemental analysis, H/C and O/C ratios, higher heating value and density. Bulk properties include flash point, kinematic viscosity, carbon residue, pour point and TAN (total acid number).

1.2. Bio-crude assay and co-processing challenges

One of the most apparent differences between crude and bio-crude is the oxygen heteroatom content and subsequently the TAN number. Compared to conventional crude with an oxygen content of 0.05–1.5% [5], bio-crude from HTL typically contains 4–10 wt.% oxygen [4] depending on the biomass feedstock and process conditions used during conversion. Since refineries are complex chemical plants, highly optimized to the crude feed as well as to the markets they serve, an upgrading pathway prior to co-processing of the bio-crude needs to be developed. The goal is to meet conventional crude oil requirements prior to introduction at a refinery stage. Focus is hereby set on the oxygen removal prior to co-processing since conventional refineries are not optimized to handle oxygen rich oils. High oxygen contents and high TAN numbers would lead to corrosion problems during refining. The overall target should hereby be to introduce the bio-feed with as little detrimental impact as possible to the refinery, potentially even exploring chemical synergetic effects that may arise through co-processing of bio-feed and conventional feed.

This study will focus on the bulk as well as fractional assay properties of HTL bio-crude produced from a hardwood feedstock. As HTL bio-crude has the major advantage of being thermally stable compared to e.g. bio-oil from pyrolysis, fractionation of the crude by distillation is possible and thereby fractional properties can be obtained. Comparing the heteroatom distribution as function of boiling in the HTL bio-crude to that characteristic for petroleum crude oil yields important information on the design of the downstream stages. If only parts of the bio-crude fractions contain heteroatoms, the necessity for upgrading could be limited to these fractions and a more sustainable and economic upgrading process could be designed. The distillation also gives insight into the yield for each fraction and consequently to the value of the bio-crude. Oxygenated hydrocarbons have higher boiling points compared to their non-oxygenated hydrocarbon group, which impacts the boiling point curve and may shift it to a misleading 'heavier' crude boiling point curve [6].

Although significant work has been published on hydrothermal liquefaction of biomass to produce bio-crudes, distillation of these bio-crudes has not been studied extensively. In literature only very few works on fractional distillation of HTL bio-crude that also include analysis of the collected fractions can be found. In 1980 Elliott and Elliott [7] included a similar distillation study on HTL bio-crude from a woody feedstock. In this work, the ASTM D1160 was used, and 5 fractions were included for analysis. In fact, no works have been published on the particular subject up until very recent, where [8] characterized the physical and chemical properties of bio-crude distillates from glycerol assisted HTL of swine manure. The fractional distillation by [8] was carried out using a so-called advanced distillation setup under atmospheric pressure and up until 500 °C, which is well beyond the critical temperature (310 °C) suggested by ASTM 2892 to avoid thermal cracking. Thermal cracking is observed by [8] through char formation during distillation, but the fact that their fractional viscosities decrease as function of boiling point above 400 °C also indicate thermal cracking and destructive distillation. Such distillation changes the bio-crude and its properties, which results in an incorrect oil assay. Thus, it has been of high priority in the current work not to affect the bio-crude by decomposition of any degree.

Fractional distillation in this study is done in a 15:5 theoretical plate column. Fractions with temperature intervals of 25 °C have been collected and elemental analysis, HHV, density and FT-IR have been evaluated and related to the boiling point distribution. Based on the distillation results and the subsequent analysis, pre-treatment of the HTL bio-crude prior to co-processing will be proposed. Further analysis on the bio-crude should also include metal content in the crude, since metals can poison refinery catalyst severely and removal of those would need to be considered prior to co-processing. The second part of this paper includes a parametric study on the removal of oxygen from the bio-crude to enable co-processing without the need for major refinery modifications. [6]

2. Methods

2.1. Materials

2.1.1. Bio-crude

The bio-crude used in this study has been obtained from processing ligno-cellulosic biomass (hardwood 20 kg/h) with supercritical water at ~400° C and ~320 bar in a continuous HTL research facility at Aalborg University. Designed and built by Steeper Energy, the Continuous Bench Scale 1 (CBS1) facility provides a versatile research platform to investigate continuous HTL under a wide range of process conditions and feedstocks. At pressures in the range of 280–350 bar and reaction temperatures in the range of 360–450 °C, wet biomass slurry can be processed into a crude oil phase, a water phase containing soluble organics, and a gas phase. Mechanically the CBS1 plant has been designed for

maximum operating pressures up to 400 bar and temperatures up to 550 °C, and a feed capacity up to approximately 30 kg per hour.

2.2. Experimental set-up

The distillation set-up used in this study is shown in Fig. 1. The set-up consists of a 15 theoretical plate column with an inner diameter of 25 mm and a Pro-Pack filling. To avoid heat loss and provide adiabatic conditions the column is surrounded by a temperature controllable heating jacket (not shown in Fig. 1). The pot flask in the bottom of the column has a volume of 2 liters. The set-up has a total of 8 fractionation collectors with a volume of 250 ml respectively (Fig. 2). The vacuum pump is connected to the top of the upper condenser as well as to the fractionation arm. The present set-up is able to reach an operating pressure of 0.1 torr. To protect the vacuum pump from light gases a dry ice cold trap is used. Light ends from the cold trap are kept for further analysis.

The ASTM standard D2892 [9] used as guideline in present study is capable of producing fractions with a final cut temperature of 400 °C. The standard does not specify at which vacuum pressures the distillation should be performed. The standard suggests operating pressures in the range from atmospheric to 2 torr. However, the maximum boiling temperature reached in the present study is approximately 400 °C at 0.1 torr. The intermediate pressure is selected according to the course of the distillation process. Before vacuum distillation the set-up has been leak tested according to ASTM D 5236 [10].

During vacuum distillation the observed vapor column head temperature must be converted to atmospheric equivalent temperatures to be able to obtain a TBP curve. This is done using

Fig. 1. Picture of the distillation column. (1) Reflux condenser. (2) Reflux valve. (3) Column head. (4) Vapor temperature. (5) Distillation column. (6) Pot flask with heating mantel. (7) Pressure transducer. (8) Cold trap. (9) Vacuum pump. (10) Product receivers.

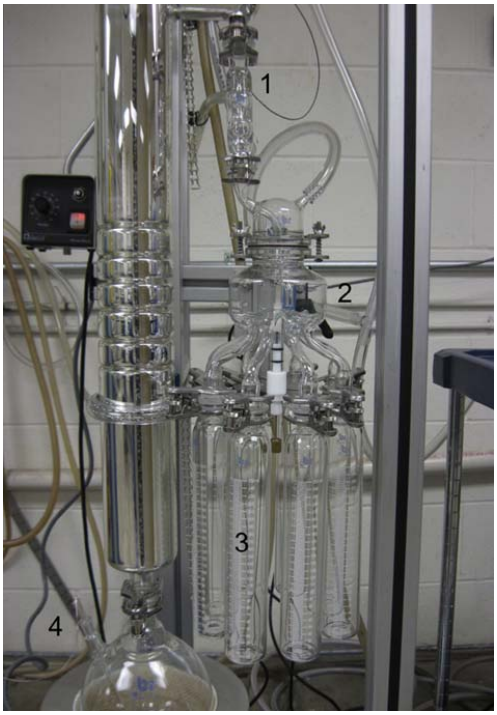

Fig. 2. Close-up view of the product receiver. (1) Product condenser. (2) Fractionation spider. (3) Fractionation receiver. (4) Thermocouple pot-flask.

the Maxwell and Bonnell derived equation described in ASTM D5236, 1999 [10]. For pressures above 2 torr the correlation between observed temperature and AET is linearized. As the pressure is decreased below 2 torr, this linearized correlation becomes inaccurate and another correlation must be applied from 2 to 0.1 torr. The equations applied in order to convert the observed temperatures to AET are given in Eqs. (1)–(3) [10]

$$\mathrm{AET} = 748.1/([1/(T+273.1)] + 0.3861 \cdot A - 0.00051606) \quad [^{\circ}\mathrm{C}] \tag{1}$$

The factor A is determined through Eq. (2) if the pressure is above 2 torr, and Eq. (3) applies for pressures between 0.1 and 2 torr.

$$A = (6.761559 - 0.987672 \cdot \log 10 \cdot P)/(3000.538 - 43.00 \cdot \log 10 \cdot \mathrm{P}) \quad \text{for } 0.1 < P < 2 \text{ torr } [-] \tag{2}$$

$$A = (5.994295 - 0.972546 \cdot \log 10 \cdot P)/(2663.129 - 95.76 \cdot \log 10 \cdot P) \quad \text{for } P > 2 \text{ torr } [-] \tag{3}$$

2.2.1. Dehydration

Prior to distillation the bio-crude has to be dehydrated. ASTM 2892 allows 0.3 wt.% of water in the sample to achieve clean cuts of the fractions. It has been observed from previous experiments that water in the sample leads to unsteady boiling, low distillation efficiency and control difficulties during distillation. Presence of water in the crude oil will lead to changes in the TBP curve between 50 and 150 °C due to the risk of steam distillation [11]. Dehydration has been done at pressures of 100 torr. The standard

suggests dehydrating at atmospheric pressures; however it has been found that when initiating the distillation at vacuum conditions the risk of cracking is decreased (observed as white smoke in the pot flask at previous distillation runs). Elliott [1] describes that the decomposition point for bio-crude from wood is approximately 55 °C below that experienced for petroleum crude. This is due the fact that some oxygenates tend to crack at lower temperatures than the corresponding hydrocarbons and thus a lower pressure has been found to be advantageous in the dehydration and distillation of HTL bio- crudes. The dehydration procedure is described in ASTM standard D2892. The bio-crude sample is heated up until a vapor temperature of 130 °C is reached. The collected product contains an organic and a water phase. The organic phase is decanted at −10 °C and reintroduced into the oil sample. The water from oil is collected for further analysis. After dehydration the bio-crude has been cooled down and fresh boiling stones have been added prior to initiating vacuum distillation. After dehydration the fractional distillation has been initiated.

2.2.2. Fractional distillation

For distillation approximately 1200 ml of bio-crude have been dehydrated. To ensure even boiling, approximately 15 g boiling stones have been added. Distillation has been run at total reflux for approximately 15 min. The heating jacket temperature has been kept at 0–5 °C below AET (atmospheric equivalent temperature) vapor temperature to ensure adiabatic conditions. A reflux of 5:1 has been kept during distillation for pressure $\geqslant$10 torr and a ratio of 2:1 $\leqslant$ 10 torr. The fractions were collected in 25° C temperature intervals compare Table 3. As soon as no increase in vapor temperature is noticed anymore, the system is cooled to be able to lower the operating pressure. To avoid cracking, the pot flask temperature and the skin temperature should not exceed temperatures of 310 °C respectively for more than an hour before the distillation has to be stopped and the vapor temperature should not exceed 210 °C [9].

Vapor temperature, pressure, pot flask temperature, pot flask skin temperature and volume of collected fraction are recorded approximately every 2 min.

2.3. Bio-crude and fraction characterization

2.3.1. Fourier transform infrared (FTIR) spectroscopy analysis

The functional group composition of the bio-crude and the fractions were investigated by FTIR spectroscopy using a Thermo Scientific Nicolet 380 spectrometer. Spectra were recorded at wavelength between 600 and 4000 cm^{-1}.

2.3.2. Elemental analysis

Elemental composition has been determined in a Perkin Elmer 2400 CHNSO analyzer in CHN mode.

2.3.3. Higher heating value (HHV) analysis

The higher heating value (HHV) has been measured using an IKA bomb calorimeter. The HHV has been done in triplicates.

2.3.4. Density analysis

Density has been measured in an Anton Paar density meter at 15.6 °C according to ASTM standards D5002. [12].

2.3.5. Simulated distillation

Simulated distillation has been carried out according to ASTM D 2887 [13] by an external certified oil testing lab.

3. Results and discussion

3.1. Dehydration

A total of 3.65 wt.% water has been removed from the bio-crude sample by dehydration at 100 torr to an AET of 130 °C. From AET <100 °C organic material could be observed in the fraction receiver, which has been reintroduced to the crude after decanting at −10 °C.

3.2. Vacuum distillation

Through vacuum distillation the dehydrated bio-crude has been successfully divided in its fractions. The initial boiling point of the crude is at AET of 87 °C. During distillation a maximum skin temperature of 330 °C at 100 torr is reached and a maximum pot flask temperature of 250 °C at 0.1 torr. No signs of cracking have been observed. The highest vapor AET reached was 375.4 °C at 0.1 torr. In total 56.8 vol.% corresponding to 53.4 wt.% of the initial feed has been distilled. 11 fractions have been collected in total, compared in Table 3. The cold trap fraction includes the condensate collected at all operating pressures and is treated as one light fraction boiling <100 °C. All material not collected below 375.4 °C is considered as residue. In the current set-up no fractionation above 375.4 °C could be achieved due to limitations in the distillation apparatus. Therefore the residue fraction also includes the fuel oil part of the bio-crude. A mass balance shows that the distillation error is 2.4 wt.% of the distillation yield. This error is due to some distillation hold-up in the system that could not be quantified

Table 1
Bio-crude analysis (dehydrated).

Analysis	Result
Flash point (°C)	39
Kinematic viscosity at 40 °C (cSt)	11.97
Carbon residue (wt.%)	3.37
Ash content (wt.%)	0.069
Total sediment (wt.%)	<0.01
Pour point (°C)	−12
Total acid number (mg KOH g^{-1})	36.78
Density at 15.6 °C (kg m^{-3})	970.3
Heating value (MJ kg^{-1})	40.43

Table 2
Elemental composition of dehydrated bio-crude.

C (wt.%)	H (wt.%)	N (wt.%)	S (wt.%)	O (wt.%)	
83.88	10.41	0.4[a]	[a]	5.31[b]	
H/C	1.49	H/C_{eff}	1.39	O/C	0.047

[a] Below calibration limit.
[b] By difference.

Table 3
Temperature intervals for collected fractions.

Fraction no.	Cut temperature (°C)
Cold trap	<100 °C
1	100–125
2	125–150
3	150–175
4	175–200
5	200–225
6	225–250
7	250–275
8	275–300
9	300–325
10	325–350
11	350–375

Fig. 3. Picture of bio-crude feed, cold trap, fractions 1–11 and residue (from left to right).

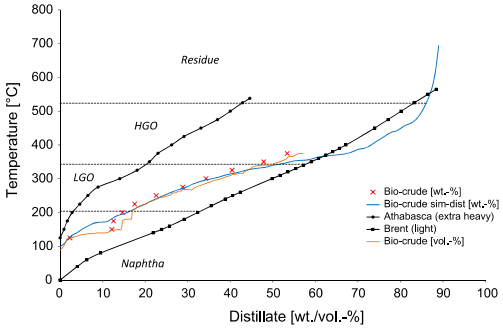

Fig. 4. Distillation curves from simulated and TBP distillation (LGO = Light gas oil, HGO = Heavy gas oil) removal would lead to an improved TAN number.

and therefore has not been included in the mass balances presented in the following section. This waxy product has been observed at the very end of the distillation procedure, as a hold-up in the glassware after cool down of the system. A picture of the bio-crude, cold-trap fraction, fraction 1 and residue is shown in Fig. 3.

3.2.1. True boiling point and simulated distillation curve

The true boiling point curve (TBP) on a cumulative mass and volume basis obtained from vacuum distillation is shown in Fig. 4, together with simulated distillation results and distillation data on conventional crudes of 2 different qualities; light benchmark Brent crude oil and Athabasca extra heavy oil [14]. The TBP mass curve contains less data points since the cumulative amount of distillate has only been logged in volume during distillation. The TBP curve and the simulated distillation curve match very well even though simulated distillation curves are obtained by calibrating with conventional crude standards. The uneven TBP curve which does not match with the sim-dist curve at temperatures between 140 and 180 °C can be explained by operational errors. The reflux valve has been opened too harshly during operation, leading to a reflux ratio of 0, which resulted in a high amount of distillate volume being flushed out of the distillation head at the same time. The operating reflux valve has been tightened immediately after a flush out of the distillation head had been noticed. This results in a separation and distribution error for fractions 2–4. Regarding bio-crude quality it can be seen that the TBP curve lies between the curves of extra heavy and light benchmark crudes. Furthermore, the flatness of the distillation curve compared to these indicates a large fraction in the middle distillate region, which is desirable in terms of market pull for fuels in this range.

3.3. Analysis of bio-crude and its fractions

A selection of bulk and fractional properties has been measured for HTL bio-crude and its fractions (see Tables 1 and 2). Elemental analysis, higher heating value (HHV), density and distillation yield in wt.% have been measured for the bio-crude, cold-trap fraction, fractions 1–11 and residue. The high viscosity of the residue at room temperature made it impossible to measure the standard density. Due to its high volatility and resulting inconsistent results elemental analysis could not be done for the cold trap fraction. The results are presented as an assay in Table 5 and discussed below. Fourier transformed infrared spectroscopy (FTIR) has been done for all samples, to get an insight into functional groups present and will be discussed in Section 3.3.2. A picture of the feed, cold trap and fractions 1–11 and the residue is given in Fig. 3.

3.3.1. Elemental analysis, HHV and density

3.3.1.1. Elemental analysis. Carbon, hydrogen and oxygen content have been determined for the bio-crude, fractions 1–11 and the residue. The molar hydrogen to carbon (H/C) ratio allows conclusion on the chemical carbohydrate structure in the samples. Fraction 1 since it is the lightest has the highest H/C ratio, suggesting short chained alkanes, like shown with FTIR analysis. The H/C generally decreases with increase in boiling point and increase in aromatic structure with the lowest ratio for the residue. The residue FTIR also shows large absorption in the 1600 cm^{-1} wavelength, suggesting C=C absorption. Fraction 8 falls slightly out of the trend which can also be recognized in the higher HHV compared to the lighter fraction 7.

Table 4
Comparison of different crudes and the equivalent gasoline and diesel fractions.

Crude equivalent		Gasoline equivalent		Diesel equivalent	
	HHV (MJ/kg)		HHV (MJ/kg)		HHV (MJ/kg)
Crude oil[a]	45.5	Conventional gasoline	46.5	Low sulfhur diesel	45.6
HTL bio-crude[b]	40.43	Bio-crude fractions 1–3[b]	43.7	Bio-crude fraction 7–10[b]	42.4
Capunitan et al.[c]/Corn stover PO[c]	35.4	Fraction (100–180 °C)[c]	37.3	Fraction (180–250 °C)[c]	37.0
Elliott[d] Wood based HTL oil[d]	36.8	Fraction (up to 138 °C)[d]	37.2	Fraction (266–382C)[d]	35.9
NA		Bio-ethanol[a]	29.8	FAME[a]	40.2

[a] [16].
[b] Weighted average.
[c] [17].
[d] [7].

Table 5
Bio-crude and fraction analysis.

	Bio-crude	Cold trap	Fraction 1 (100–125 °C)	Fraction 2 (125–150 °C)	Fraction 3 (150–175 °C)	Fraction 4 (175–200 °C)	Fraction 5 (200–225 °C)	Fraction 6 (225–250 °C)	Fraction 7 (250–275 °C)	Fraction 8 (275–300 °C)	Fraction 9 (300–325 °C)	Fraction 10 (325–350 °C)	Fraction 11 (350–375 °C)	Res (>375 °C)	Balance
Proximate															
Ash (%)[a]	0.07	n.a	n.a	n.a	n.a	n.a	n.a	n.a	n.a	n.a	n.a	n.a	n.a	n.a	n.a
Ultimate															
C (wt.%)	83.88	n.a	84.44	85.72	85.54	84.27	84.88	84.49	85.34	86.12	87.15	88.12	88.21	81.95	83.322
H (wt.%)	10.41	n.a	13.47	12.29	12.64	12.57	12.54	12.17	11.85	12.82	11.87	11.27	10.48	8.16	10.156
N (wt.%)	0.40	n.a	[c]	[c]	[c]	[c]	[c]	[c]	[c]	[c]	[c]	[c]	[c]	[c]	
S (wt.%)	n.a.	n.a	[c]	[c]	[c]	[c]	[c]	[c]	[c]	[c]	[c]	[c]	[c]	[c]	
O (wt.%)[b]	5.31	n.a	2.09	2.18	1.64	3.17	2.59	3.34	2.80	1.06	0.99	0.61	1.31	9.89	5.385
H/C	1.489	n.a	1.914	1.724	1.769	1.789	1.772	1.728	1.667	1.786	1.634	1.535	1.425	1.195	1.463
O/C	0.047	n.a	0.019	0.019	0.014	0.028	0.023	0.030	0.025	0.009	0.008	0.005	0.011	0.091	0.048
$H/C_{effective}$	1.39	n.a	1.88	1.69	1.74	1.73	1.73	1.67	1.62	1.77	1.62	1.52	1.40	1.01	1.37
HHV (MJ kg^{-1})	40.43	42.21	43.89	43.69	42.83	42.46	42.17	41.61	42.15	43.23	42.16	42.31	41.77	38.58	40.803
Density ($kg\ m^{-3}$)[d]	970.3	620.0	792	835.5	867.2	884.9	906.9	911.7	926.5	931.2	950.5	952.9	995.7	n.a	
Yield (wt.%)	100	1.11	2.29	9.86	0.37	2.09	2.9	5.08	6.2	5.48	6.13	7.44	5.53	43.13	97.61

[a] Dry basis.
[b] Calculated by difference.
[c] Below calibration.
[d] At 15.6 °C.

Fig. 5 shows the elemental oxygen content of the HTL bio-crude and its fractions. Oxygen is present in all fractions. This is also supported by the FTIR results, compare 3.3.2. Fractions 4–7 contain higher amounts of oxygen, with the highest for fraction 6 with 3.34 wt.% resulting in a slightly lower HHV. The higher oxygen can also be seen in the FT-IR spectra through alcohol groups in these specific fractions. Fractions 1–3 have oxygen contents between 1.6 and 2.2 wt.%. Fractions 8–11 have a very low oxygen content of 0.6–1.3 wt.%. As expected the highest oxygen content can be found in the residue fraction with 9.9 wt.% resulting in a lower effective H/C ratio compared to the other fractions. The effective H/C ratio is generally used to estimate the upgrading/deoxygenation effort needed. The lower H/C_{eff}, the more severe the upgrading has to be.

Compared to conventional crude with an oxygen content of 0.05–1.5 wt.%, HTL bio-crude contains 5.3 wt.% overall and a minimum of oxygen 0.6 wt.% in fraction 10 and maximum of 9.9 wt.% oxygen in the residue. Approximately 25 wt.% (fractions 8–11) would not need deoxygenation prior to co-processing. The higher oxygen content compared to conventional crude also leads to a higher total acid number (TAN) of 36.8 mg KOH g^{-1}. A high acid number will lead to corrosion problems during refining and it is expected that oxygen.

3.3.1.2. Distillation balance. Fig. 6 shows the elemental and energy balance of the collected distillation product compared to the bio-crude that has been distilled. The amount of paraffinic distillation hold up could not be obtained since it stuck to the glass parts of the distillation set-up (condensers, fractionation arm) and no analysis could be done on it. Elemental analysis on the cold trap fraction could not be obtained as described earlier. These factors have to be considered when interpreting the balances. The total distillation loss sums up to 2.4 wt.%.

The highest error can be seen in the hydrogen balance. These deviations can be explained by the missing analysis of the cold trap and paraffinic fraction since the FTIR of the cold trap fraction suggest that it contains oxygen rich aliphatic ketones. Since nitrogen and sulfhur during elemental analysis were below the calibration value, and oxygen has been calculated by difference a slight error in the elemental balance is expected as well.

3.3.1.3. Density. The density increases with increasing boiling point as expected. In general the densities are higher than those of petroleum crude boiling in the same range. Fig. 7 visualizes the densities of HTL bio-crude fractions with the corresponding fractions of two different petroleum crude oils found in [15]. The figure also gives standard fuel specifications, it can be seen that the densities of the bio-crude fractions are higher than specifications, which is due to oxygenates present throughout every boiling fraction. Bio-crude fractions would need more extensive refinery processing in regard to decreasing the density compared to processing of conventional crude.

3.3.1.4. Higher heating value. The higher heating value (HHV) has been measured for the HTL bio-crude as well as for its fractions, compare Fig. 5. The HHV is rather constant throughout the fractions with the residue having the lowest HHV as expected and the cold-trap fraction having the highest. Fig. 5 also shows the dependency of HHV to the oxygen content, the lower the oxygen content the higher the HHV. To enable comparison of energy content of the HTL bio-crude to conventional fuels, bio-fuels and -oils from other conversion processes, state of the art literature data on HHV has been collected and listed in Table 4. It contains the HHV literature data of petroleum crude oil [16], corn stover pyrolysis oil [17], wood based HTL oil from the literature [7] and the HHV of their equivalent gasoline and diesel fractions. No fraction boiling

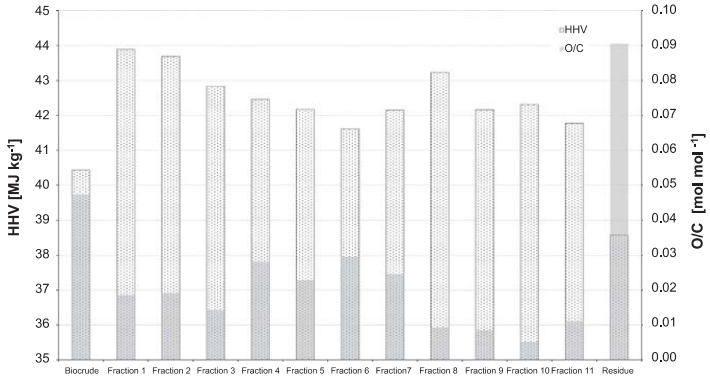

Fig. 5. Elemental oxygen content and HHV over the fractions.

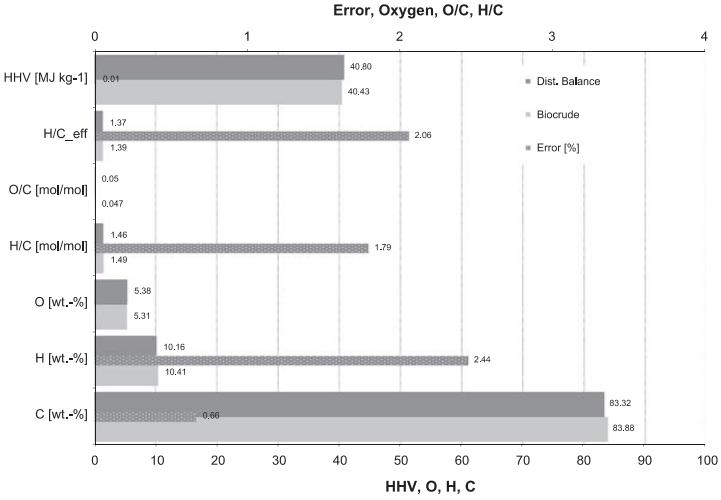

Fig. 6. Energy and elemental balance.

in the diesel range was distilled by Capunitan and Capareda [17], so the 180–250 °C is used for comparison. The HHV of pyrolysis oil and the Elliott wood based HTL oil and their fractions are significantly lower, whereas the HTL bio-crude and its fractions are slightly lower than the conventional crude oil and the respective gasoline and diesel equivalent. The HHV of bio-ethanol and FAME are also given for comparison with the HTL bio-fractions. These biofuels are presently used to a great extend worldwide, but with limitations on drop-in ability and mileage. Considering the HHV only, the HTL bio-crude shows potential as a sustainable fuel providing a longer mileage than bio-ethanol and FAME. Furthermore, unlimited refinery drop-in ability is believed to be achievable by deoxygenation prior to co-processing.

3.3.2. FTIR analysis

Interpretation of the main bands in the FTIR absorption spectra was based on [18,19]. The overall bio-crude FTIR is hard to interpret and analyzing the fractions as well gives a clearer idea of the functional groups present in the crude. In Figs. 9 and 10 the FTIR spectra of the bio-crude fractions compared to conventional refinery cuts are being presented. In Fig. 8 fractions 1 and 2 and the CBS27 bio-crude are shown. The bio-crude and consequently all fractions show 3 medium-strong sharp C-H peaks around 2853–2955 cm^{-1} along with the C—C peak at 1450 cm^{-1} and absorptions at 1375 cm^{-1} and 720 cm^{-1} which indicate paraffinic hydrocarbons. The stronger intensity of the 3300–3600 cm^{-1} band (—OH stretch) and the C—O stretch at 1260–1050 cm^{-1} for the overall bio-crude suggest the presence of alcohol and carbonyl functional groups, and underline the presence of oxygenates in the crude.

Fig. 8 indicates with peaks at 2900, 1450, 1375, 720 that fractions 1 and 2 mainly contain aliphatic compounds with a distinct peak at 1715 cm^{-1} indicating aliphatic ketones for fraction 2. The FTIR of fraction 1 also indicates 5-membered cyclic ketones due to a sharp peak at 1745 cm^{-1}. The presence of aliphatic esters is underlined in fraction 1 by the presence of the carbonyl (C=O) stretch at 1745 cm^{-1} together with a C—O stretch between 1200 and 1300 cm^{-1}, the peaks at 1720 and 1745 cm^{-1} also suggest

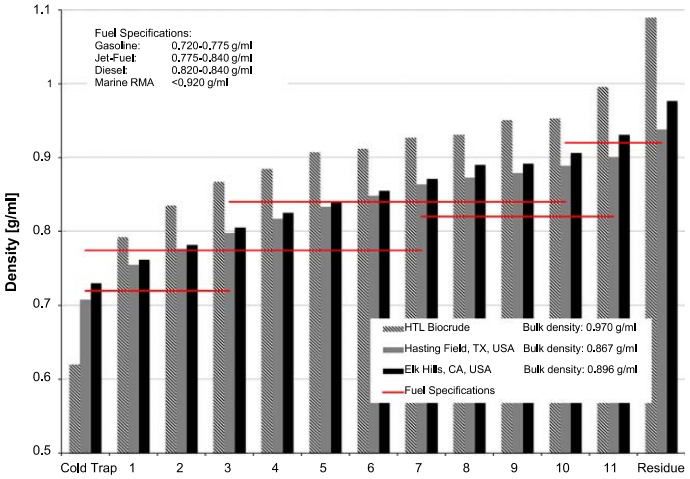

Fig. 7. Comparison of fraction densities to fuel specifications. Gasoline: fractions 1–3; jet-fuel: fractions 4–7, diesel: fractions 7–10, Marine Residual Fuels (RMA): fraction > 10, the density of the residue has been estimated.

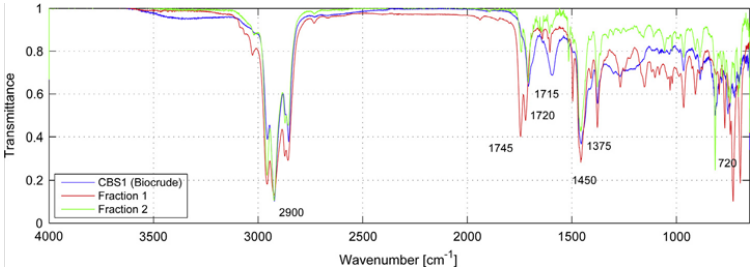

Fig. 8. Fractions 1 and 2 and bio-crude feed.

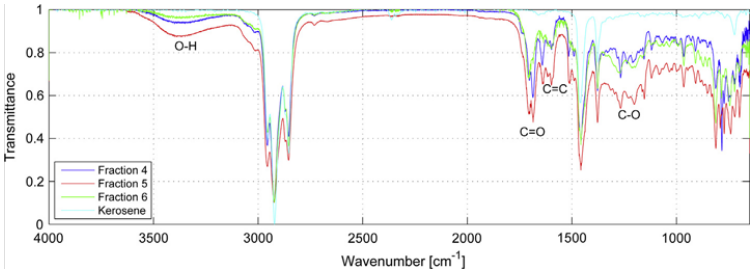

Fig. 9. FT-IR diagram of fractions 4–6 compared to kerosene.

unsaturated esters for fraction 1. The C—O stretch also suggests the presence of ethers in fraction 1. Table 6 shows a summary of possible functional groups in the fractions.

Fig. 9 compares the kerosene fractions of the bio-crude to a conventional kerosene spectrum. It is apparent that differences can mainly be seen as oxygen containing carbonyl stretches. The kerosene FTIR diagram is less noisy and more distinct, which is probably due to the paraffinic and pure nature of kerosene. The FTIR diagrams of fractions 4–6 look quite similar, whereas fraction 5 seems to have a stronger intensity in the overall bands and peaks. The fractions also contain aliphatic compounds as well as cyclic. Alcohol functional groups are suggested due to O—H and C—O stretches as described earlier. Esters and ethers are indicated by absorption between 1735 and 1740 cm^{-1} (C=O) and due to the C—O absorption between 1200 and 1300 cm^{-1}. It is suggested that all 3 fractions contain cyclic compounds and more detailed

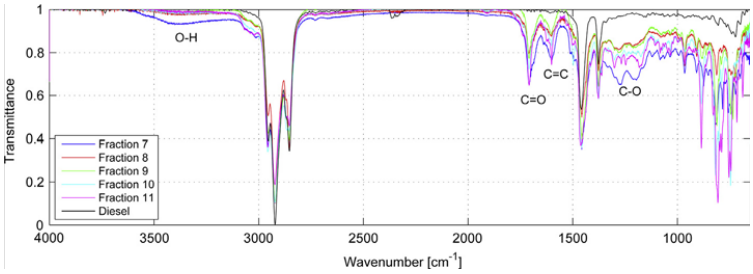

Fig. 10. FT-IR diagram of fractions 7–11 compared to diesel.

Table 6
Interpretation of FT-IR spectra of the various fractions. Only major absorptions are evaluated.

Sample	Hydrocarbon Structure	Functional Groups
Cold trap	Alkanes	Aliphatic ketones
Fraction 1	Alkanes	Aliphatic ketones 5-Membered cyclic ketone Esters/ethers
Fractions 2 and 3	Alkanes	Aliphatic ketones
Fractions 4–6	Alkanes Cyclic (less)	Alcohols Esters/ethers 7-Membered cyclic ketones
Fraction 7	Alkanes Substituted aromatics	Alcohols Esters/ethers Aromatic ketones
Fractions 8–11	Alkanes (less) Substituted aromatics	Esters/ethers Aromatic ketones
Residue	Substituted aromatics	Esters/ethers Carbonyl groups (less)

7-membered ketones due to the sharp peak at 1700 cm^{-1}, indicating a carbonyl group sitting on a 7-membered ring or larger [18].

Fig. 10 shows the FTIR diagram of diesel boiling range fractions (7–11) of the bio-crude compared to conventional diesel fuel. Diesel has a paraffinic nature, which becomes obvious looking at the IR spectra. The spectra of the 4 fractions indicate alkanes with peaks at 2900, 1450, 1375 and 720 cm^{-1}. Furthermore absorptions at 1500 to 1600 cm^{-1} indicate some aromatic compounds. The identified peak around 700–850 cm^{-1} suggests substituted aromatic compounds [18]. Fraction 7 also contains alcohol functional groups due to the O—H stretch between 3300 and 3600 cm^{-1} and the C—O stretch 1050–1150 cm^{-1}. Compared to conventional diesel fuels C—O (ester) stretches at wavenumbers <1300 cm^{-1} and the carbonyl C=O stretches with peaks at 1708 cm^{-1} of the bio-crude fractions make the main difference.

Fig. 11 shows the FT-IR spectra of the cold trap and distillation residue. Compounds in the cold trap have alkane structure due to C—H bond absorption from 2850 to 2960 cm^{-1} and methylene CH_2 scissoring at 1450 cm^{-1}. The additional peak at 1375 cm^{-1} indicates CH_3 methyl group. Functional groups in the cold trap are mainly saturated aliphatic ketones (C=O stretch at 1715 cm^{-1}).

The residue fraction with an H/C ratio of 1.18 is proposed to mainly contain aromatics. The significant peak at 1550 cm^{-1} along with the different peaks around 700–850 cm^{-1} indicate substituted aromatics. The clear C—H peaks around 2900, 1450 and 1375 cm^{-1} are probably related to substitution on aromatic rings. The high O/C ratio indicates oxygen containing functional groups, the strong broad peak at 1130 cm^{-1} indicates C—O bonding along with the carbonyl peak around 1745 cm^{-1} esters/ethers can be indicated.

3.3.2.1. Summary of FTIR analysis. Table 6 summarizes the expected compounds of the fractions and the residue according to the IR spectra.

4. Conclusion

Fractional distillation on HTL bio-crude has been carried out successfully with an overall mass recovery of 97.7% and a yield of 53.4 wt.% at AET 375 °C. It has been seen that HTL bio-crude is thermally stable and fractional separation under vacuum possible. A major outcome of this study is the distillation profile and the oxygen distribution along the temperature profile. Previous work on HTL non-destructive fractionation and analysis could not be found in literature.

The equivalent gasoline fraction of the bio-crude is relatively small at 12.5 wt.%, whereas the diesel and jet-fuel fraction are relatively large at 25.3 and 16.6 wt.% respectively. In terms of product

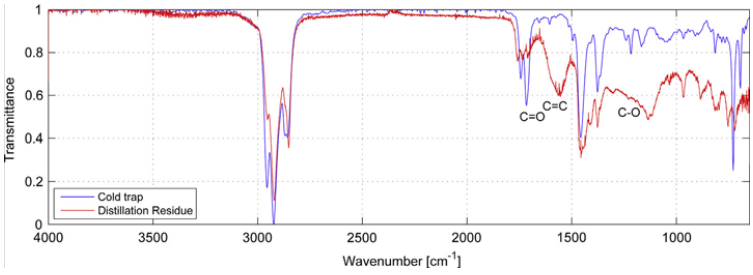

Fig. 11. FT-IR diagram the cold trap and the distillation residue.

value, the middle distillate region is expected to dominate future fuel markets. Elemental analysis and FTIR show that the oxygen content is distributed to a higher content in the gasoline and jet-fuel fraction (fractions 1–7) and to a lower content (0.86 wt.% O) in the mostly diesel range (fractions 8–10). To ensure compatibility during co-processing of the bio-crude to existing petroleum refinery infrastructures, bio-crude characteristics need to be similar to their petroleum counterparts. The overall HTL bio-crude would need light hydroprocessing to remove oxygenates prior co-processing, to prevent corrosion issues of processing equipment which will be studied in the 2nd part of this publication.

Nevertheless the overall co-processing potential of bio-crude from HTL is very promising. It would allow a straight forward introduction to the market and keeping in mind the current over capacities existing modern refineries, which are even expected to rise over the next years, co-processing of HTL bio-crude becomes even more appealing.

Acknowledgements

The authors are grateful to Steeper Energy ApS for providing state-of-the-art HTL bio-crude from the Continuous Bench Scale Unit. Additionally, we acknowledge with appreciation the Shell Refinery in Fredericia, Denmark for supplying hydrotreating catalyst and a sample of North Sea fossil crude oil. The authors would also like to acknowledge funding of this work by C3BO DSF Grant No. 1305-00030B and FlexiFuel Grant No. 10-094552.

References

[1] BP, BP statistical review of world energy 2014, 2014.
[2] International energy outlook, administration, U.S. energy information, 2010.
[3] Chang A-F, Pashikanti K, Liu YA. Refinery engineering. Weinheim: Wiley-VCH; 2012.
[4] Mortensen PM, Grundwaldt J, Jensen PA, Knudsen KG, Jensen AD. A review of catalytic upgrading of bio-oil to engine fuels. Appl Catal A 2011;407:1–19.
[5] Speight JG. Refinery of the future. Oxford: Elsevier; 2011.
[6] Jensen CU, Hoffmann J, Rosendahl LA. Co-processing potential of HTL bio-crude at petroleum refineries; Part 2: A parametric hydrotreating Study. 2015. http://dx.doi.org/10.1016/j.fuel.2015.08.047.
[7] Elliott D, Elliott DC. Process development for biomass liquefaction, 1980.
[8] Cheng D, Wang L, Shahbazi A, Xiu S, Zhang B. Characterization of the physical and chemical properties of the distillate fractions of crude bio-oil produced by the glycerol-assisted liquefaction of swine manure. Fuel 2014;130:251–6.
[9] International A. D2892 standard test method for distillation of crude petroleum (15-theoretical plate column), 2005.
[10] ASTM. D5236 standard test method for distillation of heavy hydrocarbon mixtures (vacuum potstill method), 1999.
[11] Montemayor RG. Distillation and vaor pressure measurement in petroleum products. ASTM International; 2008.
[12] ASTM. D5002 standard test method for density and relative density of crude oils by digital density analyzer. ASTM International; 2003.
[13] ASTM. D2887 standard test method for boiling range distribution of petroleum fractions by gas chromatography. ASTM International; 2014.
[14] TOTSA, 2006. <http://www.totsa.com/pub/crude/index2.php?&iback=3&rub=11&expand=3&image=europe>.
[15] Gary JH, Handwerk GE, Kaiser MJ. Petroleum refining, technology and economics. CRC Press; 2007.
[16] Boundy B, Diegel SW, Wright L, Davis SC. Biomass energy databook. 4th ed. Office of the Biomass Program, U.S. Department of Energy; 2011.
[17] Capunitan JA, Capareda SC. Characterization and separation of corn stover bio-oil by fractional distillation. Fuel 2013;112:60–73.
[18] Nakanishi K. Infrared absorption spectroscopy: practical. Nankodo Company Limited; 1962.
[19] Wade LG. Organic Chemistry volume 1. 8th ed. Prentice Hall; 2013.

Paper F

Co-processing Potential of HTL Bio-crude at Petroleum Refineries - Part 2: A Parametric Hydrotreating Study

Claus Uhrenholt Jensen, Jessica Hoffmann, Lasse A. Rosendahl

The manuscript has been published in the
Journal of Fuel, vol. 165, pp. 536–543, 2016.

The layout has been revised.

Fuel 165 (2016) 536–543

Contents lists available at ScienceDirect

Fuel

journal homepage: www.elsevier.com/locate/fuel

Co-processing potential of HTL bio-crude at petroleum refineries. Part 2: A parametric hydrotreating study

Claus Uhrenholt Jensen [a,*], Jessica Hoffmann [b], Lasse A. Rosendahl [b]

[a] Steeper Energy ApS, Sandbjergvej 11, DK-2970 Hørsholm, Denmark
[b] Aalborg University, Department of Energy Technology, Pontoppidanstræde 101, DK-9220 Aalborg, Denmark

ARTICLE INFO

Article history:
Received 16 March 2015
Received in revised form 5 August 2015
Accepted 20 August 2015
Available online 1 September 2015

Keywords:
Biooil
Hydrotreating
Hydrothermal liquefaction
Co-processing
Biomass
Upgrading

ABSTRACT

An experimental study on hydrotreatment of ligno-cellulosic hydrothermal liquefaction (HTL) bio-crude to achieve a bio-feed compatible for co-processing at a refinery was made to investigate the effect of operating temperature, pressure and hydrogen to oil ratio. Using a conventional $NiMo/Al_2O_3$ hydrotreating catalyst at 350 °C and 337 NL H_2/L bio-crude, a promising bio-feed with 0.3 wt.% O, a HHV of 43.9 MJ/kg, a density of 894 kg/m^3 and an FT-IR spectra very similar to Northern Sea fossil crude oil was obtained. This work suggests that a gradual and sustainable phase-in of bio-feed through co-processing at existing refineries can be facilitated by intermediate hydrotreating of the bio-crude from hydrothermal liquefaction.

1. Introduction

Global energy demand in the transportation sector is increasing due to emerging markets and global growth [1]. The energy supply is however limited by depleting petroleum resources and decreasing resource quality [2]. Fig. 1 emphasises how the input to refineries on a long term scale is of decreasing quality, due to increasing densities and sulphur contents. The sulphur content has almost doubled since 1985, while sulphur allowances in fuel products are becoming stricter with a recent EU directive reducing the allowed sulphur content in marine fuel from 3.5% to 0.5% by 2020 [3]. Furthermore, it is a fact that greenhouse gas (GHG) emissions rise with refining of heavier crudes [4]. Meanwhile, environmental concerns necessitate ambitious efforts in mitigating GHG emissions. To resolve the mismatch between increasing environmental concerns, a growing energy demand and depleting resources of declining quality, the global dependence on fossil resources within transportation must be replaced by partly electric engines and partly a renewable feedstock that encloses the CO_2 cycle [5]. Pyrolysis and hydrothermal liquefaction (HTL) are thermochemical processes capable of converting biomass into liquid energy carriers [6]. In particular, HTL enables a feedstock-flexible conversion of non-food biomass to a liquid bio-crude with a higher heating value (HHV) reported around 35–40 MJ/kg [7], but recently measured above 40 MJ/kg [8]. Part 1 of this publication presents a TBP distillation curve for a HTL bio-crude with a large middle distillate fraction and around 47 wt.% atmospheric residue (>375°). Additionally, HTL bio-crudes possess higher quality than pyrolysis bio-oils as intermediate for biofuel production [9], due to oxygen contents around 5–10 wt.%, lower contents of corrosive carboxylic acids, kinematic viscosities as low as 10–20 cSt and lower water content around 0–5 wt.% depending on the separation method [8]. Though, with the above mentioned characteristics, the HTL bio-crude is still an intermediate that needs further, but significantly less, upgrading to be classified as compatible with existing transportation infrastructure [10]. In 2014 an extensive technoeconomic and lifecycle assessment made for the U.S. Department of Energy modelled the large scale production cost of liquid fuels from wood by pyrolysis+hydrotreating and HTL+hydrotreating respectively. HTL was concluded both more energy efficient and cheaper compared to pyrolysis and the production cost of a completely deoxygenated HTL fuel was estimated to 0.53 $ per litre gasoline equivalent [9]. The study is considered the most updated of its kind and the conclusions emphasise HTL as a relevant technology for drop-in biofuel production. Fig. 2 illustrates the HTL path from biomass feedstock to direct drop-in biofuel or bio-crude compatible for co-processing at an existing refinery.

Co-processing bio-crude with petroleum crude oil at existing facilities is considered a potential method towards obtaining com-

* Corresponding author. Tel.: +45 29 46 86 12.
E-mail address: cuj@steeperenergy.com (C.U. Jensen).

http://dx.doi.org/10.1016/j.fuel.2015.08.047
0016-2361/

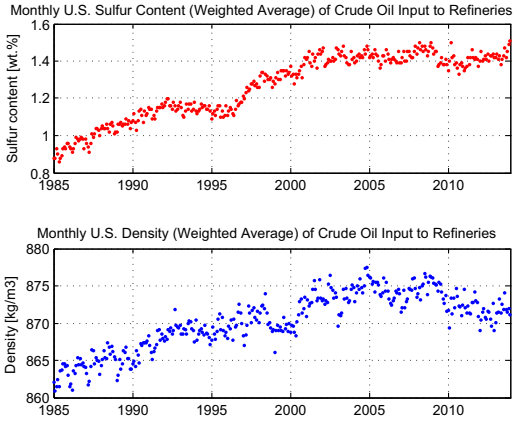

Fig. 1. Petroleum crude oil feeding U.S. refineries are generally becoming heavier and contain more sulphur [2].

petitive production prices of drop-in biofuels [11,4,12]. A currently accepted dogma that biofuels must be delivered as finished, transport grade fuels, is associated with costly drawbacks. Firstly, a potential bio-refinery that produces final fuel products from bio-crude only, requires complex and thus expensive processing units that can handle a varying bio-crude composition in order to produce on-specification products. This is due to the heterogeneous nature of biomass that the bio-crude will be made from [12,13]. Secondly, market penetration will become difficult by competing rather than cooperating with the petroleum industry. By co-processing the bio-crude at conventional refineries the point of market introduction is moved upstream, which make it an attractive market proposition compared to producing transport grade finished fuels. This paper will focus on the required upgrading path for HTL biocrude to be refinery co-processing compatible. Specifically, a parametric study on the influence of temperature, pressure and hydrogen availability is made to show that upgrading HTL bio-crude to a fossil substitute with unlimited drop-in abilities seem to be a promising addition to the overall conversion of biomass to refinery bio-feed.

Fig. 3 illustrates the concept of co-processing petroleum and bio-crude oil. For illustrative purposes, the drop-in location is chosen prior to the distillation column in this specific example, but may be located differently as discussed later. Given that the bio-crude has unlimited drop-in abilities, unlike bio-ethanol and bio-diesel, the drop-in percentage may be increased gradually along with an increase in the production capacity of the bio-crude. A gradual increase of the drop-in percentage enables a smooth phase-in, where feasibility of co-processing and availability of both bio- and petroleum crude oil can be balanced.

1.1. Refinery's perspective on co-processing

Bio-crude forms an alternative source of feedstock for the refinery. A feedstock that matches a demand for renewable fuel products that is likely to grow with global focus on sustainable energy resources [12]. Additionally, a feedstock that forms an alternative, when expenses related to processing crude oil increases due to a decrease in crude oil quality [12]. Finally, co-processing ensures full usage of capital intensive refinery capacity on a long term basis.

Bio-crudes that are possible alternatives for petroleum crude oil as refinery feedstock are sometimes included in the class of opportunity crudes [12]. Characteristics that make opportunity crudes differ from the benchmark petroleum crude include a TAN above 1 mg of KOH/g oil and a higher overall density (>900 kg/m^3) [12]. An opportunity crude is not necessarily renewable, but the characteristics match those of the HTL bio-crude studied in present study. Corrosion issues in refinery units are increased by processing a high TAN feedstock. Likewise, fouling, cetane reduction and product stability are risks that arise with the processing of an

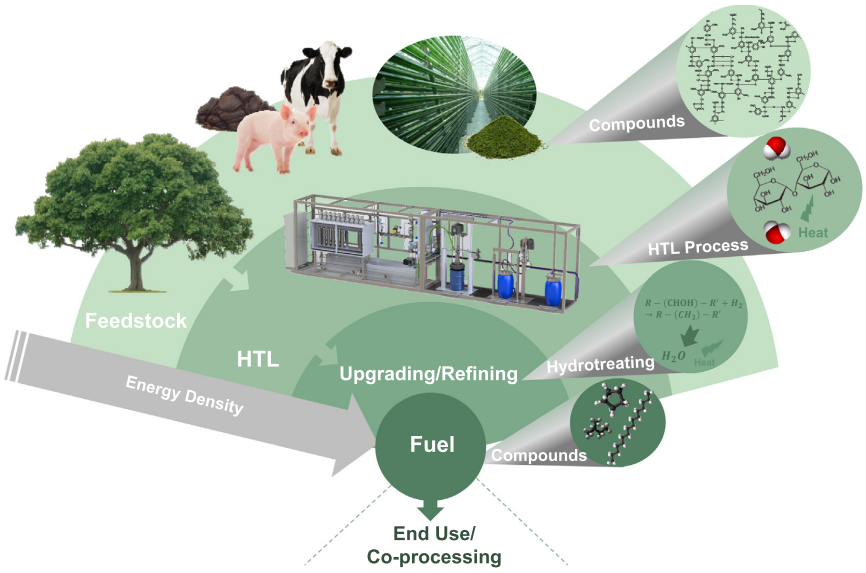

Fig. 2. HTL conversion of biomass to bio-crude, and subsequent upgrading/refining of the intermediate into drop-in biofuel [10].

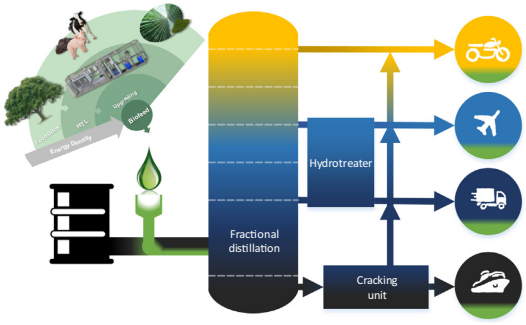

Fig. 3. Co-processing enables a gradual phase-in of the use of biofuels in existing infrastructure. The drop-in percentage of liquid biofuels into conventional liquid fuels is depicted with green in the different product circles. (For interpretation of the references to colour in this figure legend, the reader is referred to the web version of this article.)

opportunity crude. As a result, opportunity crudes are often sold at a discount compared to benchmark crude oils [12]. However, bio-crudes will probably not be sold at a discount, due to the sustainability element and the fact that a refinery will obtain operational cost savings through CO_2 reduction, when off-setting petroleum crude with bio-crude.

1.2. Considerations on the drop-in location

What is the appropriate drop-in location in relation to co-processing petroleum and bio-crude oil? Refineries are designed differently, due to the fact that crude oils have very different characteristics, depending on the origin. Thus, the specific quality requirement to a bio-crude that must be met to enable co-processing, depends on the particular refinery. Though, generally most of the heteroatom removal operations are focused on the heavy boiling fractions, since it is characteristic for all petroleum crude oils that the concentration of heteroatoms (N,S,O) increase with boiling point [13]. As a result, a similar distribution of heteroatoms is required in the bio-crude to enable blending of petroleum and bio-crude at the front end of a refinery as depicted in Fig. 3. Part 1 of this publication investigates heteroatom distribution in HTL bio-crude as function of boiling point by use of 15:5 fractional distillation and subsequent analysis. It is concluded that heteroatoms are distributed evenly in every boiling fraction. This is an issue in relation to co-processing, but may be overcome by an intermediate upgrading step prior to blending, where heteroatoms in the low boiling fractions are removed by mild operating conditions.

Alternatively, the bio-crude should be blended with the 'dirty' ADU (Atmospheric Distillation Unit) residue prior to various cracking units. This option is suggested in numerous studies on co-processing, where pyrolysis and vegetable oils are blended with heavy gas oil and treated under FCC [14–16] or hydroprocessing conditions [4,17]. This option however, introduces an imbalance in volume flow in the refinery, since the capacity of the residue processing units must be increased if a significant amount of bio-crude is blended in prior to these units. Furthermore, HTL bio-crude is considered of too high quality to do the blending in the residue end of a refinery. Consequently, this study focus on the possibility of upgrading HTL bio-crude into a biofeed with unlimited drop-in abilities that can be blended with petroleum bio-crude prior to the ADU.

1.3. Deoxygenation of HTL bio-crude

HTL bio-crudes have low (<0.5 wt.%) sulphur and nitrogen contents due to the origin from ligno-cellulosic biomass [6,8]. Thus, deoxygenation of HTL bio-crude is the major object of hydrotreating. Due to the relatively high appearance of hydroxy and carbonyl groups in HTL bio-crude (see Part 1), deoxygenation is mainly expected to follow the hydrogenation (HYD) then hydrodeoxygenation (HDO) reaction path [11,18–20]. Due to the innumerable chemical species detected in biocrudes, many different reactions e.g. deoxygenation through decarboxylation and decarbonylation will occur. These pathways are however considered less important, since the precursors for such reactions are carboxylic acids and aldehydes [11,21], which were found in relatively low concentrations in the current bio-crude (see Part 1).

A common characteristic of different petroleum crude oils is that the heteroatom content is a function of boiling point. There is roughly no traces of N and S in the low boiling point fractions, whereas the major part of total N and S atoms are concentrated in the high boiling components [13]. In relation to bio-crude co-processing in existing utility, a similar distribution of heteroatoms in the bio-crude is required. However, it is concluded in Part 1 that oxygenates appear in significant quantities throughout every fraction of HTL bio-crude. In the same paper FT-IR spectra visualised, how the oxygenates appear in different configurations depending on the boiling range. Different oxygenates have different deoxygenation reactivity. Fig. 4 orders the HDO reactivity and hydrogen consumption during HDO of different oxygenates.

The oxygenates present in this particular HTL bio-crude are mainly medium to high HDO reactivity compounds, such as phenols, alcohols, carbonyls and carboxylic acids. See Part 1 for more details on the bio-crude composition. This is satisfactory, since the process conditions can be eased and the hydrogen consumption will be in the low end. This makes the deoxygenation step prior to co-processing less costly. Though, based on the FT-IR additional phenols, cyclic ketones, esters and ethers are also expected in the higher boiling fractions. Most likely as part of polycyclic structures in the residue fraction. Deoxygenation of these require severer conditions and consumes more hydrogen due to hydrogenation of the aromatics. Meanwhile, it may turn out that

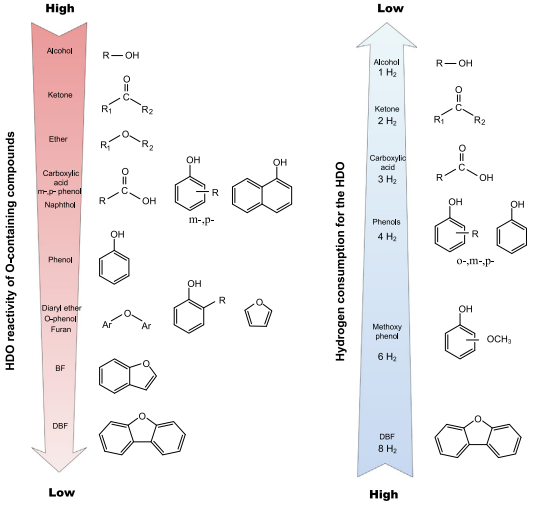

Fig. 4. HDO reactivity and hydrogen consumption associated with complete deoxygenation of different oxygenates by HDO [22].

relatively mild HDO will convert enough medium to high HDO reactivity oxygenates to facilitate co-processing at a refinery. In fact, it is considered an ideal outcome, if the deoxygenation step prior to co-processing can be designed to convert all the medium to high HDO reactivity oxygenates in the bio-crude. Thereby, only the low HDO reactivity oxygenates that require severe process conditions and consume relatively large amounts of hydrogen are remaining in the bio-crude. These cyclic oxygenates are mostly expected in the residue fraction, and in a refinery the residue fractions is directed to robust process units, where severe conditions are used to remove heteroatoms and reduce the boiling point distribution by cracking reactions [13]. The process conditions used in these particular units, should be sufficient to convert the remaining oxygenates present in the bio-crude into pure hydrocarbons.

The above discussion forms the objective of the current parametric study, where tuning of hydrotreating severity enables adjustment of the product properties in order to achieve a co-processing compatible bio-feed.

2. Experimental section

2.1. Materials

2.1.1. HTL bio-crude

An advanced hydrothermal research facility, the Continuous Bench Scale 1 (CBS1), was installed at Aalborg University in 2013. It is bio-crude from this facility, designed and constructed by Steeper Energy ApS, that is subject to hydrotreating in present study. The CBS1 unit has provided very promising and state-of-the-art leading results with respect to oil quality [7]. The particular bio-crudes applied in present study have been obtained from processing ligno-cellulosic biomass (hardwood, 20 kg/h) with supercritical water at ≈400 °C and ≈320 bar [8]. Properties of the dehydrated bio-crude subject to upgrading are listed in Table 1. Details and dehydration procedure can be found in Part 1 of the publication.

2.1.2. Catalyst

The Shell Refinery in Fredericia, Denmark has provided a conventional $NiMo/Al_2O_3$ hydrotreating catalyst in the form of spherical pellets that are preactivated and stabilised. At the refinery this catalyst is applied in hydrotreatment of diesel and jet-fuel streams at 340 °C and 60 bar. Pre-sulfided $NiMo/Al_2O_3$ catalysts are associated with good HDO conversion based on a review by Furimsky [11].

2.2. Experimental set-up

The experimental set-up consists of two 25 ml Swagelok microbatch reactors, a Techne SBL-2D fluidised sandbath and a specially designed shaking device to enable mixing of the reactants. Finally, the set-up features temperature and pressure measurements. Fig. 5 illustrates a flowchart of the experimental procedure, while Table 2 lists details on the procedure and subsequent analysis. The range of operating temperatures is chosen to be relatively large to investigate the hypothesis about different HDO reactivity found by [11,18–20] and presented in relation to Fig. 4.

Reactant mixing in the microbatch reactors has been identified as a key issue that directly affects repeatability of experiments due to mass transfer limitations. To ensure reproducible results, comparable to those expected from continuous-flow operation, a shaking device is designed and every experiment is made in duplicates and compared. Three stainless steel balls (=4 mm) are added to each reactor to improve mixing of the heterogeneous reactants during shaking. The same steel balls are recycled in every experiment. Product gasses have not been analysed in present study so hydrogen consumption is estimated based on initial purge pressure and reaction pressure drop.

Table 1
HTL bio-crude subject to hydrotreating.

Density [kg/m^3]	HHV [MJ/kg]	Elemental Comp. [wt.%]				
		C	H	N	S	O
970[a]	40.43	83.9	10.4	0.4[b]	[b]	5.3[c]

[a] @ 15.6 °C.
[b] Below calibration limit.
[c] By difference.

3. Results and discussion

Table 3 presents the deoxygenation experiments conducted in this work, and the corresponding chemical and thermophysical properties of the hydrotreated oils. References will be made to this table throughout this Section. It must be mentioned that the nitrogen content measured by elemental analysis is below the calibration level for the instrument and thus they will not be commented.

Fig. 6 illustrates temperature and pressure measurements of a representative upgrading experiment. Sandbath temperature is relatively steady within ±5 °C, and rapid heat-up and cool-down are clear from the pressure changes at 0 and 2 h. Hydrogen consumption is marked with ΔP and together with almost matching pressure profiles of the two independent reactors, these indicate repeatability. All upgrading experiments presented in Table 3 have similar pressure profiles as in Fig. 6. Though, ΔP changes, since it reflects degree of conversion, which depends on operating conditions.

From the pressure profiles in Fig. 6 it seems that an equilibrium is approached after 2 h of reaction and that extending the reaction time is without benefit. To verify that this tendency is not due to deactivated catalyst, equal experiments, but with recycled catalyst, have been conducted three times, and in every case the pressure profiles are identical to the experiment with fresh catalyst. As a result, the gradual decrease of conversion must be related to either insufficient availability of hydrogen or reach of equilibrium at the particular operating conditions. Alternatively, the steady pressure could reflect that gaseous products such as CO_2 and CO are formed to a degree that equals the pressure reduction caused by hydrogen consumption. Decarbonylation and decarboxylation is however expected as minor reaction pathways at ⩽350 °C and relatively high pressures compared to dehydration reactions. This is partly based on literature [11,21], and partly due to the fact that the current HTL bio-crude contains few carboxylic acids and aldehydes (see Part 1) that are the precursors for decarbonylation and decarboxylation reactions. Water droplets are observed in all upgraded products indicating that deoxygenation follows the HDO mechanism. It is expected that carbonyl groups are hydrogenated into an alcohol intermediate by the metal sites of the $NiMo/Al_2O_3$ catalyst. Subsequently, alcohols are converted to the corresponding hydrocarbon under HDO by formation of water.

The degree of conversion is visible from the colour and viscosity of the upgraded bio-oils. Generally good conversion is reflected by a lower viscosity and a lighter colour relative to the bio-crude, which is also clear from Fig. 7. Furthermore, the odor becomes very similar to that characteristic for petroleum crude.

It is clear from Table 3 how bio-crude quality (HHV, density, oxygen content, H/C ratio) can be improved and approach that of petroleum crude oil during deoxygenation.

Potential coke and gas formation during hydrotreating are considered minor relative to liquid losses related to product separation

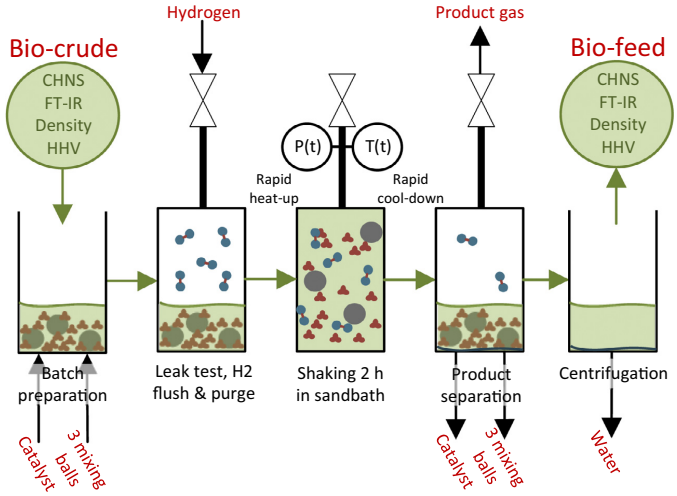

Fig. 5. Experimental procedure as flowchart. Bio-crude path marked with green. Material streams labelled with red. (For interpretation of the references to colour in this figure legend, the reader is referred to the web version of this article.)

Table 2
Experimental procedure.

Prior to experiment	
Catalyst	$NiMo/Al_2O_3$
Catalyst loading	0.20 g/g oil
Reactor volume	2 × 25 mL
Heating/cooling rate	>100 °C/min
Leaktested at	150 bar of N_2
Hydrogen flush	2 × 50 bar H_2
Op. conditions	
Temperature	150–350 °C
Pressure	55–140 bar
H_2/oil ratio	152–550 NL/L
Reaction time	2 h
Shaking frequency	450 min^{-1}
Analysis	
Centrifugation	3828 g, 30 min
Elemental analysis	Perkin-Elmer 2400 CHN
Bomb calorimeter	IKA C2000 Basic v2
FT-IR	Thermo Scientific Nicolet380
Density	Anton Paar DMA500

from catalyst and microbatch reactors. Thus, estimations on yield of upgraded bio-oil are left out of the current study in order not to present an inaccurate picture. Though, the liquid recovery including water was around 90 wt.% ±5 after product separation throughout all experiments. The present study focus on proof of concept and determination of a viable route towards obtaining a co-processing compatible bio-feed. This is done through a parametric study for which batch reactors are suitable. A detailed evaluation of the parametric study is given in the following.

3.1. Effect of hydrogen availability (HDO1-3)

Availability of hydrogen during hydrotreating is important to ensure maximum conversion and avoid catalyst deactivation [11]. Hydrogen availability is given as normal litre hydrogen per litre bio-crude (NL/L).

FT-IR spectra are given in Fig. 8 for the bio-crude and three different upgraded bio-oils that are hydrotreated with different hydrogen availability. Details on operating conditions and remaining analyses are given in Table 3. Fig. 8 clearly presents the reduction in absorbance of both alcohol-, carbonyl- and C—O bonds. Note also the significant hydrogenation that is visible from the reduction in C=C double bond absorption. More specifically, the IR spectra of HDO1, with a hydrogen availability of 152, reveals slight absorbance around 1715 cm^{-1}. This indicates incomplete deoxygenation and when comparing to HDO2 with a doubled availability of hydrogen, this incomplete deoxygenation seems to be caused by insufficient hydrogen. Furthermore, by comparing the IR spectra of HDO2 and HDO3, it can be concluded that increasing the hydrogen availability further does not have a clear impact on conversion. However, it needs mentioning that interpretation of FT-IR are qualitative only. According to Table 3 the HDO3 oil does have slightly better HHV, density and oxygen content compared to the HDO2 oil, and it must be mentioned that a higher hydrogen partial pressure is likely to have an improving effect on catalyst lifetime.

The IR spectra of a Northern Sea fossil crude oil provided by Shell is also given in Fig. 8. The difference between the IR spectra of the fossil and bio-crude are very distinct with respect to oxygen bonds and unsaturated carbon bonds. However, this difference is eliminated by hydrotreating the bio-crude with 355 NL H_2 per litre oil. In order to reduce operational costs associated with intermediate deoxygenation of the bio-crude it is both relevant to minimise hydrogen consumption, but also interesting to evaluate if the operating temperature can be lowered without sacrificing deoxygenation conversion.

3.2. Effect of operating temperature (HDO2;4-6)

Operating temperature is found to have significant influence on conversion during deoxygenation of the bio-crude. Pressure curves as function of operating temperature are given in Fig. 9 for the four different temperature set points investigated in present study. Different operating temperatures lead to different operating pressures at constant hydrogen availability in batch experiments. This explains the difference in operating pressure in Fig. 9. However, it will be presented in the next Subsection, how the effect of operating pressure is minor compared to temperature.

Table 3
List of experiments with operating conditions, chemical and thermophysical properties.

	Operating conditions			Density[a] [kg/m^3]	HHV [MJ/kg]	C	H	N[b]	S	O[c]	H/C ratio
	T [°C]	P_{max} [bar]	H_2/oil [NL/L]			[wt.%]					
Bio-crude	–	–	–	970	40.43	83.9	10.4	0.4	–[b]	5.3	1.48
Northern sea crude	–	–	–	846	44.4	86.6	13.1	–[b]	–[b]	0.3	1.80
Effect of hydrogen availability											
HDO1	350	94–100	152	911	43.49	87.7	11.6	0.3	–[b]	0.4	1.58
HDO2	350	95–98	355	904	43.73	87.5	12.0	0.2	–[b]	0.2	1.63
HDO3	350	97	550	890	43.88	87.4	12.1	0.4	–[b]	0.1	1.65
Effect of operating temperature											
HDO4	150	75	374	966	40.58	83.8	10.8	0.5	–[b]	5.0	1.54
HDO5	250	84–86	356	943	40.90	83.9	11.0	0.5	–[b]	4.6	1.56
HDO6	300	93–96	355	927	42.51	86.2	11.5	0.5	–[b]	1.8	1.59
HDO2	350	95–98	355	904	43.73	87.5	12.0	0.2	–[b]	0.2	1.63
Effect of operating pressure											
HDO6	300	93–96	355	927	42.51	86.2	11.5	0.5	–[b]	1.8	1.59
HDO7	300	134	318	925	42.67	86.5	11.7	0.2	–[b]	1.6	1.60
HDO8	350	62–63	338	902	43.50	86.5	11.6	0.6	–[b]	1.3	1.60
HDO2	350	95–98	355	904	43.73	87.5	12.0	0.2	–[b]	0.2	1.63
HDO9	350	146–148	337	894	43.90	87.2	12.2	0.4	–[b]	0.3	1.67

[a] Density @ 15.6 °C.
[b] N & S below calibration limit.
[c] Oxygen by difference.

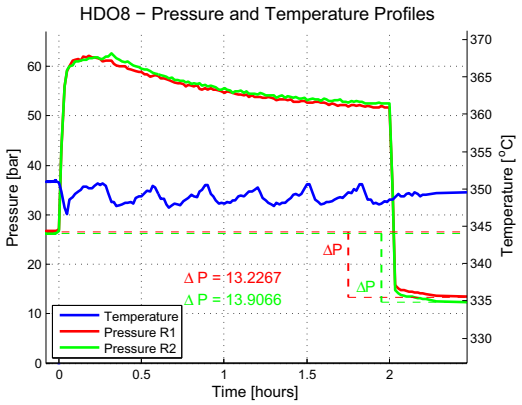

Fig. 6. Temperature and pressure data from HDO8. The two independent reactors (R1 and R2) indicate repeatability.

The pressure profile at 150 °C is rather constant with a small ΔP, indicating only little conversion. Generally the pressure profiles change from linear at the low operating temperature to more polynomic at higher operating temperatures. This matches an expectation of kinetics being the rate determining parameter at low temperatures, whereas concentration of reactants most likely become rate determining at higher temperatures.

Fig. 10 illustrates the IR spectra of the four upgraded bio-oils that have been exposed to different operating temperatures. The effect of temperature is clear from change in absorbance of both oxygen bonds and unsaturated carbons. Significant absorption in e.g. the carbonyl range is still present from the bio-oils hydrotreated at 300 °C. The elemental analysis, density and HHV measurements in Table 3 also indicate incomplete deoxygenation at lower temperatures than 350 °C. The objective presented in relation to Fig. 4 is to convert medium to high reactivity oxygenates, which includes all carbonyl groups. Thus it is concluded based on the variation of temperature that operating temperatures above 300 °C is required.

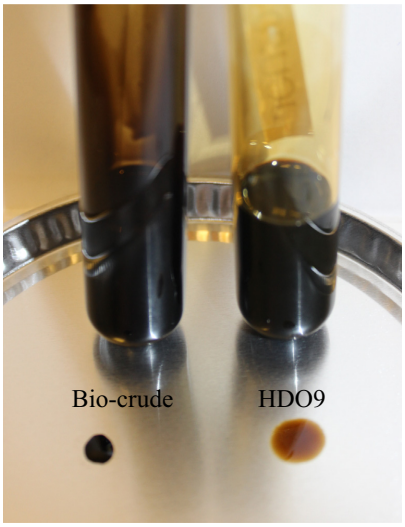

Fig. 7. Picture of raw bio-crude and upgraded bio-feed to visualise colour change. (For interpretation of the references to colour in this figure legend, the reader is referred to the web version of this article.)

3.3. Effect of operating pressure (HDO2;6-9)

Operating pressures effects on conversion during hydrotreating are investigated at an operating temperature of 350 °C. At lower operating temperatures it has been found that the effect of pressure is less visible. This can be inferred from HDO6 and HDO7 in Table 3, where the chemical and thermophysical properties are very similar. This is believed to be due to the significant influence operating temperature has on conversion, eliminating the effect of pressure.

Fig. 11 presents IR spectra of the upgraded bio-oils hydrotreated at 350 °C under different operating pressures. The effect of pressure is evident from the saturation of carbon–carbon double bonds,

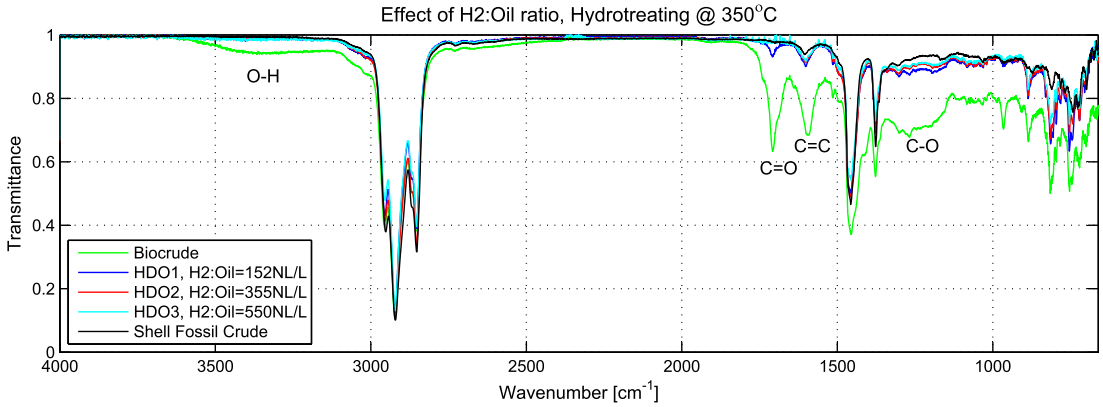

Fig. 8. Normalised FT-IR spectra of bio-crude and bio-feeds upgraded with different hydrogen availability.

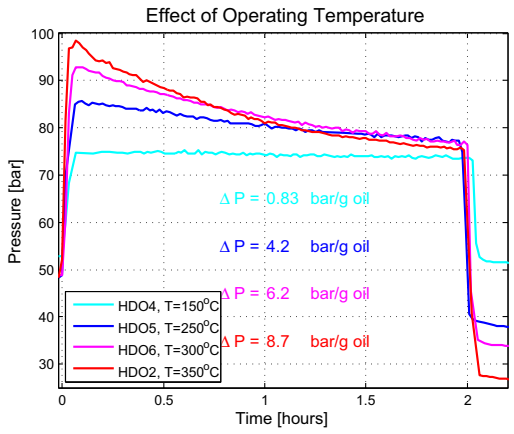

Fig. 9. Pressure curves obtained during hydrotreating at different temperatures. Read ΔP as indicative values.

which absorb infrared light at 1600 cm^{-1}. As expected, a higher operating pressure increase the saturation that also leads to a lower density and a higher HHV, which matches the analysis in Table 3.

Elemental analysis of HDO8 indicate incomplete deoxygenation compared to HDO2 and HDO9 that were hydrotreated at higher operating pressures. The IR spectra of HDO8 does not show any alcohol or carbonyl absorption, so remaining oxygenates are mainly expected as ethers absorbing infrared light around 1200 cm^{-1}. Based on this, pressure can be concluded to have an effect on deoxygenation of the low reactivity oxygenates at 350 °C.

In relation to co-processing, the crude oils that feed different refineries have different properties with respect to amount of heavy residue, heteroatom content and e.g. the correlation index, which is a measure of how parafinnic or cyclic a crude oil is [13]. Qualitatively, the IR spectra of HDO9 in Fig. 11 indicates significant similarities with the Northern Sea fossil crude oil, which is a quite parafinnic crude oil. To substitute a different crude oil with a more aromatic nature, the operating pressure can be lowered to decrease saturation and not overdo the upgrading. Likewise, the operating conditions of HDO8 might be sufficient to enable refinery co-processing, since complete deoxygenation of low reactivity oxygenates may be excessive. In other words, tuning of hydrotreating

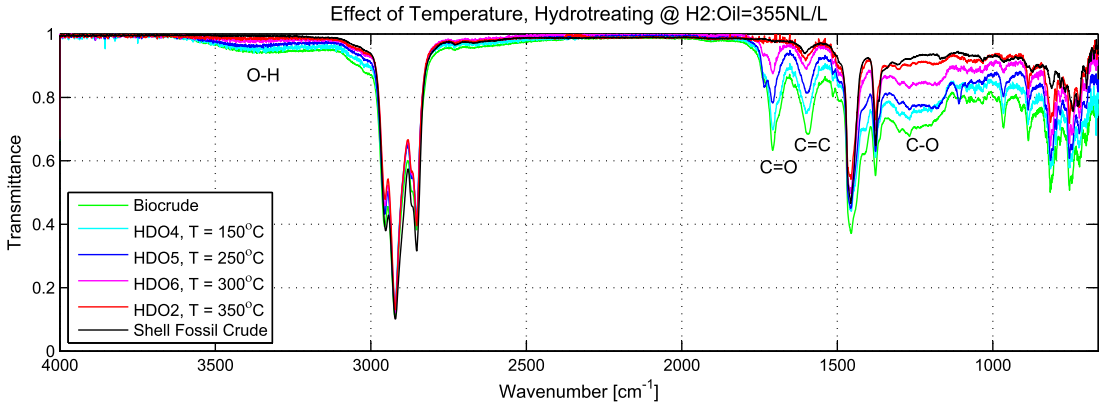

Fig. 10. Normalised FT-IR spectra of bio-crude and bio-feeds upgraded under different operating temperatures.

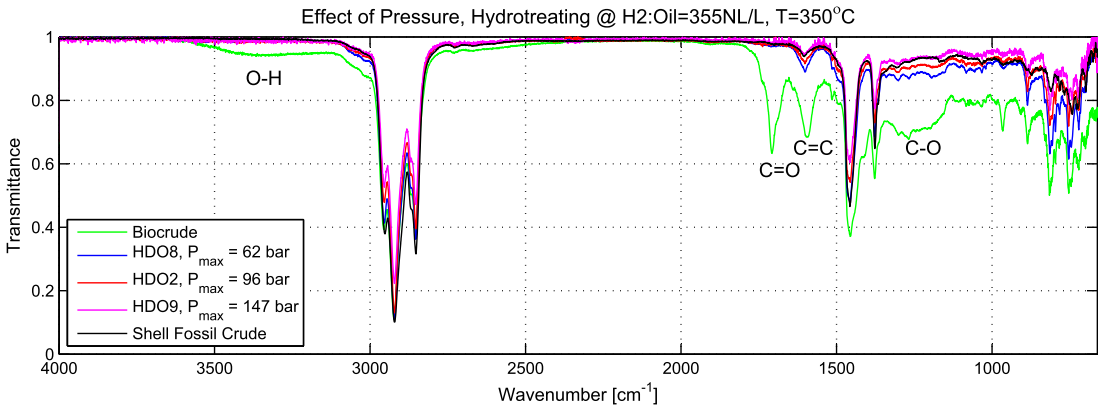

Fig. 11. Normalised FT-IR spectra of bio-crude and bio-feeds upgraded under different operating pressures.

severity enables adjustment of the product properties required for substitution of a particular fossil crude.

4. Conclusions

The present study focuses on proof of concept and determination of a viable route towards obtaining a co-processing compatible bio-feed. This is done through a parametric study on hydrotreating HTL bio-crude in micro-batch reactors using conventional $NiMo/Al_2O_3$. Operating temperature and hydrogen to oil ratio are found to have key influence on HDO and HYD conversion, while operating pressure mainly affects degree of HYD and HDO of low reactivity oxygenates. 350 °C, 95 bar and 355 NL/L is required to achieve good HDO conversion and at these conditions a bio-feed with 0.3 wt.% O, HHV above 43.7 MJ/kg and density below 904 kg/m^3 was obtained. Furthermore, FT-IR spectra of the bio-feed showed significant similarities with that of Northern Sea fossil crude. Given these encouraging results, intermediate hydrotreating seem to be a promising path to effectively deoxygenate HTL bio-crude to achieve a bio-feed compatible for co-processing at a refinery.

Acknowledgements

The authors are grateful to Steeper Energy ApS for providing state-of-the-art HTL bio-crude from the continuous facility at Aalborg University. Additionally, we acknowledge with appreciation the Shell Refinery in Fredericia, Denmark for supplying hydrotreating catalyst and a sample of Nothern Sea fossil crude oil. The authors would also like to acknowledge funding of this work by C3BO DSF Grant No. 1305-00030B and FlexiFuel Grant No. 10-094552.

References

[1] EIA. International energy statistics; 2014. <www.eia.gov>.
[2] EIA. U.S. refinery crude oil input qualities; 2014. <www.eia.gov>.
[3] EMSA. The 0.1% sulphur in fuel requirement as from 1 January 2015 in SECAs. Tech rep. European Maritime Safety Agency; 2010.
[4] Chen J, Farooqi H, Fairbridge C. Experimental study on co-hydroprocessing canola oil and vacuum gas oil blends. Energy Fuels 2013(27):3306–15.
[5] EG FTF. Future transport fuels. Tech rep. European Expert Group on Future Transport Fuels; 2011.
[6] Toor S, Rosendahl L, Rudolf A. Hydrothermal liquefaction of biomass: a review of subcritical water technologies. Energy 2011;36(5):2328–42.
[7] Jin F. Application of hydrothermal reactions to biomass conversion. Springer; 2014. iSBN:978-3-642-54457-6.
[8] Steeper Energy ApS and Aalborg University and Aarhus University. Turning low value commodities into high value syncrude. Technical report EUDP grant no 64012-0004; 2014.
[9] Tews I, Zhu Y, Drennan C, Elliott D, Snowden-Swan L, Onarheim K, et al. Biomass direct liquefaction options: technoeconomic and life cycle assessment. Tech rep. Prepared for U.S. Department of Energy; 2014.
[10] Hoffmann J. Biooil production, process optimization and product quality. Tech rep. Aalborg University; 2013.
[11] Furimsky E. Hydroprocessing challenges in biofuels production. Catal Today 2013;217:13–56.
[12] Speight JG. The refinery of the future. Elsevier Inc.; 2011. iSBN-13:978-0-8155-2041-2.
[13] Gary JH, Handwerk GE, Kaiser MJ. Petroleum refining. Technology and economics. CRC Press; 2007. iSBN:0-8493-7038-8.
[14] Mercader FDM, Groeneveld M, Kersten S, Way N, Schaverien C, Hogendoorn J. Production of advanced biofuels: co-processing of upgraded pyrolysis oil in standard refinery units. Appl Catal B: Environ 2010;96:57–66.
[15] Fogassy G, Thegarid N, Toussaint G, van Veen AC, Schuurman Y, Mirodatos C. Biomass derived feedstock co-processing with vacuum gas oil for second-generation fuel production in FCC units. Appl Catal 2010;96:476–85.
[16] Lappas A, Bezergianni S, Vasalos I. Production of biofuels via co-processing in conventional refining processes. Catal Today 2008;145:55–62.
[17] Huber GW, O'Connor P, Corma A. Processing biomass in conventional oil refineries, production of high quality diesel by hydrotreating vegetable oils in heavy vacuum oil mixtures. Appl Catal 2007;329:120–9.
[18] Mohammad M, Kandaramath T, Yaakob Z, Sharma YC. Overview on the production of paraffin based-biofuels via catalytic hydrodeoxygenation. Renew Sust Energy Rev 2013;22:121–32.
[19] Furimsky E. Catalytic hydrodeoxygenation. Appl Catal A: Gen 2000;199 (2):147–90.
[20] Durand R, Geneste P, Moreau C, Pirat J. Heterogeneous hydrodeoxygenation of ketones and alcohols on sulfided $NiO-MoO_3/\gamma-Al_2O_3$ catalyst. J Catal 1984;90:147–9.
[21] Mortensen P, Grunwaldt J, Jensen P, Knudsen K, Jensen A. A review of catalytic upgrading of bio-oil to engine fuels. Appl Catal A: Gen 2011;407:1–19.
[22] Hoffmann J, Pedersen TH, Rosendahl LA. Near-critical and supercritical water and their applications for biorefineries. Springer; 2014. iSBN 978-94-017-8922-6, [chapter 14].

Paper G

Process for producing low sulphur renewable oil

Steen Brummerstedt Iversen, Claus Uhrenholt Jensen, Julie Katerine Rodriguez Guerrero, Göran Olofsson

The patent application has been filed as
International PCT Application no. PCT/EP2017/067264.

Paper H

Separation system for high pressure process system

Steen Brummerstedt Iversen, Claus Uhrenholt Jensen, Julie Katerine Rodriguez Guerrero, Göran Olofsson

The patent application has been filed as
Danish patent application no. PA201770234.

Paper I

Heating system for high pressure process system

Steen Brummerstedt Iversen, Claus Uhrenholt Jensen, Andrew Ironside, Göran Olofsson

The patent application has been filed as
Danish patent application no. PA201700160.

Paper J

Continuous hydrothermal co-liquefaction of aspen wood and glycerol with water phase recirculation

T.H. Pedersen, I.F. Grigoras, J. Hoffmann, S.S. Toor, I.M. Daraban, C.U. Jensen, S.B. Iversen, R.B. Madsen, M. Glasius, K.R. Arturi, R.P. Nielsen, E.G. Søgaard, L.A. Rosendahl

The manuscript has been published in the
Journal of Applied Energy, vol. 162, pp. 1034–1041, 2016.

The layout has been revised.

Applied Energy 162 (2016) 1034–1041

Contents lists available at ScienceDirect

Applied Energy

journal homepage: www.elsevier.com/locate/apenergy

Continuous hydrothermal co-liquefaction of aspen wood and glycerol with water phase recirculation

T.H. Pedersen [a], I.F. Grigoras [a], J. Hoffmann [a], S.S. Toor [a], I.M. Daraban [a], C.U. Jensen [b], S.B. Iversen [b], R.B. Madsen [c], M. Glasius [c], K.R. Arturi [d], R.P. Nielsen [d], E.G. Søgaard [d], L.A. Rosendahl [a,*]

[a] Department of Energy Technology, Aalborg University, Pontoppidanstræde 101, 9220 Aalborg Øst, Denmark
[b] Steeper Energy Aps, Sandbjergvej 11, 2970 Hørsholm, Denmark
[c] Department of Chemistry and iNANO, Aarhus University, Langelandsgade 140, 8000 Aarhus C, Denmark
[d] Department of Chemistry and Bioscience, Aalborg University, Niels Bohrs Vej 8, 6700 Esbjerg, Denmark

HIGHLIGHTS

- Biocrude compounds from woody biomass can be classified into two groups: cyclopentenones and oxygenated aromatics.
- Biocrude quality can be predicted based on the feedstock model compound composition.
- Elemental composition is almost invariant to feedstock composition.
- Reaction scheme from model compound, through intermediates, to biocrude is proposed.
- Residual oxygen in the biocrude is mainly positioned in ketones and phenolic alcohols.

ARTICLE INFO

Article history:
Received 26 August 2015
Received in revised form 27 October 2015
Accepted 29 October 2015

Keywords:
Biofuel
Continuous processing
Biocrude
Biomass
Hydrothermal liquefaction
Sustainability

ABSTRACT

Hydrothermal liquefaction is a promising technology for the conversion of a wide range of bio-feedstock into a biocrude; a mixture of chemical compounds that holds the potential for a renewable production of chemicals and fuels. Most research in hydrothermal liquefaction is performed in batch type reactors, although a continuous and energy-efficient operation is paramount for such process to be feasible. In this work an experimental campaign in a continuous bench scale unit is presented. The campaign is based on glycerol-assisted hydrothermal liquefaction of aspen wood carried out with the presence of a homogeneous catalyst at supercritical water conditions, 400 °C and 300 bar. Furthermore, in the experimental campaign a water phase recirculation step is incorporated to evaluate the technical feasibility of such procedure. In total, four batches of approximately 100 kg of feed each were processed successfully at steady state conditions without any observation of system malfunctioning. The biocrude obtained was characterized using several analytical methods to evaluate the feasibility of the process and the quality of the product. Results showed that a high quality biocrude was obtained having a higher heating value of 34.3 MJ/kg. The volatile fraction of the biocrude consisted mostly of compounds having number of carbon atoms in the C_6–C_{12} range similar to gasoline. In terms of process feasibility, it was revealed that total organic carbon (TOC) and ash significantly accumulated in the water phase when such is recirculated for the proceeding batch. After four batches the TOC and the ash mass fraction of the water phase were 136.2 [g/L] and 12.6 [%], respectively. Water phase recirculation showed a slight increase in the biocrude quality in terms on an effective hydrogen-to-carbon ratio, but it showed no effects on the product gas composition or the pH of the water phase. The successful operation demonstrated the technical feasibility of a continuous production of high quality biocrude.

1. Introduction

Hydrothermal conversion of biomass in hot-compressed water is a viable, scalable, and energy-efficient thermo-chemical route for converting biomass into synthetic solid, liquid, or gaseous fuels and chemicals. At near and supercritical water conditions, biomass fragments into a bulk liquid phase, better known as biocrude. It consists of low molecular weight and deoxygenated chemical species compared to the original biomass macromolecules. The biocrude may be further processed into platform chemicals or infrastructure-compatible fuels. Hydrothermal conversion of

* Corresponding author.
E-mail address: lar@et.aau.dk (L.A. Rosendahl).

http://dx.doi.org/10.1016/j.apenergy.2015.10.165
0306-2619/

biomass has been widely studied experimentally, mostly in batch reactors and less so in continuous systems, and has been reviewed in the many process aspects, such as near-critical water synthesis properties [1,2], the effects of various process conditions [3], effects of biomass composition [4–7], process developments [8–10], and upgrading of the biocrude [11–13].

Although the vast majority of research is carried out in batch reactors, development of continuous operation and technology upscaling of near-critical water technologies has been ongoing since the mid-seventies – but has not yet reached commercialization [9]. The continuous process was first demonstrated at a bench scale system at the Pittsburgh Energy Research Center (PERC) which was later scaled to the Albany plant, Oregon [14]. The production facility utilized a recycle concept in which wood (Douglas fir) was slurried in recycled process water and initially in anthracene oil and eventually in recycled biocrude as it became available. The following three aspects of the process were identified as critical: (1) the energy intensive pre-drying and grinding step required for wood flour preparation, (2) wood–biocrude–water slurries could not be fed at concentrations greater than 10% without causing system plugging, (3) high recycle ratios of biocrude (up to 19:1) required excessive heat [15]. Many process improvements have since been done, and it is believed that the critical aspects can be overcome or greatly reduced to an extent for the process to become feasible. One aspect of the process optimization is to maximize the biocrude whilst decreasing the amount of solid byproducts. During liquefaction, reactive biomass fragments rearrange to biocrude compounds through condensation, cyclization, and re-polymerization, and for prolonged process severity a solid fraction insoluble in most solvents is formed, which is generally termed char.

In a lignocellulosic context, char formation results primarily from two counteracting mechanisms; (1) dehydration reactions of free sugars favored at intermediate temperatures, high feed concentrations [16], and acidic conditions [17] and (2) radical formation during lignin degradation leading to retrogressive char formation [18]. Char formation from carbohydrates can be suppressed by applying high heating rates to reach high reaction temperatures, preferably above supercritical conditions, and alkaline conditions [16,19,20]. Lignin radical formation purely a thermal effect, hence supercritical conditions tends to enhance lignin char formation [21]. Means of overcoming these counteracting thermal effects includes the addition of a reducing agent such hydrogen or carbon monoxide, or by the addition of a stabilizing co-solvent acting as a radical scavenger through hydrogen donation. Alcohols may undergo thermal scission causing hydrogen abstraction in the form of ·H, ·OH, or $\cdot CH_2OH$ radicals, amenable to cap lignin radicals and hence preventing lignin repolymerization [22–24]. Low molecular weight co-solvents such as phenol [25], propanol [26], ethanol [27,28], methanol [29], and glycerol [30,31] have been applied, and are preferable in order to obtain low molecular weight product compounds, when transport fuel precursors are targeted.

Among co-solvents, glycerol is of particular interest since it is already produced in large quantities. Today, glycerol is mainly a refined bio-based by-product from biodiesel production, and its market value has been declining since the market entry of biodiesel production, making it economically interesting. Xiu et al. investigated in batch the potential of utilizing crude glycerol, the unrefined by-product, as a co-substrate in hydrothermal processing of swine manure. It was found that crude glycerol enhanced both the yield and the quality of the biocrude based on the elemental composition [32–37]. In the same studies it was attempted to understand the conversion chemistry involved through model studies using pure glycerol, methanol, and fatty acids as model co-substrates, but the reaction mechanisms of the different organic compounds in the crude glycerol on the biocrude production were not fully established. Moreover, in house, but yet unpublished, model studies in batch reactors have shown that by hydrothermally liquefying aspen wood in the presence of glycerol or crude glycerol, char formation can be significantly reduced whilst maintaining a high yield of high quality biocrude [38].

The objective and novelty of the present study is to investigate and demonstrate continuous co-liquefaction at bench scale conditions of aspen wood and glycerol as a co-solvent as a viable route to process lignocellulose at high organic concentrations in the feed. The technical feasibility of process water phase recirculation is incorporated to evaluate benefits and eventual complications of such procedure. The process is evaluated based on system performance, recirculation effects on phase characteristics, and a product assessment to examine the quality of the obtained biocrude.

2. Materials and methods

2.1. Materials

Supercritical co-liquefaction of aspen wood and glycerol was demonstrated in the continuous bench scale reactor unit (CBS1) at the Department of Energy Technology, Aalborg University. In total, four batches of approximately 100 kg of feed each were processed, all prepared from the same recipe. Table 1 shows the properties of the aspen wood. Glycerol (99.5%), potassium carbonate (K_2CO_3), and carboxymethyl cellulose (CMC) were purchased from Brenntag Nordic A/S.

2.2. Process feed composition

Table 2 shows the feed composition used in the experimental campaign. Aspen wood and glycerol were mixed in nearly 50/50 ratios in recycled water phase together with K_2CO_3 and CMC. In the absence of product water phase, the feed for Batch #1 was prepared using distilled water.

2.3. Description of the Continuous Bench-Scale Unit (CBS1)

A process flow diagram (PFD) of the CBS1 is presented in Fig. 1. Pretreatment and feed slurry preparation is done in a stand-alone mixer, where aspen wood, glycerol, water phase and catalyst are mixed. Steady state conditions at the preset operating conditions are reached by circulating hot-compressed water (HCW) through

Table 1
Elemental and chemical analysis of aspen wood used in continuous hydrothermal liquefaction.

Elemental and chemical analysis[a] *(%, daf)*	
C	50.39 (±0.86)
H	6.19 (±0.08)
N	0.19 (±0.02)
S	N.D.
O (by difference)	43.23 (±0.08)
Fibre mass composition (%, db)[b]	
Cellulose	47.14 (±0.86)
Hemicellulose	19.64 (±0.11)
Lignin	22.11 (±0.17)
Extractives (by difference)	6.63 (±0.01)
Ash[c]	0.46 (±0.02)

daf = dry, ash-free. N.D. = Not Determined.
[a] Ultimate analysis was carried out in a Perkin Elmer 2400 Series II CHNS/O system.
[b] Fibre composition was determined by the Van Soest method in a FOSS Fibertec M6 unit.
[c] Ash content measured by heating a sample to 850 °C and held isothermally for 2 h.

Table 2
Feed slurry composition of the four batches.

Feed composition						
Compound	Aspen wood	Glycerol	Water phase	K_2CO_3	CMC	SUM
Mass fraction [%]	16.9	15.7	62.3	4.2	0.8	100

the plant. Once reached, the water is replaced by a batch of the prepared feed and continuous biocrude production commences. After each batch of approximately 100 kg, HCW is again recirculated to maintain process conditions. The feed barrel is reloaded with new premixed feed and processed continuously, and so on. Small amounts of CMC are added to the feed slurry (0.8% on a mass basis) to prevent feed slurry sedimentation while processing a batch. In a single stage, the feed slurry is pressurized to process pressure (300 bar) by a high pressure piston pump. Hereafter the feed is heated in two serial heaters to process temperature (400 °C) with a heat ramp in the range of 200–400 °C/min. Two 5 L, heat-traced, serial reactors accommodate the reaction residence time. Reactor effluent phases are pre-cooled in a concentric-tube heat exchanger prior entering two parallel high-pressure filters. Depressurization and feed slurry mass flow is controlled by serial capillary tubes of various lengths and various diameters. Finally, the product phases are cooled to ambient conditions in a secondary cooler before separation.

2.4. Process conditions for liquefaction experiments

Process conditions were kept constant at 400 °C and 300 bar. Mass flow rate was approximately 9 kg/h for Batch #1 and approximately 14 kg/h for Batch #2, #3, and #4. During each batch run, mass balance samples were collected to evaluate process yields. In total, 14 mass balances were collected over the four batches.

2.5. Product separation procedure

Product phases (water phase and biocrude phase) were separated gravimetrically in a separation funnel. In contrast to small scale lab-experiments, using only a gravimetric separation procedure alleviates the need for expensive solvents and provides a more realistic picture of economically viable yields. The biocrude and water phases were left to settle (30–60 min) before the water phase was tapped from the bottom of the funnel. Biocrude yields were measured right after the gravimetric separation. Product gases were collected and analyzed online for H_2, CO_2, CO, CH_4, and O_2.

2.6. Methods for biocrude and water phase analyses

Prior to biocrude analyses, the biocrude was centrifuged in a Sigma 6-16 HS centrifuge (2153 RCF) for 60 min to extract free water. Bound water was determined by Karl Fischer titration using a TitroLine 7500 KF. Elemental composition was measured using a Perkin Elmer 2400 Series II CHNS/O system (ASTM D5291). Calorific values were measured using an IKA C2000 oxygen combustion calorimeter (ASTM D2015). Qualitative analyses of all biocrude samples were carried out on a Thermo Scientific Trace 1300 ISQ GC–MS system, using a TG-SQC column (Length: 15 m, i.d.: 0.25 mm, film: 0.25 μm film). Prior to analysis, all samples were diluted in diethyl ether (DEE) and subjected to the following oven temperature profile: 40 °C was held for 3 min, then ramped to 325 °C at 8 °C/min and finally kept at this temperature for 4 min. Injector and ion source temperatures were 280 °C, split ratio was 1:20, and flow rate of the carrier gas (helium) was 1.0 mL/min.

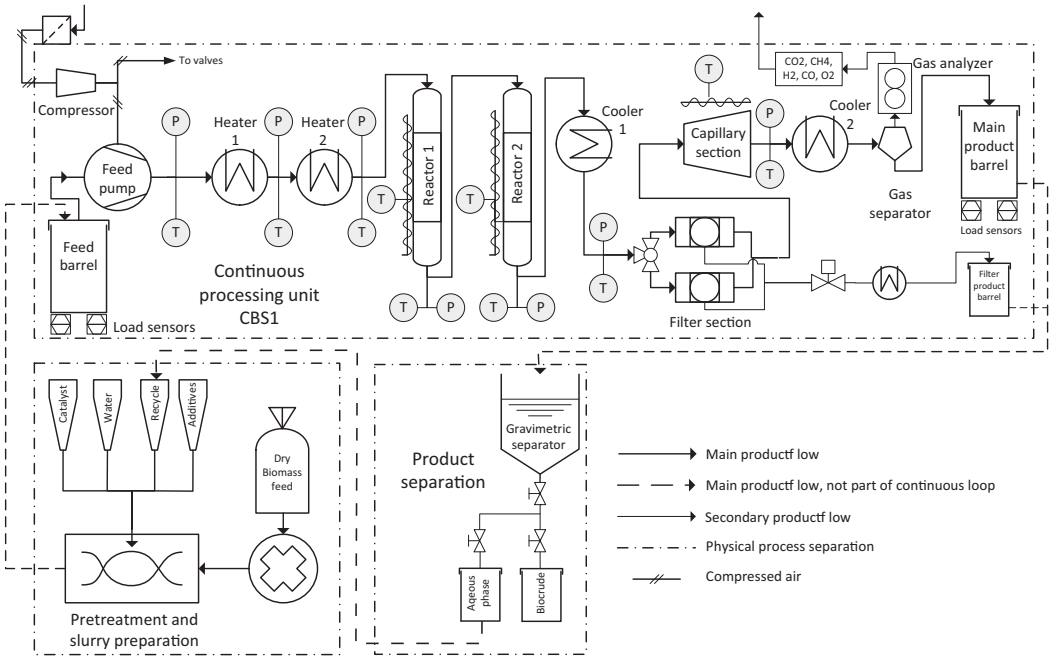

Fig. 1. PFD of the CBS1 unit.

Compounds were identified by mass spectra comparison with the NIST mass spectral data library. Identification of all compounds by GC–MS is challenged by the complexity of the mixture and due to the fact only the volatile fraction is identifiable (roughly 50% of the bulk biocrude). The identification of the reported compounds on the specific instrument was confirmed by a round robin test. Total organic carbon (TOC) and potassium analyses of the water phases were performed on a Hach Lange Spectrophotometer with RFID.

Energy Recovery (ER), Carbon Recovery (CR), and the effective hydrogen-to-carbon ratio (H/C_{eff}) were calculated according to Eqs. (1)–(3):

$$ER = \frac{\text{HHV of biocrude} \cdot \text{mass of biocrude}}{\text{HHV of feedstock} \cdot \text{mass of feedstock}} \quad (1)$$

$$CR = \frac{\text{mass of C in the biocrude}}{\text{mass of C in the feedstock}} \quad (2)$$

$$H/C_{eff} = \frac{H - 2O}{C} \quad (3)$$

3. Results and discussion

3.1. CBS1 performance

The performance and process stability in terms of process temperature, pressure, and mass flow rate of the CBS1 system is illustrated in Fig. 2. The figure displays trend curves for a typical batch run, operating at a flow rate of approximately 14 kg/h. It is readily observed that process conditions remains stable throughout the entire batch. Small pressure fluctuations in the beginning and in the end of a batch are observed, but these are explained by viscosity changes when feed is pumped into the system instead of HCW, and vice versa. The tiny oscillations in the pressure profile are due to the use of a piston pump.

For each mass balance sample roughly 20 kg of product (biocrude and water phase) was loaded into the funnel and left to separate gravimetrically before the water phase was tapped off at the bottom of the funnel. Fig. 3 clearly shows a resulting hydrophobic supernatant biocrude. The yields of biocrude were based on this initial gravimetric separation, where bound water was not included. Furthermore, later centrifugal runs of the biocrude samples revealed yet unsettled water which naturally introduced unaccounted experimental errors on the biocrude yields. Fig. 3 shows the yield calculations based on the mass balance samples obtained from the four batches. Due to significant yield variations within each batch, effects of water phase recirculation on the biocrude yields are somewhat inconclusive. As a result it is concluded that the separation procedure was not adequate for producing reliable yield results and a more robust and standardized separation procedure is under evaluation. Based on analysis of variations (ANOVA) calculations, it can only be concluded that yields from Batch #3 are statistically higher than the yields from Batch #4 (on a 95% confidence interval). During the liquefaction process water-soluble organics (WSO) are formed and contained in the aqueous phase. For Batch #1, for which the feed slurry was prepared using demineralized water, it appears from Table 3 that the total organic carbon (TOC) content of the aqueous phase reaches a value of 54.1 g/L. after the first batch. Due to the recirculation procedure adopted, commenced after Batch #1, it is observed that the TOC of the aqueous phase increases almost linearly to 136.2 g/L after the last batch. As the fraction of WSO in the aqueous phase increases, the biocrude and aqueous phase separation weakens since WSO act as co-solvents, leading ultimately to a single phase mixture, as it was found by Oasmaa et al. in a study on pyrolysis biooil separation [39]. As the amount of WSO increases, biocrude compounds become more soluble in the aqueous phase which could explain the tendency to a lower biocrude yield. The yield fluctuations also cause fluctuations in the energy

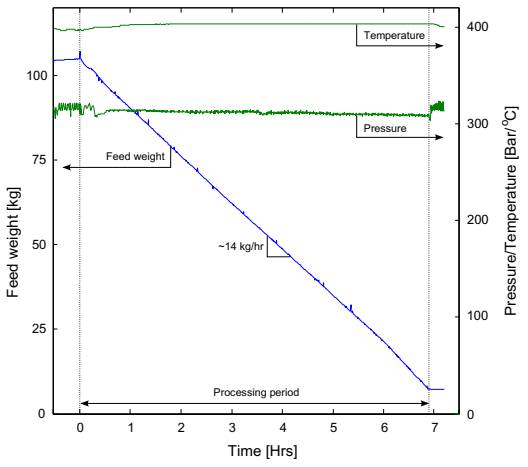

Fig. 2. Process conditions, temperature, pressure, and feed barrel weight during a continuous batch run.

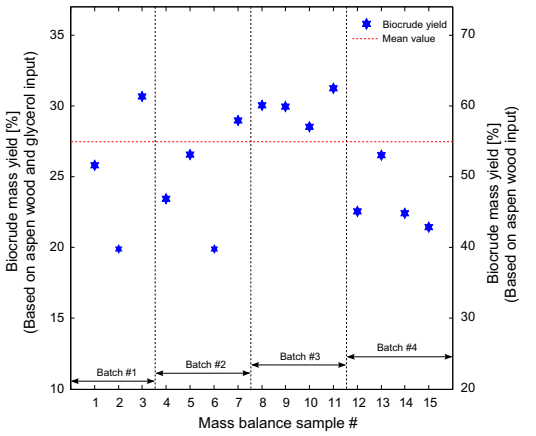

Fig. 3. Biocrude yields obtained from mass balance samples during the four batches. Mean value of all the mass balance samples are presented. In the plot; display of a typical supernatant biocrude and water phase sample. The hydrophobic biocrude readily separates gravimetrically.

Table 3
Aqueous phase analyses: mass fraction of ash, total organic carbon (TOC), pH and potassium (K) content of the four different batches.

	Batch #1	Batch #2	Batch #3	Batch #4
Ash [%]	6.20	9.41	10.7	12.6
TOC [g/L]	54.1	96.9	106.3	136.2
pH	5.28	5.91	6.02	5.35
K [g/L]	27.2	50	56.4	61.7

(ER) and carbon recovery (CR) in the biocrude. In the present experiments, biocrude ER and CR ranges from 39% to 62% and 42% to 66%, respectively. Due to the fact that glycerol forms mostly WSO or gaseous products, the ER and CR are generally penalized when including the co-solvent fraction in the ER and CR calculations, which is only measured with respect to the biocrude.

Table 3 also shows that accompanying the accumulation of WSO in the aqueous phase, ash is likewise observed to accumulate as an equal amount of K_2CO_3 is added for each batch. Starting at an aqueous phase ash content of 6.2%, resembling that of the original feed composition, the ash content is increasing linearly to a final value of 12.6% after three recycles. Tracing the potassium in the water phase, it is observed that potassium accumulates linearly in the water phase. The mass fraction of potassium to the total water phase is almost half of the mass fraction of the TOC to the total water phase. It is also evident that after four batches (3 recycles) steady state values of the water phase has yet not been reaches. During hydrothermal processing of glycerol, glycerol is mainly converted into WSO and hence the observation of WSO accumulation is likely to be a contribution from the high amount of glycerol added for each batch. Möller and Vogel investigated hydrothermal conversion of glycerol at 400 °C [16]. Even after 60 min, more than 10% of the glycerol was unconverted. During the present experiments, product analysis showed intact glycerol, but it was not clear how much glycerol was actually converted during processing. For continuous industrial operation with water phase recycling, ash accumulation presents an operational challenge to be addressed, as failing to do so may lead to operational malfunction. It has yet not been investigated, if the WSO containing water phase possess similar effects as glycerol on retardation of char formation. If so, glycerol may gradually by phased out as a feed additive as a work around for limiting the accumulation of WSO and still obtaining a stable process. The polarity of water as a solvent is known to diminish as it approaches near and supercritical water conditions, leading to solubility reduction for some salts, causing precipitation and ultimately plugging of the system. For the experiments reported here plugging was not experienced, nor did the campaign show signs of impending blockage, which would manifest itself as an increased pressure drop across the system.

Table 3 shows that after conversion the water phase is noticed to be acidic despite of the significant addition of alkaline catalyst. Lignocellulose and glycerol are known to form acidic compounds under hydrothermal processing, especially under alkaline conditions, which first neutralizes the K_2CO_3, then later acidifies the water phase [16,40]. Over the four batches the water phase pH appears almost invariant to the recirculation of aqueous phase.

To investigate if the aqueous recirculation affects the quality of the obtained biocrudes, an effective hydrogen-to-carbon ratio (H/C_{eff}) was calculated as a quality measure. Fig. 4 shows the results. Like for the biocrude yields, some variations within the individual batches are noticed blurring a clear trend to be observed. However, when excluding Batch #1, it seems as the quality in terms of H/C_{eff} is increasing as water phase is recirculated. The improvement in biocrude quality by aqueous phase recycling has also been demonstrated by Elliott et al. [10]. A hypothesis is that WSO act as hydrogen-donors. By aqueous phase recirculation, the concentration of WSO increases, which in turn increases the concentration of hydrogen-donors.

Gas phase composition was monitored continuously for carbon dioxide, hydrogen, methane, carbon monoxide, and oxygen throughout each batch. Fig. 5 displays typical gas trends. Initially, oxygen is diluted by producer gases and ultimately vanishes. It must be stated that the gas composition measured prior and in between batches is not precise, since gas detectors are calibrated only in a narrow band resembling process gas composition. It is noticed that the volume fractions CO_2 and H_2 reach steady state values of approximately 62% and 30%, respectively, and hence being the most abundant gases. The volume fractions of CH_4 and CO are 4–5% and 2–3%, respectively. During each mass balance samples, product gases are involuntarily exposed to surrounding conditions, allowing air to enter the gas stream. This is observed by an increased oxygen concentration, followed by decreasing product gases. After each mass balance sample steady state process conditions are reestablished as soon as the system is resealed. The gas mass flows were registered to approximately 0.6–0.7 kg/h, amounting to a mass fraction of approximately 12–15% of the input organic fraction. In terms of energy and carbon recoveries, this corresponds to approximately 2.4% and 8.8% in the gas phase.

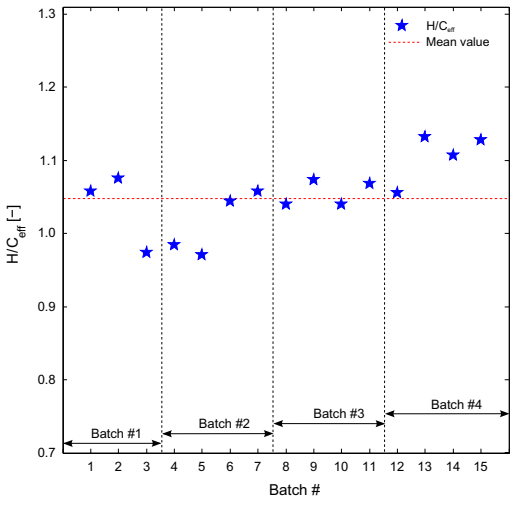

Fig. 4. H/C_{eff} of the biocrude obtained from mass balance samples during the four batches. Mean value of all the mass balance samples are presented.

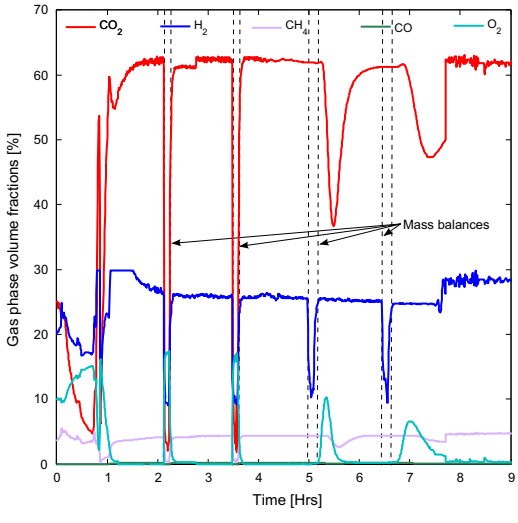

Fig. 5. Continuous process gas composition. Initiations of mass balances are indicated in the figure.

Table 4
Normalized gas composition of CO_2, CO, CH_4, and H_2.

	Gas phase volume fractions [%]			
	CO_2	CO	CH_4	H_2
Batch #1	62.1	2.9	4.6	30.5
Batch #2	62.1	2.9	4.6	30.5
Batch #3	60.8	2.7	4.5	32.0
Batch #4	63.6	3.3	4.2	28.8

At best, the carbon balance across input and output phases was established at a 96% closure.

Gas compositions obtained from the four batches are presented in Table 4, where the gas compositions have been normalized to exclude oxygen. It appears that the gas compositions are relatively invariant over the four runs and hence not affected by the water phase recirculation, although ashes and WS are observed to accumulate. The significant and insignificant shares of H_2 and CO, respectively, relative to uncatalyzed hydrothermal processing of lignocellulosic materials, indicate alternative chemical pathways [41–43]. Alkali catalysts have previously been found to enhance water–gas shift reactions, which can explain the high and low shares of H_2 and CO, respectively [44]. Steam reforming reactions may also be secondary contributors, but they proceed usually at much higher temperatures and in the presence of a transition metal catalyst [45]. A more speculative explanation is hydrogen abstraction reactions catalyzed by alkaline conditions. Glycerol deprotonation derives dihydroxyacetone, glyceraldehyde, and lactic acid, commonly observed WSO compounds, in addition to gaseous hydrogen [46].

3.2. Analyses of the biocrude

The biocrude was analyzed for determining the system performance in terms of biocrude quality. Table 5 compiles the bulk analysis obtained. First of all, it is observed that the mass fraction of oxygen in the biocrude (15.8%) is significantly lower as compared to that of the feedstock (47%, aspen wood plus glycerol). Secondly, the course of deoxygenation resulted in a hydrophobic, easily separable biocrude, with an increased gross calorific value (34.3 MJ/kg). The hydrophobicity of the biocrude is quantified by the low mass fraction of bound water in the biocrude (3.8%). It is further observed that the ash content of the biocrude is fairly high. The recycling effect of the ash content in the biocrude was not evaluated, but following the trends of the water phase, it is expected to increase from each aqueous phase recycle. A mass fraction of 0.48% of undesirable inorganics poses a potential challenge, as inorganics mount a concern from a downstream point of view. A significant part of the inorganics is alkali metals, carried over by the high amount of K_2CO_3 added for each batch cycle. If the biocrude is to be refined, inorganics may decompose and deposit in refinery hardware or even poison expensive refining catalysts.

Table 5
Elemental mass analysis, higher heating value (HHV), mass fractions of ash and bound water of the biocrude, and biocrude ash composition.

Elemental analysis [% (daf)]		Metals [mg/g]	
C	75.2	Al	0.054
H	8.2	Cr	0.035
N	0.5	Fe	0.037
S	0.3	K	1.78
O	15.8	Mg	0.136
HHV [MJ/kg]	34.3	Zn	0.01
Ash content [%]	0.48	P	0.015
Bound water [%]	3.8	Ca	0.97
		S	0.1

If the biocrude is to be combusted directly, inorganics can cause corrosion, wear, and deposit in pumps, injectors, burners, turbines, *etc.* Hence, if the aqueous phase is to be recycled, procedure amendments have to be implemented. Accumulation of inorganics is of particular concern, which is why an inorganic removal step of the aqueous phase may have to be implemented downstream. A supercritical salt separator has previously been proposed as a means for precipitation various salts with high separation efficiency [47]. Furthermore, the accumulation of WSO in the aqueous phase must be investigated in greater details to understand, (1) the impact of WSO on the conversion mechanisms in terms of yields and product quality and (2) the impact of WSO on the phase separation of the aqueous phase and the biocrude.

The volatile fraction of the biocrude was further characterized to investigate the chemical composition. Table 6 presents the identified compounds by GC–MS analysis together with their

Table 6
List of compounds identified in the biocrude by gas chromatography–mass spectroscopy. The table includes compound name, formula, relative peak area, and number of carbon atoms (C#). No standards were used for compound verification.

RT (min)	Identified compound	Chemical formula	Peak area (%)	C#
2.06	Cyclopentanone	C_5H_8O	0.30	5
2.59	3,5,5-Trimethyl-2-hexene	C_9H_{18}	0.39	9
2.94	2-Methyl-cyclopentanone	$C_6H_{10}O$	2.28	6
3.37	Ethylbenzene	C_8H_{10}	0.39	8
3.56	p-Xylene	C_8H_{10}	0.62	8
3.87	2,5-Dimethyl-cyclopentanone	$C_9H_{16}O$	0.86	9
4.04	3,4-Dimethyl-3-penten-2-one	$C_7H_{12}O$	1.51	7
4.38	2-Methyl-2-cyclopenten-1-one	C_6H_8O	1.58	6
5.04	1-Cyclohexylethanol	$C_8H_{16}O$	2.84	7
5.19	1,2-Dimethyl-cyclohexene	C_8H_{14}	1.26	8
5.56	3-Methyl-2-cyclopenten-1-one	C_6H_8O	1.83	6
6.93	2,3-Dimethyl-2-cyclopenten-1-one	$C_7H_{12}O$	4.33	7
7.37	2,3,4-Trimethyl-2-cyclopenten-1-one	$C_8H_{12}O$	4.32	8
7.65	p-Cresol	C_7H_8O	1.75	7
8.12	2,3-Dimethyl-phenol	$C_8H_{10}O$	2.71	8
8.50	2-Ethyldienecyclohexanone	$C_8H_{14}O$	1.34	8
8.81	3,5-Dimethyl-phenol	$C_8H_{10}O$	4.69	8
9.15	2,4,6-Trimethyl-3-cyclohexen-1-carboxaldehyde	$C_{10}H_{16}O$	1.25	10
9.35	4-Methyl-1-(1-methylethyl)-cyclohexene	$C_{10}H_{18}$	1.32	10
9.44	4-Methyl-1-(1-methylethyl)-cyclohexene	$C_{10}H_{18}$	1.73	10
9.62	2,4,6-Trimethyl-3-cyclohexen-1-carboxaldehyde	$C_{10}H_{16}O$	1.62	10
9.82	4-Ethyl-3,4-dimethyl-2,5-cyclohexadien-1-one	$C_{10}H_{14}O$	1.31	10
10.14	2,4,6-Trimethyl-3-cyclohexen-1-carboxaldehyde	$C_{10}H_{16}O$	1.50	10
10.71	2,6-Dimethoxytoluene	$C_9H_{12}O_2$	1.49	9
11.07	2,3-Dihydroxy-3-methyl-1H-inden-1-one	$C_{11}H_{12}O_3$	2.05	10
11.33	Duroquinone	$C_{10}H_{12}O_2$	0.86	11
11.71	2,6-Dimethyl-1,4-benzenediol	$C_8H_{10}O_2$	1.62	8
12.13	4-Ethylcatechol	$C_8H_{10}O_2$	1.92	8
12.42	2,5-Dimethyl-1,4-benzenediol	$C_8H_{10}O_2$	1.47	8
12.76	5-Methoxy-2,3-dimethyl-phenol	$C_9H_{12}O_2$	3.67	9
12.90	4-Ethylguaiacol	$C_9H_{12}O_2$	2.54	9
13.68	2,3,5-Trimethyl-1,4-benzenediol	$C_9H_{12}O_2$	4.21	9
13.97	3-Tert-butyl-4-hydroxyanisole	$C_{11}H_{16}O_2$	1.52	11
14.19	4-Butoxybenzyl alcohol	$C_{10}H_{16}O$	0.93	10
14.81	2,3,5,6-Tetramethyl-1,4-benzenediol	$C_{10}H_{14}O_2$	1.52	10
15.30	2,6-Dimethoxy-4-(2-propenyl)-phenol	$C_{11}H_{14}O_3$	2.61	11
16.32	6-Tert-butyl-2,4-dimethylphenol	$C_{12}H_{18}O$	1.20	12
16.44	Benzaldehyde, 3-hydroxy-4-methoxy-2-(2-propenyl)-	$C_{11}H_{12}O_3$	0.81	12
16.63	4-(2,4,4-Trimethyl-cyclohexa-1,5-dienyl)-but-3-en-2-one	$C_{13}H_{18}O$	0.64	13
18.82	Methyl dehydroabietate	$C_{21}H_{30}O_2$	0.36	21
19.79	10,18-Bisnorabieta-5,7,9(10),11,13-pentene	$C_{18}H_{22}$	0.74	18
20.82	Retene	$C_{18}H_{18}$	1.55	18

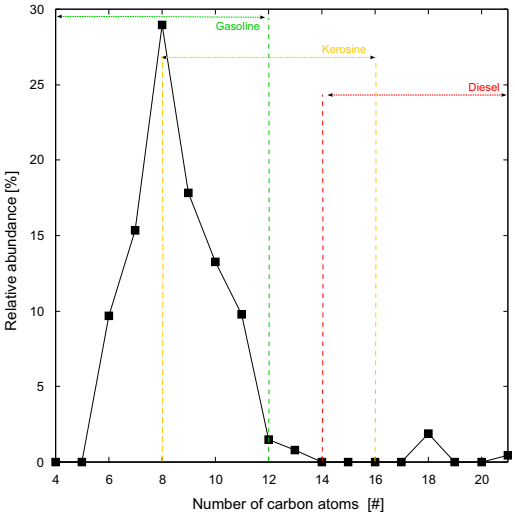

Fig. 6. Relative distribution (by relative peak area) in numbers of carbon atoms in the compounds obtained from the identified in the biocrude. The relative abundance is calculated based on summed relative peak areas. The ranges of number of carbon atoms in conventional fuels are included.

chemical formulas, relative peak area, and number of carbon atoms (C#). It is readily observed that the biocrude is a complex mixture of chemical compounds for which the majority of compounds are oxygenated cyclic structures having carbon atoms in the range of C_6–C_{21}. Unsaturated hydrocarbons compounds with higher number of carbon atoms, including fused ring structures, were also identified but in minor quantities. The major denominators for all of the compounds are cyclic C_5 or aromatic C_6 backbones, substituted with various functional groups (ketonic, aldehyde, phenolic). Ketonic functionalities are mainly observed on pentane and pentene backbones having only single heteroatoms, and are believed to be formed by condensation reactions between Retro-Aldol derived carbohydrate intermediates. A broad collection of aromatics are also observed having mainly phenolic functionalities with single, double or even triple heteroatom formulas. Despite the fact that the compound mixture is complex and diverse, the range of numbers of carbon atoms is relatively narrow. The distribution of number of carbon atoms based on the identified compounds has been calculated semi-quantitatively by total ion count. The distribution is plotted in Fig. 6, together with the common number of carbon atom ranges of conventional gasoline, kerosene-type jet fuel, and diesel. It appears that the majority of compounds lump into the C_6–C_{12} region, mainly representing gasoline range and 'low cut' jet fuel. Based only on carbon range, the diesel range is hardly represented in the biocrude.

4. Conclusion

Continuous co-liquefaction of aspen wood and glycerol at supercritical water conditions was demonstrated successfully. High organic content feeds were prepared and processed for which a water phase recycling procedure was implemented. High process stability in terms of temperature, pressure, and mass flow rate was obtained and steady state conditions were achieved throughout all experiments. High hydrophobicity of the resulting biocrudes allowed for a simple, but commercially realistic, gravimetric separation between biocrudes and water phases. Unfortunately, significant yield variations obtained from mass balance samples within each batch obscured the identification of clear effects of the water phase recirculation on the biocrude yields, but a slight decreasing tendency is observed. Conversely the biocrude yield trend, the biocrude quality in terms of an effective hydrogen-to-carbon ratio was observed to increase slightly when the water phase is recirculated. Gas phase yields and compositions were found almost invariant to the water phase recirculation. Some process inconveniences were observed with respect to water phase recirculation; TOC and ash contents of the water phase were observed to increase significantly with water phase recirculation, which may eventually lead to system failure due to salt precipitation. Moreover, the mass fraction of ash in the biocrude was found relatively high (0.48%). From the biocrude analysis it was found that the major biocrude compounds were cyclic C_5 or aromatic C_6 backbones, substituted with various oxygenated functionalities. The number of carbon atoms range of the biocrude compounds is distributed mainly in the C_6–C_{12} range similar to gasoline. In conclusion, the experimental campaign demonstrated an auspicious platform for continuous operation of hydrothermal liquefaction for the production of high quality biocrudes.

Acknowledgements

This work is part of the Flexifuel Project, a Sino-Danish collaboration, and C3BO (Center for BioOil) at the Department of Energy Technology, Aalborg University. The research was financially supported by The Danish Agency for Science, Technology and Innovation (Grant No. 10-094552) and The Danish Council for Strategic Research (Grant No. 1305-00030B).

References

[1] Kruse A, Dinjus E. Hot compressed water as reaction medium and reactant: Properties and synthesis reactions. J Supercrit Fluids 2007;39(3):362–80. http://dx.doi.org/10.1016/j.supflu.2006.03.016.
[2] Kruse A, Dinjus E. Hot compressed water as reaction medium and reactant: 2. Degradation reactions. J Supercrit Fluids 2007;41(3):361–79. http://dx.doi.org/10.1016/j.supflu.2006.12.006.
[3] Akhtar J, Amin NAS. A review on process conditions for optimum bio-oil yield in hydrothermal liquefaction of biomass. Renew Sustain Energy Rev 2011;15(3):1615–24. http://dx.doi.org/10.1016/j.rser.2010.11.054.
[4] Peterson AA, Vogel F, Lachance RP, Froling M, Antal Jr MJ, Tester JW. Thermochemical biofuel production in hydrothermal media: a review of sub- and supercritical water technologies. Energy Environ Sci 2008;1:32–65. http://dx.doi.org/10.1039/B810100K.
[5] Toor SS, Rosendahl L, Rudolf A. Hydrothermal liquefaction of biomass: a review of subcritical water technologies. Energy 2011;36(5):2328–42. http://dx.doi.org/10.1016/j.energy.2011.03.013.
[6] Pedersen TH, Rosendahl LA. Production of fuel range oxygenates by supercritical hydrothermal liquefaction of lignocellulosic model systems. Biomass Bioenergy 2015;83:206–15. http://dx.doi.org/10.1016/j.biombioe.2015.09.014.
[7] Toor S, Rosendahl L, Hoffmann J, Pedersen T, Nielsen R, Søgaard E. Hydrothermal liquefaction of biomass. Springer Publishing Company; 2014. ISBN 978-3-642-54457-6. p. 189–217. http://dx.doi.org/10.1007/978-3-642-54458-3.
[8] Bouvier J, Gelus M, Maugendre S. Wood liquefaction – an overview. Appl Energy 1988;30(2):85–98. http://dx.doi.org/10.1016/0306-2619(88)90006-2.
[9] Elliott DC. Historical developments in hydroprocessing bio-oils. Energy Fuels 2007;21(3):1792–815. http://dx.doi.org/10.1021/ef070044u.
[10] Elliott DC, Biller P, Ross AB, Schmidt AJ, Jones SB. Hydrothermal liquefaction of biomass: developments from batch to continuous process. Bioresource Technol 2015;178(0):147–56. http://dx.doi.org/10.1016/j.biortech.2014.09.132.
[11] Xiu S, Shahbazi A. Bio-oil production and upgrading research: a review. Renew Sustain Energy Rev 2012;16(7):4406–14. http://dx.doi.org/10.1016/j.rser.2012.04.028.
[12] Furimsky E. Catalytic hydrodeoxygenation. Appl Catal A: Gen 2000;199(2):147–90. http://dx.doi.org/10.1016/S0926-860X(99)00555-4.
[13] Hoffmann J, Pedersen T, Rosendahl L. Hydrothermal conversion in near-critical water – a sustainable way of producing renewable fuels. Netherlands: Springer; 2014. ISBN 978-94-017-8922-6. p. 373–400. http://dx.doi.org/10.1007/978-94-017-8923-3.
[14] Lindemuth T. Carboxylolysis of biomass. In: Sofer SS, Zaborsky OR, editors. Biomass conversion processes for energy and fuels. US: Springer; 1981. p.

99–112. ISBN 978-1-4757-0303-0. http://dx.doi.org/10.1007/978-1-4757-0301-6_10.
[15] Schaleger LL, Figueroa C, Davis HG. Direct liquefaction of biomass: results from operation of continuous bench scale unit in liquefaction of water slurries of douglas fir wood – report number: Lbl-14019. Tech rep; Energy and Environment Division, Lawrence Berkeley Laboratory; 1982.
[16] Müller JB, Vogel F. Tar and coke formation during hydrothermal processing of glycerol and glucose. Influence of temperature, residence time and feed concentration. J Supercrit Fluids 2012;70:126–36. http://dx.doi.org/10.1016/j.supflu.2012.06.016.
[17] Tran A, Rogers D. Examination of alternative catalysts for biomass direct liquefaction. 1985. <http://www.osti.gov/scitech/servlets/purl/6316343>. http://dx.doi.org/10.2172/6316343.
[18] Saisu M, Sato T, Watanabe M, Adschiri T, Arai K. Conversion of lignin with supercritical waterphenol mixtures. Energy Fuels 2003;17(4):922–8. http://dx.doi.org/10.1021/ef0202844.
[19] Karagöz S, Bhaskar T, Muto A, Sakata Y. Hydrothermal upgrading of biomass: effect of K_2CO_3 concentration and biomass/water ratio on products distribution. Bioresource Technol 2006;97(1):90–8. http://dx.doi.org/10.1016/j.biortech.2005.02.051.
[20] Zhu Z, Rosendahl L, Toor SS, Yu D, Chen G. Hydrothermal liquefaction of barley straw to bio-crude oil: effects of reaction temperature and aqueous phase recirculation. Appl Energy 2015;137(0):183–92. http://dx.doi.org/10.1016/j.apenergy.2014.10.005.
[21] Yong TLK, Matsumura Y. Kinetic analysis of lignin hydrothermal conversion in sub- and supercritical water. Ind Eng Chem Res 2013;52(16):5626–39. http://dx.doi.org/10.1021/ie400600x.
[22] Ross DS, Blessing JE. Alcohols as h-donor media in coal conversion. 1. Base-promoted h-donation to coal by isopropyl alcohol. Fuel 1979;58(6):433–7. http://dx.doi.org/10.1016/0016-2361(79)90084-X.
[23] Ross DS, Blessing JE. Alcohols as h-donor media in coal conversion. 2. Base-promoted h-donation to coal by methyl alcohol. Fuel 1979;58(6):438–42. http://dx.doi.org/10.1016/0016-2361(79)90085-1.
[24] Wolfson A, Dlugy C, Shotland Y, Tavor D. Glycerol as solvent and hydrogen donor in transfer hydrogenation–dehydrogenation reactions. Tetrahedron Lett 2009;50(43):5951–3. http://dx.doi.org/10.1016/j.tetlet.2009.08.035.
[25] Zhang Qh, Zhao Gj, Jie Sj. Liquefaction and product identification of main chemical compositions of wood in phenol. For Stud China 2005;7(2). http://dx.doi.org/10.1007/s11632-005-0018-8.
[26] Ross DS, Blessing JE. Isopropyl alcohol as a coal liquefaction agent. Am Chem Soc Fuel Div Prepr 1977;22(6):208–13. http://dx.doi.org/10.1016/0016-2361(79)90084-X.
[27] Cheng S, Dcruz I, Wang M, Leitch M, Xu CC. Highly efficient liquefaction of woody biomass in hot-compressed alcoholwater co-solvents. Energy Fuels 2010;24(9):4659–67. http://dx.doi.org/10.1021/ef901218w.
[28] Zhang J, Zhang Y, Luo Z. Hydrothermal liquefaction of chlorella pyrenoidosa in ethanol–water for bio-crude production. Energy Proc 2014;61:1961–4. http://dx.doi.org/10.1016/j.egypro.2014.12.052 [International conference on applied energy, {ICAE2014}].
[29] Long J, Xu Y, Wang T, Yuan Z, Shu R, Zhang Q, et al. Efficient base-catalyzed decomposition and in situ hydrogenolysis process for lignin depolymerization and char elimination. Appl Energy 2015;141:70–9. http://dx.doi.org/10.1016/j.apenergy.2014.12.025.
[30] Demirbas A. Liquefaction of biomass using glycerol. Energy Sources Part A: Recov Util Environ Effects 2008;30(12):1120–6. http://dx.doi.org/10.1080/15567030601100654.
[31] Seljak T, Oprešnik SR, Kunaver M, Katrašnik T. Wood, liquefied in polyhydroxy alcohols as a fuel for gas turbines. Appl Energy 2012;99:40–9. http://dx.doi.org/10.1016/j.apenergy.2012.04.043.
[32] Xiu S, Shahbazi A, Shirley V, Mims MR, Wallace CW. Effectiveness and mechanisms of crude glycerol on the biofuel production from swine manure through hydrothermal pyrolysis. J Anal Appl Pyrol 2010;87(2):194–8. http://dx.doi.org/10.1016/j.jaap.2009.12.002.
[33] Xiu S, Shahbazi A, Shirley VB, Wang L. Swine manure/crude glycerol co-liquefaction: physical properties and chemical analysis of bio-oil product. Bioresource Technol 2011;102(2):1928–32. http://dx.doi.org/10.1016/j.biortech.2010.08.026.
[34] Xiu S, Shahbazi A, Wallace CW, Wang L, Cheng D. Enhanced bio-oil production from swine manure co-liquefaction with crude glycerol. Energy Convers Manage 2011;52(2):1004–9. http://dx.doi.org/10.1016/j.enconman.2010.08.028.
[35] Ye Z, Xiu S, Shahbazi A, Zhu S. Co-liquefaction of swine manure and crude glycerol to bio-oil: model compound studies and reaction pathways. Bioresource Technol 2012;104(0):783–7. http://dx.doi.org/10.1016/j.biortech.2011.09.126.
[36] Cheng D, Wang L, Shahbazi A, Xiu S, Zhang B. Characterization of the physical and chemical properties of the distillate fractions of crude bio-oil produced by the glycerol-assisted liquefaction of swine manure. Fuel 2014;130:251–6. http://dx.doi.org/10.1016/j.fuel.2014.04.022.
[37] Cheng D, Wang L, Shahbazi A, Xiu S, Zhang B. Catalytic cracking of crude bio-oil from glycerol-assisted liquefaction of swine manure. Energy Convers Manage 2014;87(0):378–84. http://dx.doi.org/10.1016/j.enconman.2014.06.084.
[38] Pedersen TH, Jasiünas L, Casamassima L, Singh S, Rosendahl LA. Synergetic hydrothermal co-liquefaction of crude glycerol and aspen wood. Energy Convers Manage 2015;106:886–91. http://dx.doi.org/10.1016/j.enconman.2015.10.017.
[39] Oasmaa A, Sundqvist T, Kuoppala E, Garcia-Perez M, Solantausta Y, Lindfors C, et al. Controlling the phase stability of biomass fast pyrolysis bio-oils. Energy Fuels 2015;29(7):4373–81. http://dx.doi.org/10.1021/acs.energyfuels.5b00607.
[40] Yin S, Tan Z. Hydrothermal liquefaction of cellulose to bio-oil under acidic, neutral and alkaline conditions. Appl Energy 2012;92:234–9. http://dx.doi.org/10.1016/j.apenergy.2011.10.041.
[41] Mosteiro-Romero M, Vogel F, Wokaun A. Liquefaction of wood in hot compressed water: Part 1. Experimental results. Chem Eng Sci 2014;109(0):111–22. http://dx.doi.org/10.1016/j.ces.2013.12.038.
[42] Knezevic D, van Swaaij WPM, Kersten SRA. Hydrothermal conversion of biomass: I. Glucose conversion in hot compressed water. Ind Eng Chem Res 2009;48(10):4731–43. http://dx.doi.org/10.1021/ie801387v.
[43] Knezevic D, van Swaaij W, Kersten S. Hydrothermal conversion of biomass. II. Conversion of wood, pyrolysis oil, and glucose in hot compressed water. Ind Eng Chem Res 2010;49(1):104–12. http://dx.doi.org/10.1021/ie900964u.
[44] Akgül G, Kruse A. Influence of salts on the subcritical water–gas shift reaction. J Supercrit Fluids 2012;66:207–14. http://dx.doi.org/10.1016/j.supflu.2011.10.009.
[45] Guo Y, Wang S, Xu D, Gong Y, Ma H, Tang X. Review of catalytic supercritical water gasification for hydrogen production from biomass. Renew Sustain Energy Rev 2010;14(1):334–43. http://dx.doi.org/10.1016/j.rser.2009.08.012.
[46] Sharninghausen LS, Campos J, Manas MG, Crabtree RH. Efficient selective and atom economic catalytic conversion of glycerol to lactic acid. Nat Commun 2014;5(0):1–9. http://dx.doi.org/10.1038/ncomms6084.
[47] Schubert M, Regler JW, Vogel F. Continuous salt precipitation and separation from supercritical water. Part 1: Type 1 salts. J Supercrit Fluids 2010;52(1):99–112. http://dx.doi.org/10.1016/j.supflu.2009.10.002.

Paper K

Two-stage alkaline hydrothermal liquefaction of wood to biocrude in a continuous bench-scale system

I.M. Daraban, I.F. Grigoras, C.U. Jensen, S.S. Toor, T.H. Pedersen, L.A. Rosendahl

The manuscript has been published in the
Journal of Biomass Conversion and Biorefinery, vol. 7, no. 4, pp. 425–435, 2017.

The layout has been revised.

Biomass Conv. Bioref.
DOI 10.1007/s13399-017-0247-9

ORIGINAL ARTICLE

Two-stage alkaline hydrothermal liquefaction of wood to biocrude in a continuous bench-scale system

Iulia M. Sintamarean[1] · Ionela F. Grigoras[1] · Claus U. Jensen[2] · Saqib S. Toor[1] · Thomas H. Pedersen[1] · Lasse A. Rosendahl[1]

Received: 14 September 2016 / Revised: 7 December 2016 / Accepted: 8 February 2017

Abstract Feedstock pumpability is one of the main obstacles for continuous processing of biomass through hydrothermal liquefaction (HTL), due to their tendency to form heterogeneous slurries. In this work, a novel strategy is proposed to ensure lignocellulosic feed pumpability in HTL processing, even while applying elevated biomass loadings. In the first stage, a pumpable feed is prepared by an alkaline treatment of coarse wood chips at 180 °C, 120-min reaction time, and 0.35 NaOH-to-wood ratio. In a subsequent stage, the treated feedstock is converted into a biocrude in a continuously operated 20 kg/h scale unit. In total, 100 kg of wood paste with 25% dry matter is processed at 400 °C and 30 MPa, demonstrating the usefulness of this two-stage liquefaction strategy. An additional advantage liquefaction of such pretreated wood shows increased biocrude yields with approximately 10% compared to the case where non-pretreated wood is liquefied.

Keywords Lignocellulosic · Feedstock pumpability · Alkaline pretreatment · Biocrude

1 Introduction

In the transition from fossil fuels to renewables, biofuels can potentially replace up to 27% of transportation fuels by 2050, thus contributing to 7%-point reduction in CO_2 emissions, in the 2 °C global temperature increase scenario (IEA, 2012).

✉ Lasse A. Rosendahl
lar@et.aau.dk

[1] Department of Energy Technology, Aalborg University, Pontoppidanstræde 111, 9220 Aalborg, Denmark

[2] Steeper Energy, Sandbjergvej 11, 2970 Hørsholm, Denmark

Hydrothermal liquefaction (HTL) is a promising route to convert non-food biomass into liquid biofuels. The process operates on an aqueous biomass slurry that is pressurized to maintain water in its liquid state, and then heated to sub- or supercritical water conditions (300–400 °C). At these conditions, biomass decomposes into its major constituents, which subsequently undergo further chemical changes such as depolymerization, dehydration, condensation, and cyclization. The main product of this complex process is the biocrude. The biocrude oil is insoluble in water and is composed of hundreds of oxygenated chemical compounds [1]. Depending on process parameters and the feedstock used, up to 80% of the biomass can be converted into biocrude [2, 3]. The rest of the biomass is converted into water-soluble compounds, gaseous products, and a small fraction of solids.

As continuous processing is a prerequisite for implementing the HTL process at relevant scales, feedstock must be pumpable at high dry matter loading. This has been and still is one of the major obstacles that must be overcome. Because most HTL studies are focused on batch experiments, this problem is often ignored in literature and poorly understood. When a biomass feedstock is processed in a continuous HTL system, slurry dewatering may occur, causing dry processing giving rise to char deposit formation and even clogging. In small scale systems, the problem has been tackled by reducing the particle size below 0.250 mm and/or the solids content below 10% [4–6]. In larger scale continuous systems, where feedstock biomass loading is important for the process economy, efforts have been made to increase the dry matter content of the feed stream. Options tested have been to use an oil vehicle to carry the solid particles (the PERC process), to decompose the wood into fibers by acid hydrolysis (the LBL process) [7], or to use biomass streams that are already in liquid form (e.g., sewage sludge, manure). Even so, the dry matter content of the feedstock could not exceed 15% mass fraction in case of lignocellulosic

Published online: 22 February 2017

materials [8]. To reduce the energy consumption for particle size reduction and to allow higher biomass loadings, this work proposes a two-stage hydrothermal liquefaction process where extensive biomass dissolution is achieved in the first stage at 180 to 200 °C followed by conversion of the resulting biomass paste into biocrude at sub- or supercritical water conditions (see Fig. 1). The first stage—pretreatment—is performed in alkaline conditions with excess of alkaline reactant; thus, the second stage—HTL—will also be carried out in alkaline environment. Such an alkaline environment is beneficial for both biomass pretreatment and liquefaction, as it may increase the biomass degradation effect, the biomass conversion, and the biocrude yield while reducing the gas and solid products formation [9–16].

Alkaline pretreatment is one of the methods used in the pulp and paper industry to isolate the cellulose fibers from the lignocellulosic matrix or in the second-generation bioethanol production to remove the lignin and to increase the enzymatic hydrolysis of biomass. The most common alkaline reagents used in the alkaline pretreatment of biomass are sodium hydroxide (NaOH), potassium hydroxide (KOH), sodium carbonate (Na_2CO_3), and lime ($Ca(OH)_2$) [17]. According to the pretreatment conditions employed and the alkaline reagent used, the process can be tailored to remove lignin, hemicellulose, and even cellulose from the lignocellulosic matrix. The pretreatment temperature may vary from room temperature with retention times of hours or days, up to 200 °C with shorter retention times. NaOH has the most destructive effect on the lignocellulosic biomass and was used in the first chemical pulping process in the 1850s [18]. Soda pulping process was later replaced with more lignin-selective methods and is scarcely used nowadays for chemical pulp production. However, a pretreatment process similar to soda pulping may be effectively used to prepare pumpable feeds for hydrothermal processing. The aggressive attack of NaOH on all biomass constituents (lignin, hemicellulose, cellulose) will lead to biomass dissolution, reducing considerably the difficulty to handle heterogeneous biomass aqueous slurries under high-pressure conditions. The technical feasibility of using NaOH to solubilize the biomass as pretreatment method for HTL feedstocks has not been reported yet in literature.

In this study, wood alkaline hydrothermal pretreatment followed by hydrothermal liquefaction at supercritical water conditions was performed. First, laboratory-scale experiments were carried out to identify the alkaline pretreatment conditions required to obtain pumpable feedstocks. The optimum pretreatment conditions identified were used to prepare a batch of 100 kg of wood pulp that was converted in a bench-scale continuous HTL system with a capacity of 20 kg/h feed. The effect of the first stage—pretreatment on biocrude oil yield and elemental and chemical composition—was evaluated.

2 Materials and methods

2.1 Raw material

In the pretreatment experiments, hybrid poplar chips were used, while in the bench scale, willow chips were converted. Both poplar and willow, provided by Ny Vraa Bioenergi I/S, Tylstrup, Denmark, were 5-year-old trees cut in the winter of 2014. Bark and chips from branches were removed so only the wood stem parts were used. Poplar chips were 20 mm width and were separated into three particle size classes, small (3 to 5 mm), medium (5 to 10 mm), and large (10 to 14 mm). The willow was cut into chunks of 20 to 70 mm long. The chemical and elemental composition of poplar and willow is given in Table 1. Different raw materials were used for the small- and the bench-scale tests due to the lack of availability of poplar chips in larger quantities. As shown in Table 1, poplar and willow have similar elemental and chemical composition. For this reason, it was assumed that the impact of the raw material type on the pretreatment and HTL experimental results will not be significant.

2.2 Pretreatment experiments

Small scale pretreatment experiments were performed in a 400 cm^3 electrically heated batch reactor. The reactor was equipped with stirrer and cooling coil. For a batch test, 50 g of wood slurry was prepared from 10 g wood chips and 40 g NaOH solution. The concentration of the NaOH solution varied between 8 and 10% mass fraction, corresponding to NaOH-to-wood ratio of 0.32 and 0.40, respectively. Reaction time, particle size, and temperature were varied as well. All mixtures contained 20% wood mass fraction on dry basis (liquid-to-biomass ratio 4:1). After loading and closing the reactor, a heating period of 30 to 40 min was required to reach the set temperature. When reactor temperature reached the set point, the mixture was held at this temperature for desired reaction time (30 to 240 min). At the end of reaction, the reactor was cooled down and the product collected. The reactor, cooling coil, and the stirrer were thoroughly washed with distilled water that afterwards was filtered to recover the

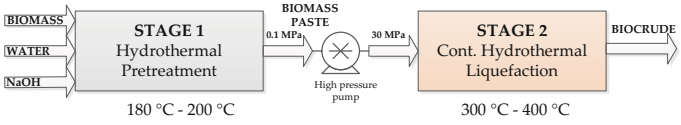

Fig. 1 Conceptual scheme of the two-stage alkaline hydrothermal liquefaction of biomass

Table 1 Elemental and chemical composition of the biomass used for alkaline pretreatment and HTL experiments. Values are given as per dry basis

	Element mass fraction				Polymer mass fraction			Ash (%)
	C	H	N	O[a]	Cellulose	Hemicellulose	Lignin	
Poplar	47	6	n.d.	46	60	18	13	1
Willow	48	6	n.d.	46	53	15	20	2

n.d. not detected

[a] By difference

solids. The amount of solids dissolved during the pretreatment was determined by filtering the pretreatment product on Whatman filter paper (qualitative filter paper grade 413, particle retention 5–13 μm) under vacuum, followed by drying at 105 °C to constant weight. Dried residue was weighed and the percent of biomass dissolved was determined gravimetrically (reported as percent of initial biomass on dry basis).

The objective of the small scale pretreatment experiments was to select the most significant factors that influence wood dissolution in the alkaline pretreatment stage. For these tests, a full factorial design with four variables at two levels and three experiments at the center points was used to study the variation of wood dissolved mass fraction with the process conditions. The process variables and their levels were (1) reaction temperature 160 and 200 °C, (2) reaction time 30 and 240 min, (3) NaOH-to-wood ratio 0.32 and 0.40, and (4) wood particle size 3 to 5 mm and 10 to 15 mm. A total of 19 experiments were carried out for factor screening. For each experiment, the percent of biomass dissolved was measured. Statistical interpretation of the results was performed using the Umetrics MODDE software and the effects of each variable were calculated. For a set of pretreatment conditions (180 °C, 120 min, 0.35 alkali-to-wood ratio), the impact of the alkaline reactant type on wood dissolution was also investigated by replacing the NaOH with Na_2CO_3, KOH, and K_2CO_3.

Bench-scale pretreatment was performed in an 80-L paddle digester, specially designed for pulping of annual plants under industry-like conditions. The equipment was provided by Thünen Institute of Wood Research, Hamburg. The reactor was heated with steam indirectly via a jacket. The digester was filled in the upright position and then was brought in horizontal position for processing. A central paddle, which can operate at different speed, provided a good mixing. One hundred kilograms of feedstock were prepared in four batches. In each batch, 5 kg of willow chips were mixed with 20 kg of NaOH solution of 10% mass fraction (NaOH-to-wood ratio of 0.40) and were processed at 180 °C for 120 min. The heating time was approximately 30 min.

2.3 Pumpability test

The pretreated feedstocks were tested for their pumpability using the syringe test. The syringe test aims at mimicking the flow of the feed forced through an orifice, albeit at lower pressures than HTL. The sample is loaded into the syringe tube and the material is discharged by applying pressure to the plunger. The feedstock is considered pumpable if the feed behaves like a homogeneous material, as shown in Fig. 2 and without slurry dewatering. The advantages of the syringe test are (a) the test is quick and easy, (b) does not require special laboratory equipment, and (c) can be implemented in laboratory or on site. However, although good indicative results come from this test, there are also several drawbacks of the syringe test like (a) the pressure applied is not comparable to the pressure at which the feed will be pumped which means that pumpability is only indicated and (b) the test result depends on the pressure applied, the volume of sample, and the syringe outlet diameter.

2.4 Hydrothermal liquefaction experiments

Small-scale HTL experiments were carried out in 10-mL stainless steel tubular batch reactors at 400 °C and 32–33 MPa for 10 min. In a typical run, approximately 7 g of feedstock was loaded into the reactor. The reactor was purged with nitrogen for removal of residual air and pre-pressurized with approximately 2 MPa nitrogen. All experiments were performed in triplicates. The reactors were heated in a pre-heated fluidized sand bath (Techne SBL-2D) and reached the final temperature in about 2 min. After that, the reactor was removed from the fluidized sand bath and cooled in a water bath. After cooling, the gases were released and the liquid and solid products in the reactor were collected and separated. First, the water phase was poured out of the reactor and filtered using a Whatman filter paper to remove the solids. Afterwards, the reactor was washed with acetone to recover the biocrude oil. The

Fig. 2 The syringe test applied to an alkaline pretreated feed showing the homogeneity of the feed after the test

acetone-biocrude mixture was filtered and evaporated under reduced pressure (0.060 MPa at 40 °C), in a rotary evaporator to remove the acetone. The biocrude obtained after acetone evaporation was mixed with hydrochloric acid (HCl)—5.12 vol.%—and centrifuged to separate the oil phase from the remaining water.

Continuous processing of the alkaline-pretreated feedstock was carried out at 400 °C and 30 MPa. The continuous bench-scale unit has a capacity of 20 kg/h feed and consists of two serial heaters (with heating rate of 200–400 °C/min), two 5-L serial reactors, a cooler, a capillary section for depressurization of the product stream, and a product separation section. The pretreated feedstock was loaded into a 100-kg feed barrel and fed into the system using a high-pressure piston pump. After approximately 4 h of continuous operation, the feed barrel was emptied and the liquid products collected (water phase and biocrude phase). The biocrude was separated gravimetrically from the water phase in a separation funnel and the biocrude yield was measured. The oil was also analyzed for elemental and chemical composition. A schematic diagram of the continuous bench-scale HTL plant is shown in Fig. 3. The system is described in more detail by Pedersen et al. [19].

A summary of the experimental conditions used for biomass pretreatment and HTL at laboratory and bench scale is given in Table 2.

2.5 Analytical procedure

The cellulose, hemicellulose, and lignin content of the biomass samples were determined using a Foss FibertecTM 1020 Fiber Analyzer according to the Foss procedure (modified to eliminate the use of amylase. Elemental analysis was performed with a PerkinElmer 2400 Series II CHNS/O Elemental Analyzer. The water content of the biocrude oils was measured by Karl Fischer titration. Higher heating value of the biomass was measured with an IKA C2000 Basic calorimeter and the ash content was measured at 575 °C for 6 h. The Na and K content in the biocrude ash was quantified using inductively coupled plasma optical emission spectroscopy (ICP-OES).

The chemical composition of the biocrude oils was analyzed by gas chromatography-mass spectrometry (GC-MS). The instrument used was Thermo Scientific Trace 1300 GC equipped with a single quadrupole MS. The analyses were carried out in electron ionization (EI) mode, with an Agilent HP 5-ms column, 30 m long, 0.25-mm ID, and 0.25-μm film thickness. The samples were diluted with dichloromethane (DCM) and analyzed using the following program: 40 °C for 2 min, 5 °C/min to 180 °C, and 10 °C/min to 300 °C.

3 Results and discussion

3.1 Stage 1 hydrothermal pretreatment—screening and optimization tests

Table 3 shows the variation of wood dissolved mass fraction with temperature, solution alkalinity, reaction time, and wood chip size. Based on these values, the impact of each variable

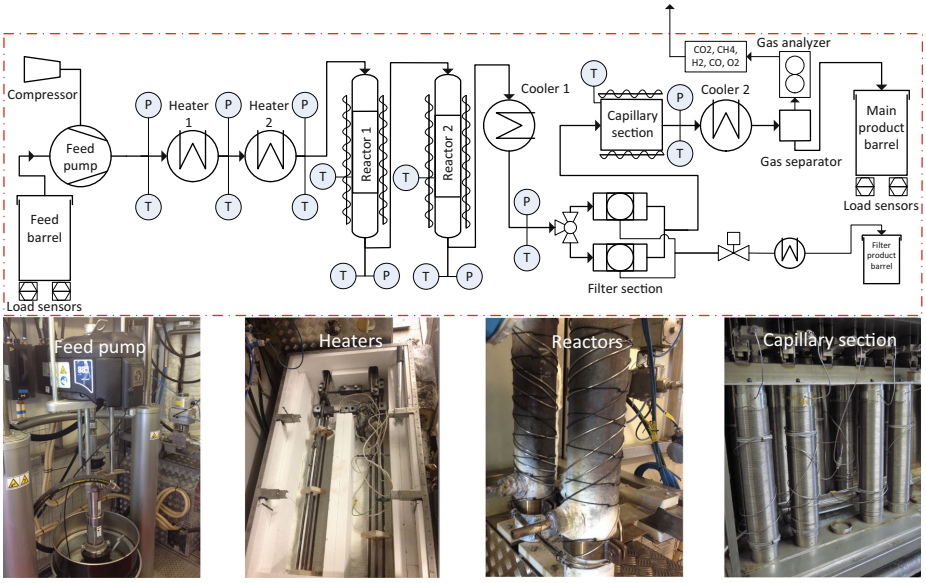

Fig. 3 Process flow diagram of the continuous bench-scale HTL plant [20]

Table 2 Experimental conditions used in the laboratory- and bench-scale experiments

Biomass	Laboratory scale Poplar chips 3–14 mm	Bench scale Willow chips 20–70 mm
Pretreatment conditions		
Reactor volume (L)	0.4	80
Liquor-to- biomass ratio	4:1	4:1
NaOH-to-biomass ratio	0.32–0.40	0.40
Temperature (°C)	160–200	180
Heating time (min)	30–40	30
Reaction time (min)	30–240	120
HTL conditions		
System size	10 mL	20 kg/h
Temperature (°C)	400	400
Reaction time (min)	10	10–15
Other alkalis	none	K_2CO_3

on the amount of wood dissolved was calculated and plotted in Fig. 4.

The results indicate that the pretreatment temperature has the highest impact on wood dissolution followed by reaction time and NaOH-to-wood ratio. The mass fraction of wood chips dissolved increases with about 35% when pretreatment temperature is raised from 160 to 200 °C. The increase of wood dissolved mass fraction with the temperature can be explained by the fact that as temperature increases, more wood constituents suffer degradation. During the heating period (up to 150 °C), carbohydrates start to degrade by peeling reactions of the reducing end groups. As temperature increases to 150–160 °C, advanced degradation of hemicellulose occurs by hydrolysis, increasing the number of reducing end groups and consequently enhancing the polymer chain erosion. Delignification accelerates significantly in the same temperature region [21–23]. However, cellulose degradation starts only around 170 °C [22]. Like hemicellulose, its degradation occurs by peeling reactions and hydrolysis. Higher temperatures enhance cellulose depolymerization until the reducing groups are stabilized [21, 23, 18]. This may explain why wood chips could not be dissolved completely. Even at the most drastic conditions, a solid fraction mainly consisting of short fibers could be separated. The formation of the solids (long chain fibers) may also be related to the high content of biomass in the slurry (20% mass fraction) that may favor the association between polymer chains [21].

Table 3 The variation of the solid dissolved mass fraction (%) with the pretreatment conditions and wood chip size. At the central points (180 °C, 0.36 NaOH-to-wood ratio, 135 min), the mass fraction of wood dissolved on average was 60.7 ± 6.2%

NaOH-T-t[a]	Particle size (mm)		NaOH-T-t[a]	Particle size (mm)	
	3–5	10–15		3–5	10–15
0.32-160-30	23	17	0.40-160-30	27	27
0.32-160-240	34	33	0.40-160-240	53	48
0.32-200-30	62	57	0.40-200-30	71	71
0.32-200-240	71	60	0.40-200-240	87	84

[a] NaOH-to-wood mass fraction-temperature (°C)-reaction time (min)

Reaction time and solution alkalinity are the second most important variables. The impact of increasing the reaction time from 30 to 240 min or the NaOH-to-wood ratio from 0.32 to 0.40 is about 15% increase of the biomass dissolved. An interaction between these two factors is indicated in Fig. 4 (B*D). This means that the effect of one of the factors on the output variable (wood dissolved mass fraction) is dependent on the value of the second factor with which it interacts. For example, the average wood dissolved mass fraction increases with the increase of sodium hydroxide concentration by 9% when reaction time is 30 min and by 19% when reaction time is 240 min.

The wood particle size has a negative but relatively low impact on wood dissolution. An increase of wood particle size from approximately 5 up to 14 mm can reduce the amount of biomass dissolved with about 5%. The effect of the alkaline hydrothermal pretreatment conditions on the product aspect can be visualized in Fig. 5.

Designed experiments showed that the impact of wood particle size on biomass dissolved fraction is not significant thus this factor can be eliminated from a further optimization study. More, it was determined that the interactions between factors have a low impact on the output variable which means that the relationship between variables and the output is approximately linear. In this context, the utilization of a single-factor design or a one-factor-at-a-time (OFAT) optimization strategy is appropriate. In this case, the optimization criterion was the pretreated feedstock response to the syringe test (yes/no).

From Table 4 and Fig. 6, it can be noticed that approximately 65% of the initial wood needs to be dissolved to pass the syringe test and that the critical pretreatment conditions are reaction temperature 180 °C, reaction time 120 min, and

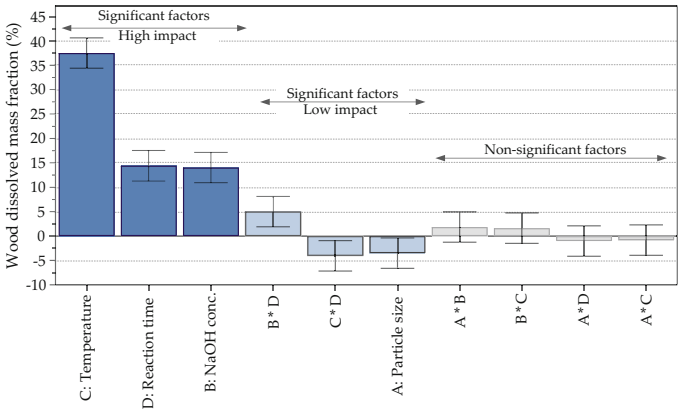

Fig. 4 The change of wood dissolved mass fraction (%) when a pretreatment process variable is increased from its low level to high level

NaOH-to-wood ratio 0.35. In Fig. 6d, the effect of NaOH is also compared with other alkaline bases and salts. Sodium and potassium carbonates were less effective in wood dissolution compared to sodium hydroxide. This is because carbonates have poor nucleophilicity, reducing the biomass delignification. Potassium hydroxide was less efficient than sodium hydroxide due to lower molar concentration of KOH solution compared to the NaOH solution at the same reactant-to-wood mass ratio.

The pretreatment experiments and the syringe test applied to the partially dissolved wood-based slurries indicate that pumpable feeds with 20% dry matter content can be obtained by treating the wood chips at 180–200 °C in NaOH solution with NaOH-to-wood ratio of 0.35–0.40. To validate these results, a batch of 100 kg of willow feedstock was prepared at 180 °C with a NaOH-to-wood ratio of 0.40 and 120 min at maximum temperature. A higher NaOH-to-wood ratio than the critical value of 0.35 was chosen because for the bench-scale pretreatment, willow chips with particle size significantly higher than the particles used in the optimization test (up to five times longer and two times thicker) were used. The wood paste obtained passed the syringe test and was used as feedstock for the second stage—HTL in the continuous bench-scale plant.

3.2 Stage 2 hydrothermal liquefaction of pretreated feedstock

3.2.1 HTL in continuous bench-scale system—proving the technological feasibility of continuous processing wood-based feeds with high dry matter content by two-stage hydrothermal liquefaction

Besides liquefaction of alkaline pretreated wood, a baseline test with non-pretreated wood was carried out into the continuous bench-scale system. To pump the non-pretreated wood, biomass grinding to fine powder was necessary as well as the addition of an oil vehicle into the feedstock composition. The same amount of oil vehicle was added to the pretreated wood slurry to obtain a feedstock with similar composition as the

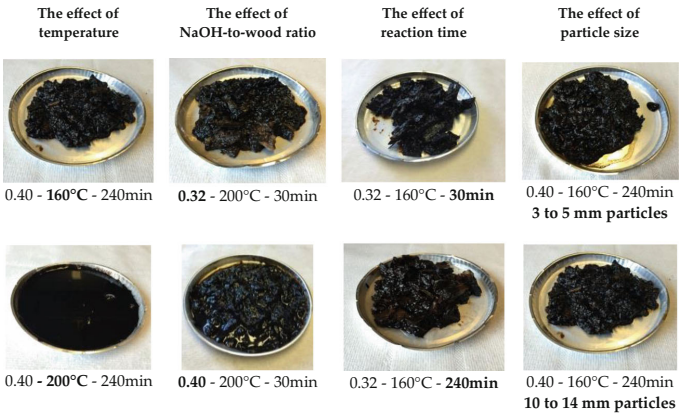

Fig. 5 The impact of process conditions on biomass dissolution and product aspect. Samples visualize the resulting pulps

Table 4 Alkaline hydrothermal pretreatment condition optimization using the one-factor-at-a-time (OFAT) strategy. Designed experiments previously performed showed that factor interactions have a low impact on the output and the factor particle size can be eliminated. For the optimization tests, medium size (5 to 10 mm) wood chips were used

Temperature (°C)	NaOH-to-wood ratio	Time at Tmax (min)	Wood dissolved mass fraction (%)	Feed pumpability (syringe test)
Fixed factors: temperature 180 °C, reaction time 120 min				
Variable factor: NaOH-to-wood ratio				
180	0.25	120	28	x
180	0.30	120	55	x[a]
180	0.35	120	65	✓
180	0.40	120	72	✓
Fixed factors: temperature 180 °C, NaOH-to-wood ratio 0.35				
Variable factor: reaction time				
180	0.35	30	56	x[a]
180	0.35	60	62	✓[a]
180	0.35	120	65	✓
180	0.35	180	68	✓
180	0.35	240	71	✓
Fixed factors: NaOH-to-wood ratio 0.35, reaction time 120 min				
Variable factor: temperature				
160	0.35	120	54	x
180	0.35	120	65	✓
200	0.35	120	88	✓

[a] The product consisted of softened wood chips that required maceration

baseline. Upon mixing the pretreated wood with oil, the feed viscosity was reduced which allowed the addition of fresh wood powder. Thus, the biomass loading of the feed containing pretreated wood was increased from 20 to 25% mass fraction. The composition of the two feedstocks is given in Table 5. Batches of 100 kg of each feedstock were prepared and pumped at 30–32 MPa using a high-pressure piston pump and were continuously processed for about 4 h into the HTL system.

Alkaline hydrothermal liquefaction of wood in a two-stage process is advantageous because it allows processing of feeds with high biomass loading and reduces the need for mechanical downsizing of the biomass. As shown in Table 5, wood chips instead of wood powder were used in the two-stage HTL strategy. More, the biomass loading of the feed in the two-stage process was increased from 18 to 25% mass fraction due to wood dissolution and co-processing with raw biomass. Continuous processing of feedstock based on woody biomass, with such high dry matter content was not reported yet. However, the high amount of NaOH used, between 35 and 40% of the biomass weight, represents the main disadvantage of the alkaline pretreatment process. Methods to reduce the NaOH consumption, e.g., by combining the chemical pretreatment with mechanical operations or alkali reactant recovery by water phase recirculation, need to be further investigated in order to make the pretreatment process economical.

Despite the high fraction of alkalis in the feedstock, the ash content in the biocrude is between 3.9 and 5.3% mass fraction. Na and K represent about 34% of the biocrude ash content, i.e., that less than 5% of the elemental Na and K added into the feedstock was transferred into the biocrude. Therefore, most of the inorganic matter in the feed is transferred into the water phase and is involved in the solid formation. This confirms that water phase recirculation could be an option to recover the alkaline reactant used in the pretreatment stage.

The results given in Table 5 indicate that the yield, the elemental composition, and the heating value of the biocrude oils were not significantly affected by the pretreatment stage. It is worth to mention that the biocrudes analyzed were not obtained under steady-state conditions which are usually achieved after processing 400 kg of feedstock or more. The main focus of the bench-scale test was to demonstrate that by pretreating the wood prior to HTL, pumpable feeds with improved biomass loading can be obtained. To further investigate the effect of wood pretreatment on the biocrude yield and composition, comparative HTL experiments in micro reactors were carried out.

3.2.2 HTL in micro reactors—the effect of biomass pretreatment stage on biocrude yield and composition

The alkaline pretreated wood paste was liquefied at 400 °C and 30 MPa in 10-mL batch reactors without the addition of other additives. A baseline test with non-pretreated wood and identical alkaline reactant concentration was carried out. The feed composition, the yield, and the elemental composition of the biocrudes obtained after the HTL conversion of the two slurries are given in Table 6.

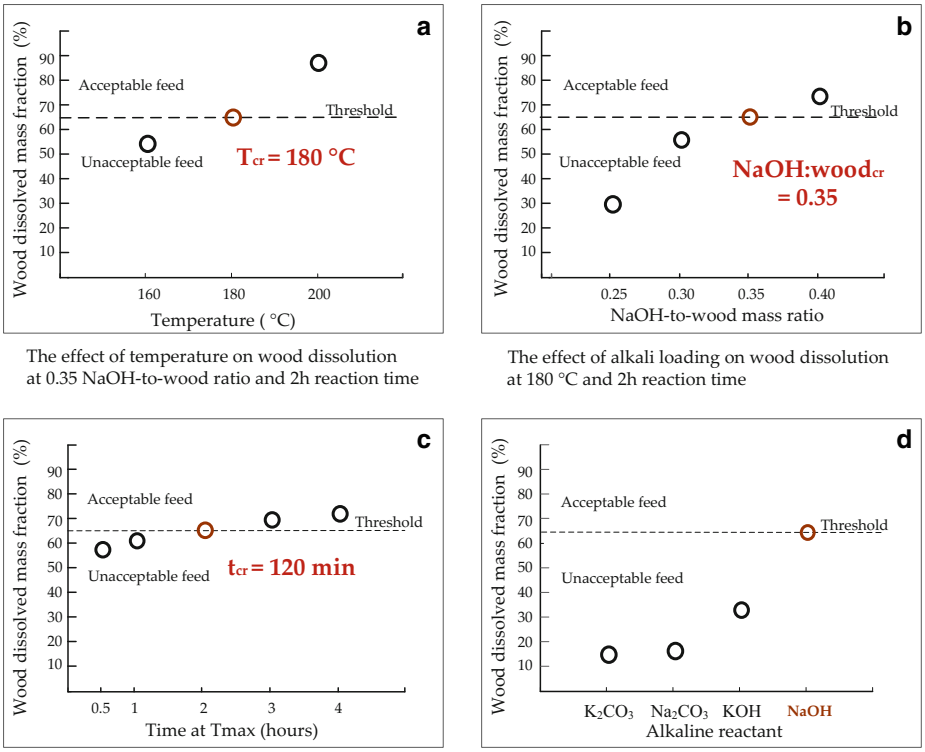

The effect of temperature on wood dissolution at 0.35 NaOH-to-wood ratio and 2h reaction time

The effect of alkali loading on wood dissolution at 180 °C and 2h reaction time

The effect of reaction time on wood dissolution at 180 °C and 0.35 NaOH-to-wood ratio

The effect of alkaline reactant type on wood dissolution at 180 °C, 0.35 alkali-to-wood ratio and 2h reaction time

Fig. 6 Identification of critical alkaline pretreatment conditions. The effect of NaOH loading, reaction time, temperature, and reactant type on wood dissolved mass fraction (%); 5–10 mm poplar wood chips were used in all experiments

Unlike the results obtained in the continuous HTL system, the alkaline pretreatment of wood determined an increase of the biocrude yield with about 10%. This may confirm the hypothesis that due to the addition of raw wood in the pretreated feedstock, the effect of the first stage pretreatment on biocrude yield was reduced. The increase of biocrude yield may be due to several reasons: (a) initial biomass dissolution created a more homogeneous medium for the HTL reactions ensuring a better distribution of reactants and higher mass transfer rates and (b) due to biomass dissolution, which is considered the rate determining step in biomass liquefaction [24], the rates of the reactions generating oil compounds were increased.

Like the biocrude oils obtained in the continuous system, the elemental composition was not affected by the pretreatment stage. Lower oxygen fractions were measured for the oils obtained in micro reactors. This might be related to the oil separation procedures applied in the two cases. Unlike the oils obtained in the bench-scale system that are separated gravimetrically, small scale liquefaction requires oil separation with solvents. During the solvent evaporation process, some of the oil compounds may be lost affecting the elemental composition of the sample. The oil separation procedure may explain also the lower biocrude yield obtained in batch experiments in the case of non-pretreated wood.

From Table 7, it can be noticed that only small variations between the peak areas of the compounds identified by GC-MS exist suggesting a very similar chemical composition of the two biocrudes. The volatile compounds identified were mainly oxygenated aromatic and cyclic structures, typical for HTL biocrudes based on lignocellulosic biomass. Most common compounds were ketones and phenols but alcohols and other compounds were also identified. The small variations in elemental and chemical composition of the biocrudes obtained by one-stage and two-stage HTL suggest that the biocrude quality is not affected by the pretreatment stage, considering that the oils were obtained from the same substrate—wood. However, it is important to mention that the characterization of the biocrudes chemical composition is based only on the volatile fraction of the oil which represents

Table 5 Feedstock composition, biocrude yield, and biocrude elemental composition from continuous HTL of pretreated and non-pretreated wood at 400 °C in 20 kg/h feed capacity system

	Continuous bench-scale system	
	One-stage HTL	Two-stage HTL
Feed		
Biomass	Non-pretreated wood powder	Alkaline pretreated wood chips and raw wood powder
Total biomass in feed (% db)	18	25
Water-to-biomass ratio	2.9	1.8
Alkaline-to-biomass ratio (NaOH and K_2CO_3)	0.27	0.30
Oil medium (%)	18	18
Other additives (ethanol, thickeners) (%)	5.0	5.0
Biocrude		
Yield (% db)	44	44
HHV (MJ/kg)	36	36
C (% db)	72	77
H (% db)	9.6	8.9
N (% db)	0.85	1.1
O[a]	18	13
H/C	1.6	1.4
O/C	0.19	0.13
Na (%)	–	1.2
K (%)	–	0.58
Ash (%)	3.9	5.3

[a] By difference (100-C-H-N)

about half of the sample weight. Characterization of the non-volatile fraction of the biocrude would provide a complete understanding of the effect of biomass alkaline pretreatment on the biocrude chemical composition and will be covered in a future work.

4 Conclusions

This work proves the technological feasibility of preparing pumpable wood feedstocks with high dry matter content by applying a two-stage hydrothermal liquefaction strategy. In the first stage,

Table 6 Feedstock composition, biocrude yield, and biocrude elemental composition from HTL of pretreated and non-pretreated wood at 400 °C in 10-mL micro reactors [25]

	Batch micro reactors	
	One-stage HTL	Two-stage HTL
Feed		
Biomass	Non-pretreated wood powder	Alkaline pretreated wood chips
Total biomass in feed (% db)	20	20
Water-to-biomass ratio	3.6	3.6
Alkaline-to-biomass ratio	0.40	0.40
Other additives	none	none
Biocrude		
Yield (% db)	31	42
C (% db)	84	82
H (% db)	9.4	9.0
N (% db)	1.6	1.6
O[a]	5.3	7.2
H/C	1.3	1.3
O/C	0.05	0.07

[a] By difference (100-C-H-N)

Table 7 Classification of chemical compounds detected by GC-MS in biocrude oils obtained from HTL of non-pretreated (one-stage HTL) and pretreated wood (two-stage HTL) in batch micro reactors (HTL conditions 400 °C, 32–33 MPa, 10 min) [25]

	Chemical compound	Formula	MW	Peak area (%)	
				One-stage HTL	Two-stage HTL
Alcohols	3-penten-2-ol	C5H10O	86	5.0	3.4
	4-methyl-2-pentanol	C6H14O	102	2.3	1.8
	5-octen-1-ol	C8H16O	128	1.5	1.5
	2-methyl-1-hexadecanol	C17H36O	256	1.6	1.5
Ketones	Cyclopentanone	C5H8O	84	0.43	0.46
	2-methyl-cyclopentanone	C6H10O	98	1.8	1.5
	4-hydroxy-4-methyl-2-pentanone	C6H12O2	116	2.8	2.7
	3-methyl-cyclohexanone	C7H12O	112	1.9	1.3
	2-methyl-2-cyclopenten-1-one	C6H8O	96	0.42	0.5
	2,3-dimethyl-2-cyclopenten-1-one	C7H10O	110	0.36	0.5
	3-methyl-2-cyclopenten-1-one	C6H8O	96	0.00	0.00
	3,4-dimethyl-2-cyclopenten-1-one	C7H10O	110	1.0	0.47
	2,3-dimethyl-2-cyclopenten-1-one	C7H10O	110	0.43	0.70
	3,4-dimethyl-2-cyclopenten-1-one	C7H10O	110	0.00	0.47
	2,3-dimethyl-2-cyclopenten-1-one	C7H10O	110	1.0	1.2
	2,3,4-trimethyl-2-cyclopenten-1-one	C8H12O	124	1.1	1.2
	3-isopropyl-2-cyclopenten-1-one	C8H12O	124	0.0	0.82
	2,3,4,5-tetramethyl-2-cyclopenten-1-one	C9H14O	138	0.6	0.75
	3-isopropyl-2-cyclopenten-1-one	C8H12O	124	0.0	0.00
	2,2-dimethylcyclohexyl methyl ketone	C10H18O	154	3.4	3.4
Phenols	Phenol	C6H6O	94	0.66	0.83
	m-cresol	C7H8O	108	0.55	0.79
	p-cresol	C7H8O	108	0.52	0.63
	2-methoxy-phenol	C7H8O2	124	1.3	1.8
	2,3-xylenol	C8H10O	122	0.60	0.72
	2-methoxy-4-methyl-phenol (creosol)	C8H12O2	138	3.0	2.7
	2,3,6-trimethyl-phenol	C9H12O	136	0.93	0.84
	4-ethyl-2-methoxy-phenol(p-ethylguaiacol)	C9H12O2	152	0.59	0.47
	2,6-dimethoxy-phenol	C8H10O3	154	0.47	0.51
	2-methoxy-4-propyl-phenol	C10H14O2	166	0.00	0.00
	4-methoxy-3-(methoxymethyl)-phenol	C9H12O3	168	0.00	0.46
	Butylated hydroxytoluene	C15H24O	220	11	11
Esters	2-propenoic acid, 3-(1-acetyl-2,2-dimethylcyclopentyl)-,methyl ester	C13H20O3	224	0.82	1.0
	Terephthalic acid, bis(2-ethylhexyl)ester	C24H38O4	390	0.00	0.00
Others	2-chloro-2-methyl-butane	C5H11Cl	106	18	13
	2,5,8-trimethyl-1,2,3,4-tetrahydro-1-naphthol	C13H18O	190	0.00	0.00
	9-hexadecenoic acid	C16H30O2	254	0.63	0.65
Total				64	60

pumpable feedstocks are prepared by alkaline hydrothermal pretreatment of biomass at 180 to 200 °C and NaOH-to-biomass ratio of 0.35 to 0.40. The pretreatment dissolves more than 65% of the biomass, improving significantly the feed pumpability. Comparative studies show that alkaline pretreatment stage has no significant impact on biocrude elemental and chemical composition or heating value. Small-scale batch studies indicate that wood pretreatment prior to HTL increase the biocrude yield with approximately 10% but the continuous bench-scale tests are less conclusive and more data from continuous processing are needed. The wood-based slurry containing 25% dry matter content was successfully pumped at 30 MPa using a high-pressure piston pump. For lignocellulosic biomass, continuous processing of feedstocks with such high solid loading is a first breakthrough.

Acknowledgements The authors would like to acknowledge the funding of this work by Innovation Fund Denmark Grant No. 1305-00030B.

References

1. Tews IJ, Zhu Y, Drennan CV et al (2014) Biomass direct liquefaction options: technoeconomic and life cycle assessment. Pacific Northwest National Laboratory, Richland
2. Mørup AJ, Christensen PR, Aarup DF et al (2012) Hydrothermal liquefaction of dried distillers grains with solubles: a reaction temperature study. Energy Fuel 26:5944–5953. doi:10.1021/ef3008163
3. Biller P, Ross AB (2011) Potential yields and properties of oil from the hydrothermal liquefaction of microalgae with different biochemical content. Bioresour Technol 102:215–225. doi:10.1016/j.biortech.2010.06.028
4. Jazrawi C, Biller P, Ross AB et al (2013) Pilot plant testing of continuous hydrothermal liquefaction of microalgae. Algal Res 2:268–277. doi:10.1016/j.algal.2013.04.006
5. Elliott DC, Hart TR, Neuenschwander GG et al (2014) Hydrothermal processing of macroalgal feedstocks in continuous-flow reactors. ACS Sustain Chem Eng 2:207–215. doi:10.1021/sc400251p
6. Elliott DC, Baker EG, Sealock LJ et al (1988) Low-temperature conversion of high-moisture biomass continuous reactor system results. Pacific Northwest Laboratory, Richland
7. Thigpen PL (1982) Final report: an investigation of liquefaction of wood at the biomass liquefaction facility, Albany, Oregon, Battelle Pacific Northwest Laboratories, Department of Energy, Wheelabrator Cleanfuel Corporation. Technical Information Center, Office of Scientific and Technical Information, U.S. Department of Energy
8. Elliott DC (2011) Hydrothermal processing. In: Brown RC (ed) Thermochem. Process. Biomass John Wiley & Sons, Ltd, pp 200–231
9. Ogi T, Yokoyama P, Koguchi K (1985) Direct liquefaction of wood by catalyst (part 1) effects of pressure, temperature, holding time and wood/catalyst/water ratio on oil yield. J Japan Pet Inst 28:239–245. doi:10.1627/jpi1958.28.239
10. Minowa T, Zhen F, Ogi T (1998) Cellulose decomposition in hot-compressed water with alkali or nickel catalyst. J Supercrit Fluids 13:253–259. doi:10.1016/S0896-8446(98)00059-X
11. Akhtar J, Kuang SK, Amin NS (2010) Liquefaction of empty palm fruit bunch (EPFB) in alkaline hot compressed water. Renew Energy 35:1220–1227. doi:10.1016/j.renene.2009.10.003
12. Mazaheri H, Lee KT, Bhatia S, Mohamed AR (2010) Subcritical water liquefaction of oil palm fruit press fiber in the presence of sodium hydroxide: an optimisation study using response surface methodology. Bioresour Technol 101:9335–9341. doi:10.1016/j.biortech.2010.07.004
13. Mazaheri H, Lee KT, Mohamed AR (2013) Influence of temperature on liquid products yield of oil palm shell via subcritical water liquefaction in the presence of alkali catalyst. Fuel Process Technol 110:197–205. doi:10.1016/j.fuproc.2012.12.015
14. Liu HM, Wang FY, Liu YL (2014) Alkaline pretreatment and hydrothermal liquefaction of cypress for high yield bio-oil production. J Anal Appl Pyrolysis 108:136–142. doi:10.1016/j.jaap.2014.05.007
15. Li Z, Cao J, Huang K et al (2015) Alkaline pretreatment and the synergic effect of water and tetralin enhances the liquefaction efficiency of bagasse. Bioresour Technol 177:159–168. doi:10.1016/j.biortech.2014.11.043
16. Toor SS, Rosendahl LA, Hoffmann J et al (2014) Hydrothermal liquefaction of biomass. In: Jin F (ed) Application of hydrothermal reaction to biomass conversion. Springer-Verlag, Berlin Heidelberg, pp 189–217
17. Kim JS, Lee YY, Kim TH (2016) A review on alkaline pretreatment technology for bioconversion of lignocellulosic biomass. Bioresour Technol 199:42–48. doi:10.1016/j.biortech.2015.08.085
18. Sjöström E (1993) Wood chemistry: fundamentals and applications, 2nd edn. Academic Press, San Diego
19. Pedersen TH, Grigoras IF, Hoffmann J et al (2016) Continuous hydrothermal co-liquefaction of aspen wood and glycerol with water phase recirculation. Appl Energy 162:1034–1041. doi:10.1016/j.apenergy.2015.10.165
20. Pedersen TH (2016) Hydrothermal liquefaction of biomass and model compounds. Dissertation, Aalborg University
21. Knill CJ, Kennedy JF (2003) Degradation of cellulose under alkaline conditions. Carbohydr Polym 51:281–300. doi:10.1016/S0144-8617(02)00183-2
22. Britt KW (1970) Handbook of pulp and paper technology, 2nd edn. Van Nostrand Reinhold, New York
23. Grace TM, Malcolm EW (1989) Pulp and paper manufacture: Volume 5 Alkaline pulping, 3rd edn. TAPPI Press, Atlanta
24. Overend RP, Chornet E (1988) A unified treatment for liquefaction. In: Bridgwater AV, Kuester JL (eds) Res. Thermochem. biomass Convers. Elsevier Science Publishing Co., pp 411–428
25. Grigoras IF, Stroe RE, Sintamarean IM, Rosendahl AL (2016) Effect of alkaline pretreatment on the product distribution and composition resulting from the hydrothermal liquefaction of short rotation coppice willow. Bioresour Technol , Manuscript submitted for publication. BITE-D-16-06754

Paper L

Process for upgrading oxygen containing renewable oil

Steen Brummerstedt Iversen, Claus Uhrenholt Jensen, Julie Katerine Rodriguez Guerrero

The patent application has been filed as
Danish patent application - no. not yet available

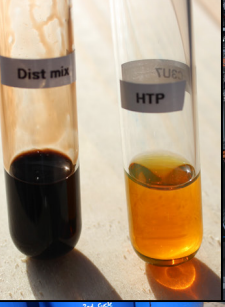


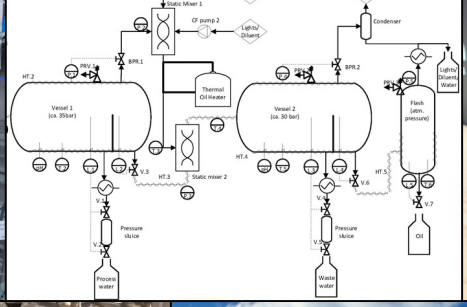


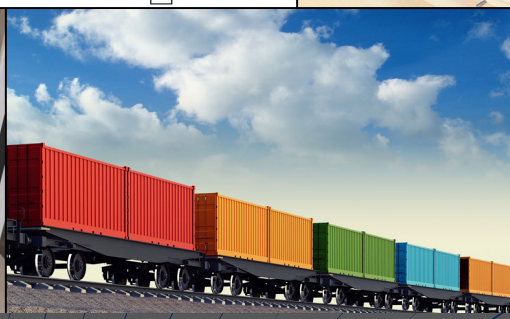

ISSN (online): 2446-1636
ISBN (online): 978-87-7210-134-7

AALBORG UNIVERSITY PRESS